

AD-A203 887

DTIC FILE COPY N-1788

NCEL

Technical Note

September 1988

By C.A. Kodres, E.E. Cooper,
and P.L. Stone

Sponsored by Naval Facilities
Engineering Command

EXPERIMENTAL EXAMINATION OF THE AEROTHERMAL PERFORMANCE OF THE T-10 TEST CELL AT NAS, CUBI POINT

DTIC
ELECTE
JAN 26 1989

S
R H

ABSTRACT This report presents results of aerodynamic and thermodynamic tests conducted on the first standard Navy air-cooled T-10 test cell. Objectives of the tests were to: (1) Determine if aerodynamic and thermodynamic design objectives for the standard T-10 test cells were met; (2) Obtain data for comparing analytical predictions and validating analytical modeling techniques, and (3) Obtain baseline data of cell performance for use in case of future changes in design or operations. Data were obtained during runs with the following engines: a J52-P-8B, a J52-P-408, a TF41-A-2C, a F404-GE-400, and a TF30-P-414. All engines were run at idle, 85%, and military power, and the engines equipped with afterburner (the TF30 and F404) were run at zone 5. Measurements included: Intake flow velocities and flow rates, cell pressure, flow velocities approaching and around the engine, exhaust section surface temperatures, and exhaust jet temperatures and velocities. Results showed that all aerothermal design objectives were met with one exception; noise measured 250 feet aft of the engine exceeded 85 db. Augmentation ratios ranged from 6.0 to 13.5. Air flow approaching the engine was smooth with velocities less than 40 ft/sec. Cell depression was less than 1.0 inch H₂O. Flow in the exhaust augmentor tube was symmetrical and indicated smooth mixing of jet exhaust with cooling air. Maximum temperature of the augmentor wall was about 800°F with the TF30 engine.

NAVAL CIVIL ENGINEERING LABORATORY PORT HUENEME CALIFORNIA 93043

REPRODUCED FROM
BEST AVAILABLE COPY

Approved for public release; distribution is unlimited.

89 1 26 05 D

Unclassified

SECURITY CLASSIFICATION OF THIS PAGE (When Data Entered)

REPORT DOCUMENTATION PAGE		READ INSTRUCTIONS BEFORE COMPLETING FORM
1. REPORT NUMBER TN-1788	2. GOVT ACCESSION NO. DN665088	3. RECIPIENT'S CATALOG NUMBER
4. TITLE (and Subtitle) EXPERIMENTAL EXAMINATION OF THE AEROTHERMAL PERFORMANCE OF THE T-10 TEST CELL AT NAS, CUBI POINT		5. TYPE OF REPORT & PERIOD COVERED Not Final; Oct 1986-Sep 1987
		6. PERFORMING ORG. REPORT NUMBER
7. AUTHOR C.A. KODRES, E.E. COOPER AND P.L. STONE		8. CONTRACT OR GRANT NUMBER(s)
9. PERFORMING ORGANIZATION NAME AND ADDRESS NAVAL CIVIL ENGINEERING LABORATORY Port Hueneme, California 93043-5003		10. PROGRAM ELEMENT, PROJECT, TASK AREA & WORK UNIT NUMBERS 63725N; Y0995-01; Y0995-01-007
11. CONTROLLING OFFICE NAME AND ADDRESS Naval Facilities Engineering Command Alexandria, VA 22332-2300		12. REPORT DATE September 1988
		13. NUMBER OF PAGES 140
14. MONITORING AGENCY NAME & ADDRESS (if different from Controlling Office)		15. SECURITY CLASS. (of this report)
		15a. DECLASSIFICATION DOWNGRADING SCHEDULE
16. DISTRIBUTION STATEMENT (of this Report) Approved for public release; distribution unlimited.		
17. DISTRIBUTION STATEMENT (of the abstract entered in Block 20, if different from Report)		
18. SUPPLEMENTARY NOTES		
19. KEY WORDS (Continue on reverse side if necessary and identify by block number) Aviation Engine Test Cell; Jet Engine Testing; Jet Engine Exhaust Flow; Turbulent Jets; Compressible Jets. (ngm) ←		
20. ABSTRACT (Continue on reverse side if necessary and identify by block number) This report presents results of aerodynamic and thermodynamic tests conducted on the first standard Navy air-cooled T-10 test cell. Objectives of the tests were to: (1) Determine if aerodynamic and thermodynamic design objectives for the standard T-10 test cells were met; (2) Obtain data for comparing analytical predictions and validating analytical modeling techni- ques, and (3) Obtain baseline data of cell performance for use in case of future changes in design or operations. Data were obtained during runs with		

DD FORM 1473 EDITION OF NOV 65 IS OBSOLETE

Unclassified

SECURITY CLASSIFICATION OF THIS PAGE (When Data Entered)

(1)

Unclassified

SECURITY CLASSIFICATION OF THIS PAGE (When Data Entered)

20. Continued

the following engines: a J52-P-8B, a J52-P-408, a TF41-A-2C, a F404-GE-400, and a TF30-P-414. All engines were run at idle, 85%, and military power, and the engines equipped with afterburner (the TF30 and F404) were run at zone 5. Measurements included: Intake flow velocities and flow rates, cell pressure, flow velocities approaching and around the engine, exhaust section surface temperatures, and exhaust jet temperatures and velocities. Results showed that all aerothermal design objectives were met with one exception: noise measured 250 feet aft of the engine exceeded 85 db. Augmentation ratios ranged from 6.0 to 13.5. Air flow approaching the engine was smooth with velocities less than 40 ft/sec. Cell depression was less than 1.0 inch H₂O. Flow in the exhaust augments tube was symmetrical and indicated smooth mixing of jet exhaust with cooling air. Maximum temperature of the augments wall was about 800 F with the TF30 engine.

Library Card

Naval Civil Engineering Laboratory
EXPERIMENTAL EXAMINATION OF THE AEROTHERMAL
PERFORMANCE OF THE T-10 TEST CELL AT NAS, CUBI
POINT (Not Final) by C.A. Kodres, E.E. Cooper,
and P.L. Stone
TN-1788 140 pp illus Sep 1988 Unclassified

1. Turbulent Jets 2. Compressible Jets I. Y0995-01-007

This report presents results of aerodynamic and thermodynamic tests conducted on the first standard Navy air-cooled T-10 test cell. Objectives of the tests were to: (1) Determine if aerodynamic and thermodynamic design objectives for the standard T-10 test cells were met; (2) Obtain data for comparing analytical predictions and validating analytical modeling techniques, and (3) Obtain baseline data of cell performance for use in case of future changes in design or operations. Data were obtained during runs with the following engines: a J52-P-8B, a J52-P-408, a TF41-A-2C, a F404-GE-400, and a TF30-P-414. All engines were run at idle, 85%, and military power, and the engines equipped with afterburner (the TF30 and F404) were run at zone 5. Measurements included: Intake flow velocities and flow rates, cell pressure, flow velocities approaching and around the engine, exhaust section surface temperatures, and exhaust jet temperatures and velocities. Results showed that all aerothermal design objectives were met with one exception: noise measured 250 feet aft of the engine exceeded 85 db.

Unclassified

SECURITY CLASSIFICATION OF THIS PAGE (When Data Entered)

CONTENTS

	Page
INTRODUCTION	1
STANDARD NAVY T-10 TEST CELL	1
DESCRIPTION OF TESTS	2
RESULTS	3
Total Airflow	3
Cell Depression	4
Augmenter Tube Gas Velocities	4
Augmenter Tube Wall Temperatures	4
Augmenter Tube Gas Temperatures	5
Augmenter Tube Gas Pressures	5
Augmenter Tube Transient Temperature Behavior	5
Test Bay Air Velocities.	5
T-10 TEST CELL AEROTHERMAL PERFORMANCE SUMMARY.	6
General	6
Cell Depression.	6
Air Velocities At The Jet Intake	6
Test Bay Air Velocities	7
Augmenter Tube Wall Temperatures	7
Augmenter Tube Pressure	7
COMMENTS	7
APPENDIXES	
A - Description of the Standard Navy Test Cell at NAS Cubi Point	A-1
B - Instrumentation	B-1
C - Accuracy of the Data	C-1
D - Data Reduction Techniques	D-1
E - Velocity Contour Plots	E-1
F - Cubi Point Weather Summaries	F-1



Accession For	
NTIC GRA&I	<input checked="" type="checkbox"/>
DTIC TAB	<input type="checkbox"/>
Unannounced	<input type="checkbox"/>
Justification	
By	
Distribution/	
Availability Codes	
Dist	Avail and/or Special
A-1	

INTRODUCTION

This report presents results of the aerodynamic and thermodynamic testing conducted at the Naval Air Station (NAS) Cubi Point, Republic of the Philippines, on the standard Navy air-cooled T-10 test cell. The tests were conducted from 9 November through 20 November 1986. Figures 1 and 2 are front and rear views of the test cell.

The objectives of the aerothermal testing were to: (1) Determine if aerodynamic and thermodynamic design objectives for the standard T-10 test cells were met; (2) Obtain data for comparing analytical predictions and validating analytical modeling techniques; and (3) Obtain baseline data of cell performance for use in case of future changes in design or operations.

The test cell at NAS Cubi Point is the first standard T-10 test cell, and will be replicated at several Navy and Marine Corps bases. This was the first opportunity to measure the performance of the standard T-10 design and to determine if design changes should be made to the standard configuration. The variety of engines maintained at NAS Cubi Point also resulted in the unique opportunity to measure cell performance with most engines to be run in the T-10 test cells. Two engines not available for the test reported here were the F402, which is not maintained at NAS Cubi Point, and the F110, which was not in production at the time of these tests.

The aerothermal testing was done concurrently with other test programs conducted at the completion of construction of test cells. The test programs were: Correlation test with "known performance engines" conducted by the Naval Air Propulsion Center and the Naval Aviation Engine Support Unit; control room equipment checkout and calibration conducted by the Naval Air Engineering Center; and measurement of internal and external noise levels conducted by the Naval Ocean Systems Center. Each agency will report separately on its test program. In addition, the Naval Civil Engineering Laboratory (NCEL) measured vibrations of the structure at several points, and ultraviolet and infrared emissions from the engines and exhaust plumes. NCEL will report its vibration and radiant emissions data separately.

STANDARD NAVY T-10 TEST CELL

Figure 3 identifies the main components of the T-10 test cell at NAS Cubi Point and indicates the paths of flows through the facility.

The T-10 test cell is a "dry augementer" cell. This means that the cell is designed to draw in large amounts of air through the intakes to mix with and cool the exhaust from the engine. The test cell acts as a large eductor. Momentum of the engine exhaust "pumps" or "drags" the needed air through the cell. Exhaust gases leave the engine as a high

velocity, relatively small diameter, jet directed into the augmentor tube, and surrounded by a layer of slower ambient air. A turbulent shear layer develops around the jet and pulls the ambient air along with the jet, i.e., the eductor effect. In pulling ambient air down the augmentor tube with the jet, a reduced pressure is created in the test bay, forcing air to be drawn in through the primary and secondary intakes to replace the air pulled down the tube.

Appendix A describes the T-10 test cell in detail.

DESCRIPTION OF TESTS

Aerothermal measurements were made at NAS Cubi Point during runs with the following engines: a J52-P-8B, a J52-P-408, a TF41-A-2C, an F404-GE-400, and a TF30-P-414. Data were taken with each engine at idle, 85%, and military (Mil) power settings. For the engines equipped with an afterburner (the TF30 and F404), data were also taken at zone 5. A complete set of data was taken with the T-10 test cell in the "as-built" configuration, specifically, with the throttle plate installed. The throttle plate is a 2-foot extension of the converging section of the augmentor. The throttle plate was included on the theory that it would delay impingement of exhaust flow on the augmentor wall. To check the theory, the throttle plate was removed and tests were repeated with the TF41, TF30, and F404 engines. Augmentation rates were slightly higher without the throttle plate, but the effects of the throttle plate were so small that reinstallation was not recommended.

The tests included measurements and observations of flow parameters and temperatures throughout the test cell. The locations and types of measurements of the tests were:

Intakes

- Primary Intake. Velocity and mass flow rate distribution at the top of the primary intake baffles.
- Secondary Intake. Velocity and mass flow rate distribution at the bottom of the secondary intake baffles.

Test Bay

- Velocity measurements up to 13 feet high at various positions in the test bay.
- Cell depression.
- Qualitative, overall flow patterns throughout the test bay.
- Air temperature.

Augmenter

- Velocity distribution and mass flow rate of the jet engine exhaust/augmentation air at 30 feet aft of the secondary intake.
- Velocity distribution and mass flow rate of the jet engine exhaust/augmentation air at 60 feet aft of the secondary intake.
- Temperature distribution of the jet engine exhaust/augmentation air at 30 feet and at 60 feet aft of the secondary intake.
- Temperature distribution of the perforated plate surfaces circumferentially and down the length of the augmenter tube.
- Static pressure distribution down the length of the augmenter tube.

Stack Ramp

- Temperature distribution on the stack ramp.

The instrumentation and the accuracy of the results are discussed in Appendixes B and C, respectively.

RESULTS

Whenever possible, duplicate runs were recorded. Several alternatives were often available when choosing the data to be used in describing the behavior of a particular variable. Plots were generated from the data set that best describes the pertinent variable, usually the data set with the least inoperative instrumentation. It follows that the data does not always match exactly from plot to plot.

Most of the plots summarize steady state values, averages of data recorded every second for 30 seconds up to a minute. A TF30 transient from Mil to A/B and back down is included, however. On the plots, the data are shown as a symbol: a circle, cross, triangle, etc. A line is faired through appropriate data to better illustrate overall trends.

The techniques used to record and reduce the data are explained in Appendix D.

Total Airflow

The total mass flow through the test cell was determined by measuring and adding airflows through the primary and secondary inlets. The procedures employed are discussed in detail in Appendix B. Major assumptions include incompressibility and symmetry.

Table 1 summarizes NAS Cubi Point T-10 test cell airflows measured during correlation tests. Augmentation ratio, a common indicator of aerothermal performance, is defined as:

$$\text{aug ratio} \equiv (\text{inlet flow} - \text{engine flow})/\text{engine flow}$$

Nearly all recorded runs are included; note the repeatability from run to run.

Cell Depression

Cell depression is defined as the static pressure inside the test bay, relative to ambient. It is always a negative value, and inches of water is used as the unit of measurement. Normally the (-) sign is omitted; the word 'depression' would suggest a negative value, regardless. For these tests, cell depression was measured on the side wall outside the control room.

Table 2 summarizes cell depression measured during the correlation tests. Again, nearly all runs are included. Here, however, the repeatability is poor. Figure 4 shows cell depression plotted as a function of total inlet airflow. Scatter in the data is even more apparent. (Fluctuations in cell depression will be discussed later.) The dashed line through the data on Figure 4 is a curve fit based on the assumption of incompressible flow,

$$\text{velocity} \propto [\text{pressure difference/density}]^{1/2}$$

$$\text{mass flow} \propto [\text{pressure difference} \times \text{density}]^{1/2}$$

or, combining the density and the constant of proportionality,

$$\text{inlet airflow} = 2390 [\text{cell depression}]^{1/2}$$

Augmenter Tube Gas Velocities

Figures 5 through 18 show gas velocities calculated from pressures measured with pitot tubes mounted on the two racks in the augmenter tube. Velocities are parallel to the tube centerline. Two profiles are shown on each figure. The first, labelled "vertical tube diameter," was developed from pressures measured along the vertical member of the racks (see Figure B-7). It is, therefore, a velocity profile through the center of the augmenter tube from top to bottom. The second profile, labelled "horizontal tube diameter," was developed from pressures measured along the horizontal member of each of the racks.

Gas velocities measured during several runs are also plotted as contours in Appendix E.

Augmenter Tube Wall Temperatures

Wall surface (skin) temperatures were measured with thermocouples permanently mounted around the circumference of the tube at three axial locations. These temperatures are plotted as Figures 19 through 22. Figure 23 shows wall temperatures with engine alignment (yaw) as a parameter.

Augmenter Tube Gas Temperatures

Temperature of the gases as they pass through the augmenter tube are plotted as Figures 24 through 37. Temperature profiles in both the vertical and horizontal directions are shown together, in a manner analogous to that used for the gas velocities.

Also included on these figures are the temperatures of the surface of the exhaust ramp. These are metal temperatures, not gas temperatures, but they closely approximate the temperatures of the gases as they strike the ramp. Although the thermocouples were mounted on the surface of a 45-degree plane, the data were plotted as if the plane was vertical; i.e., the ramp "diameter" in the vertical direction was multiplied by sine 45 degrees. Thus, the ramp temperatures compare sequentially with the two rack temperatures.

Figure 38 is a plot of augmenter tube gas temperatures with misalignment (yaw) as a parameter.

Augmenter Tube Gas Pressures

Static pressures of the gases passing through the tube were measured every 10 feet along the sidewall; gas pressures were also measured at the top and bottom of the two racks. These pressures are summarized in Figures 39 through 44. Pressures are plotted relative to ambient. It is assumed that cell depression is representative of the static pressure at the inlet to the augmenter tube.

Augmenter Tube Transient Temperature Behavior

Data were recorded continuously during a TF30 transition from military (Mil) power to afterburner power (A/B) and back down to Mil. Temperatures recorded during this run are plotted against time on Figures 45a, b, c.

Figure 45a describes aerothermal behavior at the forward instrumentation rack, i.e., in a vertical plane about 30 feet into the tube. The temporal variations of gas temperatures at the tube centerline and near the wall are plotted alongside tube wall metal temperatures measured at the same location. Figure 45b shows these same temperatures at the rear instrumentation rack, i.e., in a vertical plane 60 feet into the tube. The temperature in the center of the ramp is also plotted on Figure 45b, an approximate indication of tube centerline gas temperature at the tube exit. Figure 45c shows the variation of the tube wall metal temperature at different circumferential locations both 30 and 60 feet into the augmenter tube.

To keep from cluttering the plots, not all data points are shown.

Test Bay Air Velocities

Figures 46 through 64 are schematics of the test bay portion of the test cell. The top schematic shows a side view; the bottom schematic shows the top view. A series of vectors has been drawn on each of these figures. The length of these vectors is proportional to the air velocity

measured with the anemometers. The magnitude of the air velocity in feet per second is printed alongside each vector. Locations are defined by the tail of the "arrow" in the side view and the "cross" in the top view. Velocities are parallel to the tube centerline.

T-10 TEST CELL AEROTHERMAL PERFORMANCE SUMMARY

There were no aerothermal problems observed and none are anticipated for any of the engines that were tested. Except for excessive noise from the stack being propagated directly aft, all design objectives set for the T-10 test cell were met. (Noise levels will be discussed in a separate report.)

General

The throttle plate decreases augmentation ratio by about 10%. Its effect on test cell performance appears to be negligible.

Augmentation ratios at military and afterburner power settings ranged from 6.3 to 13.4. The engine exhaust flow and the augmentation air mixed effectively without premature attachment to the wall. About 60% of the intake flow was drawn in through the primary intake and 40% through the secondary. This airflow split remained approximately constant regardless of power setting, engine type, or with or without the throttle plate.

Based on one incident with the J52, the test cell is sensitive to engine alignment. (See comments that follow.)

Nearly all maximum pressures, temperatures, and velocities occurred while testing the TF30 at A/B. Maximum mass flow rates were generated by the TF41.

Cell Depression

The maximum cell depression recorded was about 1.0 inches of water measured near the test bay wall just outside the control room. The correlation team observed a maximum cell depression of 0.75 inches of water* (see comments that follow).

Air Velocities at the Jet Intake

The maximum engine intake velocity observed was 36 ft/sec, near the center of the nacelle about 10 feet directly in front of the engine. This was as close as the anemometers were placed.

*NAPC LR-87-8. Final Report: Jet engine test cell correlation, Naval Air Station, Cubi Point, Republic of the Philippines, 31 Mar 1987.

Test Bay Air Velocities

Air velocity reached a maximum 40 ft/sec inside the test bay. Velocities of about this magnitude were observed at several locations: in front of the primary air inlet, down the side of the test bay, and over the top of the engine.

The flow in the test bay was steady, evenly distributed, and free of eddies or recirculation. There was no indication of any hot flow reversal, i.e., engine exhaust entering the test bay.

Augmenter Tube Wall Temperatures

The highest tube wall (skin) temperature observed was 580 °F reached during A/B testing of the TF30. As shown on Figure 20, this maximum occurs very near the end of the tube. At military power, the wall temperature reached a maximum of 180 °F. Ramp temperatures reached about 470 and 180 °F at A/B and military power, respectively. Durations of the afterburner runs were only about 30 seconds, however, and temperatures were still rising. For prolonged afterburner runs with the TF30 engine, it is estimated that temperatures on the augmenter wall and stack ramp would reach 750 to 800 °F.

Augmenter tube walls were slightly cooler with the throttle plate removed, perhaps 25 degrees cooler when testing the TF30 at A/B.

Augmenter Tube Pressures

The pressure difference across the tube wall, outside to inside, reached about 5.5 inches of water.

COMMENTS

Weather did not influence the tests. Weather conditions encountered during the correlation tests are summarized in Appendix F.

The static pressure measured in the test bay varied by as much as 100% between the probe located outside the control room and the one beneath the secondary inlet. Location of the probe used to measure cell depression, therefore, can be expected to strongly influence the pressures encountered. Cell depression, even at the same location, fluctuated greatly, particularly at high power settings. An examination of Table C-3 is enlightening. Instantaneous values of cell depression are probably meaningless as indicators of test cell performance.

The jet was skewed slightly upward and to the left. This has no apparent effect on the engine performance, nor is there significant effect on the structural temperatures or other design parameters. However, there is academic interest in determining whether the cause is simply due to engine misalignment, or whether there is some secondary flow effect, such as spin of the exhaust as it leaves the nozzle, which should be included in analytical flow models.

During one of the early J52 runs, the test stand was misaligned. The misalignment was detected during the subsequent runs and corrected. This provided an opportunity to study the effects of engine alignment on the aerothermal behavior of the augmenter tube. The difference in yaw of the test engine between the aligned and misaligned runs was determined

by measuring the distance between the "feet" of the test stand and the grate located along the centerline of the test bay. A yaw of 2.3 degrees to the left (when standing in the augmeter and facing the engine) was measured for the misaligned runs; this same angle was 1.0-degrees after the engine was aligned. Only the difference is pertinent; a 1.0-degree yaw relative to the grate does not necessarily represent perfect alignment with the centerline of the augmeter tube.

Alignment of the jet has a strong influence on augmeter tube flow characteristics, stronger than geometrical considerations would suggest. Figures 23, 38, and E-1a,b were developed to see how far the jet is displaced by a known misalignment of the engine. Figure 38 is particularly informative. It shows the center of the jet being shifted about 2.5 feet by the extra 1.3 degree misalignment when measured 30 feet down the augmeter tube. Trigonometry predicts a 1.1-foot radial deflection.

Table 1. NAS Cubi Point T-10 Test Cell Air Flow Summary

Engine	Power Setting	With Throttle Plate			Without Throttle Plate			
		Primary Inlet (lb/sec)	Secondary Inlet (lb/sec)	Aug Ratio	Primary Inlet (lb/sec)	Secondary Inlet (lb/sec)	Aug Ratio	
J52-P-8B	Mil	900	625	10.1				
		840	790	10.9				
		910	750	11.1				
		920	700	10.8				
	85%	775	570					
		680	490					
	Idle	300	210					
		295	190					
	J52-P-408	Mil	1020	850	11.8			
			1010	870	11.9			
1020			840	11.7				
85%		740	610					
		780	600					
Idle		310	230					
		330	230					
		325	230					
		310	220					
TF41-A-2C	Mil	1170	890	7.2	1240	990	7.8	
		1130	825	6.8	1235	935	7.6	
		1140	815	6.8	1235	890	7.4	
					1220	890	7.4	
	85%	730	580		800	650		
		245	205		320	240		
	Idle	280	190					
		270	210					
TF30-P-414A	A/B	1020	760	6.3	1160	880	7.1	
		1030	810	6.6	1150	910	7.2	
		1030	790	6.5	1140	910	7.2	
		1020	830	6.6	1155	880	7.1	
		1030	830	6.7	1135	875	7.0	
		1020	820	6.5	1170	880	7.2	
		1030	800	6.5				
		1040	830	6.7				
	Mil	1050	890	6.8	1200	945	7.6	
					1180	990	7.7	
	85%	640	550		720	580		
		300	210		340	240		
	Idle							

(Continued)

Table 1. (Continued)

Engine	Power Setting	With Throttle Plate			Without Throttle Plate		
		Primary Inlet (lb/sec)	Secondary Inlet (lb/sec)	Aug Ratio	Primary Inlet (lb/sec)	Secondary Inlet (lb/sec)	Aug Ratio
F404-GE-400	A/B	1000	870	12.3	1120	900	13.4
		1020	800	12.0	1100	870	13.1
		1005	855	12.3	1095	810	12.6
					1105	840	12.9
					1100	880	13.2
	Mil	990	820	11.9	1080	910	13.2
		1080	800	12.4	1030	860	12.5
		1000	810	11.9			
	85%	595	545		680	570	
		640	500		800	525	
	Idle	245	125				

Table 2. NAS Cubi Point T-10 Test Cell Depression Summary

Engine	Power Setting	With Throttle Plate		Without Throttle Plate	
		Total Inlet Airflow (lb/sec)	Cell Depression (in. water)	Total Inlet Airflow (lb/sec)	Cell Depression (in. water)
J52-P-8B	M11	1525	0.56		
		1630			
		1660	0.55		
	85% Idle	1345	0.15		
		510	0.040		
J52-P-408	M11	1870	0.52		
		1880	0.78		
		1860	0.83		
	85%	1350	0.39		
		1380	0.35		
		540	0.030		
	Idle	560	0.044		
		555	0.045		
		540	0.039		
TF41-A-2C	M11	2060	0.58	2230	0.84
		1955	0.72	2140	0.84
		1955	0.75	2125	0.82
				2110	0.82
	85% Idle	1310	0.31	1450	0.54
		450	0.031	560	0.0058
		470	0.039		
		480	0.038		
TF30 P-414A	A/B	1780	0.56	2040	0.53
		1840	0.72	2060	0.70
		1820	0.84	2050	0.53
		1850	0.59	2030	0.54
		1860	0.42	2010	
		1840	0.69	2050	1.00
		1830	0.69		
		1870			
	M11	1940	0.66	2145	0.64
				2170	0.74
	85%	1190	0.38	1300	0.26
		510	0.055	580	
	Idle				
F404-GE-400	A/B	1870		2020	
		1820		1970	
		1860		1905	0.24
	M11			1945	0.32
		1810		1980	0.46
		1880	0.74	1990	
	85% Idle				



Figure 1. Front view of Standard T-10 test cell at NAS Cubi Point.

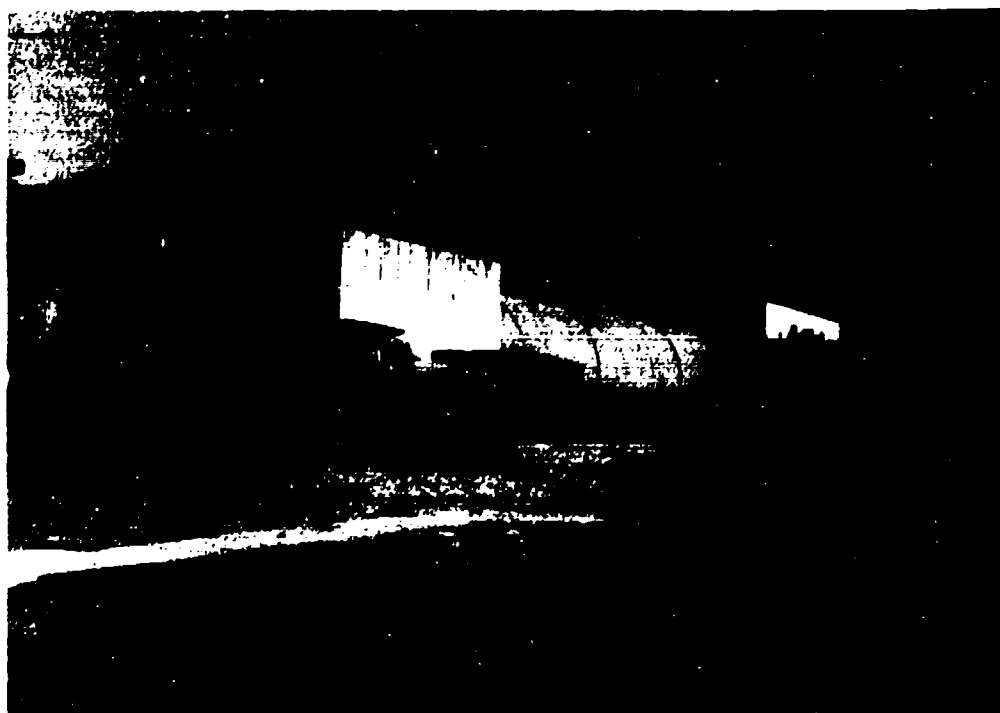


Figure 2. Rear view of Standard T-10 test cell at NAS Cubi Point.

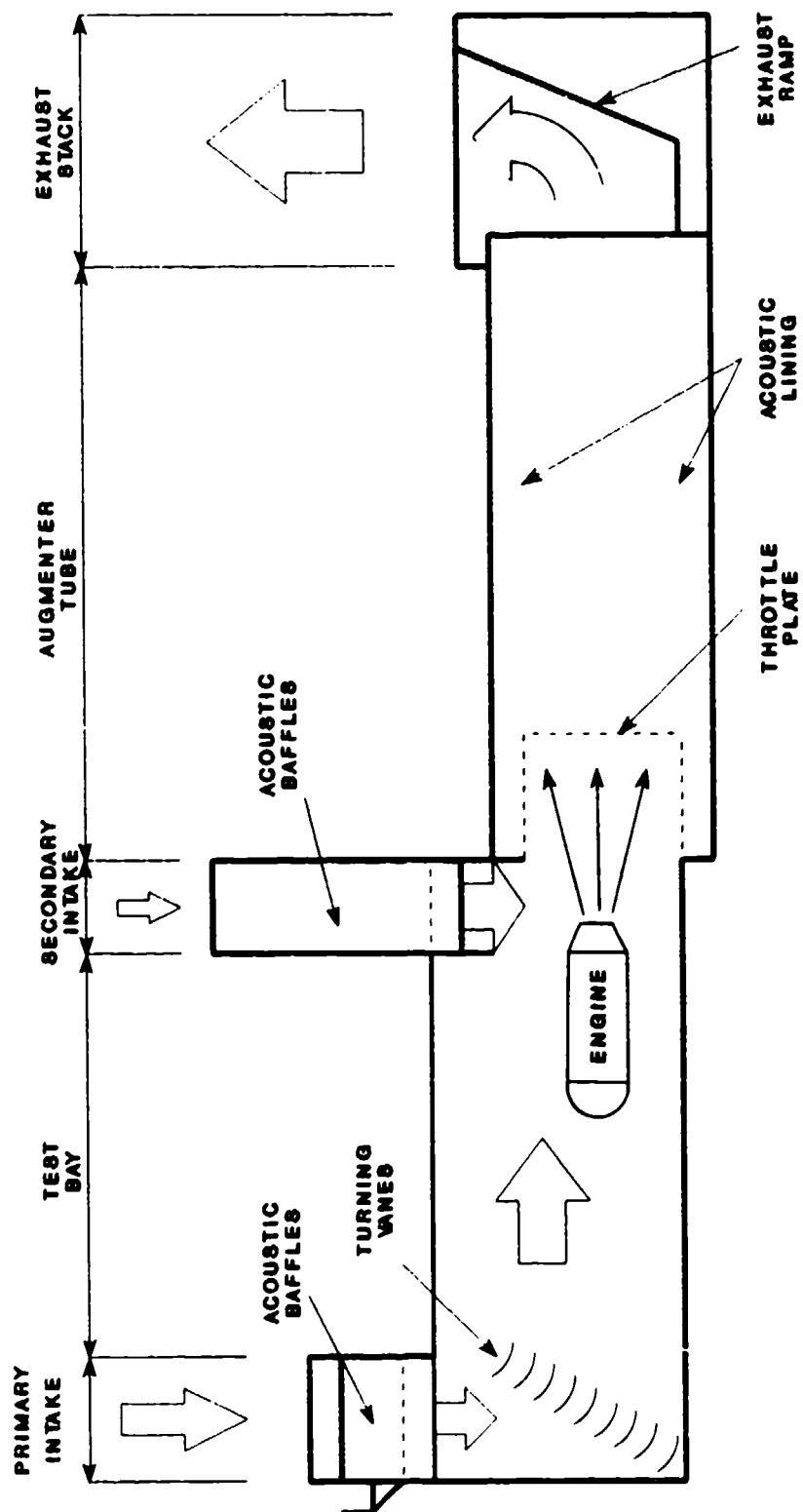


Figure 3. Components of the standard Navy test cell, NAS Cubi Point.

NOTES:

- (1) PRESSURES MEASURED ON TEST BAY WALL NEAR CONTROL ROOM
- (2) CELL DEPRESSION DEFINED AS ABSOLUTE VALUE OF RELATIVE PRESSURE INSIDE TEST BAY

- ◆ J52-P-88 WITH THROTTLE PLATE
- ⊕ J52-P-408 WITH THROTTLE PLATE
- ▲ TF41-A-2C WITH THROTTLE PLATE
- △ TF41-A-2C WITHOUT THROTTLE PLATE
- TF30-P-414A WITH THROTTLE PLATE
- TF30-P-414A WITHOUT THROTTLE PLATE
- F404-GE-400 WITH THROTTLE PLATE
- F404-GE-400 WITHOUT THROTTLE PLATE

$\text{INLET AIRFLOW} = 2390 \cdot \text{SQRT}(\text{CELL DEPRESSION})$

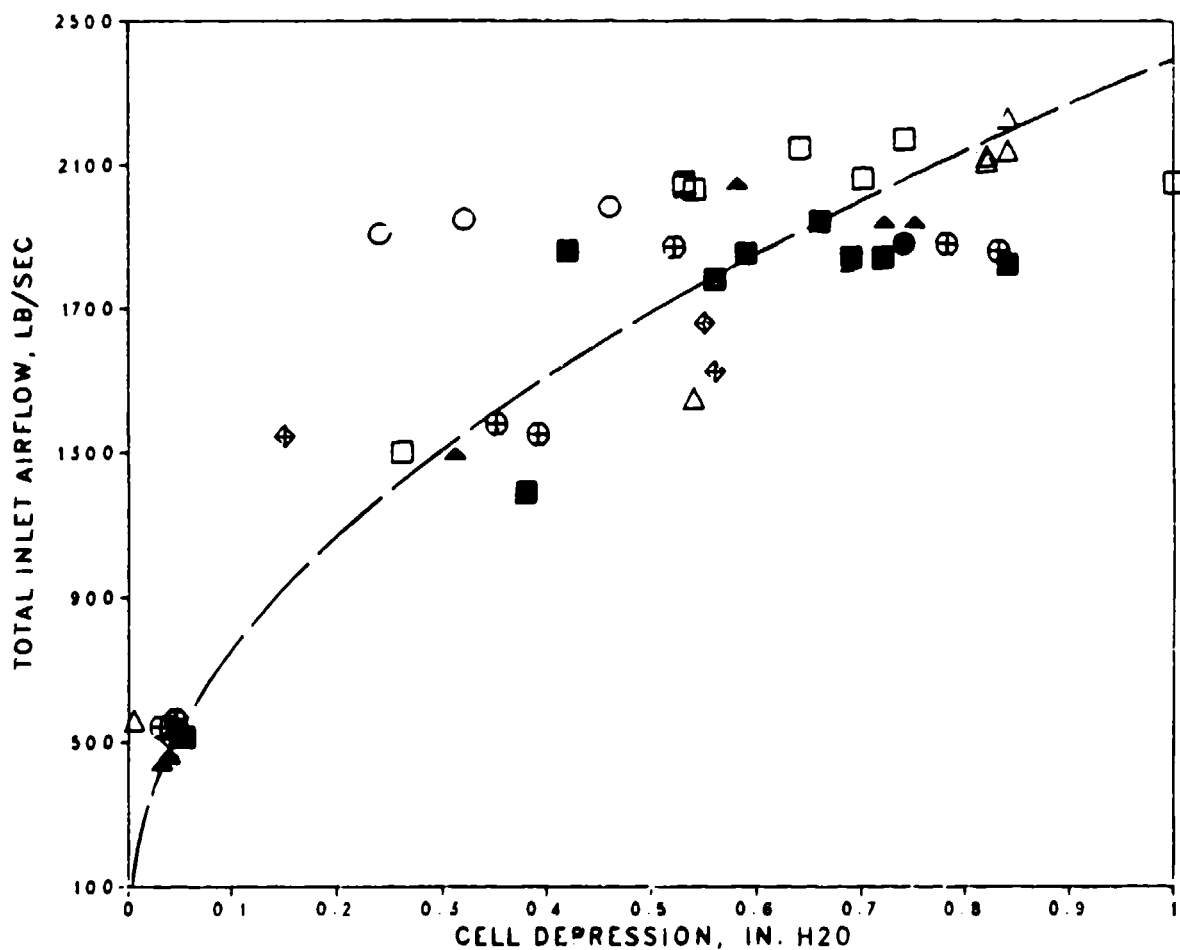


Figure 4. NAS Cubi Point T-10 test cell depression summary.

NOTE:
AVERAGED OVER 56 SECONDS

MEASURED 11/11/86

- ALONG VERTICAL TUBE DIAMETER
- ▲ ALONG HORIZONTAL TUBE DIAMETER

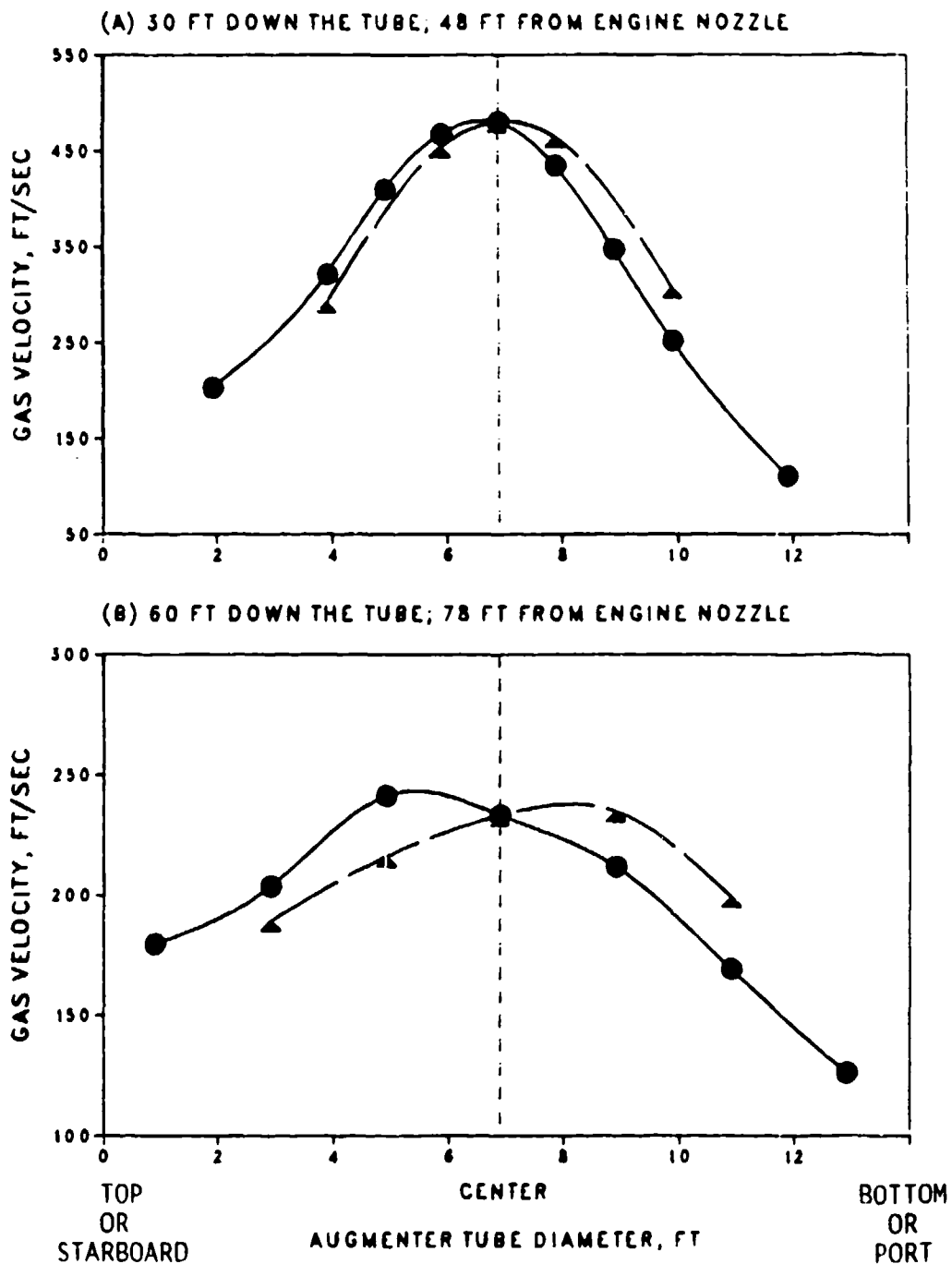


Figure 5. Velocity profiles across augmentor tube while testing J52-P-408 at Mil with throttle plate.

NOTE:
AVERAGED OVER 66-SECOND BURN

MEASURED 11/12/86

- ALONG VERTICAL TUBE DIAMETER
- ▲ ALONG HORIZONTAL TUBE DIAMETER

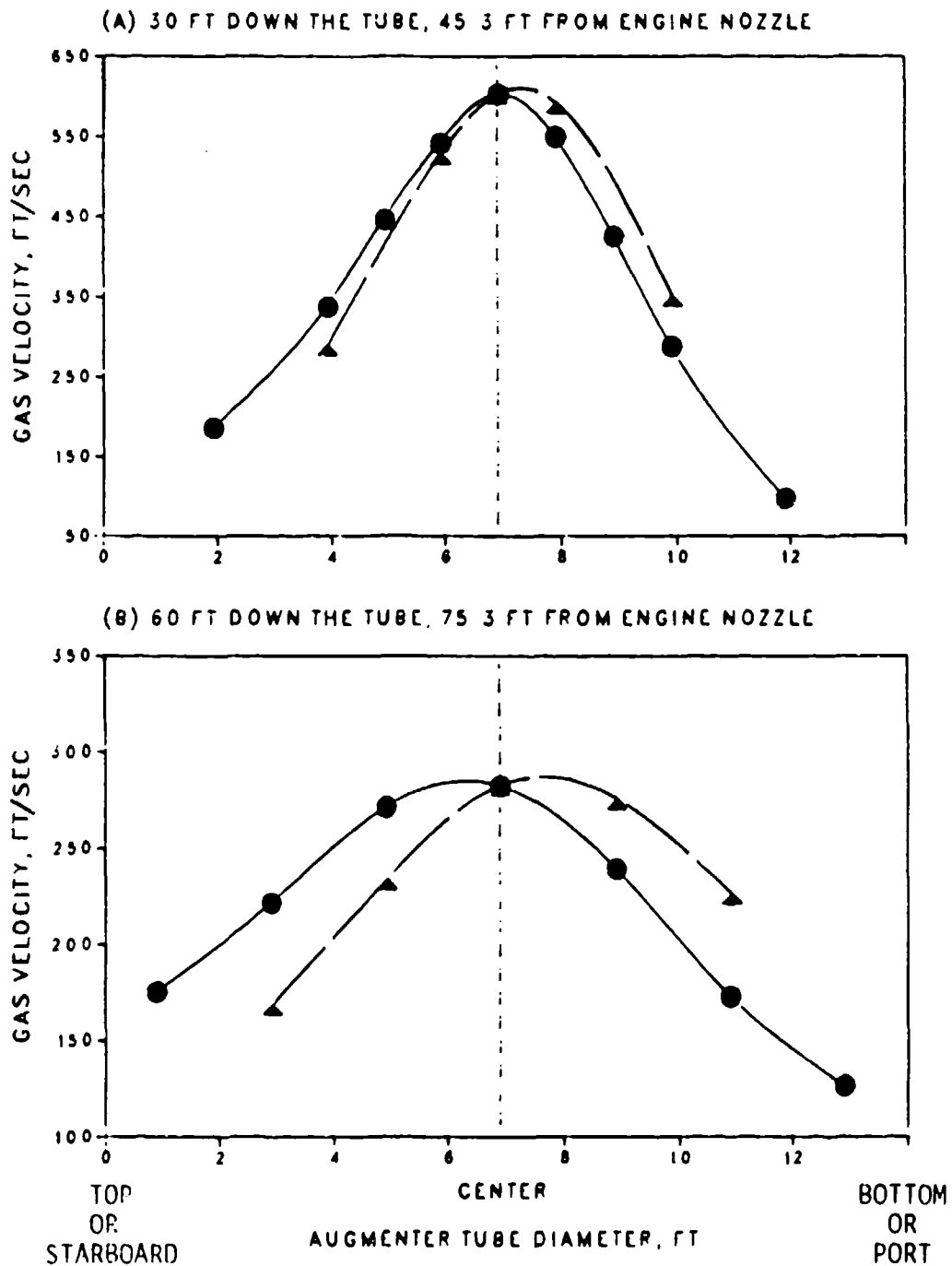


Figure 6. Velocity profiles across augmeter tube while testing TF41-A-2C at Mil with throttle plate.

NOTE:
AVERAGED OVER 55 SECONDS

MEASURED 11/12/86

- ALONG VERTICAL TUBE DIAMETER
- ▲ ALONG HORIZONTAL TUBE DIAMETER

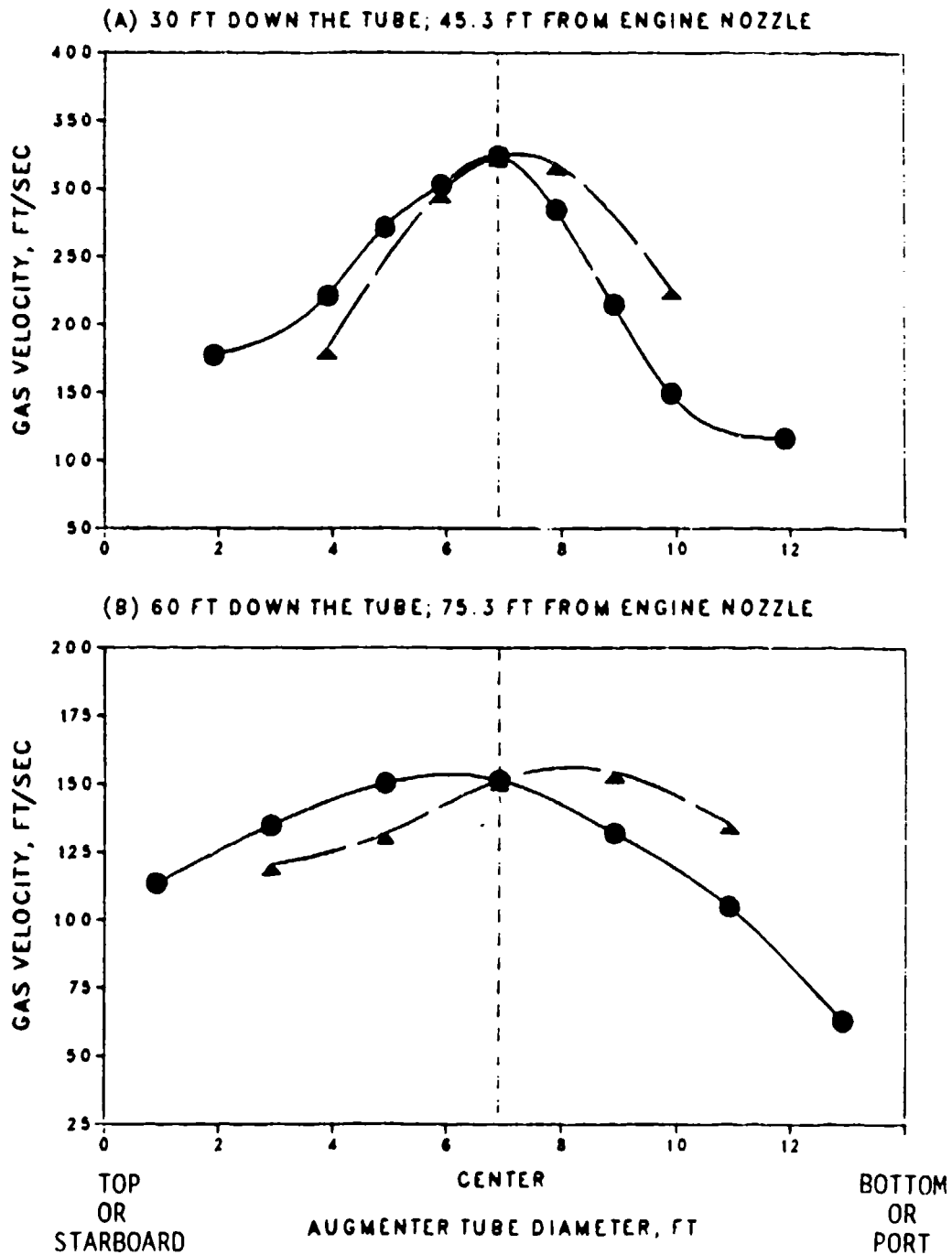


Figure 7. Velocity profiles across augmeter tube while testing TF41-A-2C at 85% with throttle plate.

NOTE:
AVERAGED OVER 60 SECONDS

MEASURED 11/12/86

- ALONG VERTICAL TUBE DIAMETER
- ▲ ALONG HORIZONTAL TUBE DIAMETER

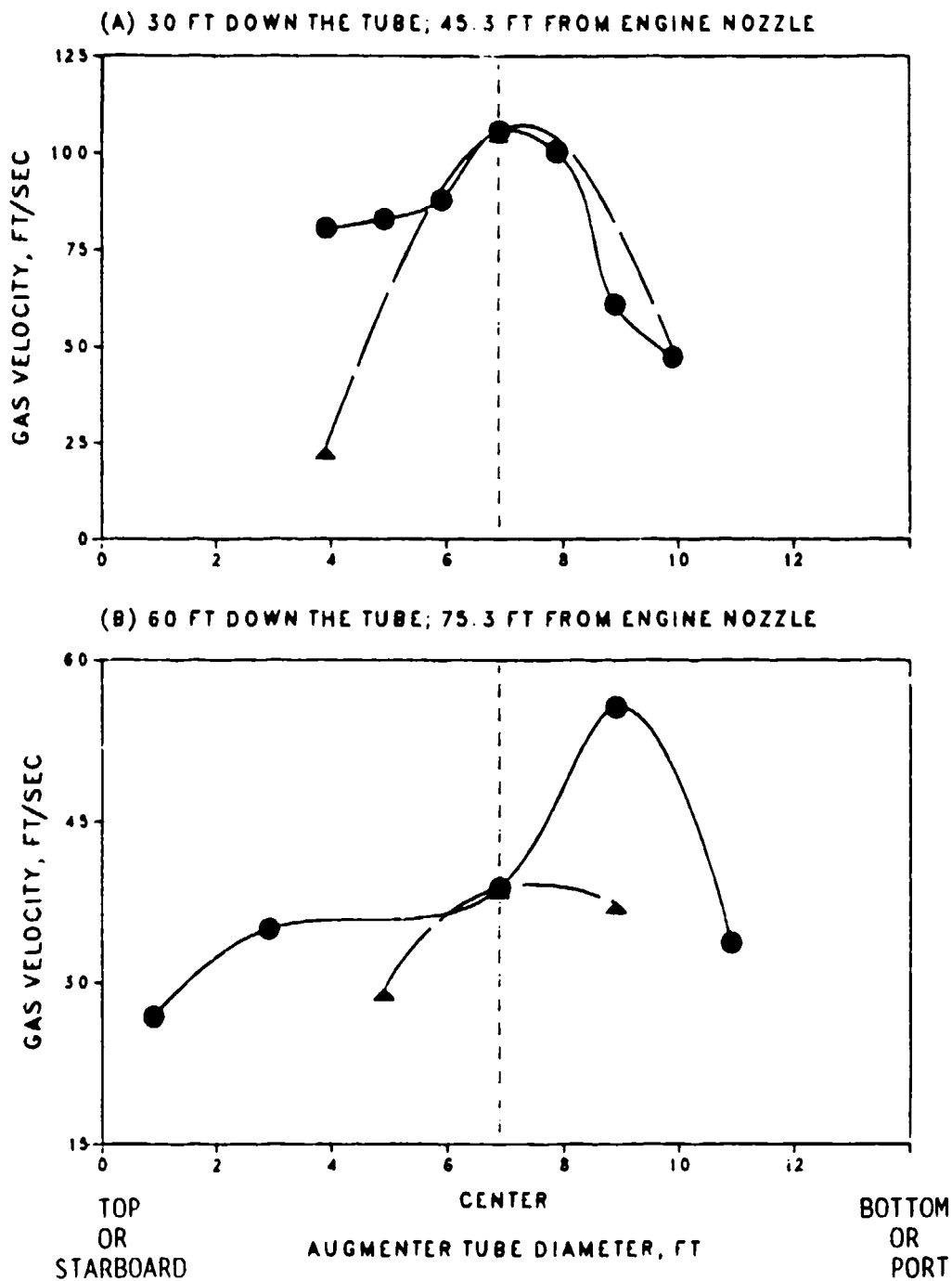


Figure 8. Velocity profiles across augmeter tube while testing TF4J-A-2C at idle with throttle plate.

NOTES:

(1) AVERAGED OVER A 30-SECOND BURN

(2) 60 FT DOWN THE TUBE; 75.3 FT FROM ENGINE NOZZLE

MEASURED 11/19/86

- ALONG VERTICAL TUBE DIAMETER
- ▲ ALONG HORIZONTAL TUBE DIAMETER

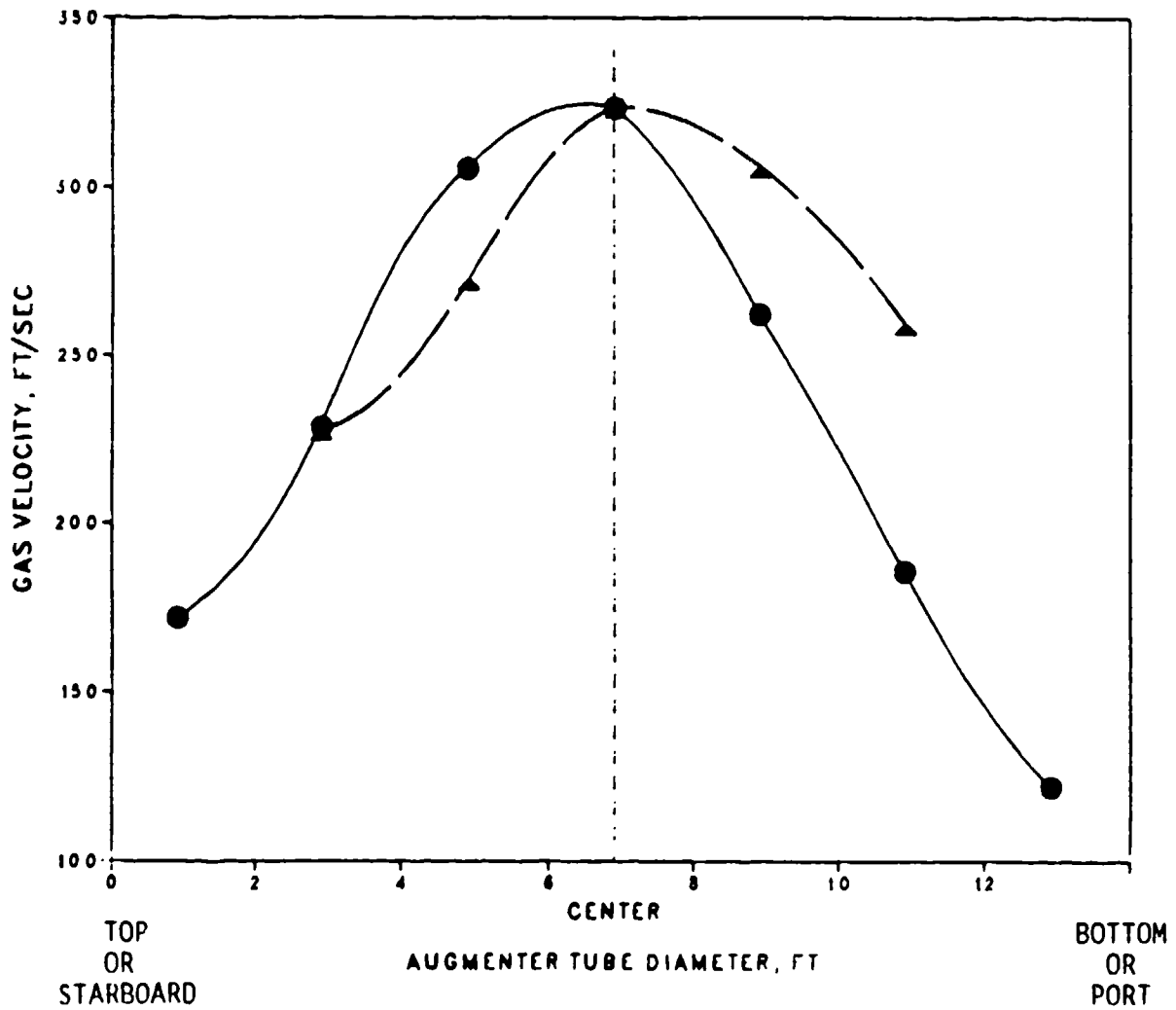


Figure 9. Velocity profile across augmenter tube while testing TF41-A-2C at M11 without throttle plate.

NOTES:

(1) 30-SECOND BURN

(2) NOZZLE AND TUBE ALIGNED TO WITHIN 2 INCHES

MEASURED 11/14/86

● ALONG VERTICAL TUBE DIAMETER

▲ ALONG HORIZONTAL TUBE DIAMETER

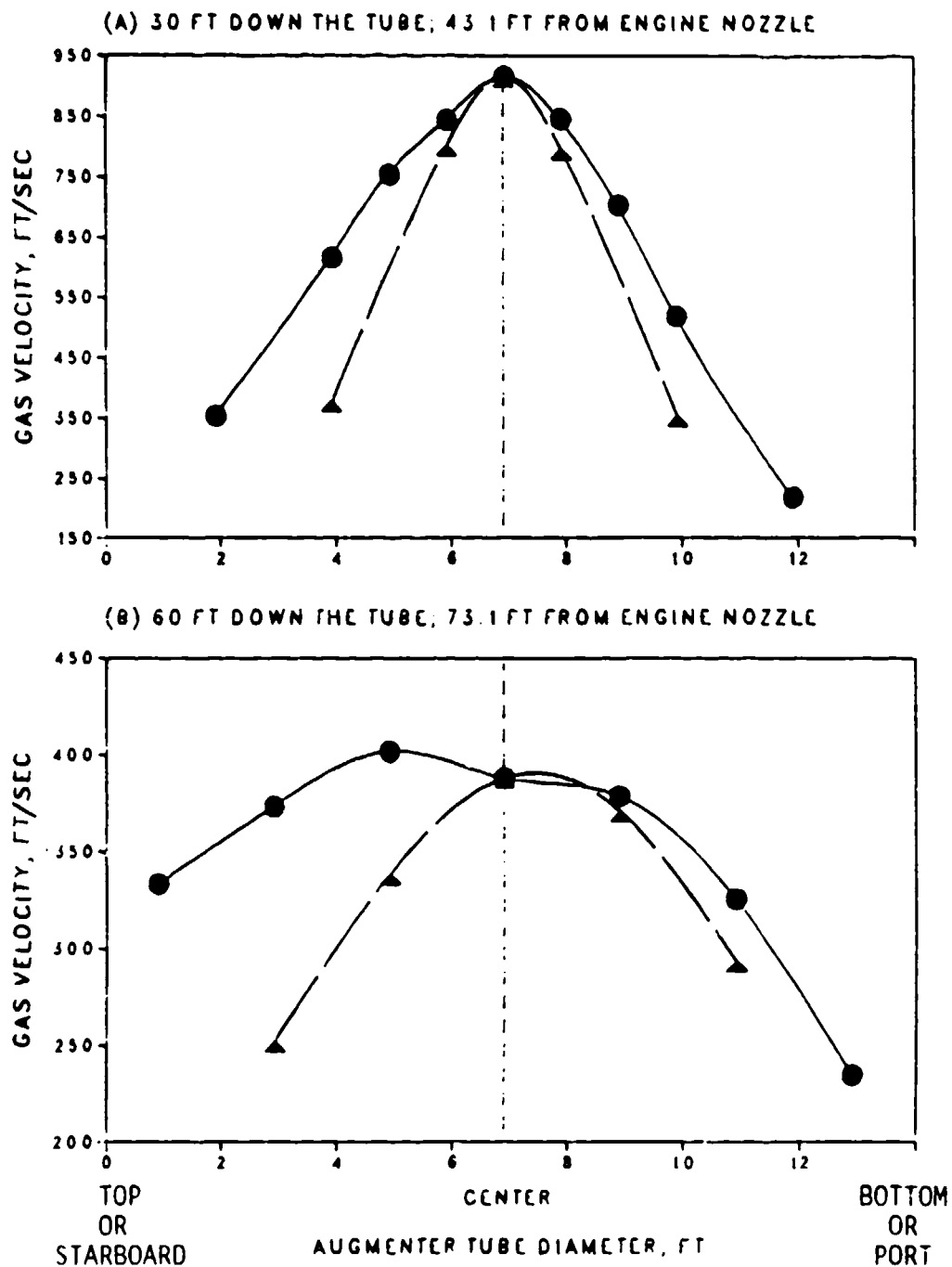


Figure 10. Velocity profiles across augmentor tube while testing TF30-P414A at A/B with throttle plate.

NOTE:
AVERAGED OVER 60 SECONDS

MEASURED 11/14/86

- ALONG VERTICAL TUBE DIAMETER
- ▲ ALONG HORIZONTAL TUBE DIAMETER

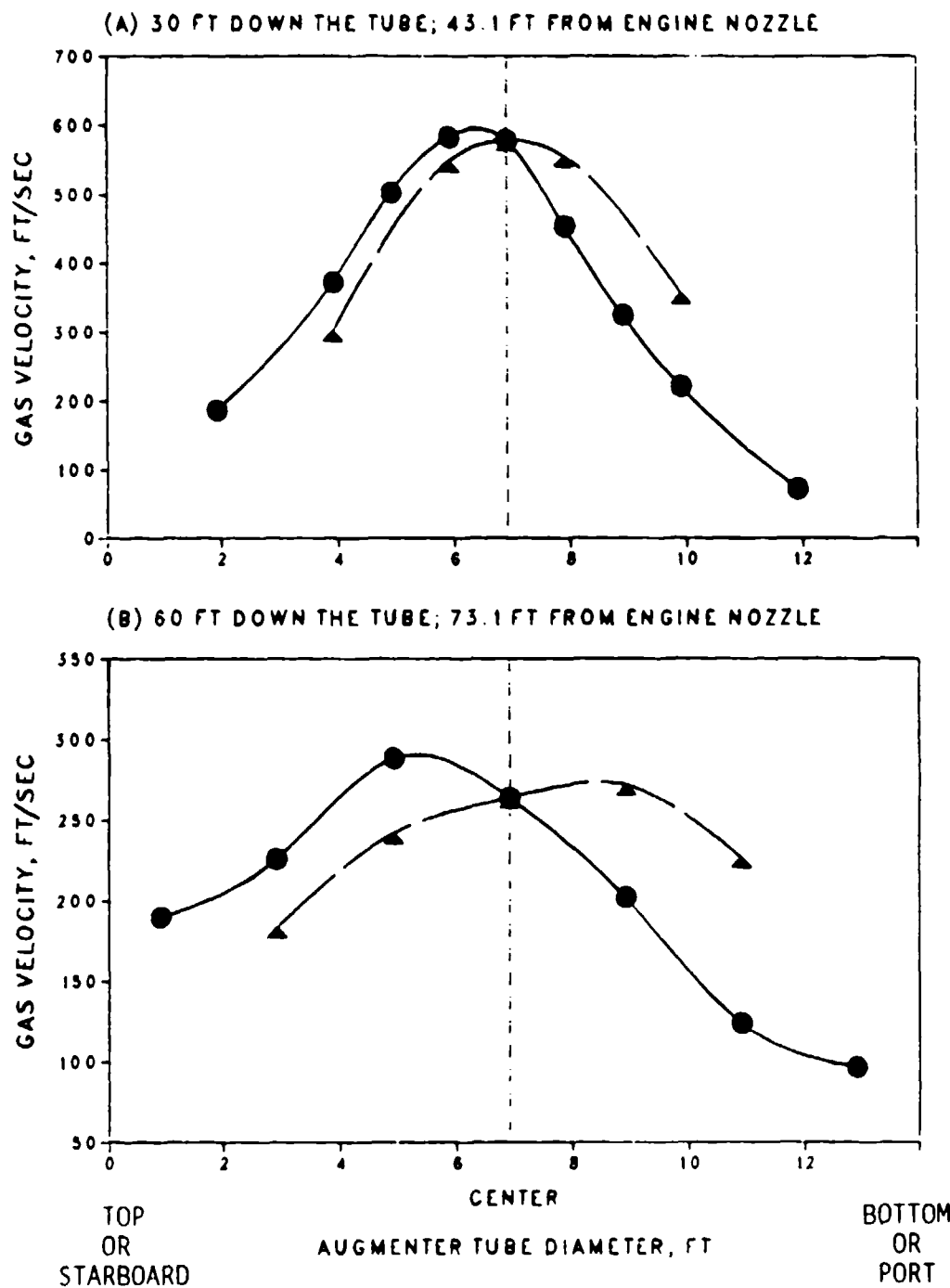


Figure 11. Velocity profiles across augmenter tube while testing TF30-P-414A at Mil with throttle plate.

NOTE:
AVERAGED OVER 65 SECONDS

MEASURED 11/14/86

- ALONG VERTICAL TUBE DIAMETER
- ▲ ALONG HORIZONTAL TUBE DIAMETER

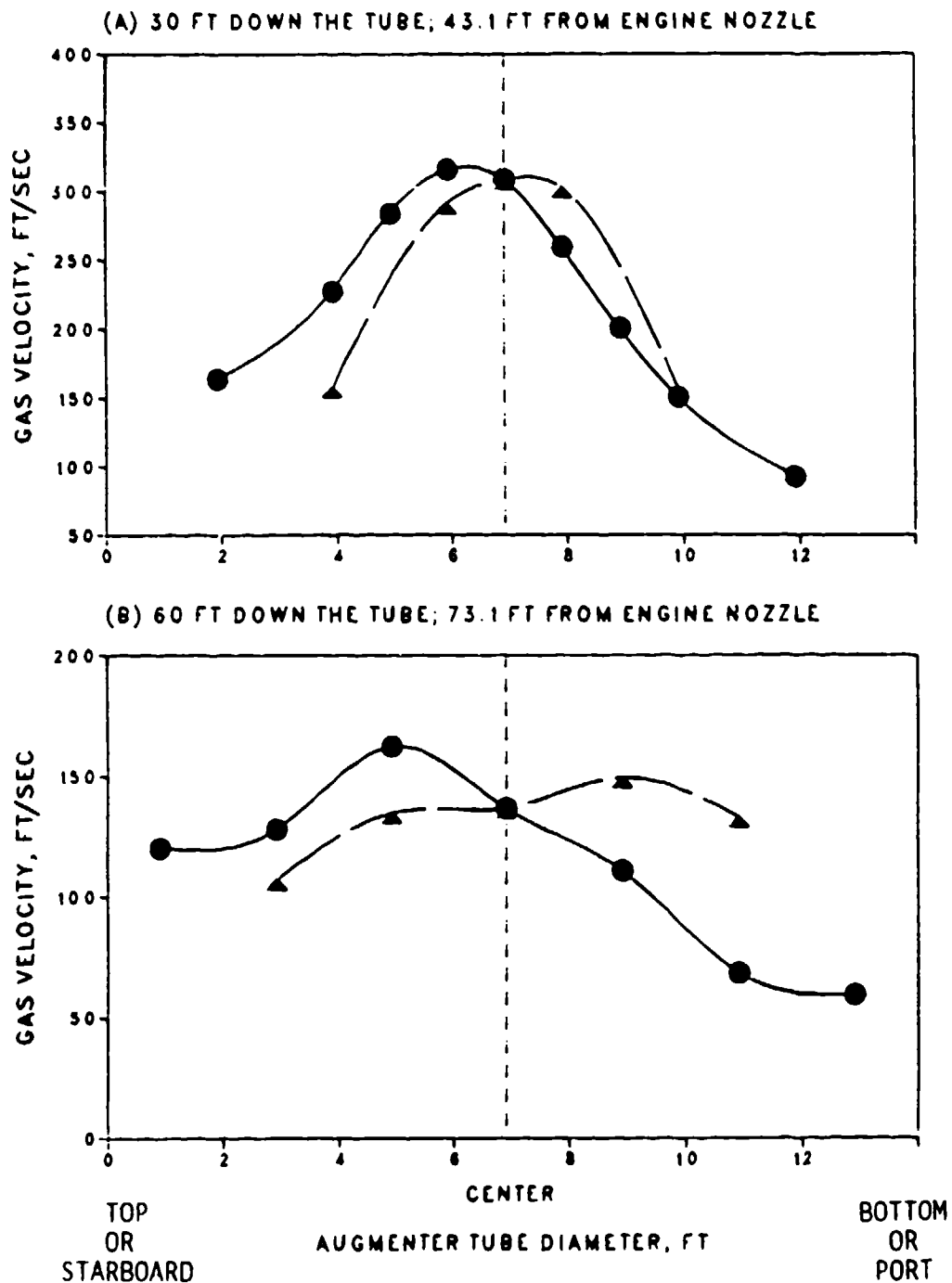


Figure 12. Velocity profiles across augmeter tube while testing TF30-P-414A at 85% with throttle plate.

NOTE:
AVERAGED OVER 60 SECONDS

MEASURED 11/14/86

- ALONG VERTICAL TUBE DIAMETER
- ▲ ALONG HORIZONTAL TUBE DIAMETER

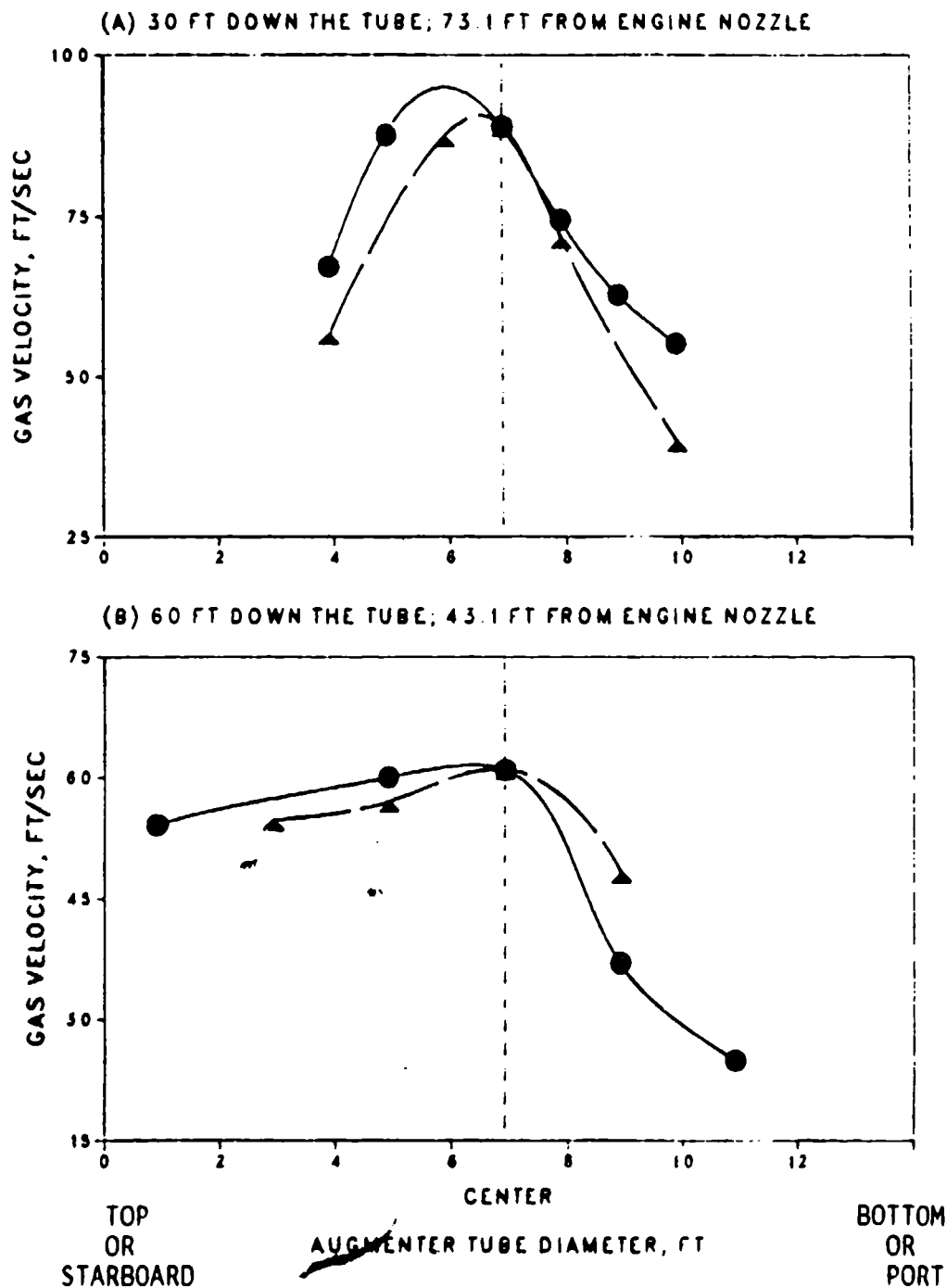


Figure 13. Velocity profiles across augmentor tube while testing TF30-P-414A at idle with throttle plate.

NOTES:

(1) AVERAGED OVER A 30-SECOND BURN

(2) 60 FT DOWN THE TUBE; 75.3 FT FROM ENGINE NOZZLE

MEASURED 11/18/86

- ALONG VERTICAL TUBE DIAMETER
- ▲ ALONG HORIZONTAL TUBE DIAMETER

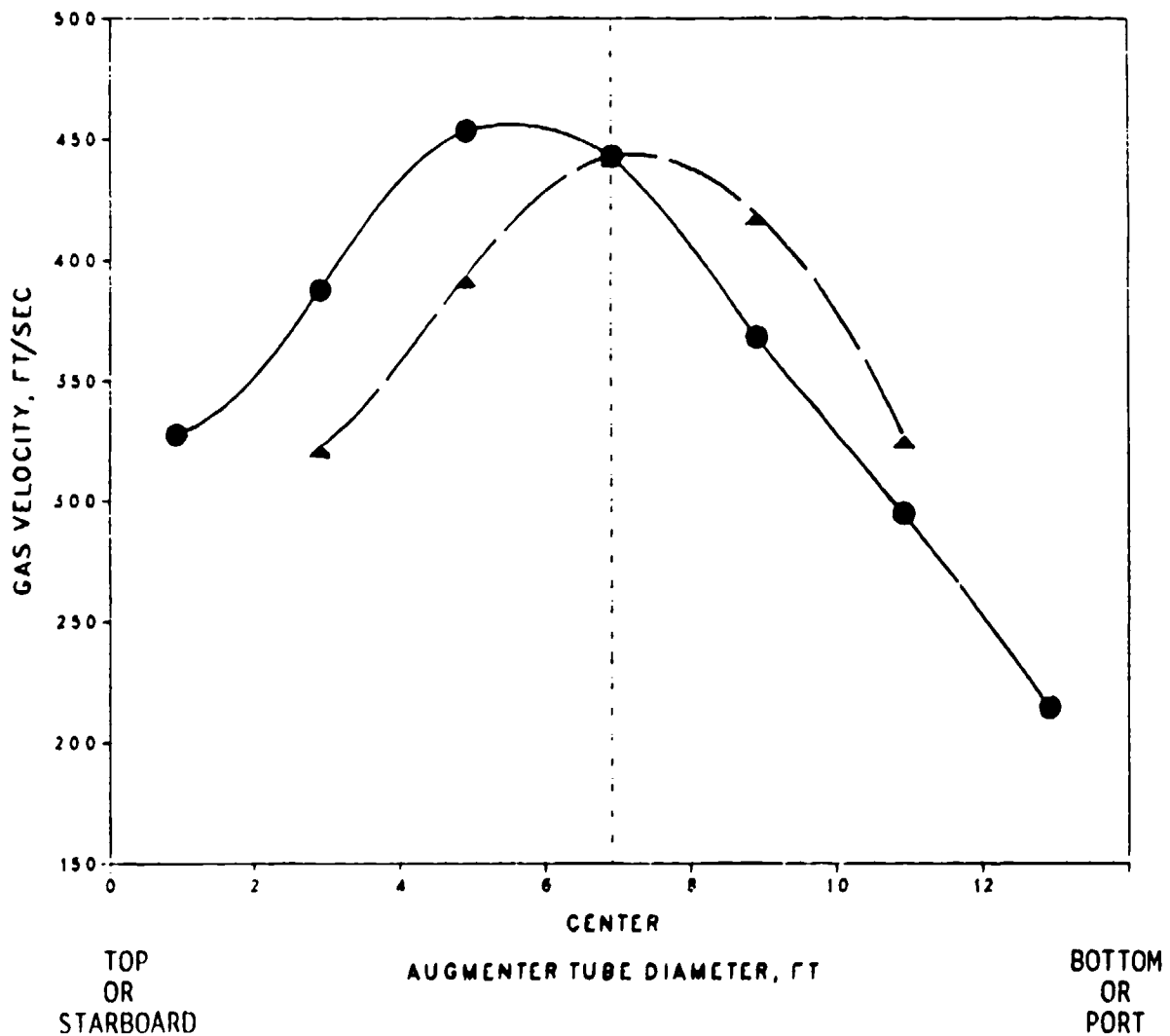


Figure 14. Velocity profile across augmentor tube while testing TF30-P414A at A/B without throttle plate.

NOTES:

(1) AVERAGED OVER 60-SECOND RUN

(2) 60 FT DOWN THE TUBE; 73.1 FT FROM ENGINE NOZZLE

MEASURED 11/18/86

● ALONG VERTICAL TUBE DIAMETER

▲ ALONG HORIZONTAL TUBE DIAMETER

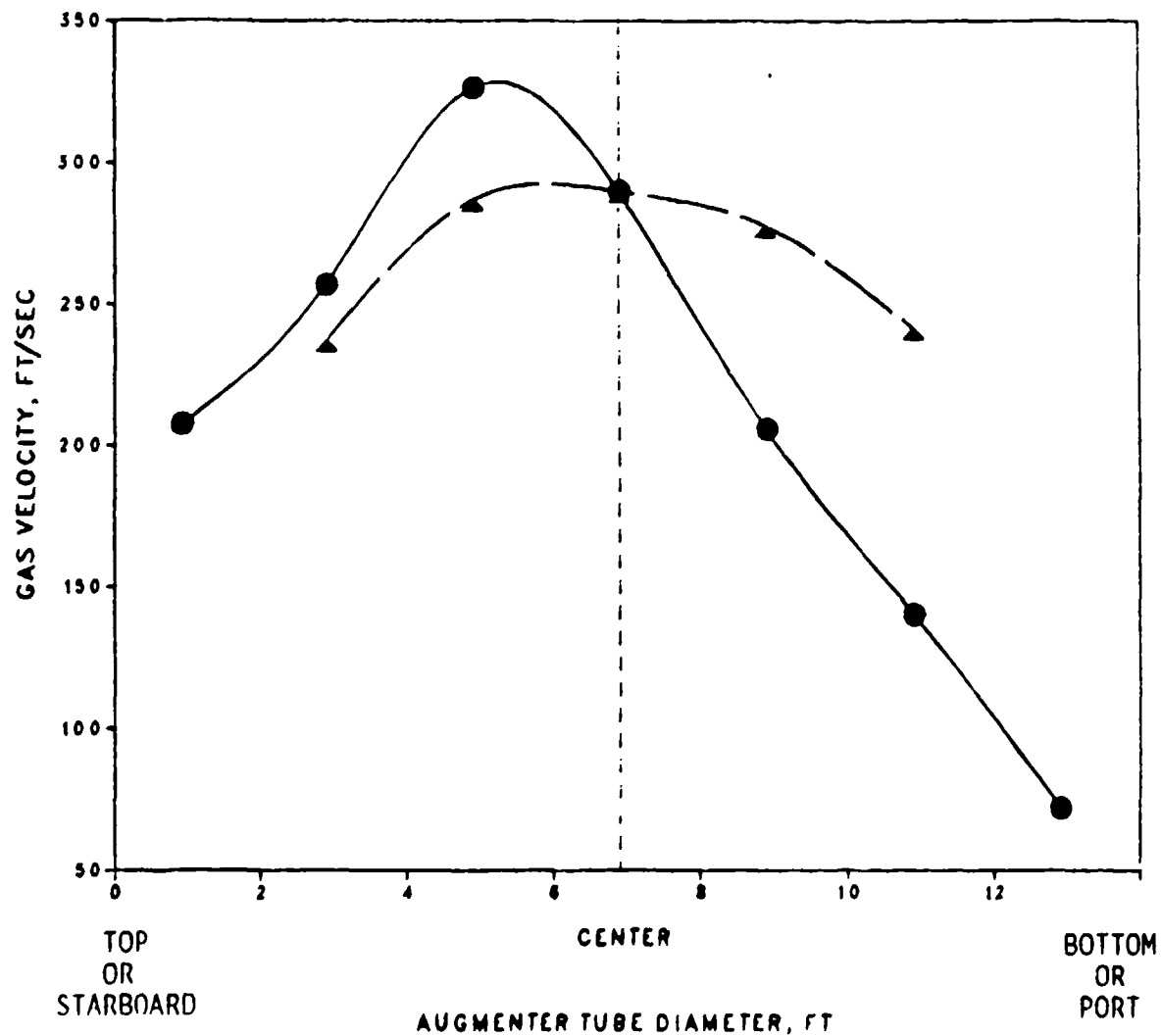


Figure 15. Velocity profiles across augmentor tube while testing TF30-P-414A at Mil without throttle plate.

NOTE:
AVERAGED OVER 30-SECOND BURN

MEASURED 11/11/86

- ALONG VERTICAL TUBE DIAMETER
- ▲ ALONG HORIZONTAL TUBE DIAMETER

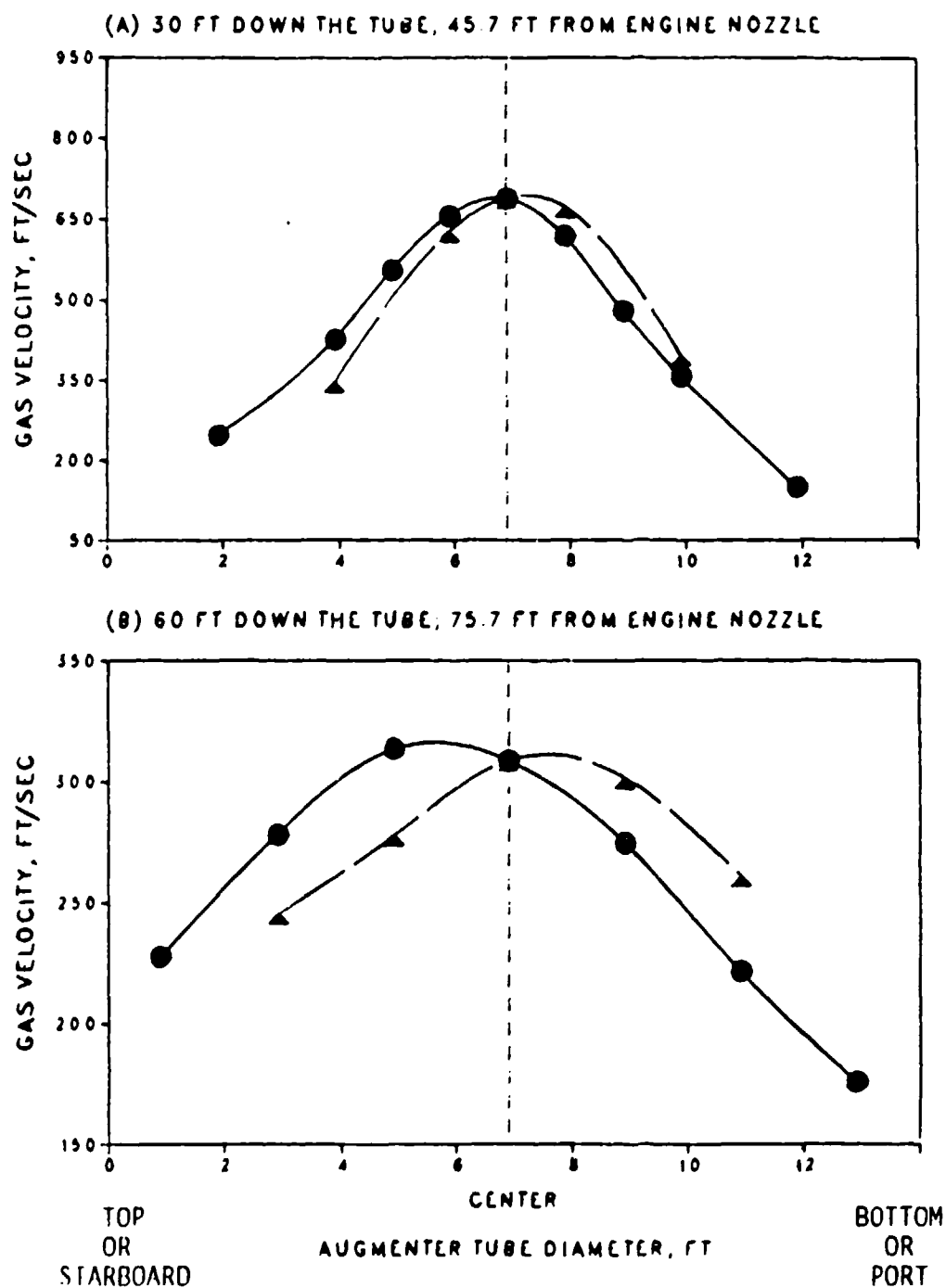


Figure 16. Velocity profiles across augmeter tube while testing F404-GE-400 at A/B with throttle plate.

NOTE:
AVERAGED OVER 38 SECONDS

MEASURED 11/11/86

- ALONG VERTICAL TUBE DIAMETER
- ▲ ALONG HORIZONTAL TUBE DIAMETER

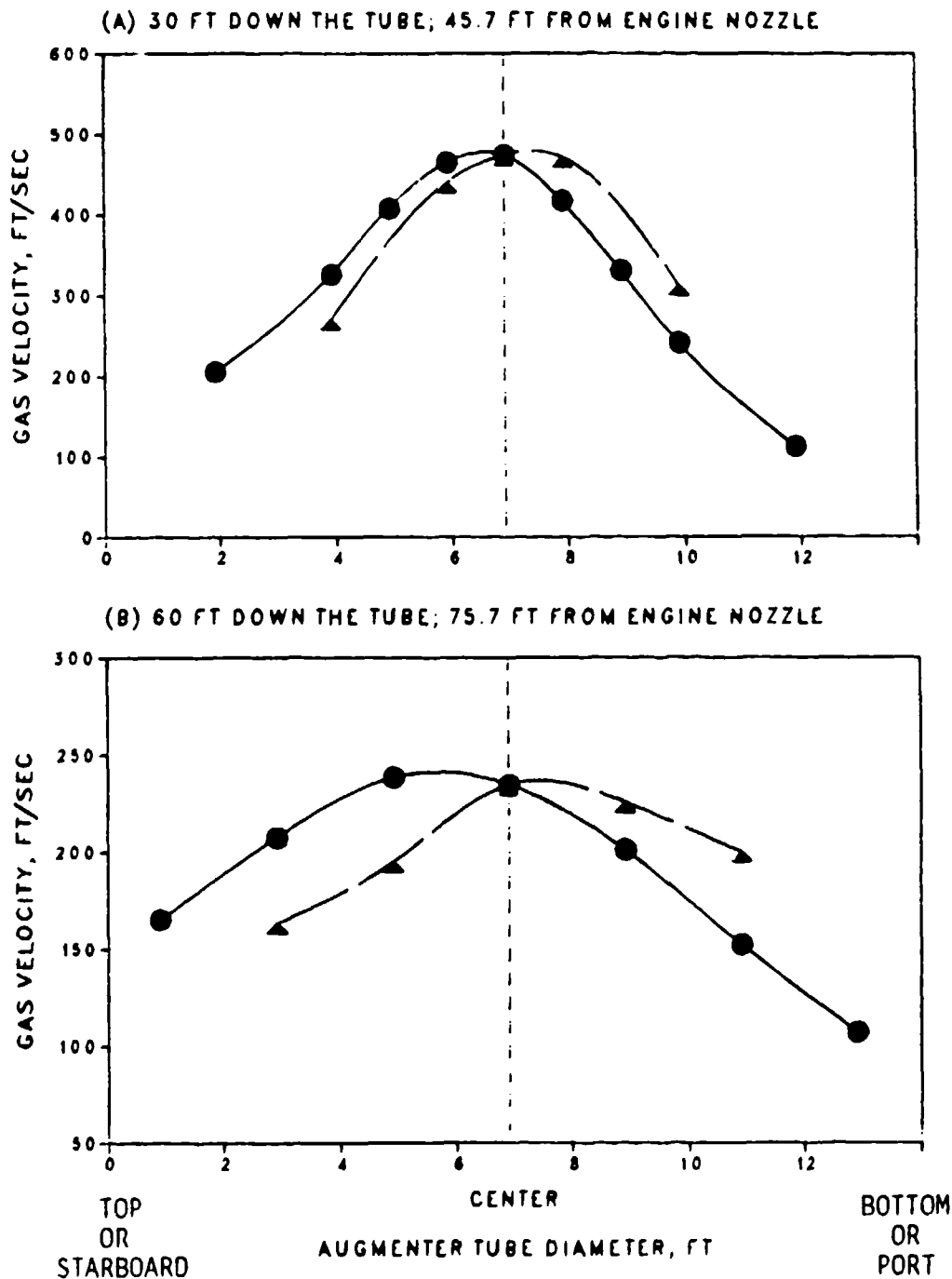


Figure 17. Velocity profiles across augmenter tube while testing F404-GE-400 at Mil with throttle plate.

NOTES:

(1) AVERAGED OVER A 30-SECOND BURN

(2) 60 FT DOWN THE TUBE; 75.7 FT FROM ENGINE NOZZLE

MEASURED 11/19/86

● ALONG VERTICAL TUBE DIAMETER

▲ ALONG HORIZONTAL TUBE DIAMETER

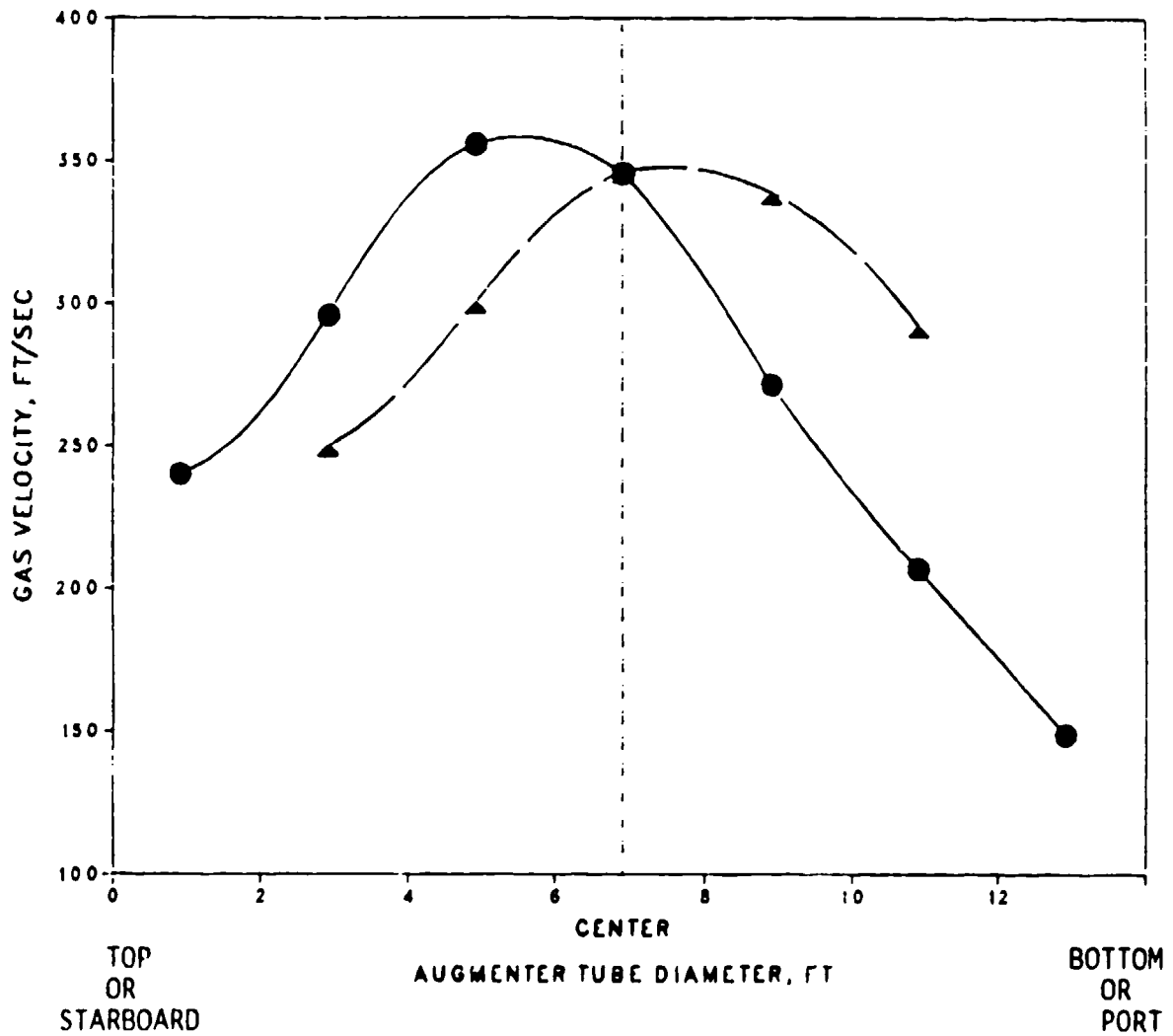


Figure 18. Velocity profiles across augmentor tube while testing F404-GE-400 at A/B without throttle plate.

NOTE:
INSTANTANEOUS VALUES

MEASURED 11/12/86 (W/THROTTLE), 11/19/86 (W/O THROTTLE)

- × AT TOP OF TUBE
- ▲ AT BOTTOM OF TUBE
- STARBOARD SIDE
- PORT SIDE

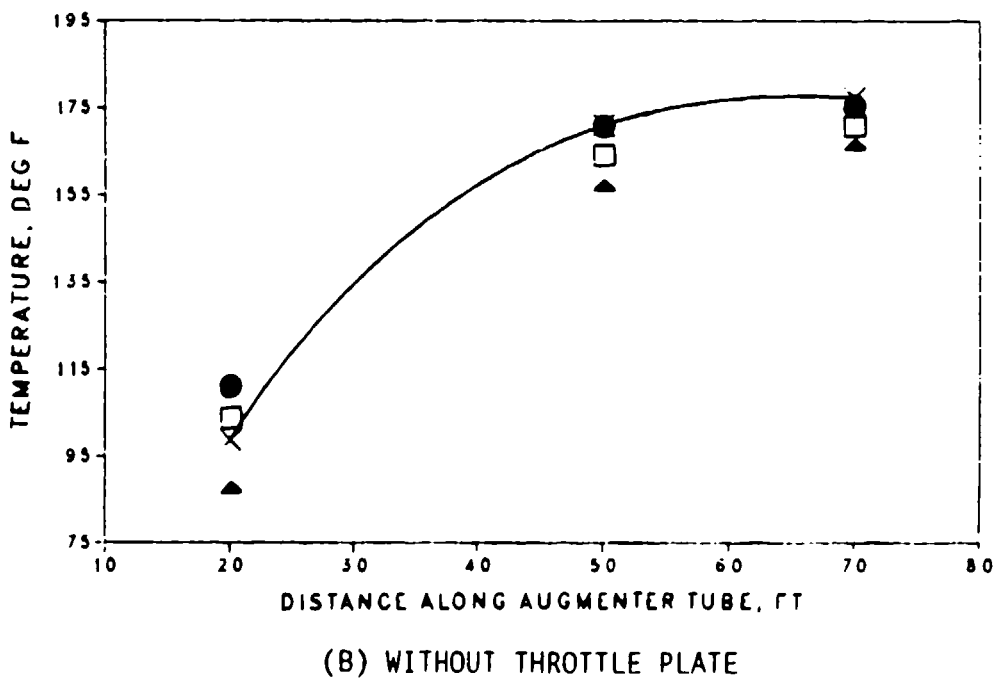
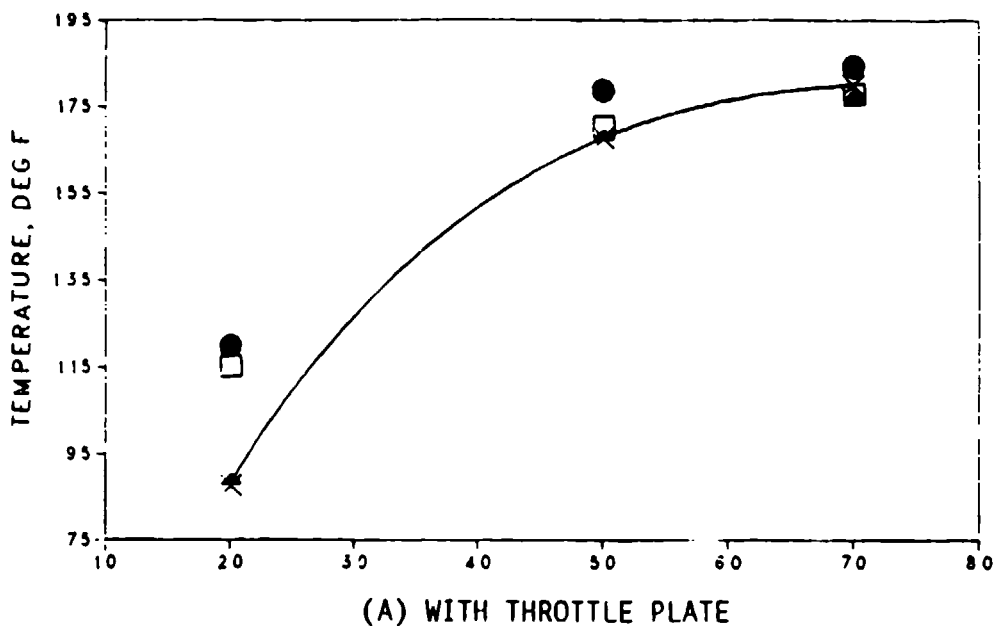


Figure 19. Wall temperatures along augmenter tube while testing TF41-A-2C at Mil.

NOTE:

INSTANTANEOUS VALUES; RECORDED NEAR THE END OF A 30-SECOND BURN

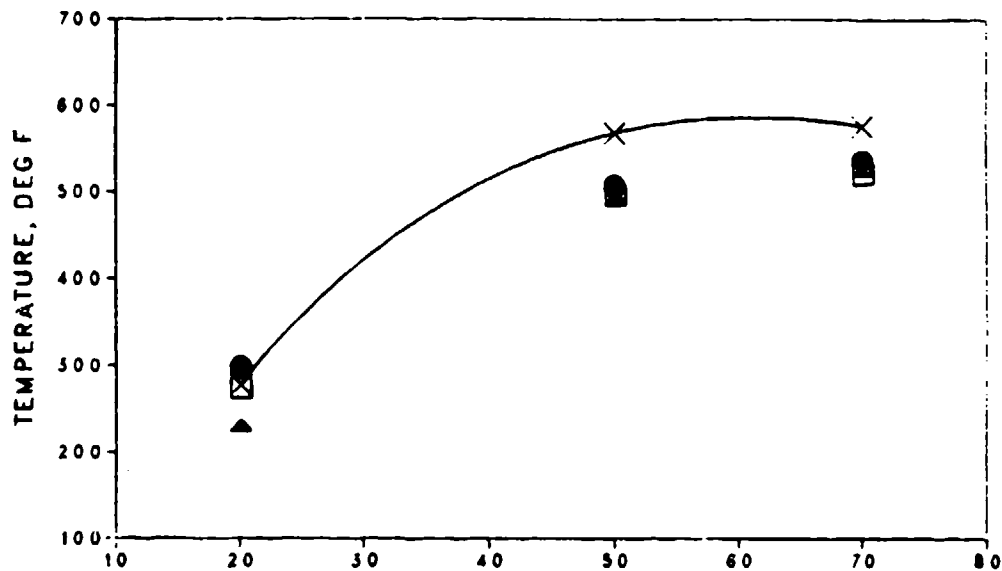
MEASURED 11/14/86 (W/THROTTLE), 11/18/86 (W/O THROTTLE)

× AT TOP OF TUBE

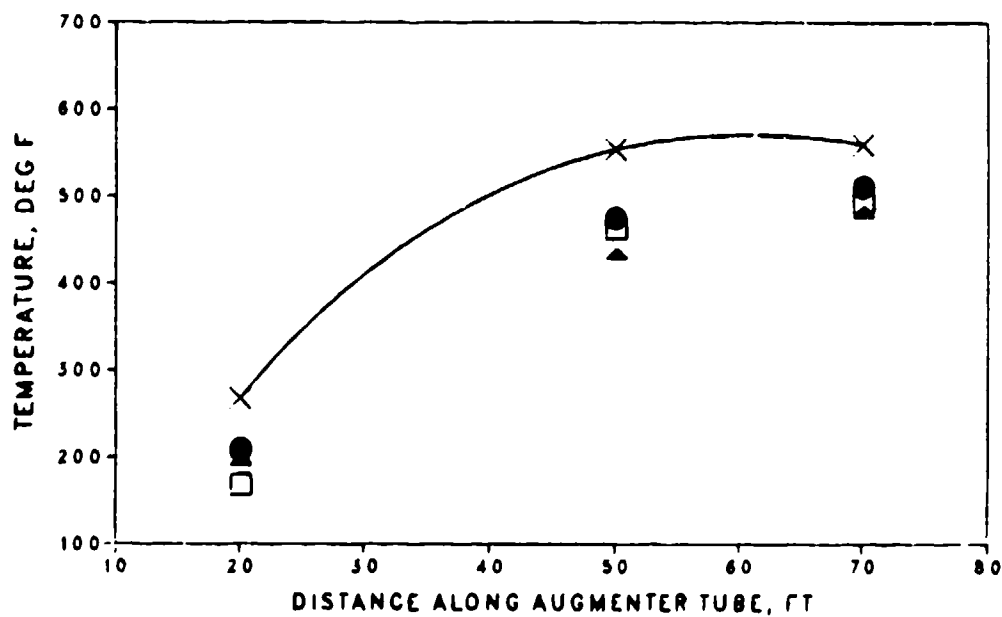
▲ AT BOTTOM OF TUBE

□ STARBOARD SIDE

● PORT SIDE



(A) WITH THROTTLE PLATE



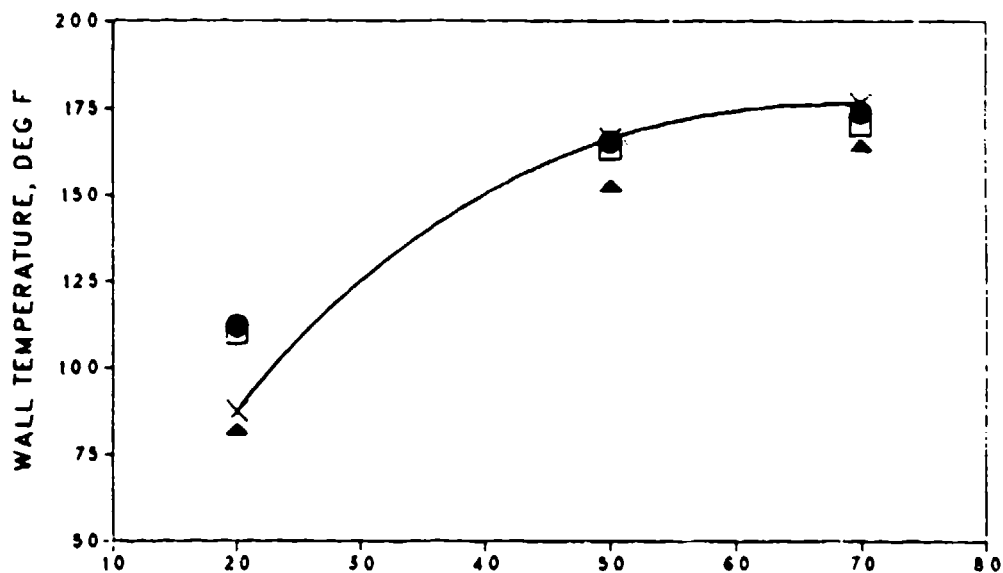
(B) WITHOUT THROTTLE PLATE

Figure 20. Wall temperatures along augmeter tube while testing TF30-P-414A at A/B.

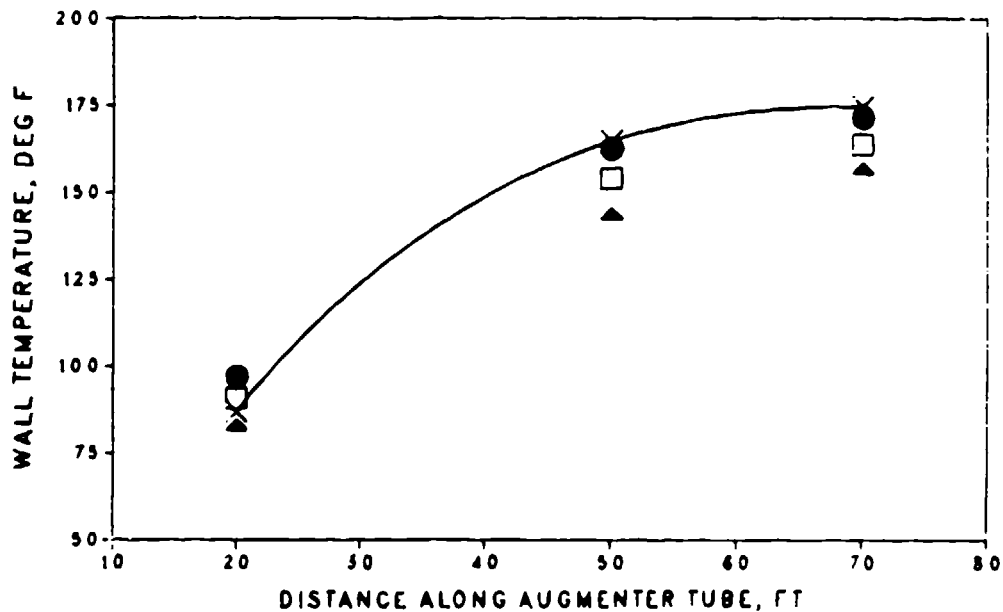
NOTE:
INSTANTANEOUS VALUES; RECORDED NEAR END OF 2-MINUTE RUN

MEASURED 11/14/86 (W/THROTTLE), 11/18/86 (W/O THROTTLE)

- × AT TOP OF TUBE
- ▲ AT BOTTOM OF TUBE
- STARBOARD SIDE
- PORT SIDE



(A) WITH THROTTLE PLATE



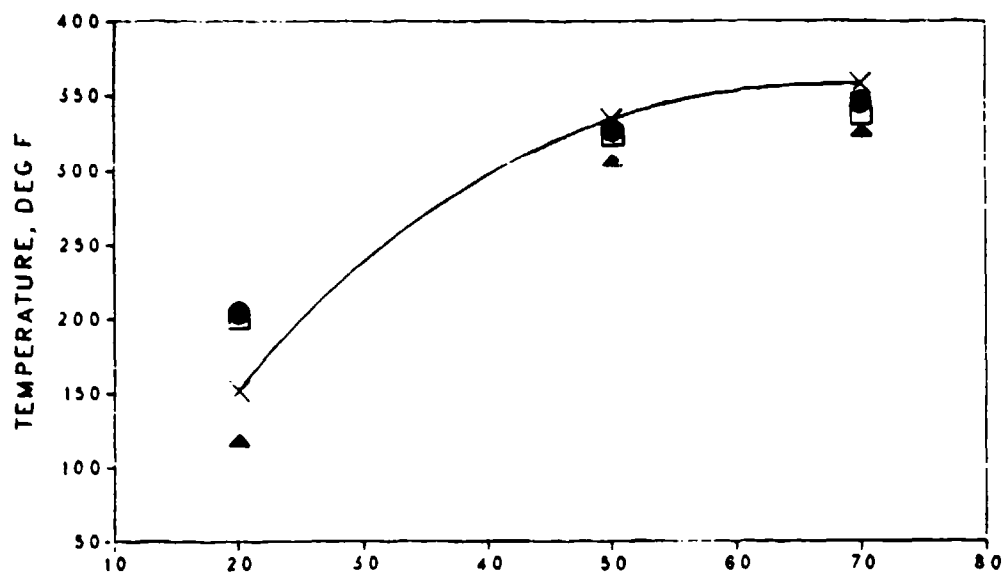
(B) WITHOUT THROTTLE PLATE

Figure 21. Wall temperatures along augmenter tube while testing TF30-P-414A at M11.

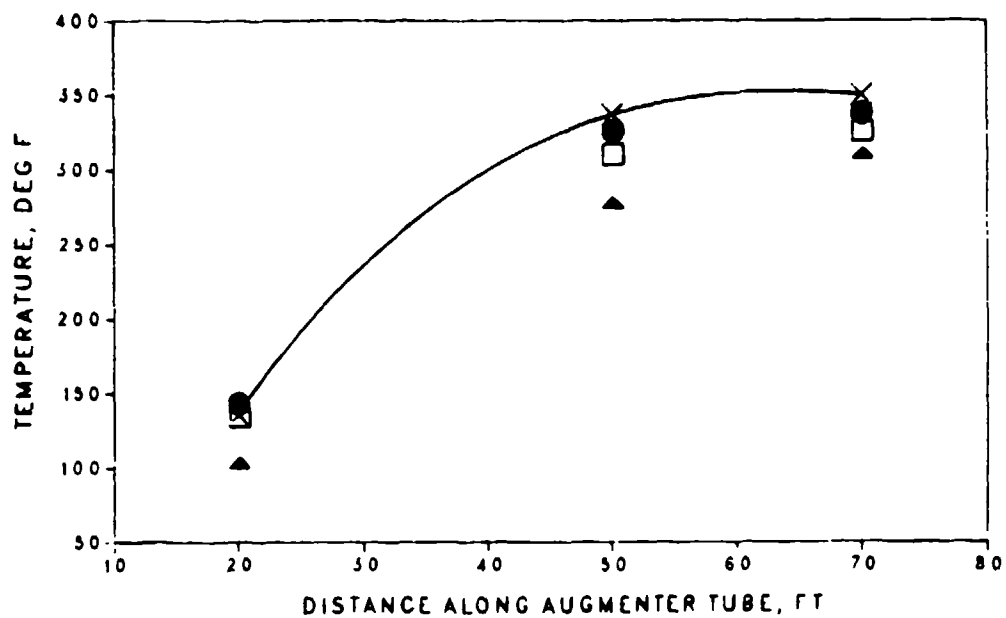
NOTE:
INSTANTANEOUS VALUES; RECORDED NEAR THE END OF A 30-SECOND BURN

MEASURED 11/11/86 (W/THROTTLE), 11/19/86 (W/O THROTTLE)

- × AT TOP OF TUBE
- ▲ AT BOTTOM OF TUBE
- STARBOARD SIDE
- PORT SIDE



(A) WITH THROTTLE PLATE



(B) WITHOUT THROTTLE PLATE

Figure 22. Wall temperatures along augments tube while testing F404-GE-400 at A/B.

NOTE:

(1) J52-P-8B AT MIL

(2) WITH THROTTLE PLATE

(A) MISALIGNED 2.3 DEGREES TO THE LEFT

- AT TOP OF TUBE
- ▲ AT BOTTOM OF TUBE
- ⊗ STARBOARD SIDE
- PORT SIDE

(B) MISALIGNED 1.0 DEGREE TO THE LEFT

- AT TOP OF TUBE
- △ AT BOTTOM OF TUBE
- × STARBOARD SIDE
- PORT SIDE

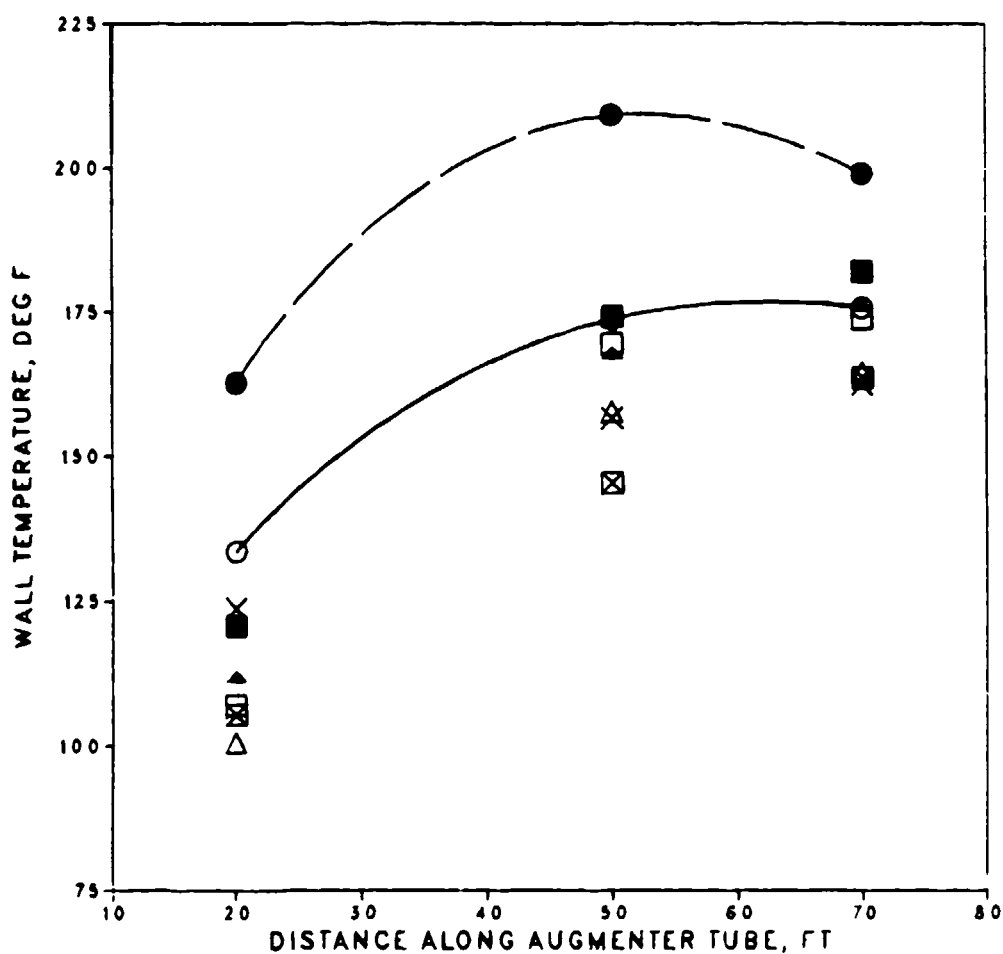


Figure 23. Effect of engine misalignment on augmentor tube wall temperatures.

NOTES:

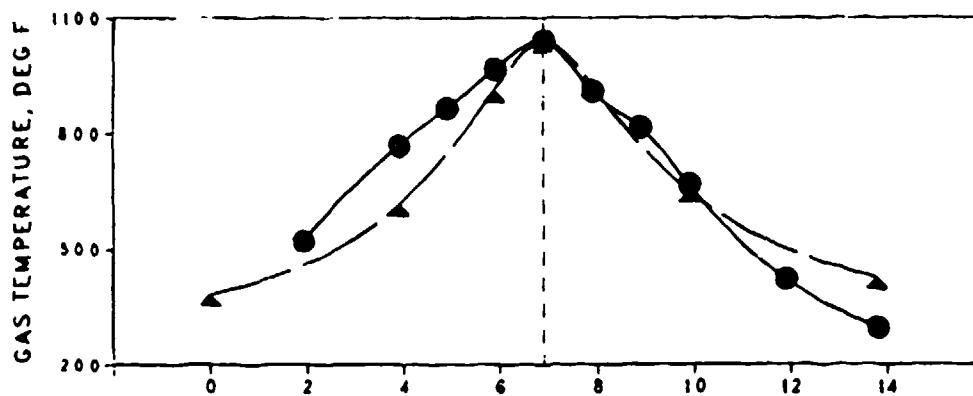
(1) AVERAGED OVER A 30-SECOND BURN

(2) RAMP TEMPS AND THOSE MEASURED AT STARBOARD, PORT, AND BOTTOM OF TUBE DIAM ARE WALL SURFACE VALUES; ALL OTHERS ARE GAS TEMPS

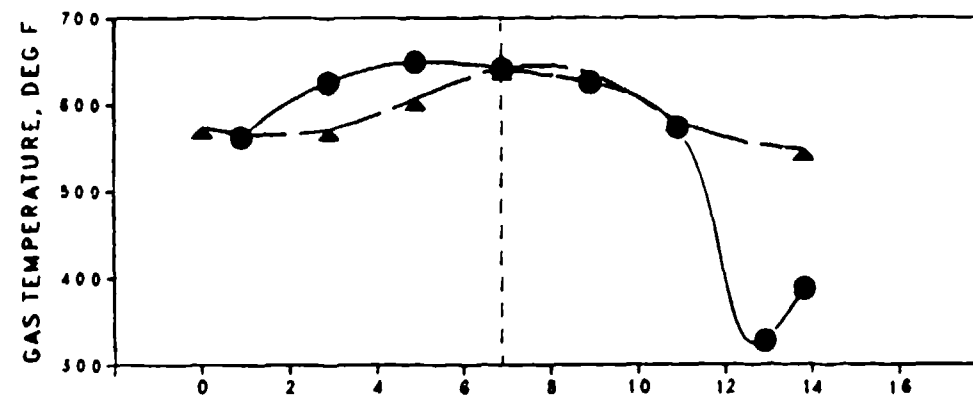
MEASURED 11/14/86

- ALONG VERTICAL TUBE DIAM OR RAMP PROJECTED SURFACE
- ▲ ALONG HORIZONTAL TUBE DIAM OR RAMP PROJECTED SURFACE

(A) 30 FT DOWN THE TUBE; 43.1 FT FROM ENGINE NOZZLE



(B) 60 FT DOWN THE TUBE; 73.1 FT FROM ENGINE NOZZLE



(C) EXHAUST RAMP PROJECTED TO VERTICAL PLANE

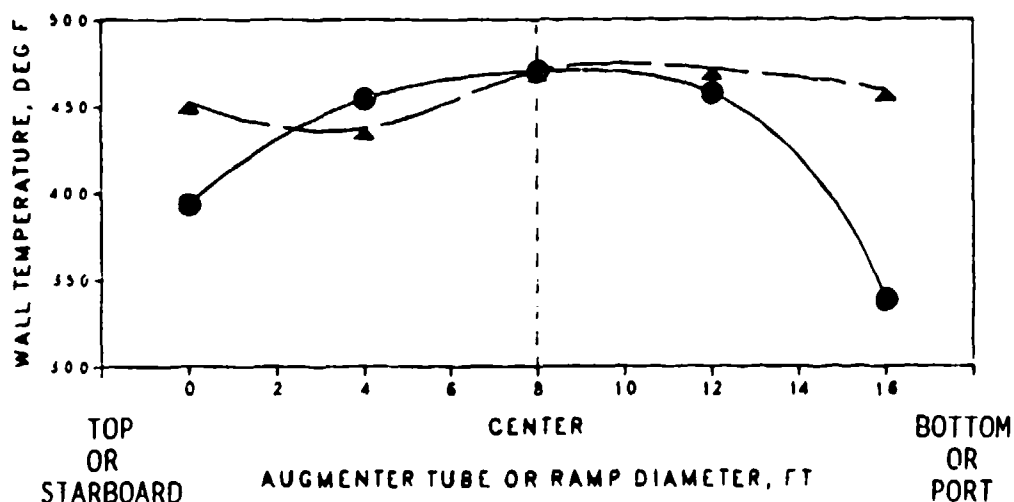


Figure 24. Temperature profiles across augmenter tube and ramp while testing TF30-P-414A at A/D with throttle plate.

NOTES:

- (1) AVERAGED OVER A 60-SECOND BURN
- (2) RAMP TEMPS AND THOSE MEASURED AT STARBOARD, PORT, AND BOTTOM OF TUBE DIAM ARE WALL SURFACE VALUES; ALL OTHERS ARE GAS TEMPS

MEASURED 11/14/86

- ALONG VERTICAL TUBE DIAM OR RAMP PROJECTED SURFACE
- ▲ ALONG HORIZONTAL TUBE DIAM OR RAMP PROJECTED SURFACE

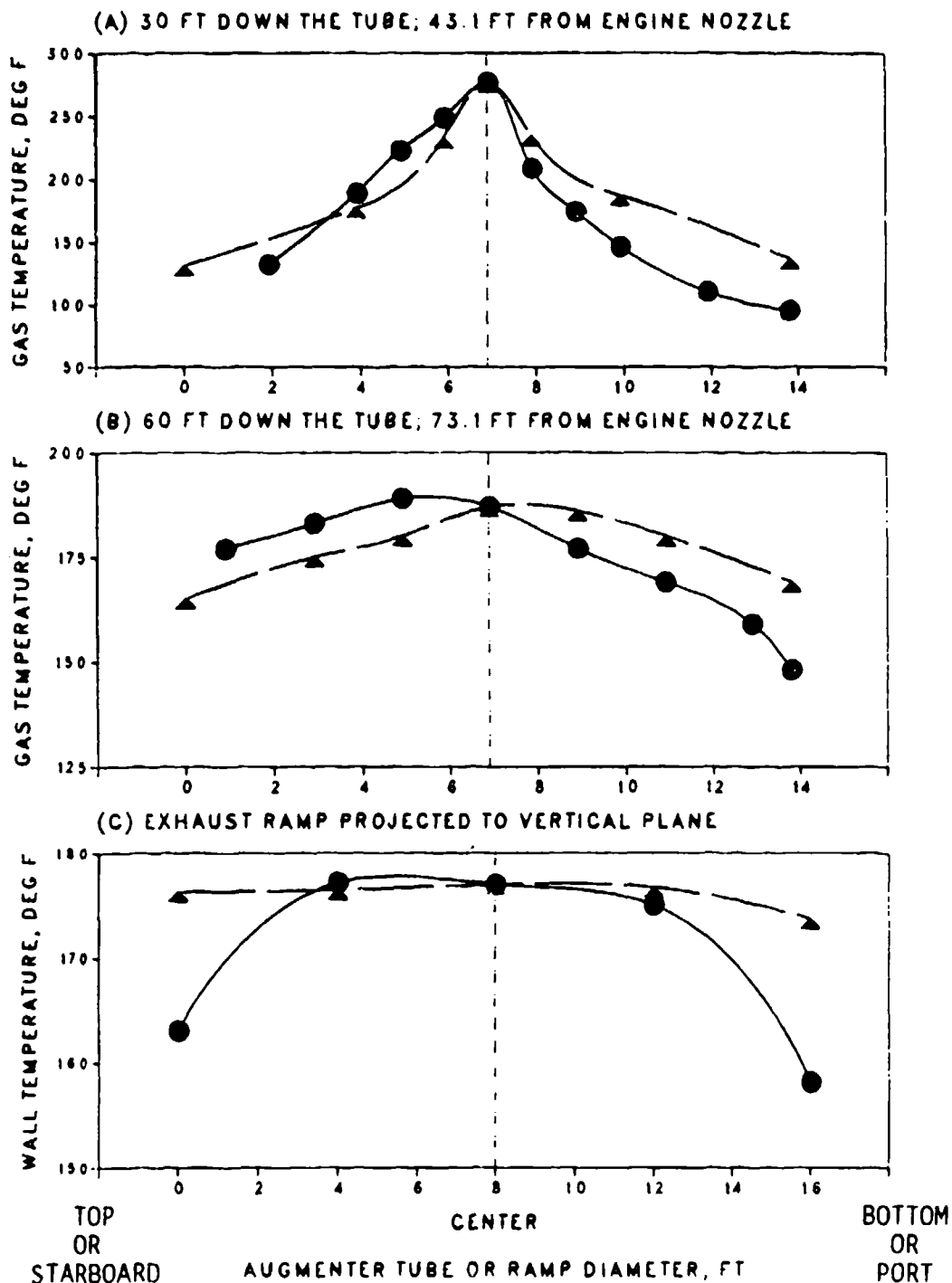


Figure 25. Temperature profiles across augmenter tube and ramp while testing TF30-P-414A at Mil with throttle plate.

NOTES:

(1) AVERAGED OVER A 70-SECOND BURN

(2) RAMP TEMPS AND THOSE MEASURED AT STARBOARD, PORT, AND BOTTOM OF TUBE DIAM ARE WALL SURFACE VALUES; ALL OTHERS ARE GAS TEMPS

MEASURED 11/14/86

- ALONG VERTICAL TUBE DIAM OR RAMP PROJECTED SURFACE
- ▲ ALONG HORIZONTAL TUBE DIAM OR RAMP PROJECTED SURFACE

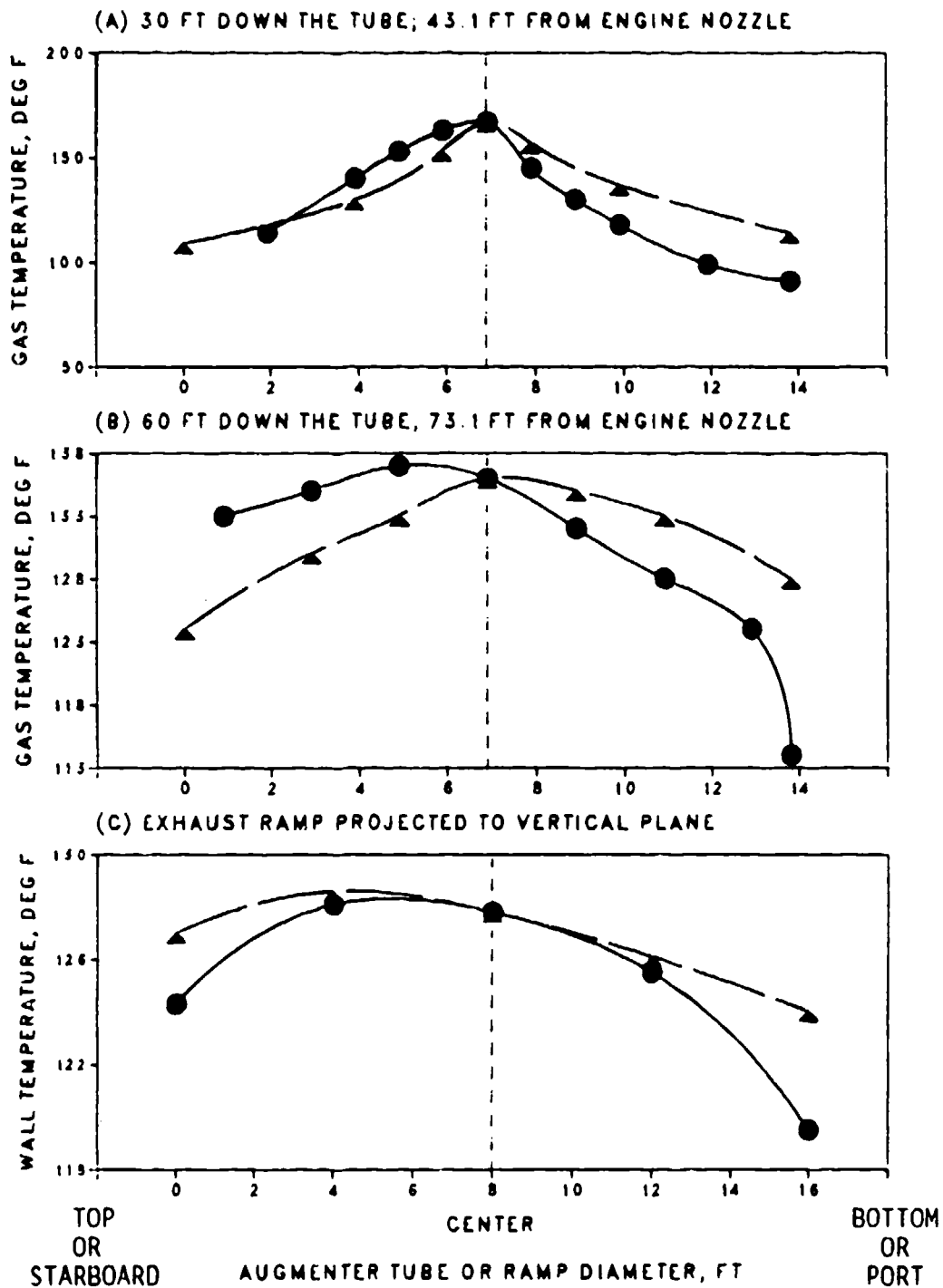


Figure 26. Temperature profiles across augmentor tube and ramp while testing TF30-P-414A at 85% with throttle plate.

NOTES:

- (1) AVERAGED OVER A 80-SECOND RUN
- (2) RAMP TEMPS AND THOSE MEASURED AT STARBOARD, PORT, AND BOTTOM OF TUBE DIAM ARE WALL SURFACE VALUES; ALL OTHERS ARE GAS TEMPS

MEASURED 11/14/86

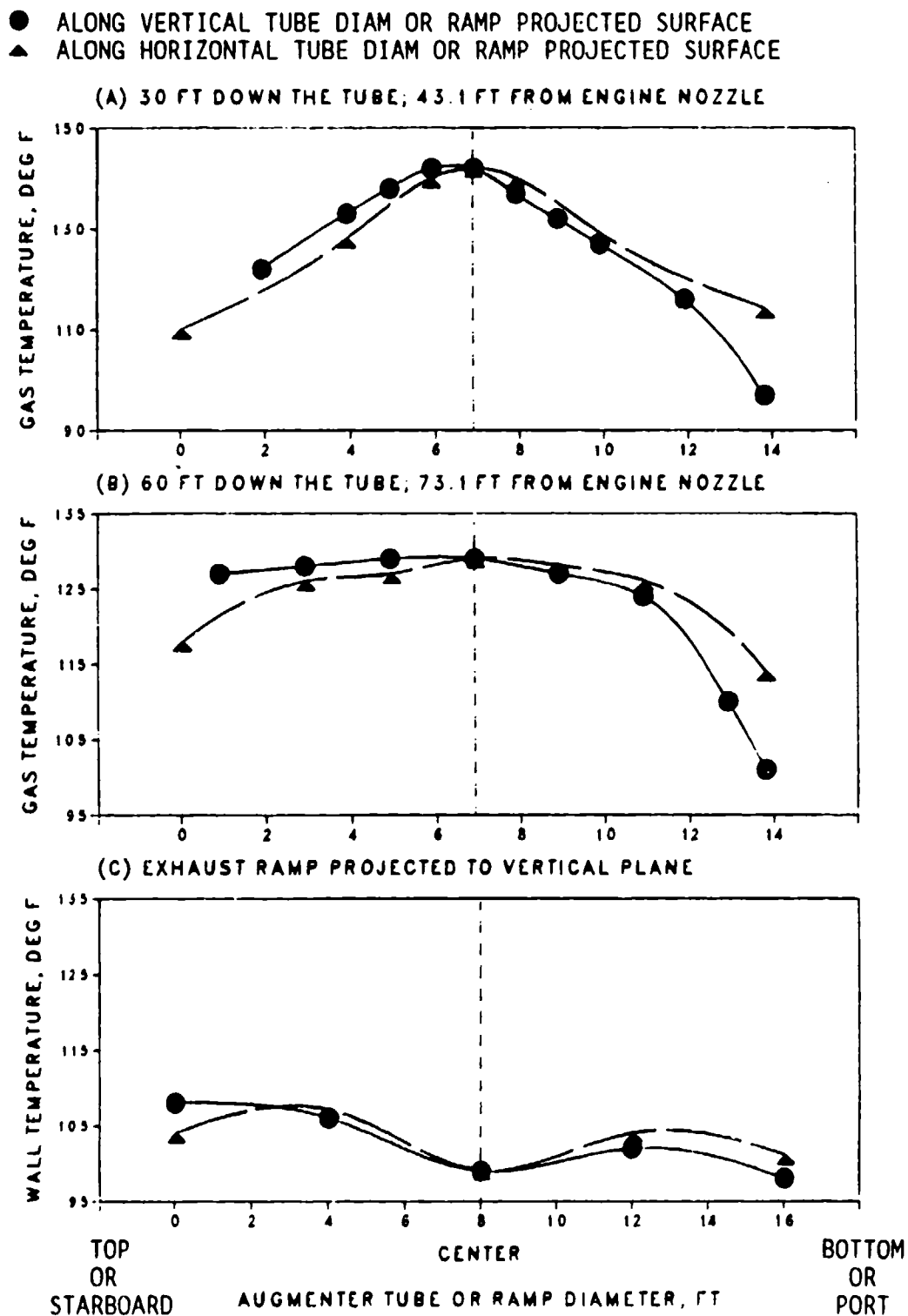


Figure 27. Temperature profiles across augmentor tube and ramp while testing TF30-P-414A at idle with throttle plate.

NOTES:

- (1) AVERAGED OVER A 37-SECOND RUN
- (2) RAMP TEMPS AND THOSE MEASURED AT STARBOARD, PORT, AND BOTTOM OF TUBE DIAM ARE WALL SURFACE VALUES; ALL OTHERS ARE GAS TEMPS

MEASURED 11/18/86

- ALONG VERTICAL TUBE DIAM OR RAMP PROJECTED SURFACE
- ▲ ALONG HORIZONTAL TUBE DIAM OR RAMP PROJECTED SURFACE

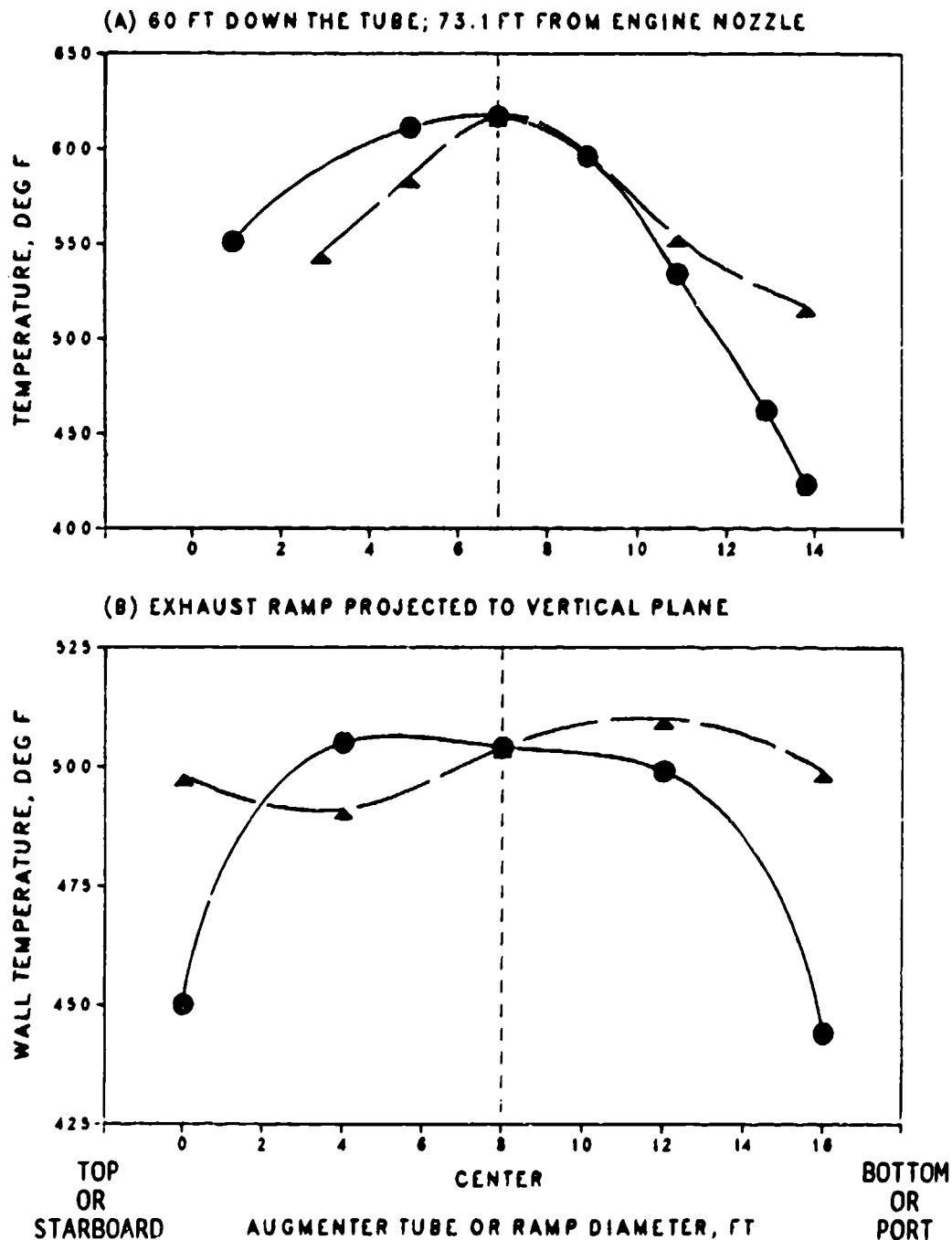


Figure 28. Temperature profiles across augmeter tube and ramp while testing TF30-P-414A at A/B without throttle plate.

NOTES:

- (1) AVERAGED OVER A 59-SECOND RUN
- (2) RAMP TEMPS AND THOSE MEASURED AT STARBOARD, PORT, AND BOTTOM OF TUBE DIAM ARE WALL SURFACE VALUES; ALL OTHERS ARE GAS TEMPS

MEASURED 11/18/86

- ALONG VERTICAL TUBE DIAM OR RAMP PROJECTED SURFACE
- ▲ ALONG HORIZONTAL TUBE DIAM OR RAMP PROJECTED SURFACE

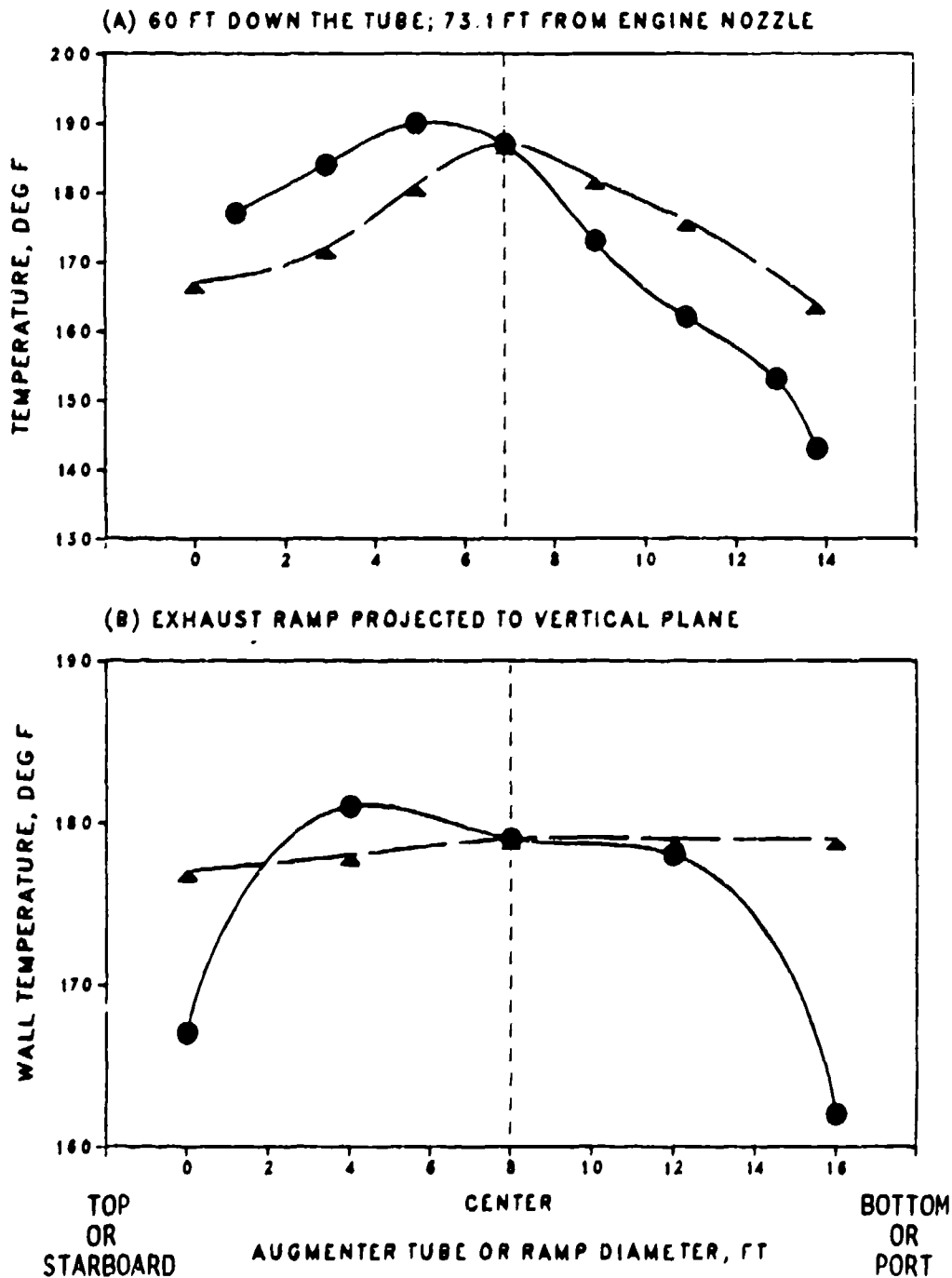


Figure 29. Temperature profiles across augmentor tube and ramp while testing TF30-P-414A at M1 without throttle plate.

NOTES:

(1) AVERAGED OVER A 60-SECOND RUN

(2) RAMP TEMPS AND THOSE MEASURED AT STARBOARD, PORT, AND BOTTOM OF TUBE DIAM ARE WALL SURFACE VALUES; ALL OTHERS ARE GAS TEMPS

MEASURED 11/18/86

- ALONG VERTICAL TUBE DIAM OR RAMP PROJECTED SURFACE
- ▲ ALONG HORIZONTAL TUBE DIAM OR RAMP PROJECTED SURFACE

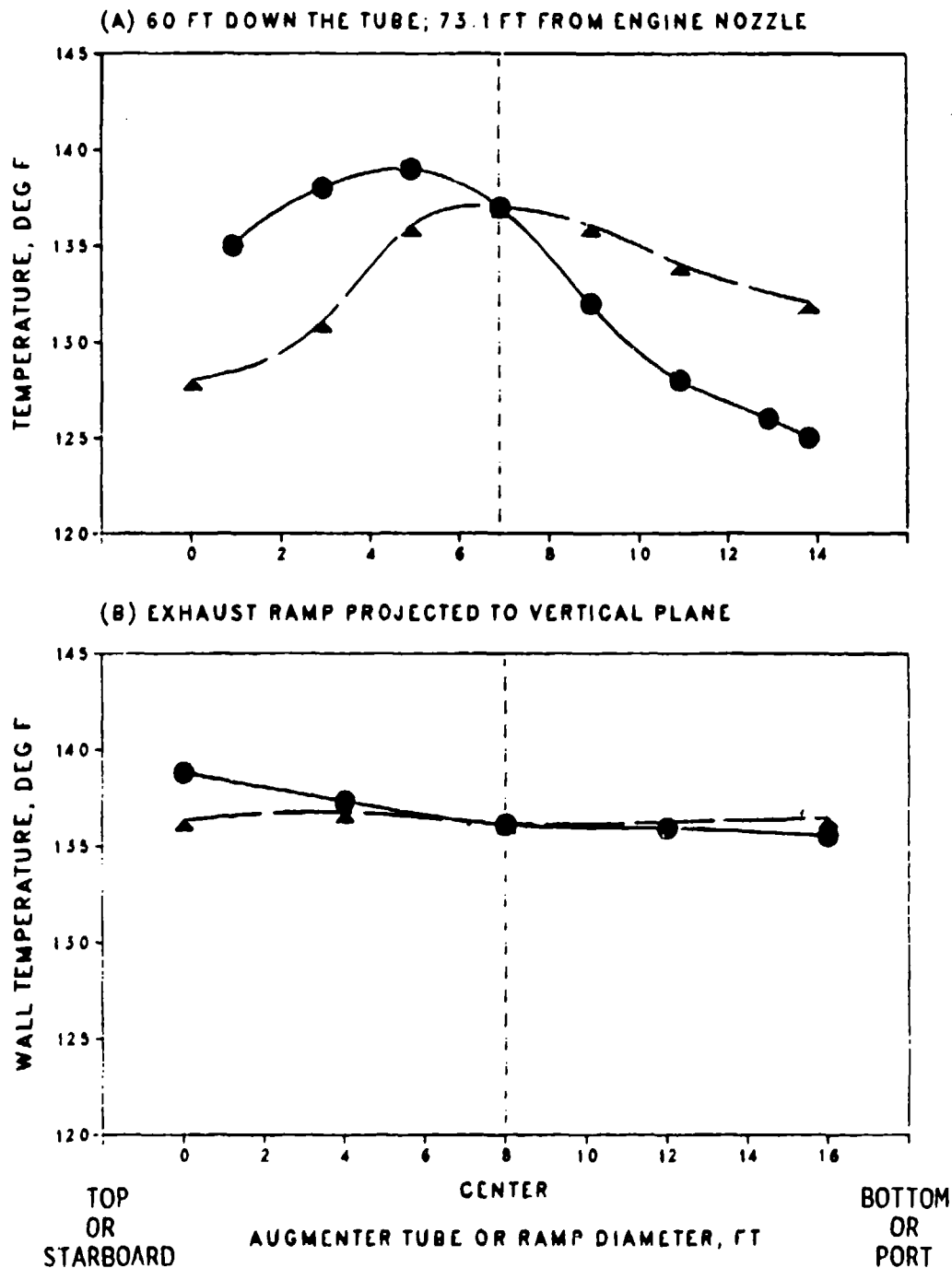


Figure 30. Temperature profiles across augmenter tube and ramp while testing TF30-P-414A at 85% without throttle plate.

NOTES:

- (1) AVERAGED OVER A 26-SECOND BURN
- (2) RAMP TEMPS AND THOSE MEASURED AT STARBOARD, PORT, AND BOTTOM OF TUBE DIAM ARE WALL SURFACE VALUES; ALL OTHERS ARE GAS TEMPS

MEASURED 11/11/86

- ALONG VERTICAL TUBE DIAM OR RAMP PROJECTED SURFACE
- ▲ ALONG HORIZONTAL TUBE DIAM OR RAMP PROJECTED SURFACE

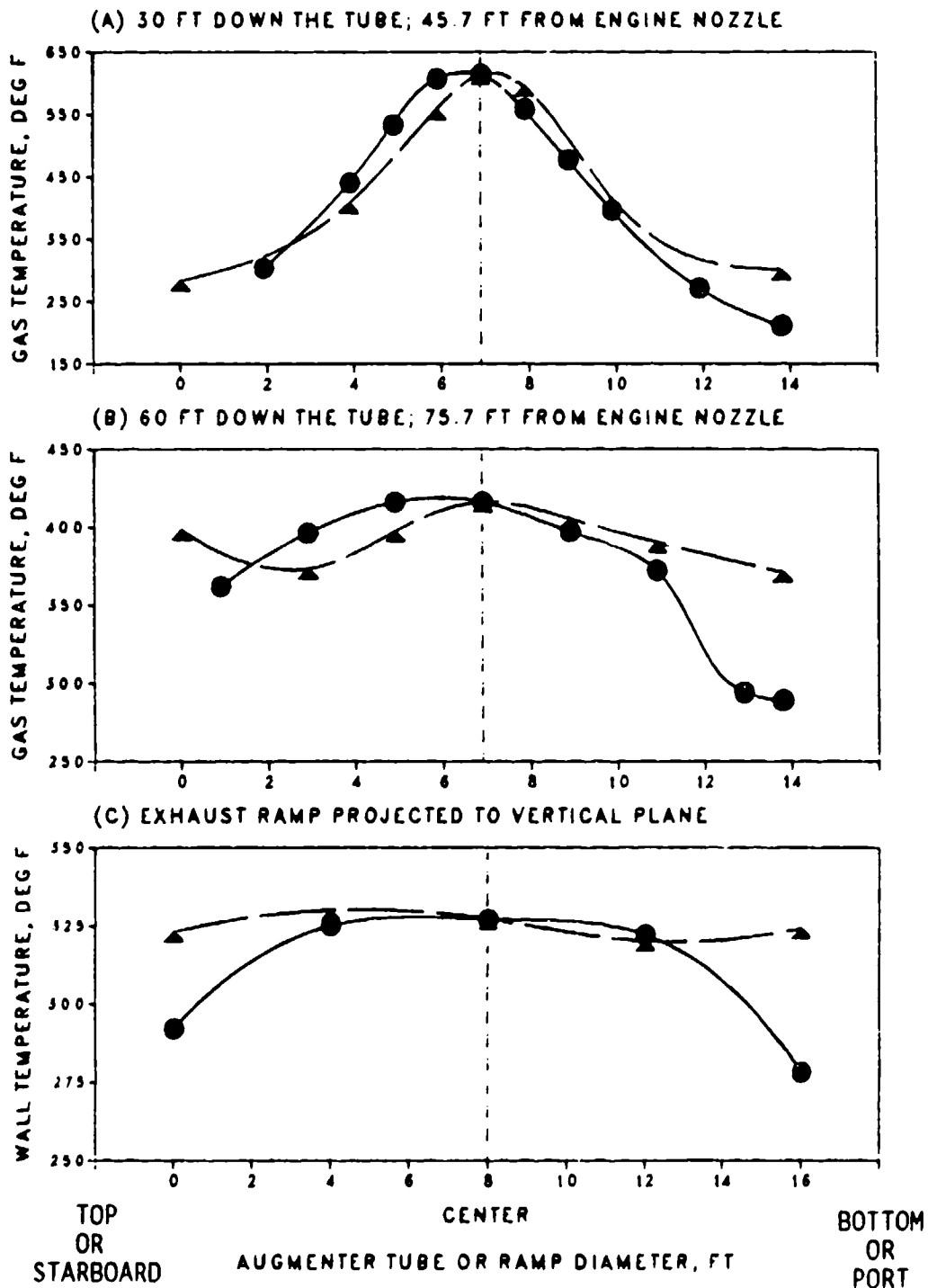


Figure 31. Temperature profiles across augmenter tube and ramp while testing F404-GE-400 at A/B with throttle plate.

NOTES:

- (1) AVERAGED OVER A 92-SECOND RUN
- (2) RAMP TEMPS AND THOSE MEASURED AT STARBOARD, PORT, AND BOTTOM OF TUBE DIAM ARE WALL SURFACE VALUES; ALL OTHERS ARE GAS TEMPS

MEASURED 11/11/86

- ALONG VERTICAL TUBE DIAM OR RAMP PROJECTED SURFACE
- ▲ ALONG HORIZONTAL TUBE DIAM OR RAMP PROJECTED SURFACE

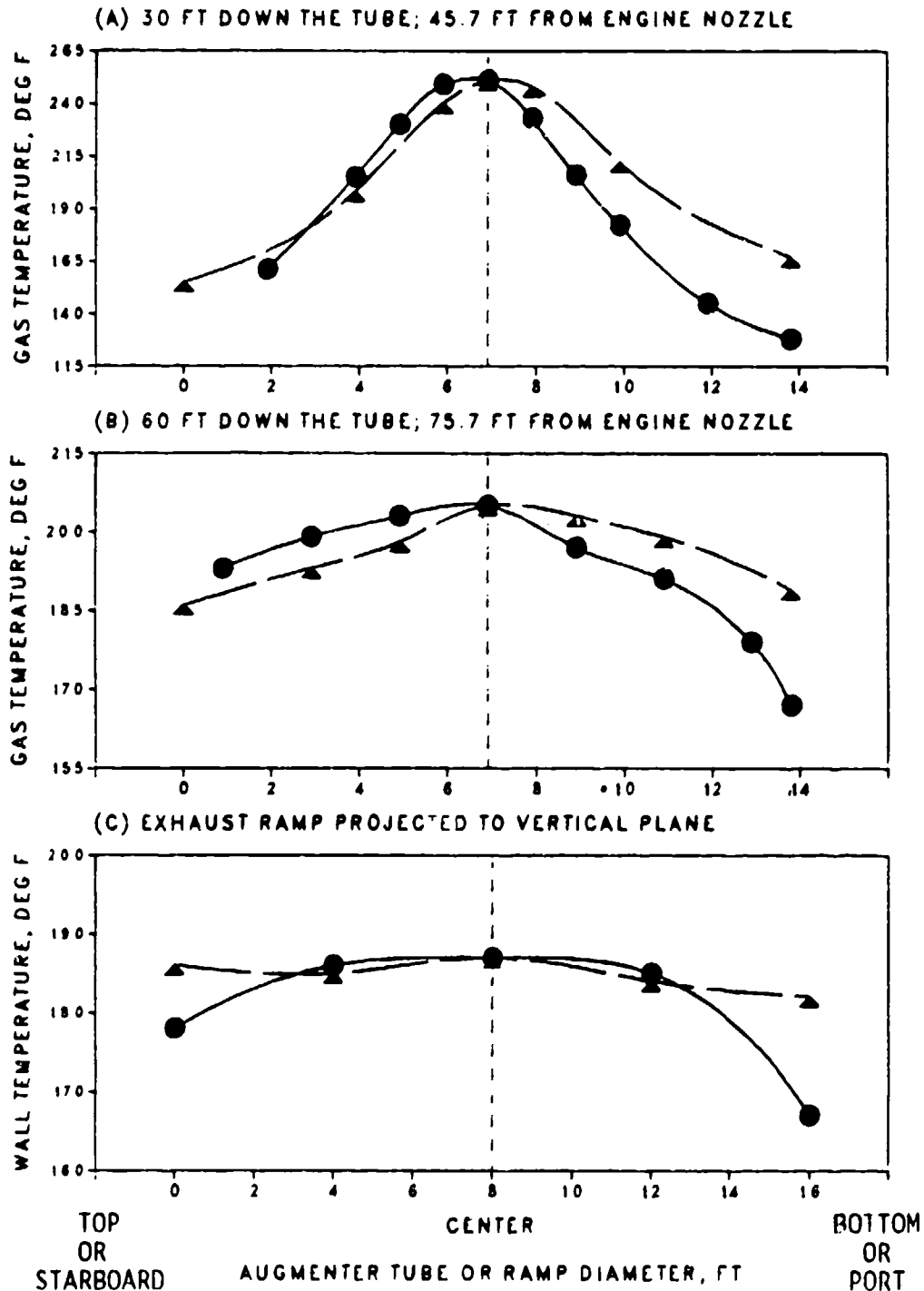


Figure 32. Temperature profiles across augmeter tube and ramp while testing F404-GE-400 at M11 with throttle plate.

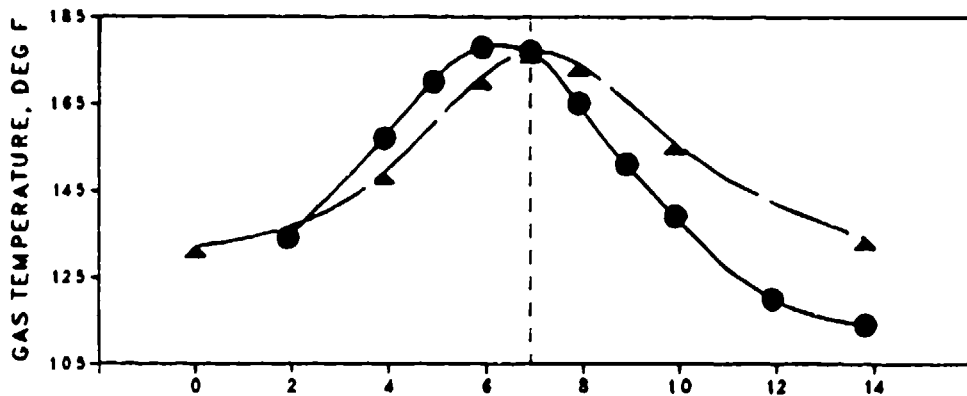
NOTES:

- (1) AVERAGED OVER A 42-SECOND RUN
- (2) RAMP TEMPS AND THOSE MEASURED AT STARBOARD, PORT, AND BOTTOM OF TUBE DIAM ARE WALL SURFACE VALUES; ALL OTHERS ARE GAS TEMPS

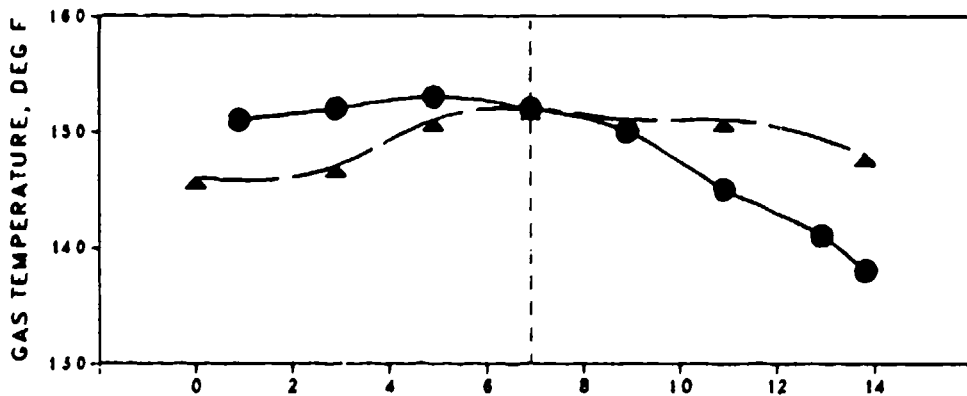
MEASURED 11/11/86

- ALONG VERTICAL TUBE DIAM OR RAMP PROJECTED SURFACE
- ▲ ALONG HORIZONTAL TUBE DIAM OR RAMP PROJECTED SURFACE

(A) 30 FT DOWN THE TUBE; 45.7 FT FROM ENGINE NOZZLE



(B) 60 FT DOWN THE TUBE; 75.7 FT FROM ENGINE NOZZLE



(C) EXHAUST RAMP PROJECTED TO VERTICAL PLANE

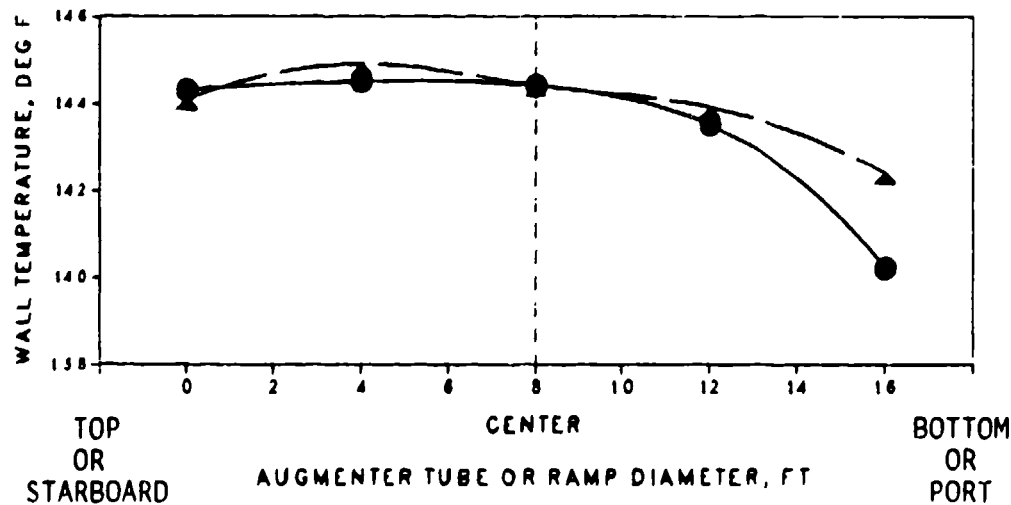


Figure 33. Temperature profiles across augmenter tube and ramp while testing F404-GE-400 at 85% with throttle plate.

NOTES:

- (1) AVERAGED OVER A 52-SECOND BURN
- (2) RAMP TEMPS AND THOSE MEASURED AT STARBOARD, PORT, AND BOTTOM OF TUBE DIAM ARE WALL SURFACE VALUES; ALL OTHERS ARE GAS TEMPS

MEASURED 11/11/86

- ALONG VERTICAL TUBE DIAM OR RAMP PROJECTED SURFACE
- ▲ ALONG HORIZONTAL TUBE DIAM OR RAMP PROJECTED SURFACE

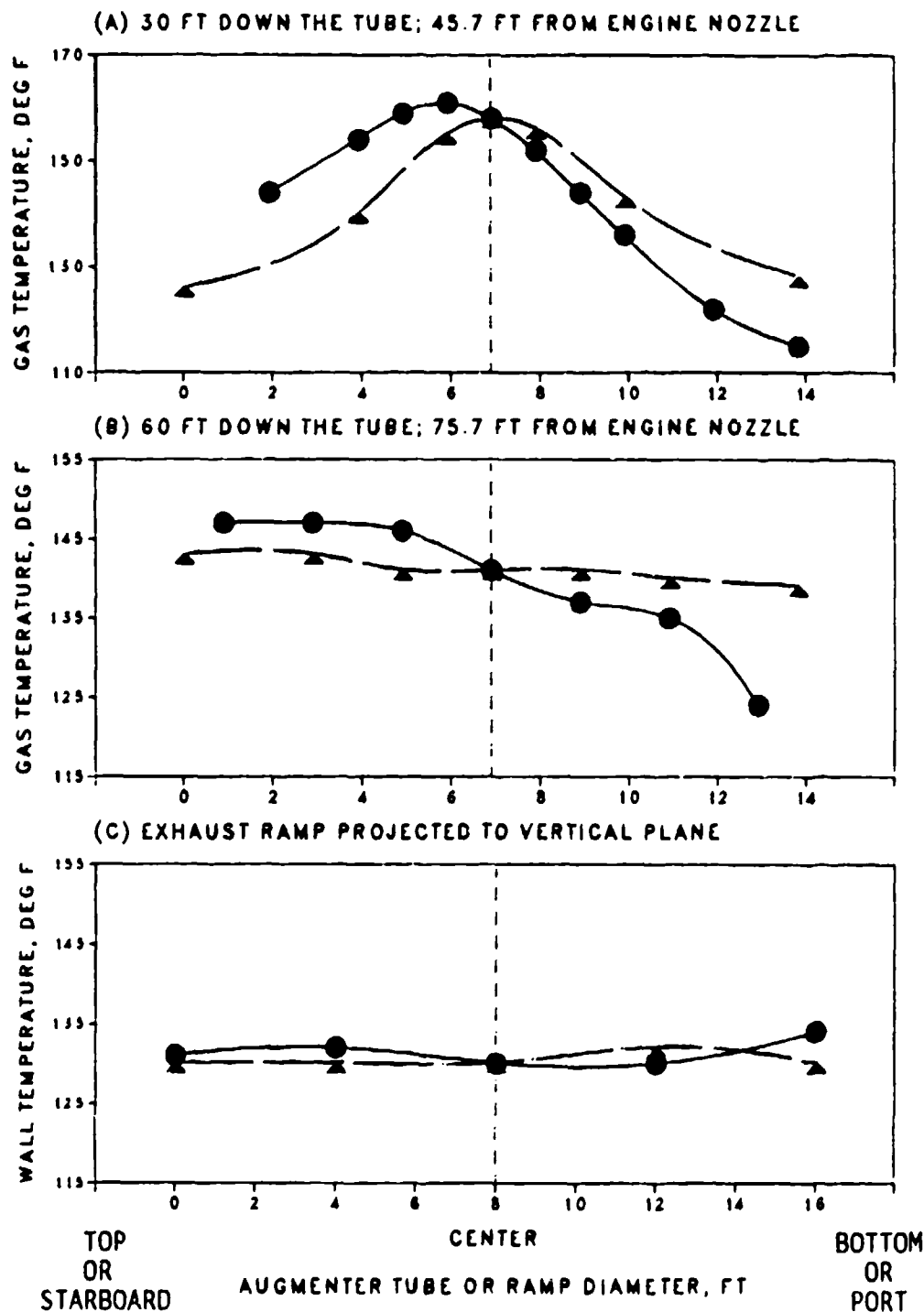


Figure 34. Temperature profiles across augmentor tube and ramp while testing F404-GE-400 at idle with throttle plate.

NOTES:

- (1) AVERAGED OVER A 27-SECOND RUN
- (2) RAMP TEMPS AND THOSE MEASURED AT STARBOARD, PORT, AND BOTTOM OF TUBE DIAM ARE WALL SURFACE VALUES; ALL OTHERS ARE GAS TEMPS

MEASURED 11/19/86

- ALONG VERTICAL TUBE DIAM OR RAMP PROJECTED SURFACE
- ▲ ALONG HORIZONTAL TUBE DIAM OR RAMP PROJECTED SURFACE

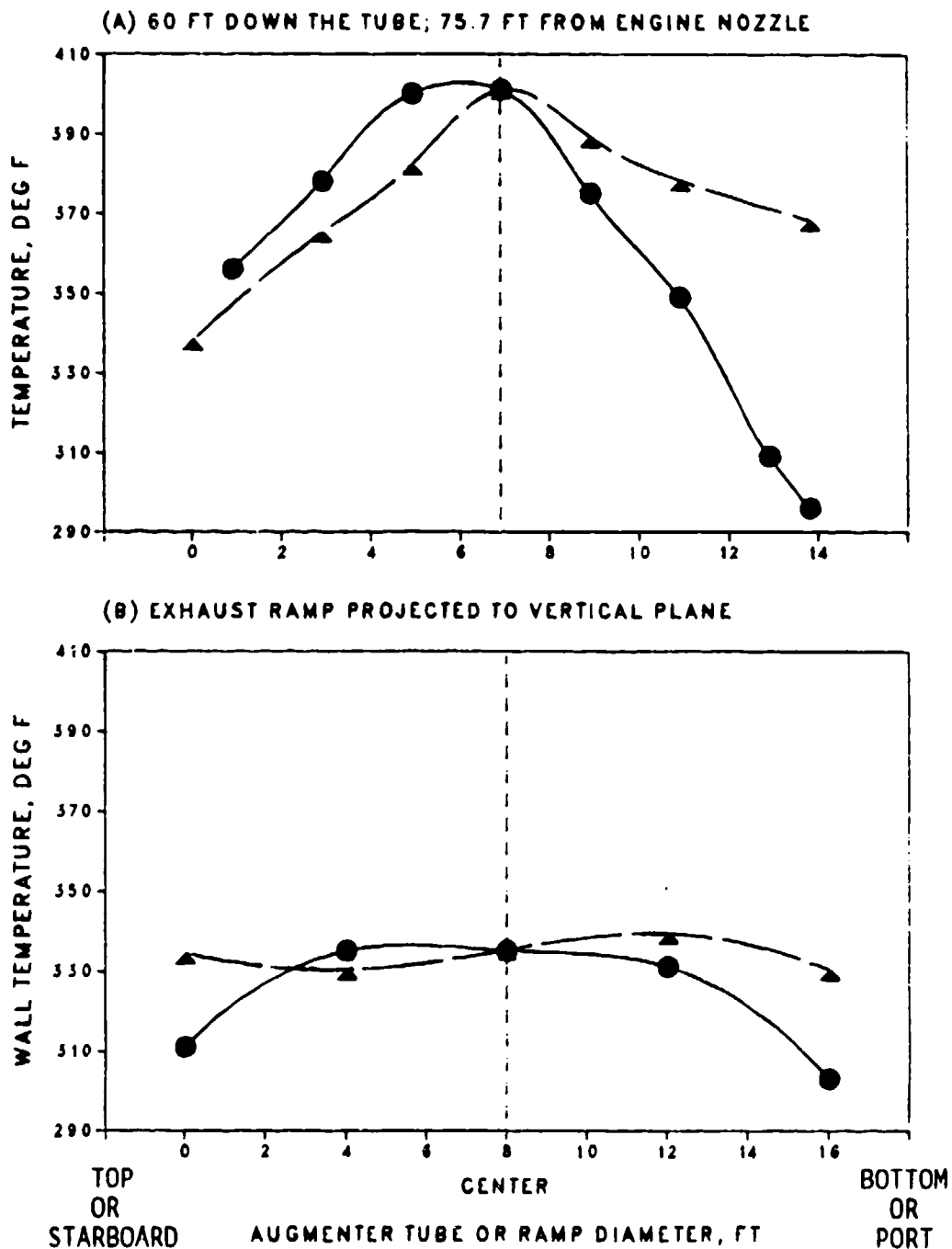


Figure 35. Temperature profiles across augmeter tube and ramp while testing F404-GE-400 at A/B with out throttle plate.

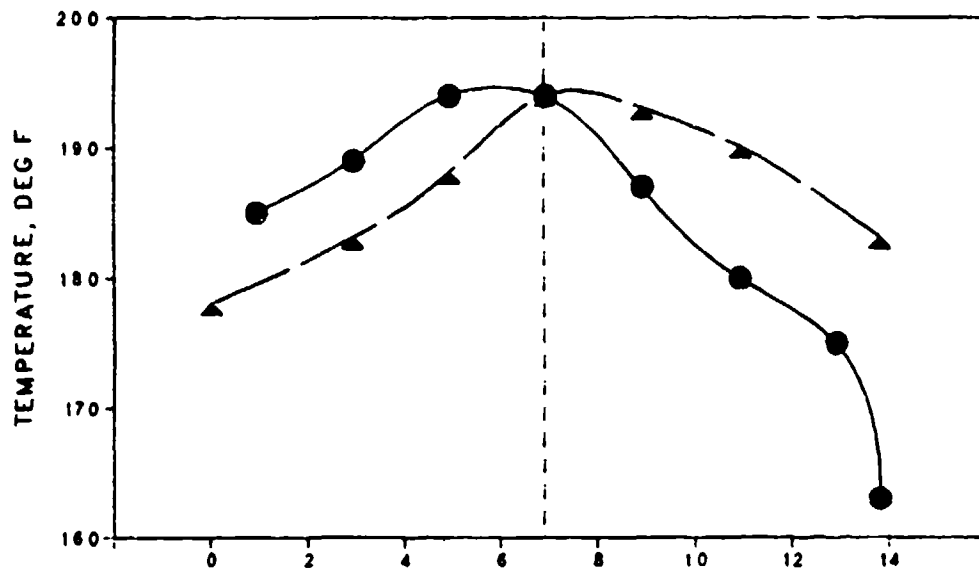
NOTES:

- (1) AVERAGED OVER A 73-SECOND RUN
- (2) RAMP TEMPS AND THOSE MEASURED AT STARBOARD, PORT, AND BOTTOM OF TUBE DIAM ARE WALL SURFACE VALUES; ALL OTHERS ARE GAS TEMPS

MEASURED 11/19/86

- ALONG VERTICAL TUBE DIAM OR RAMP PROJECTED SURFACE
- ▲ ALONG HORIZONTAL TUBE DIAM OR RAMP PROJECTED SURFACE

(A) 60 FT DOWN THE TUBE; 75.7 FT FROM ENGINE NOZZLE



(B) EXHAUST RAMP PROJECTED TO VERTICAL PLANE

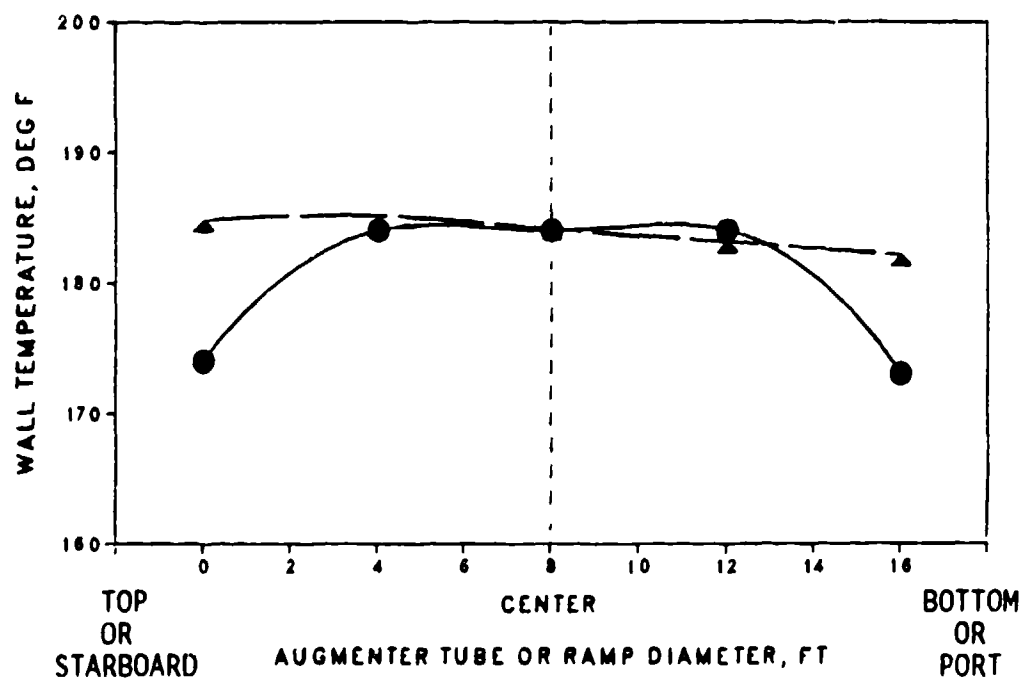


Figure 36. Temperature profiles across augments tube and ramp while testing F404-GE-400 at Mil with out throttle plate.

NOTES:

- (1) AVERAGED OVER A 60-SECOND RUN
- (2) RAMP TEMPS AND THOSE MEASURED AT STARBOARD, PORT, AND BOTTOM OF TUBE DIAM ARE WALL SURFACE VALUES; ALL OTHERS ARE GAS TEMPS

MEASURED 11/19/86

- ALONG VERTICAL TUBE DIAM OR RAMP PROJECTED SURFACE
- ▲ ALONG HORIZONTAL TUBE DIAM OR RAMP PROJECTED SURFACE

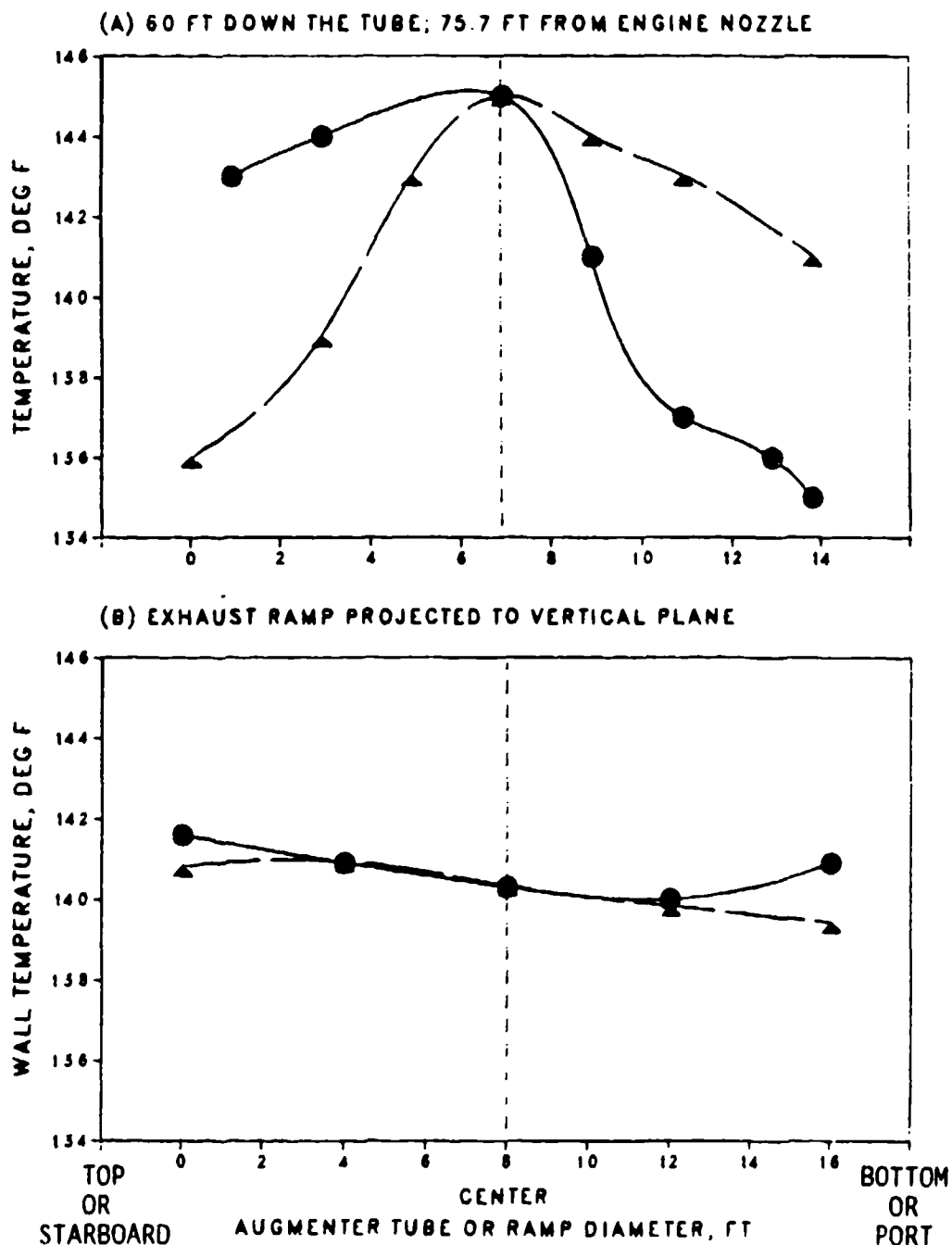


Figure 37. Temperature profiles across augmentor tube and ramp while testing F404-GE-400 at 85% without throttle plate.

NOTES:

(1) J52-P-8B AT MIL

(2) WITH THROTTLE PLATE

● ENGINE MISALIGNED 2.3 DEGREES TO PORT

▲ ENGINE MISALIGNED 1.0 DEGREE TO PORT

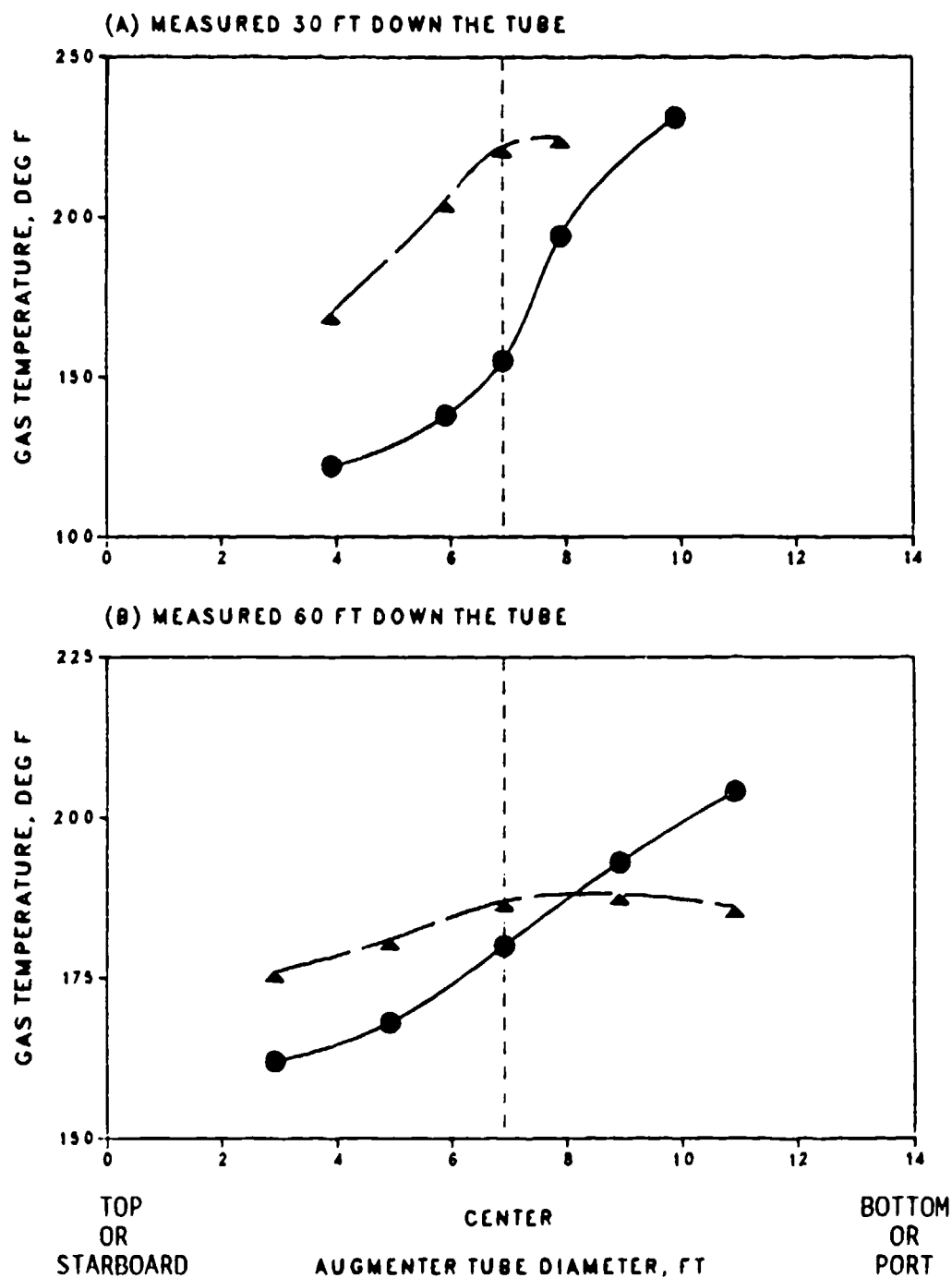
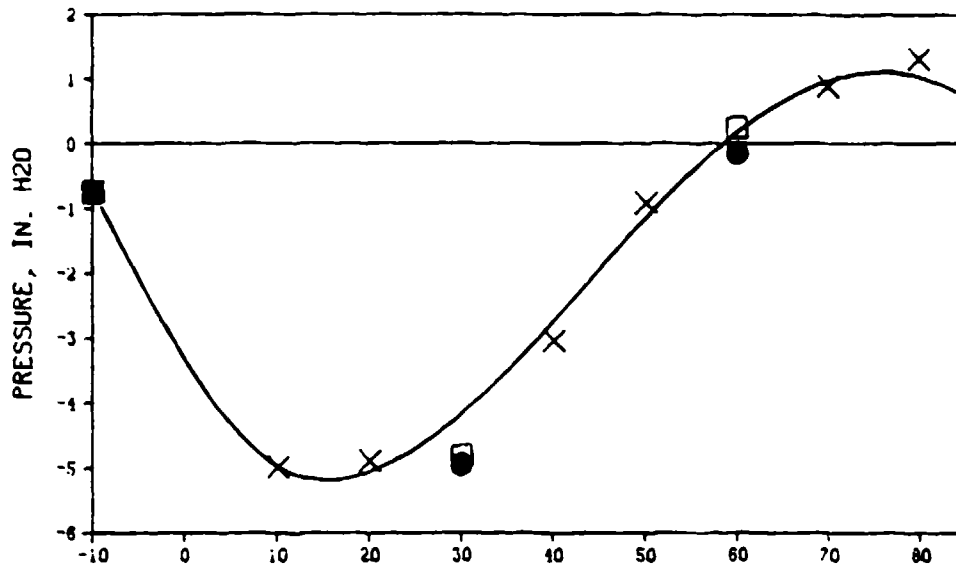


Figure 38. Effect of misalignment on augmeter tube gas temperatures.

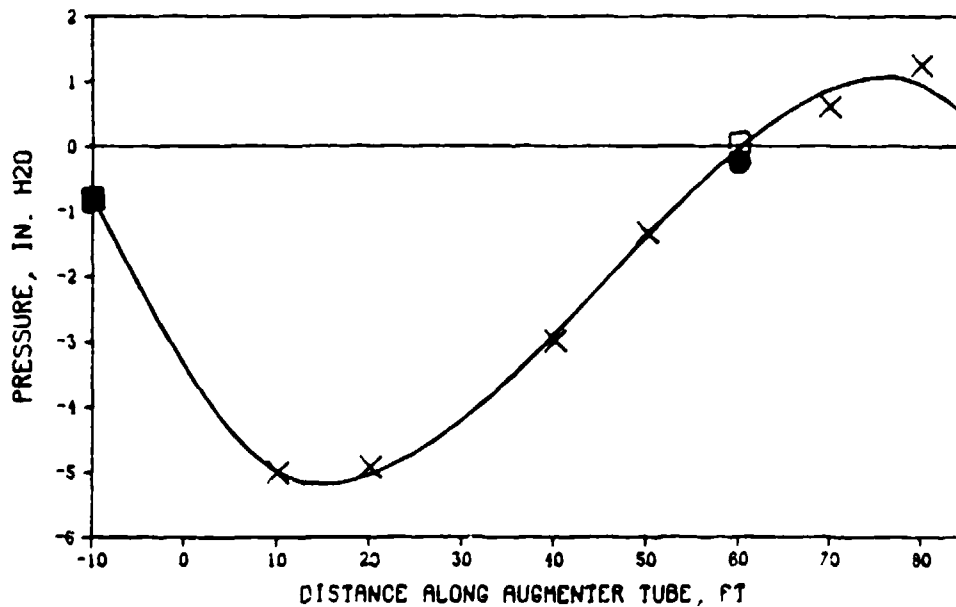
NOTE:
TUBE STARTS 15.3 FT FROM ENGINE NOZZLE

MEASURED 11/12/86 (W/THROTTLE), AND 11/19/86

- CELL DEPRESSION
- × PORT SIDEWALL
- TOP OF TUBE
- BOTTOM OF TUBE



(A) WITH THROTTLE PLATE



(B) WITHOUT THROTTLE PLATE

Figure 39. Static pressure distribution along augmeter tube while testing TF41-A-2C at Mil.

NOTE:

(1) AVERAGED OVER A 30-SECOND BURN

(2) AUGMENTER TUBE STARTS 13.1 FT FROM ENGINE NOZZLE

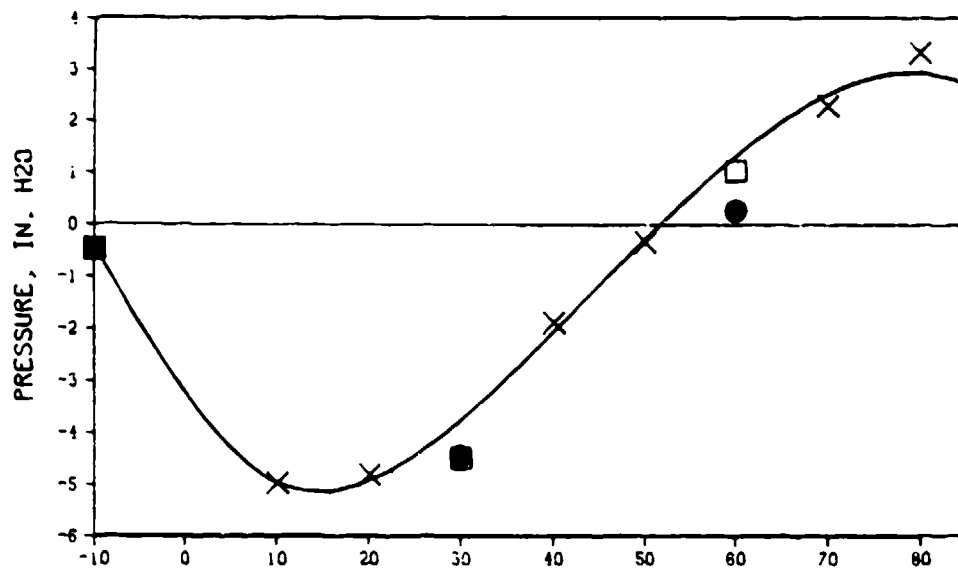
MEASURED 11/14/86 (W/THROTTLE), AND 11/18/86

● CELL DEPRESSION

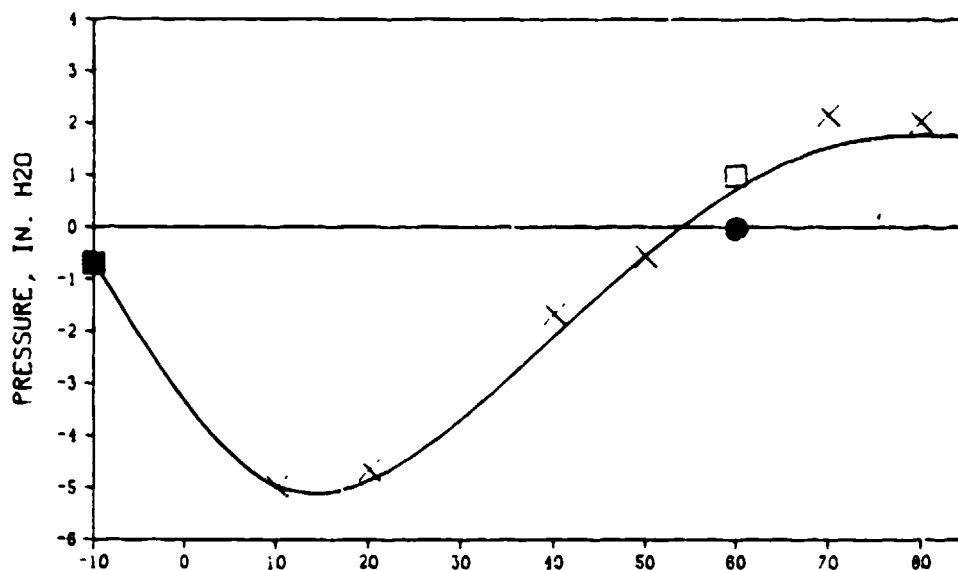
□ PORT SIDEWALL

× TOP OF TUBE

■ BOTTOM OF TUBE



(A) WITH THROTTLE PLATE



DISTANCE ALONG AUGMENTER TUBE, FT

(B) WITHOUT THROTTLE PLATE

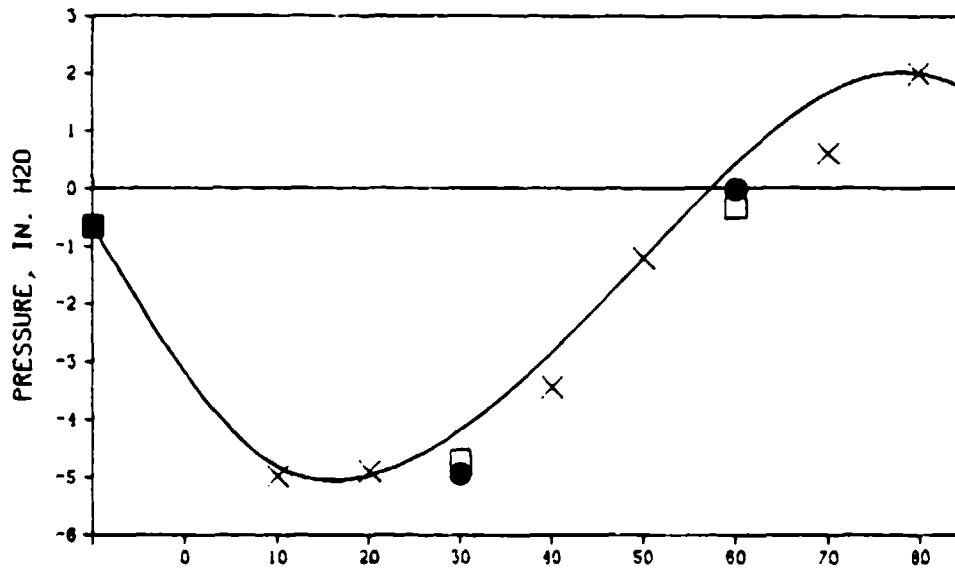
Figure 40. Static pressure distribution along augmeter tube while testing TF30-P-414A at A/B.

NOTE:

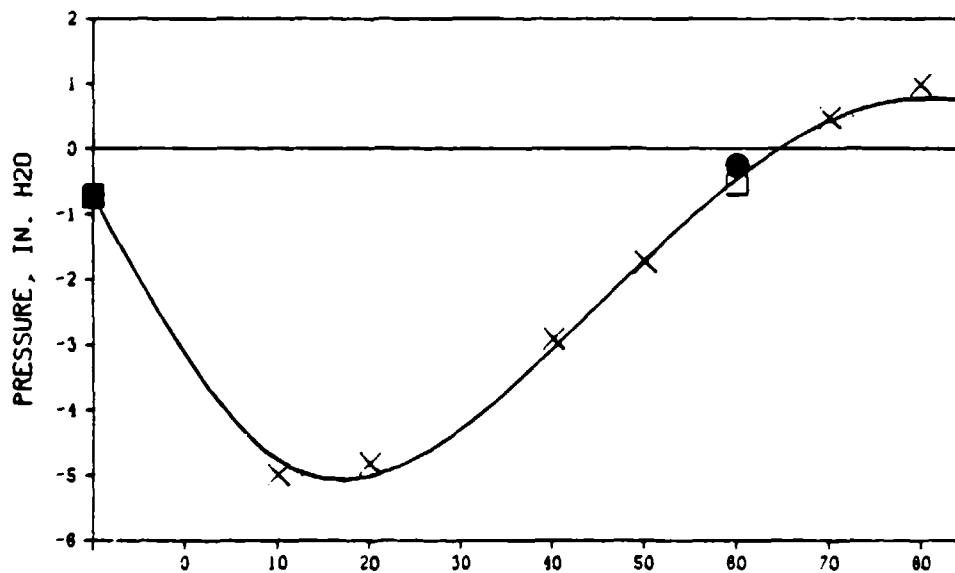
- (1) AUGMENTER TUBE STARTS 13.1 FT FROM ENGINE NOZZLE
- (2) PRESSURES AVERAGED OVER 60-SECOND RUN

MEASURED 11/14/86 (W/THROTTLE), AND 11/18/86

- CELL DEPRESSION
- × PORT SIDEWALL
- TOP OF TUBE
- BOTTOM OF TUBE



(A) WITH THROTTLE PLATE



DISTANCE ALONG AUGMENTER TUBE, FT

(B) WITHOUT THROTTLE PLATE

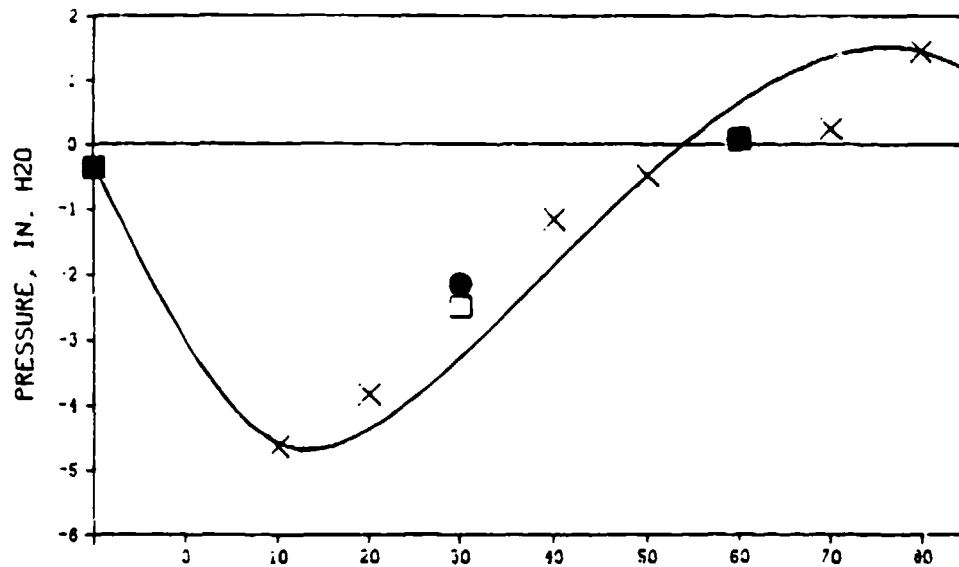
Figure 41. Static pressure distribution along augmenter tube while testing TF30-P-414A at Mil.

NOTE:

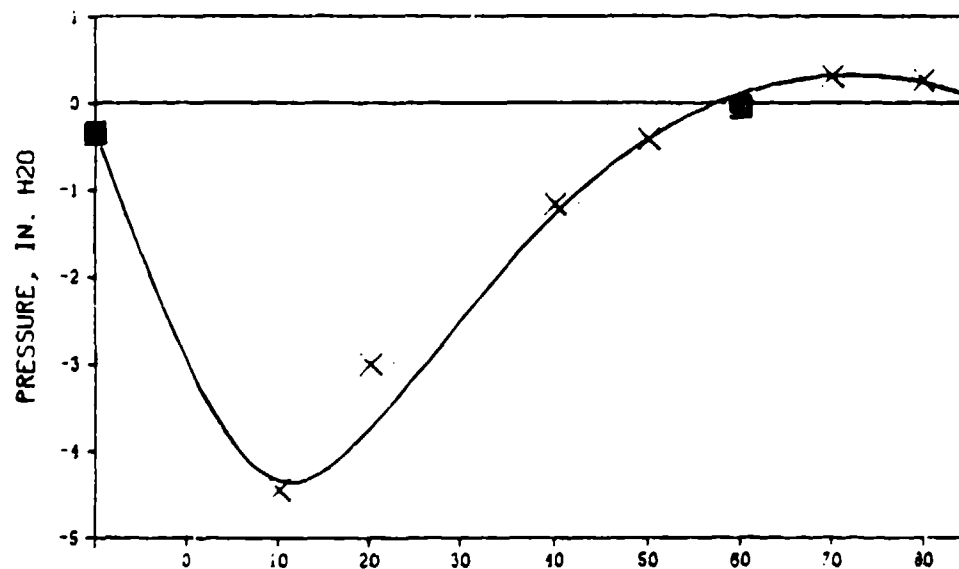
- (1) AUGMENTER TUBE STARTS 13.1 FT FROM ENGINE NOZZLE
- (2) PRESSURES AVERAGED OVER 60-SECOND RUN

MEASURED 11/14/86 (W/THROTTLE), AND 11/18/86

- CELL DEPRESSION
- × PORT SIDEWALL
- TOP OF TUBE
- BOTTOM OF TUBE



(A) WITH THROTTLE PLATE



DISTANCE ALONG AUGMENTER TUBE, FT

(B) WITHOUT THROTTLE PLATE

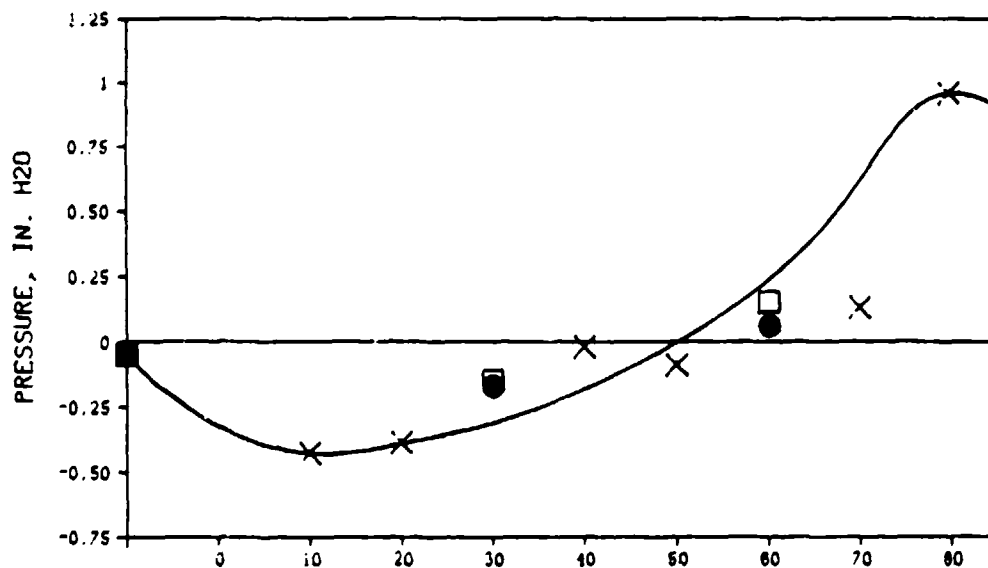
Figure 42. Static pressure distribution along augmenter tube while testing TF30-P-414A at 85%.

NOTE:

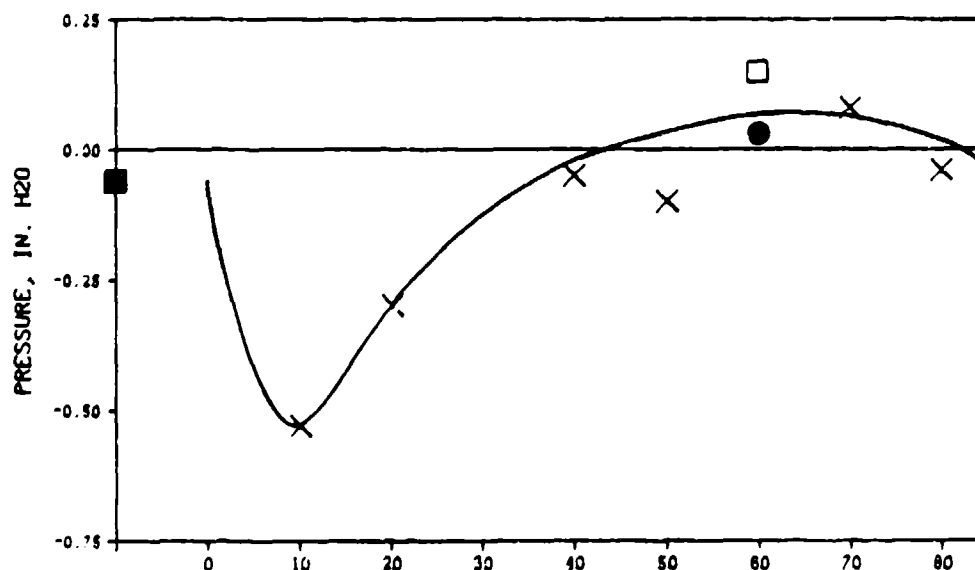
- (1) AUGMENTER TUBE STARTS 13.1 FT FROM ENGINE NOZZLE
- (2) PRESSURES AVERAGED OVER 60-SECOND RUN

MEASURED 11/14/86 (W/THROTTLE), AND 11/18/86

- CELL DEPRESSION
- × PORT SIDEWALL
- TOP OF TUBE
- BOTTOM OF TUBE



(A) WITH THROTTLE PLATE



DISTANCE ALONG AUGMENTER TUBE, FT

(B) WITHOUT THROTTLE PLATE

Figure 43. Static pressure distribution along augmenter tube while testing TF30-P-414A at idle.

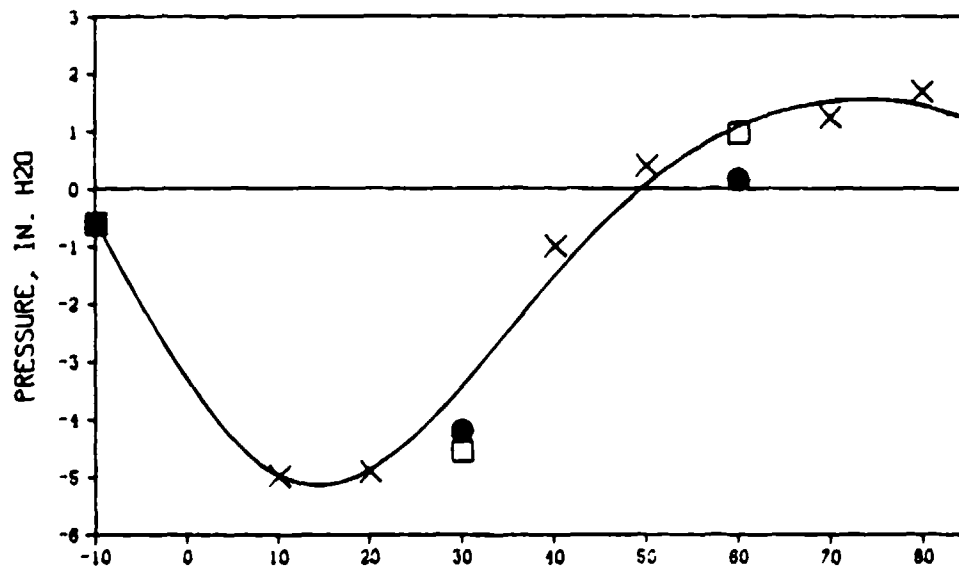
NOTE:

(1) AVERAGED OVER 30-SECOND BURN

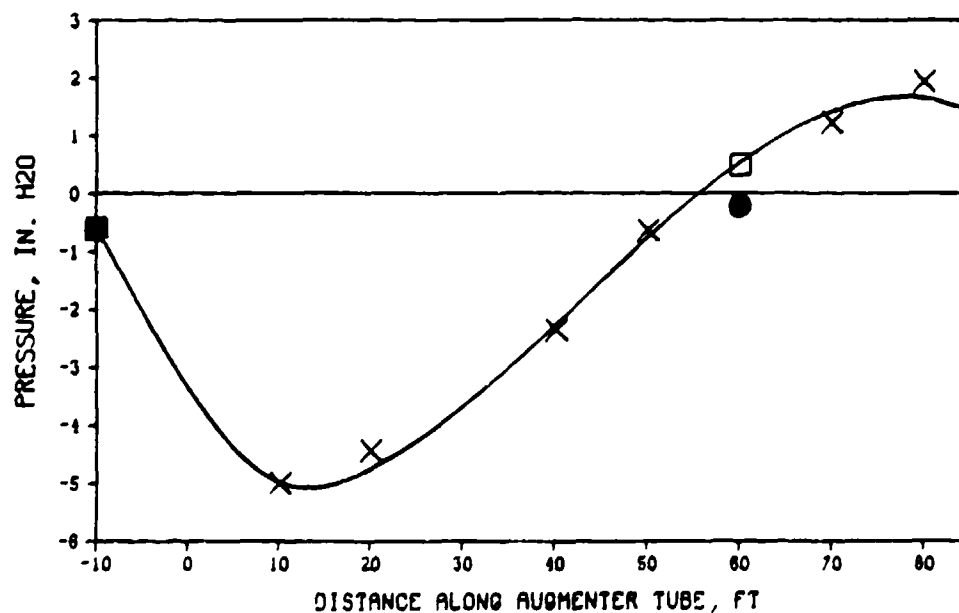
(2) AUGMENTER TUBE STARTS 15.7 FT FROM ENGINE NOZZLE

MEASURED 11/11/86 (W/THROTTLE), AND 11/19/86

- CELL DEPRESSION
- × PORT SIDEWALL
- TOP OF TUBE
- BOTTOM OF TUBE



(A) WITH THROTTLE PLATE



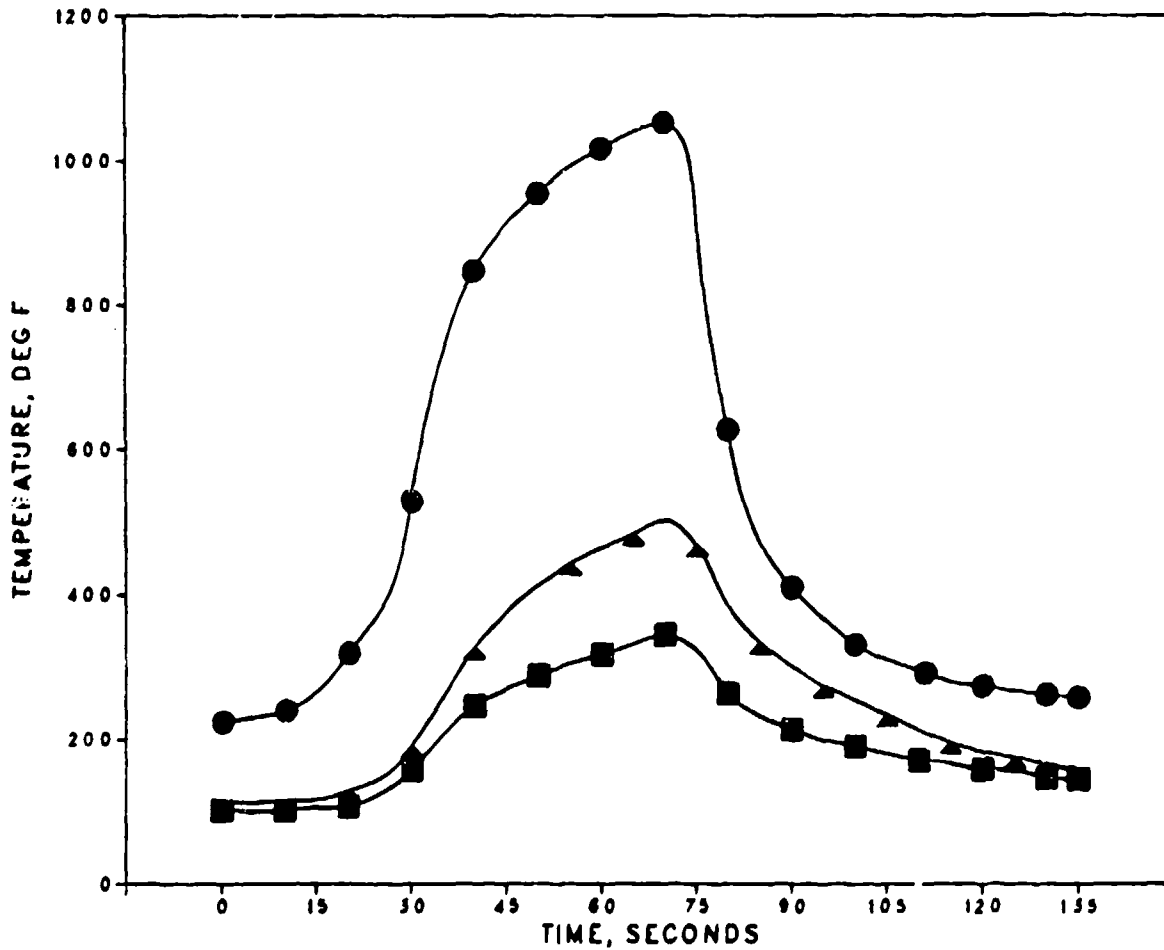
(B) WITHOUT THROTTLE PLATE

Figure 44. Static pressure distribution along augmeter tube while testing F404-GE-400 at A/B.

NOTES:

- (1) THROTTLE PLATE INSTALLED
- (2) 30 FT DOWN THE TUBE; 4.3.1 FT FROM ENGINE NOZZLE
- (3) MEASURED 11/14/86

- GAS TEMPERATURES AT TUBE CENTERLINE
- ▲ GAS TEMPERATURES 2 FT OUT FROM BOTTOM OF TUBE
- TUBE WALL AT BOTTOM



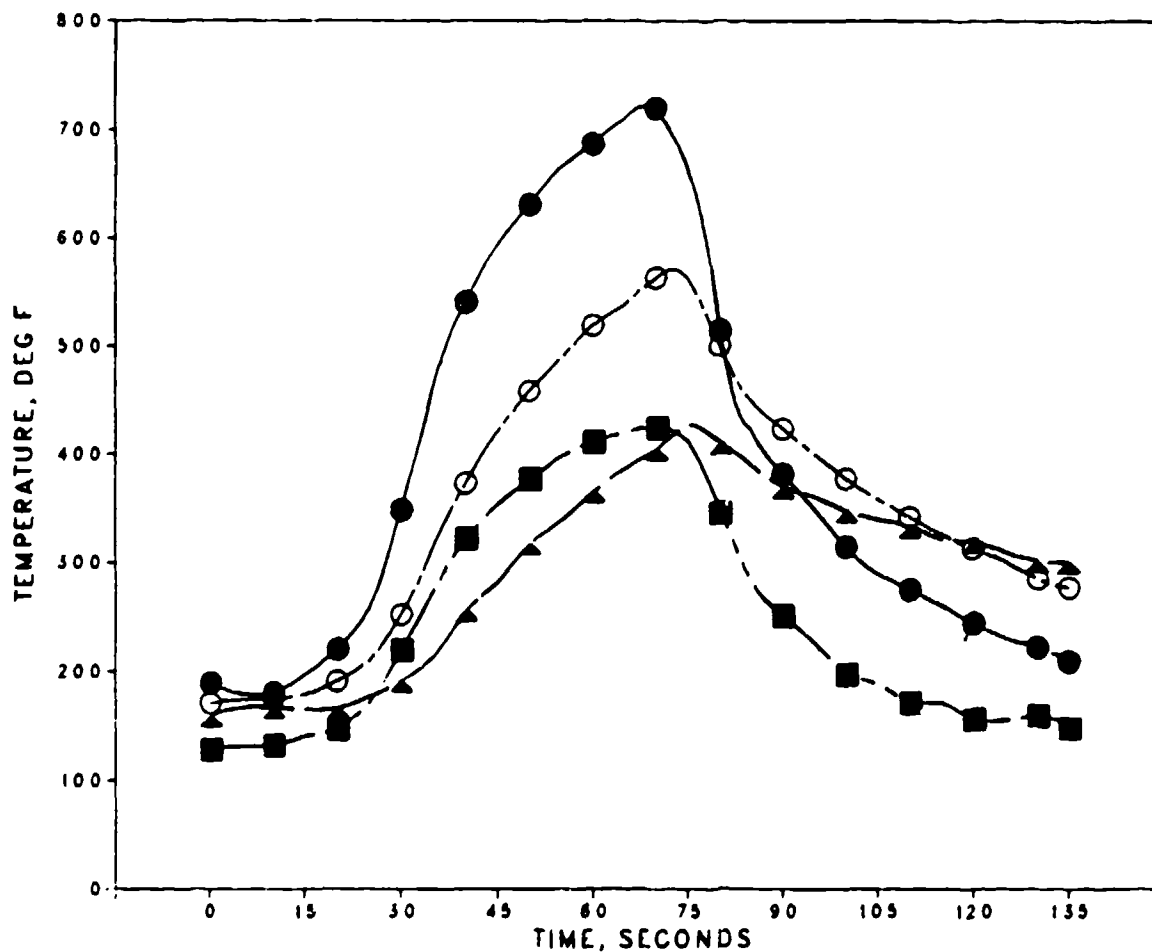
(a) Aerothermal temperatures on forward instrumentation rack.

Figure 45. Augmenter tube temperatures during TF30 transient from M11 to A/B and back down to M11.

NOTES:

- (1) THROTTLE PLATE INSTALLED
- (2) 60 FT DOWN THE TUBE; 7.3.1 FT FROM ENGINE NOZZLE
- (3) MEASURED 11/14/86

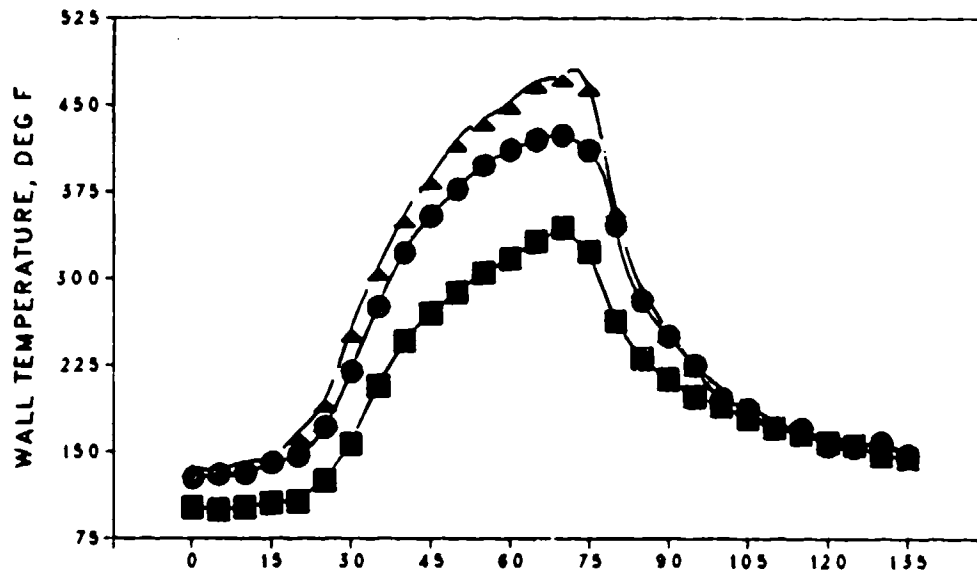
- GAS TEMPERATURES AT TUBE CENTERLINE
- ▲ GAS TEMPERATURES 1 FT UP FROM BOTTOM OF TUBE
- TUBE WALL AT BOTTOM
- RAMP



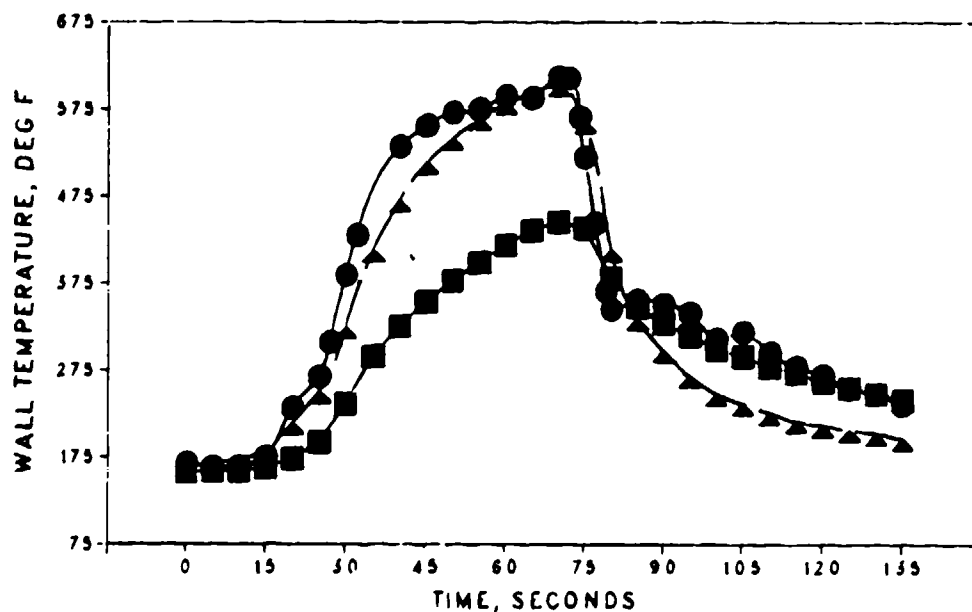
(b) Aerothermal temperatures on rear instrumentation rack.

NOTES:
THROTTLE PLATED INSTALLED
MEASURED 11/14/86

- STARBOARD SIDE
- ▲ PORT SIDE
- BOTTOM OF WALL

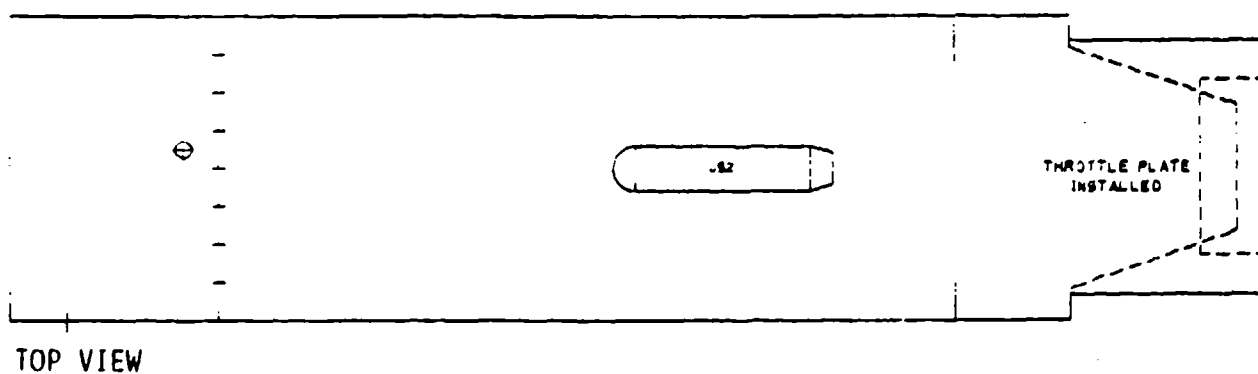
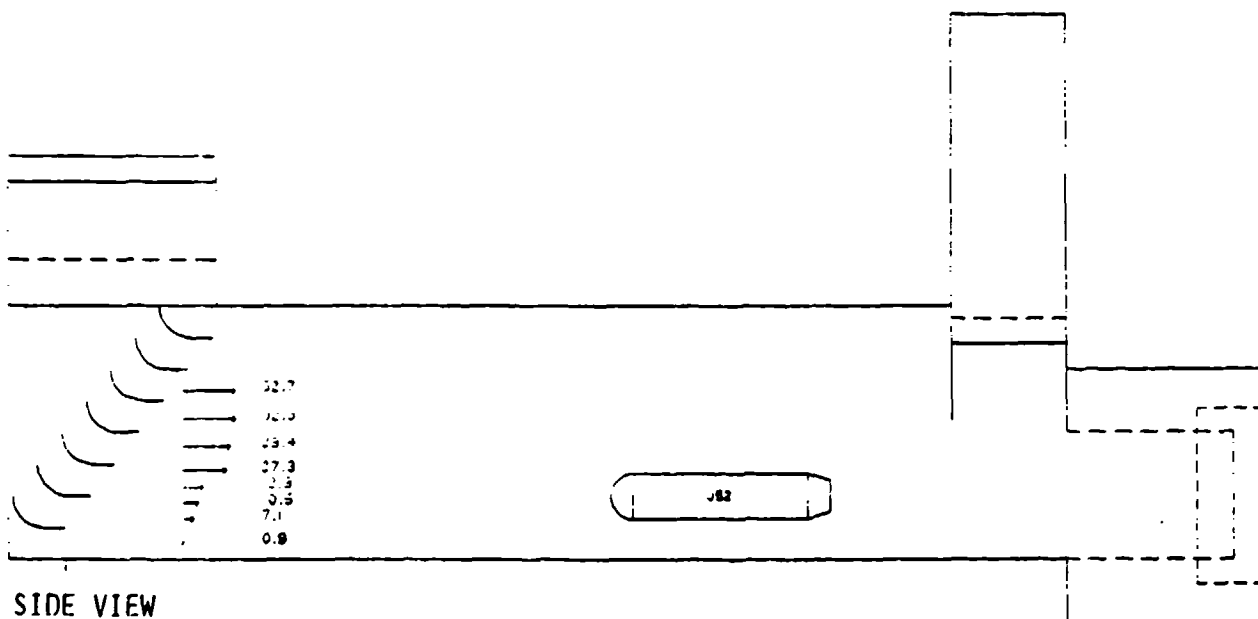


30 FT DOWN THE TUBE



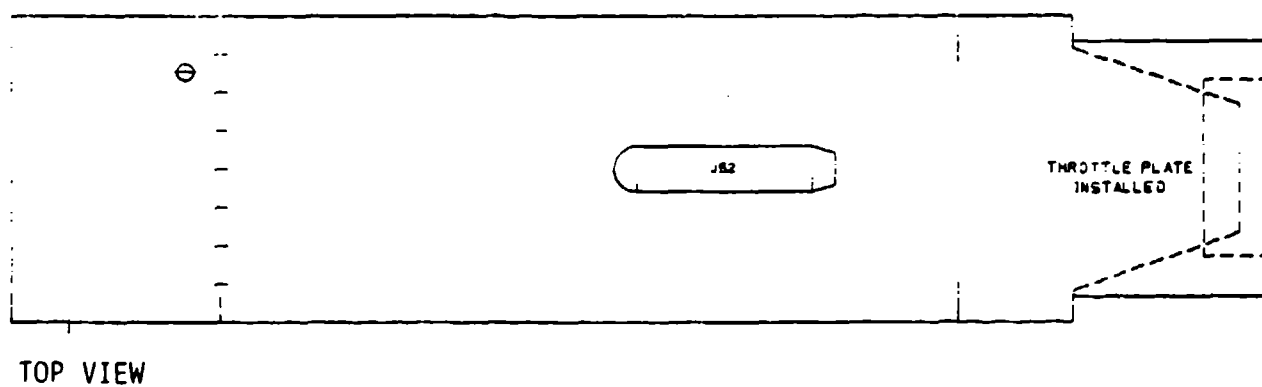
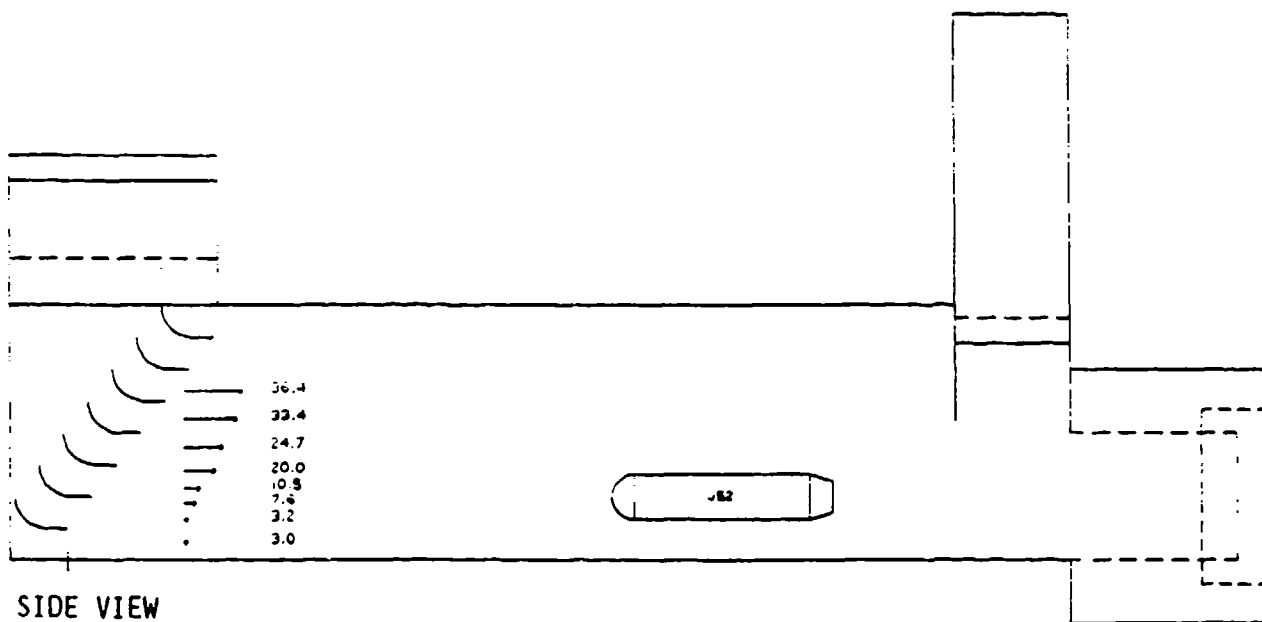
60 FT FOWN THE TUBE

(c) Variation of tube wall temperatures, at different circumferential location.

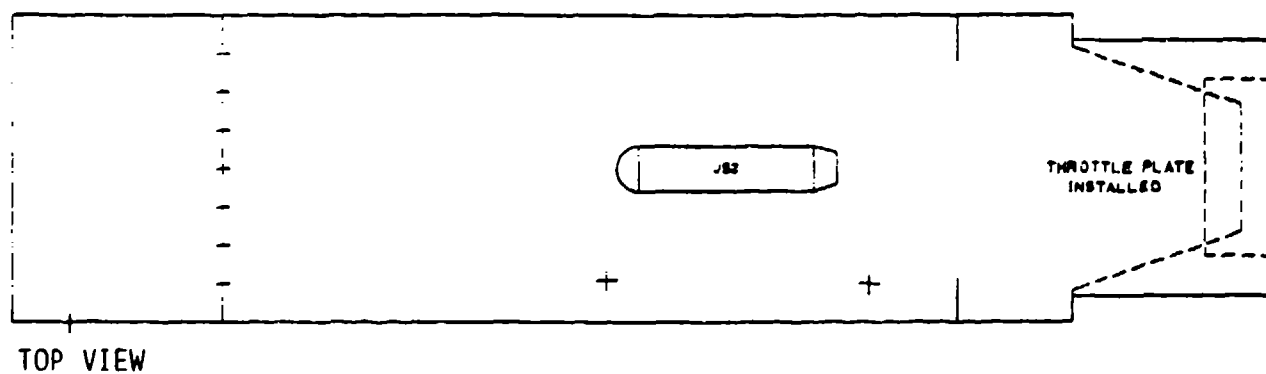
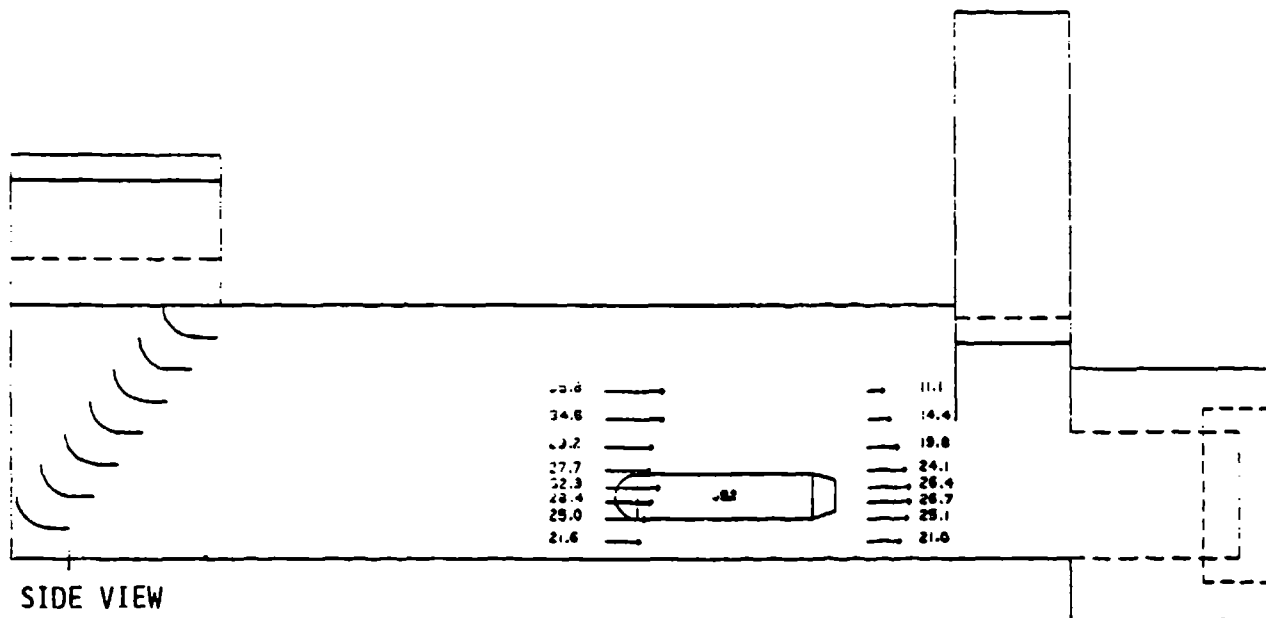


^ Airflows (ft/sec) inside test bay while testing J52-P-8B
at Mil: Test run 1.

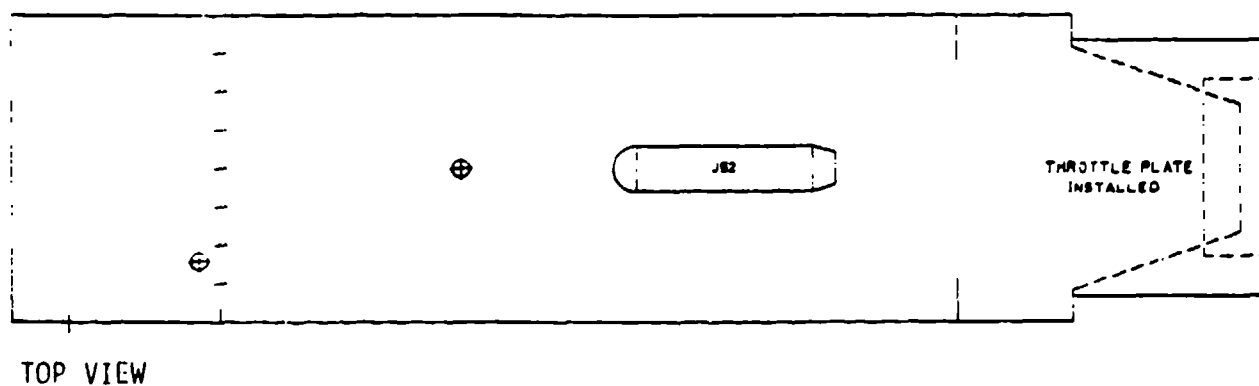
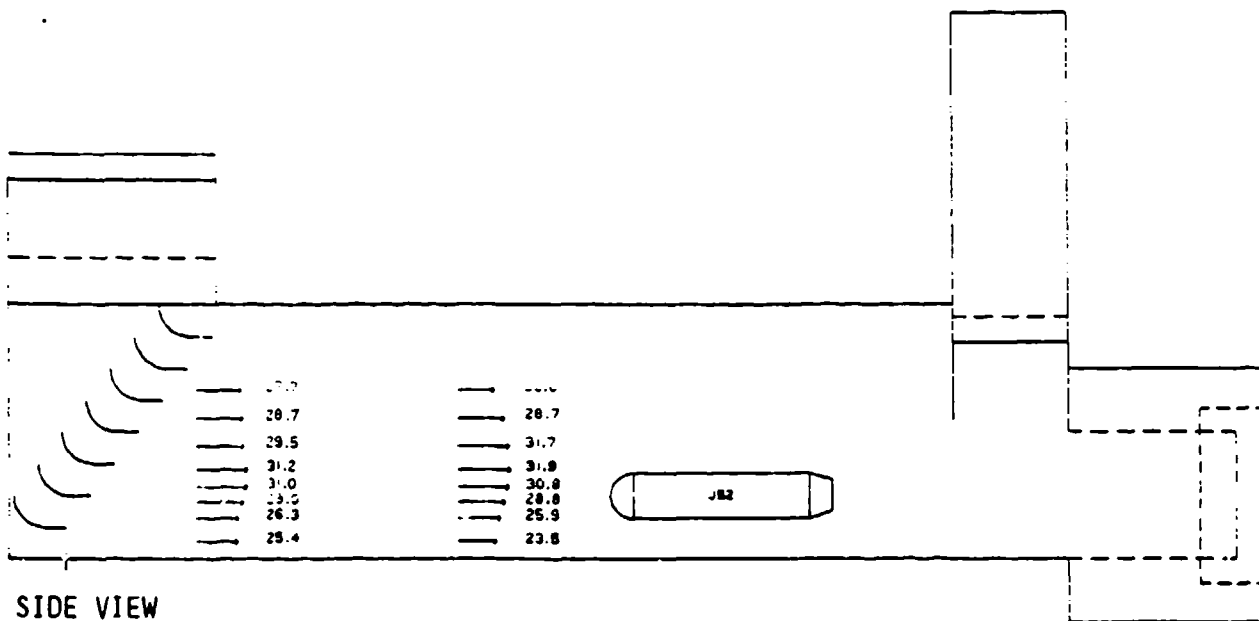
Figure 46. Airflows (ft/sec) inside test bay while testing J52-P-8B.



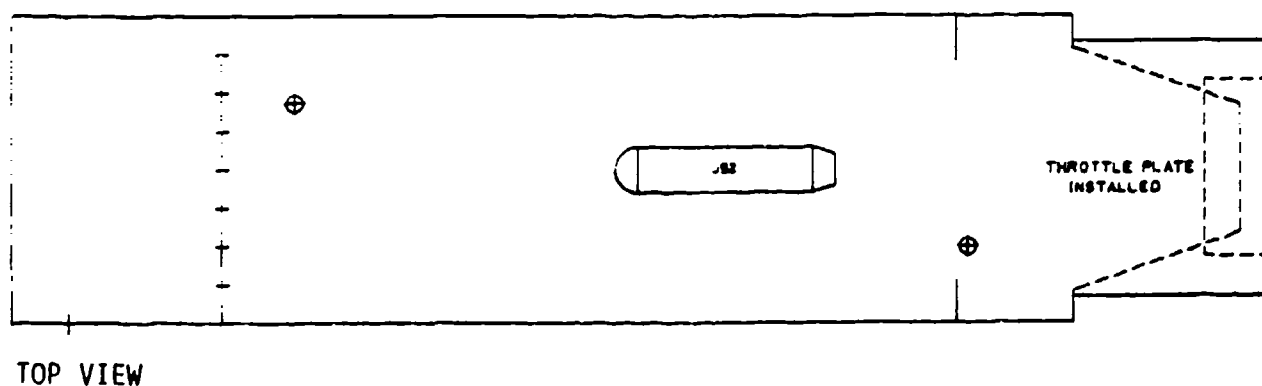
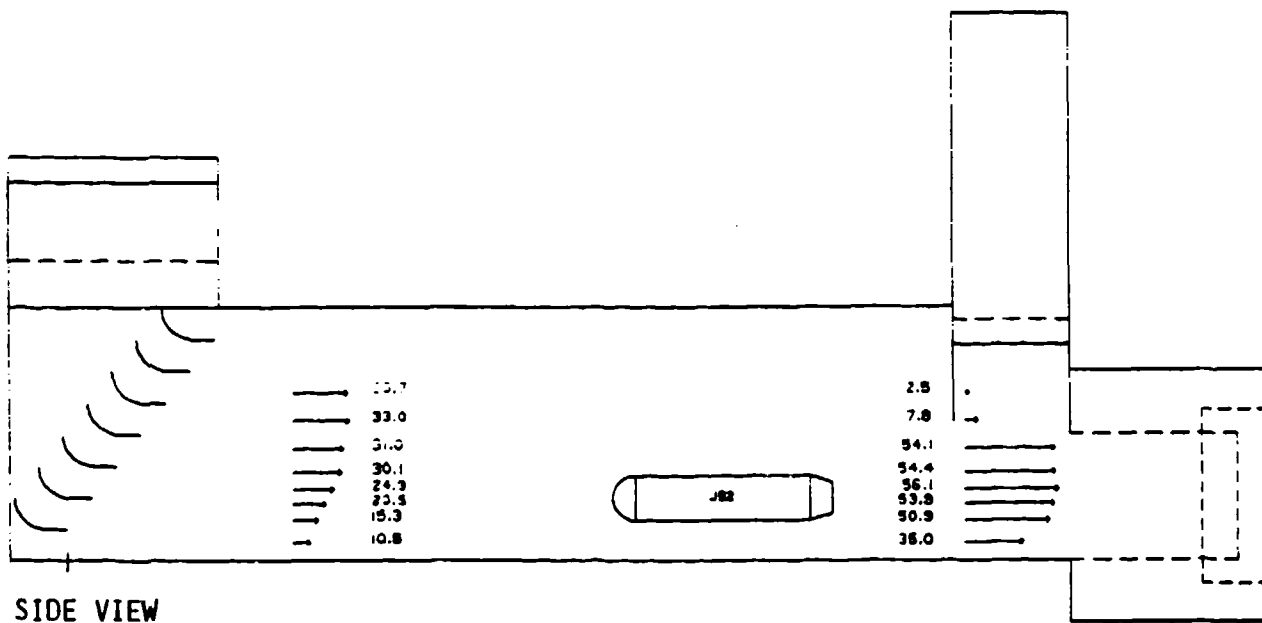
R Airflows (ft/sec) inside test bay while testing J52-P-8B
at M1: Test run 2.



C Airflows (ft/sec) inside test bay while testing J52-P-8B at M11: Test run 3.

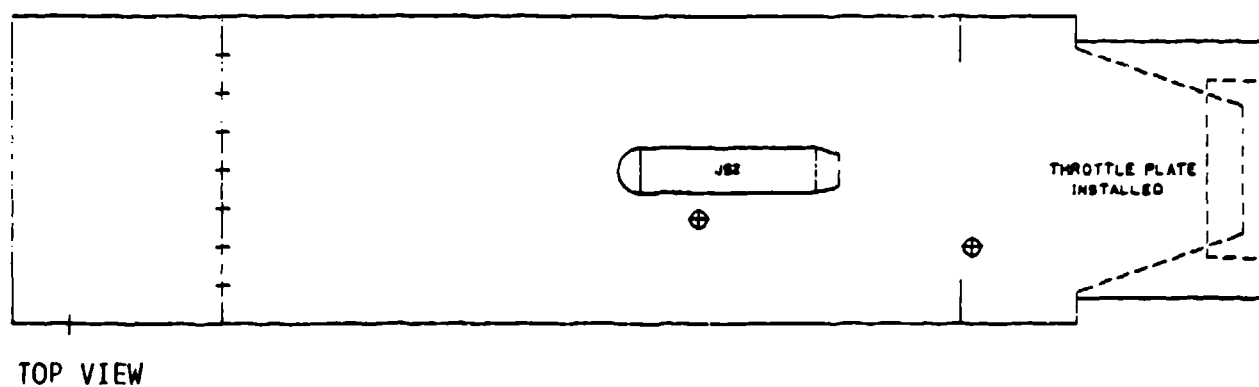
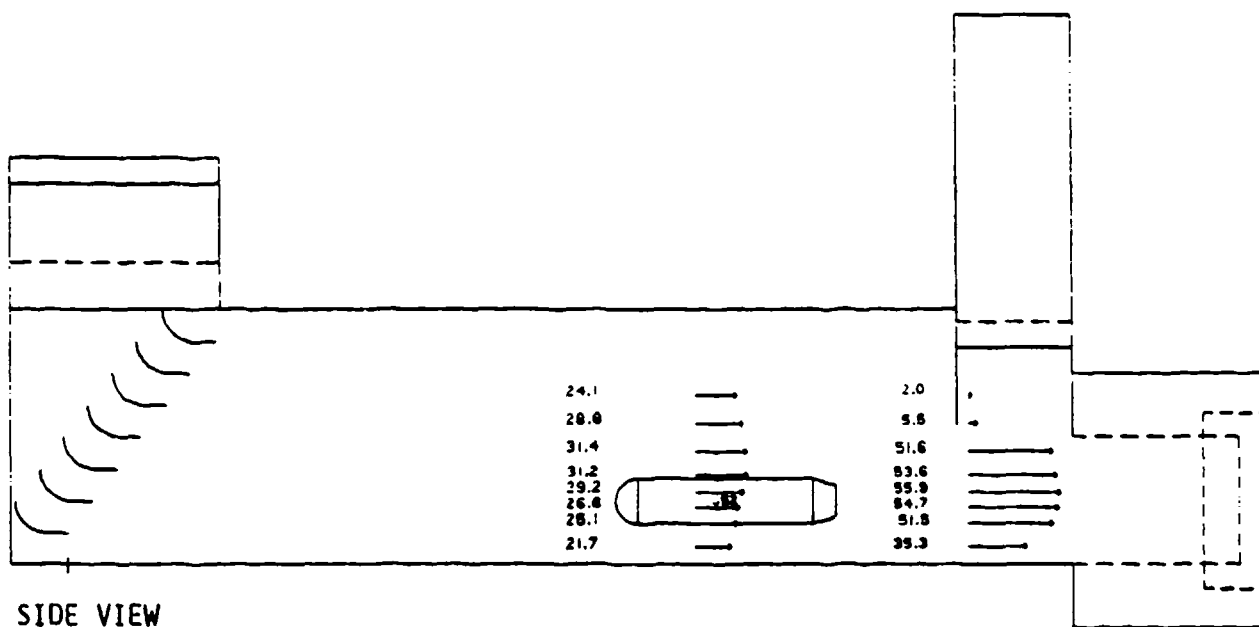


D Airflows (ft/sec) inside test bay while testing J52-P-8B at M1: Test run 4.



A Airflows (ft/sec) inside test bay while testing J52-P-408 at Mil: Test run 1.

Figure 47. Airflows (ft/sec) inside test bay while testing J52-P-408.



B Airflows (ft/sec) inside test bay while testing J52-P-408 at Mil: Test run 2.

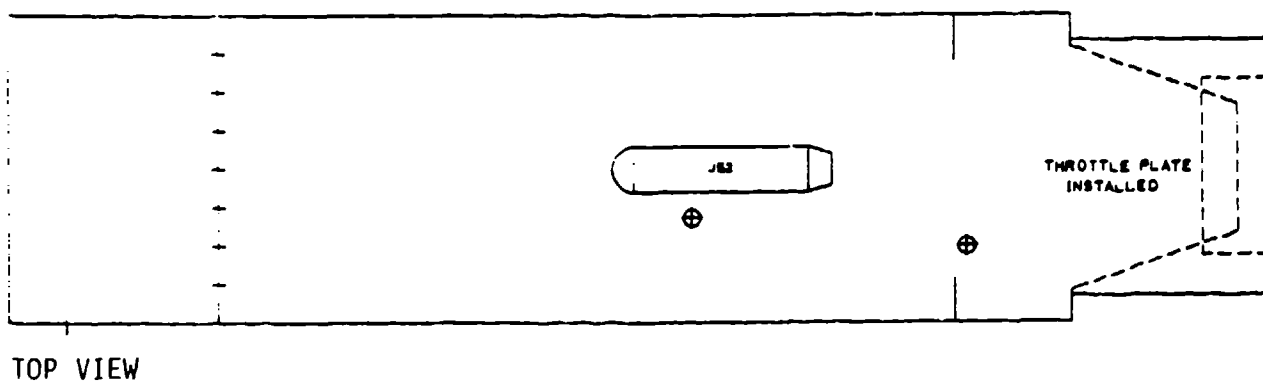
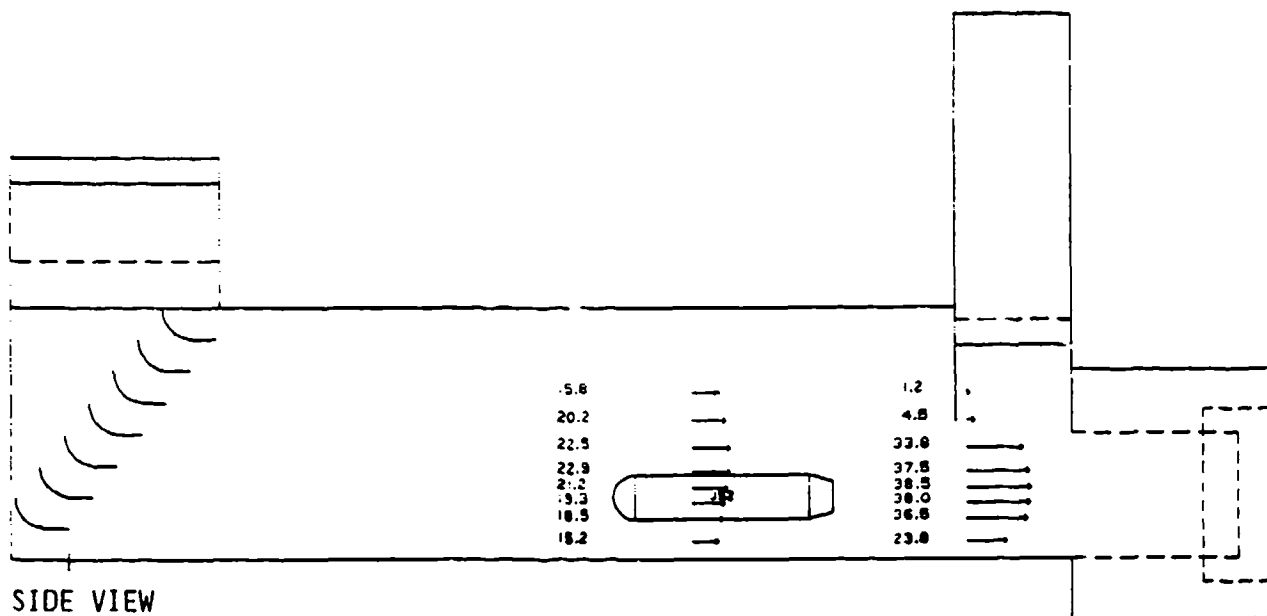


Figure 48. Airflows (ft/sec) inside test bay while testing J52-P-408 at 85%.

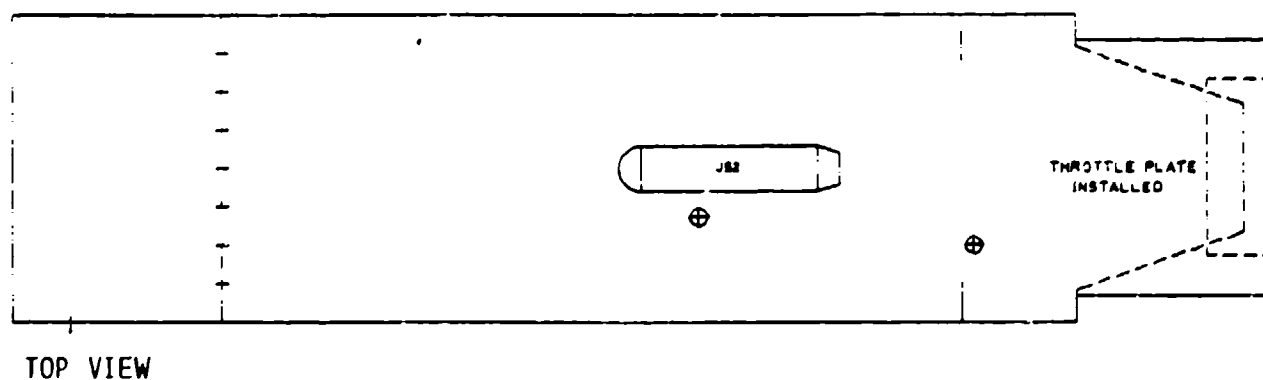
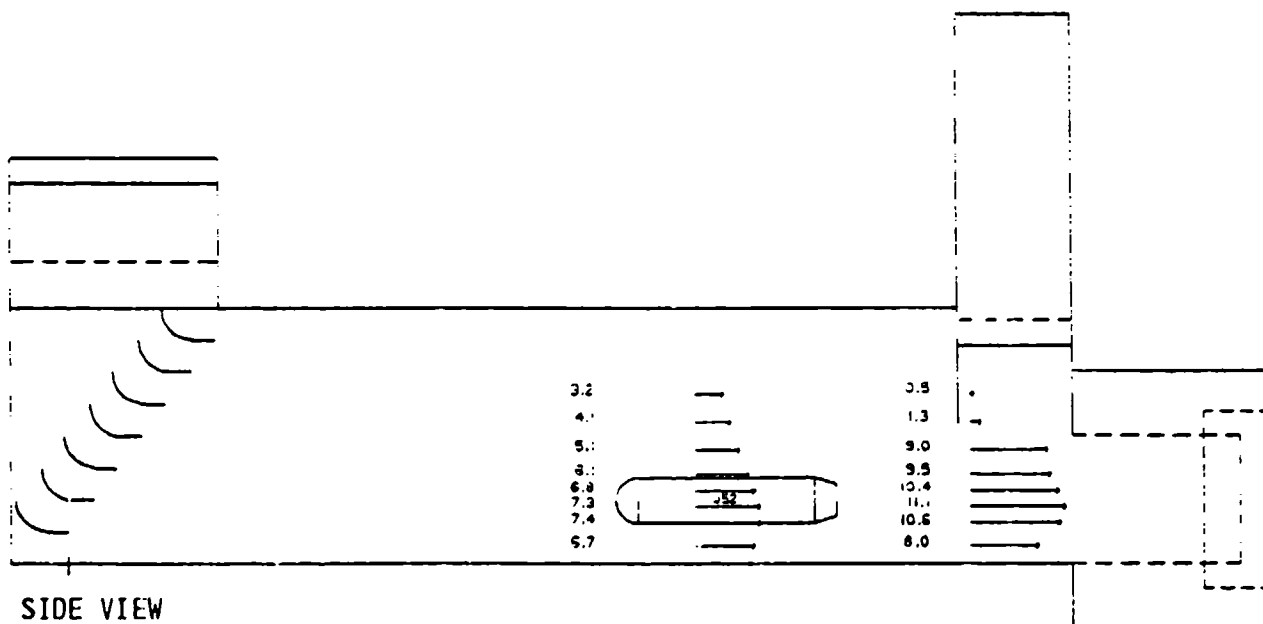
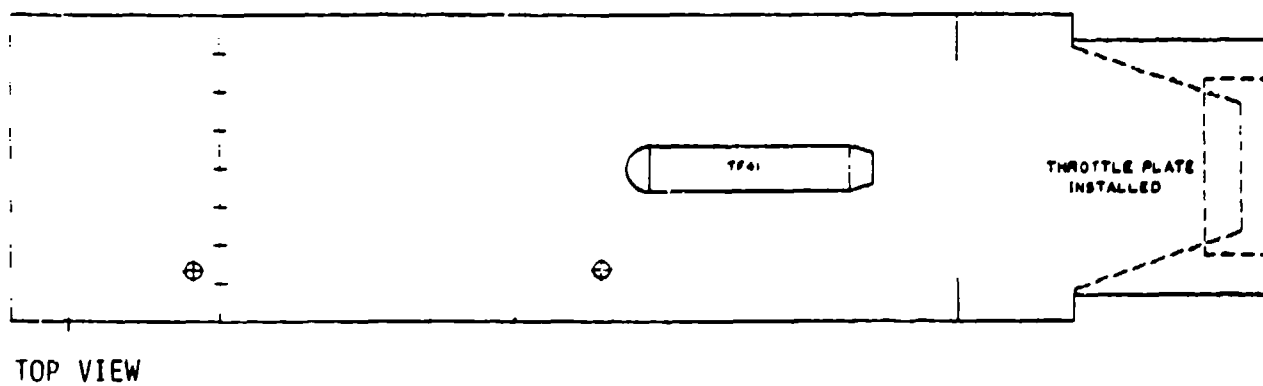
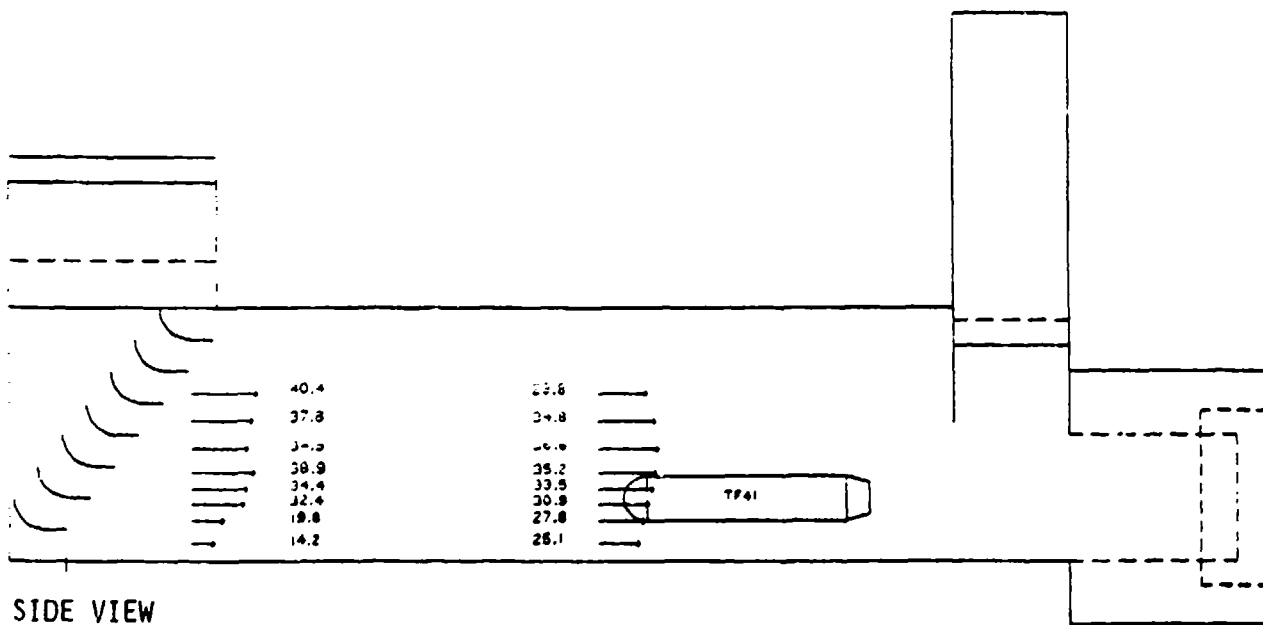
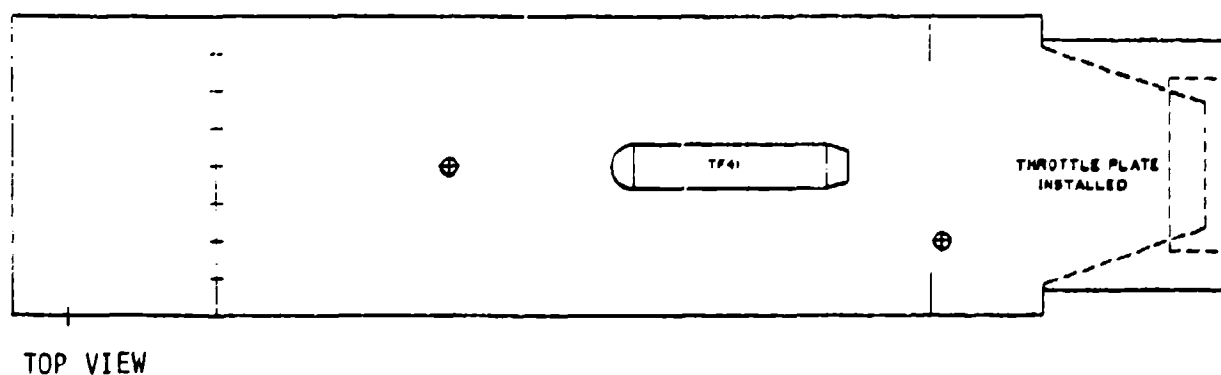
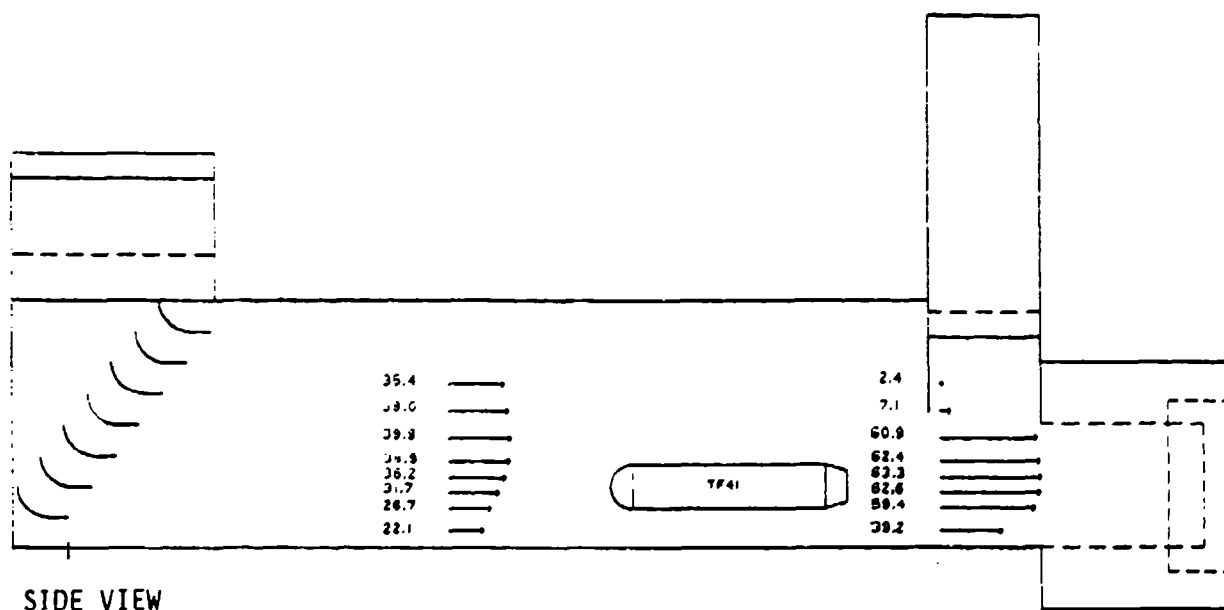


Figure 49. Airflows (ft/sec) inside test bay while testing J52-P-408 at idle.



A Airflows (ft/sec) inside test bay while testing TF41-A-2C at M1; Test run 1.

Figure 50. Airflows (ft/sec) inside test bay while testing TF41-A-2C.



B Airflow (ft/sec) inside test bay while testing TF41-A-2C at M11: Test run 2.

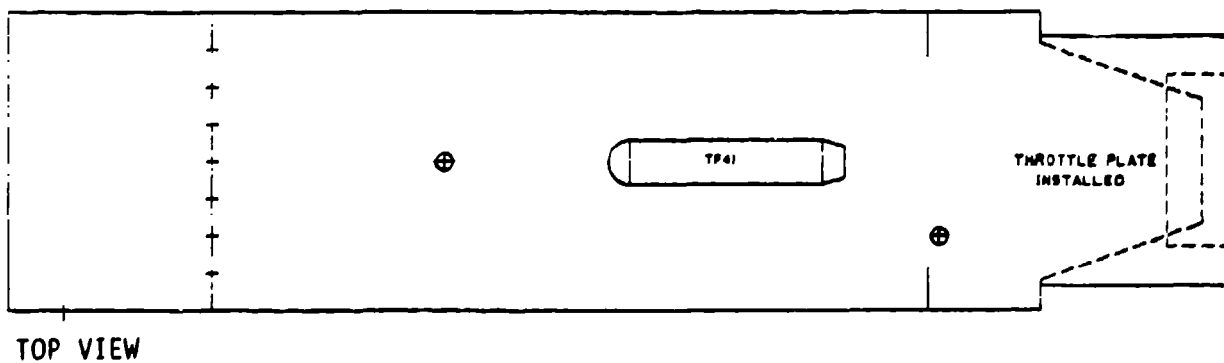
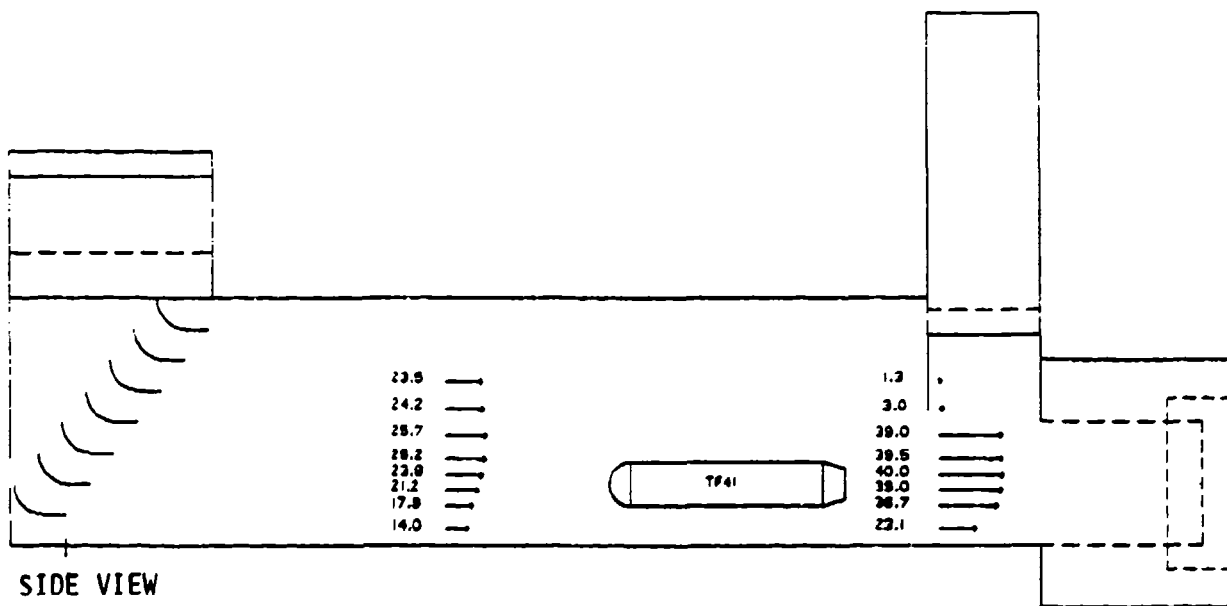


Figure 51. Airflows (ft/sec) inside test bay while testing TF41-A-2C at 85%.

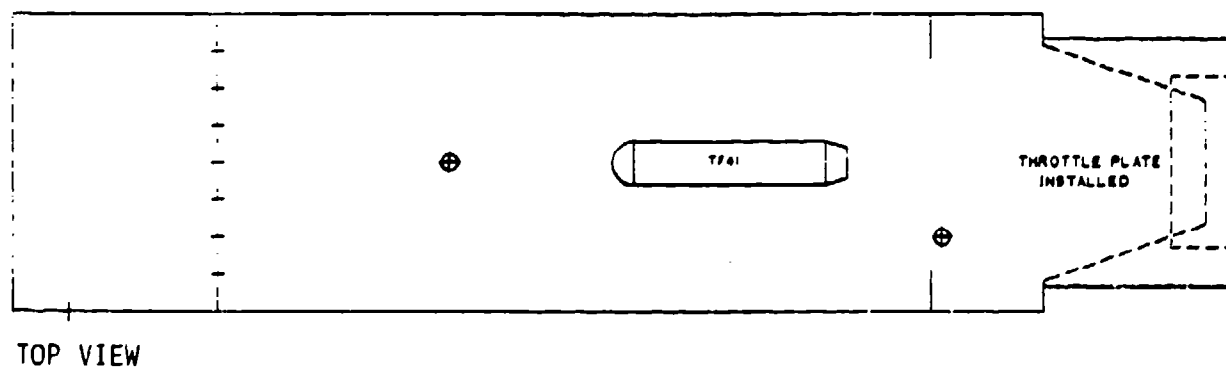
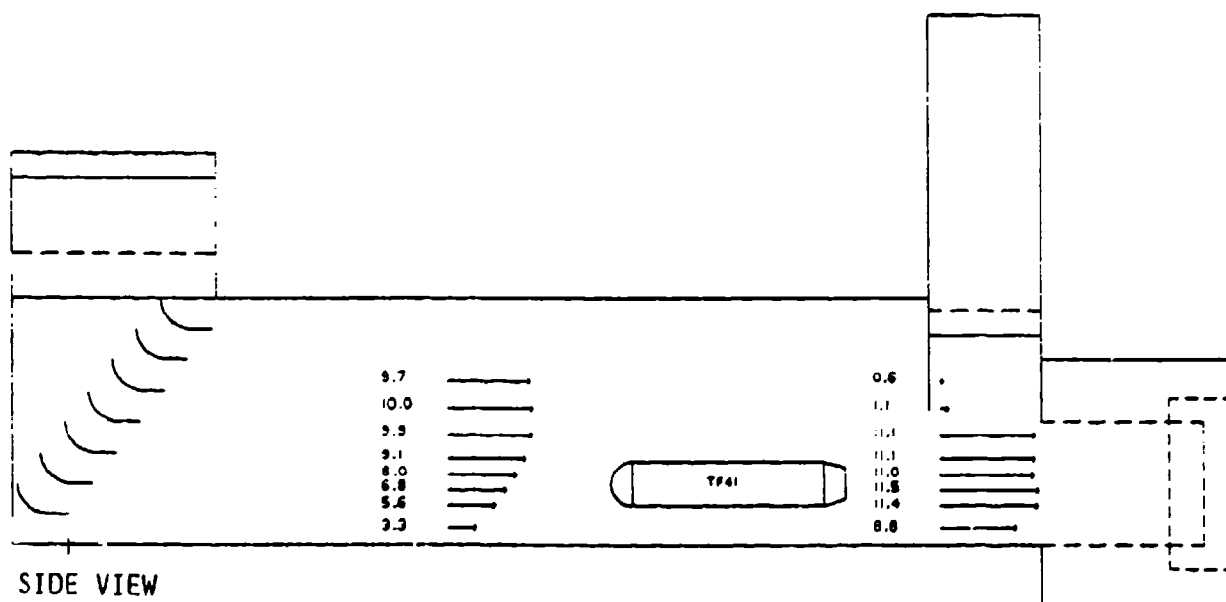


Figure 52. Airflows (ft/sec) inside test bay while testing TF41-A-2C at idle.

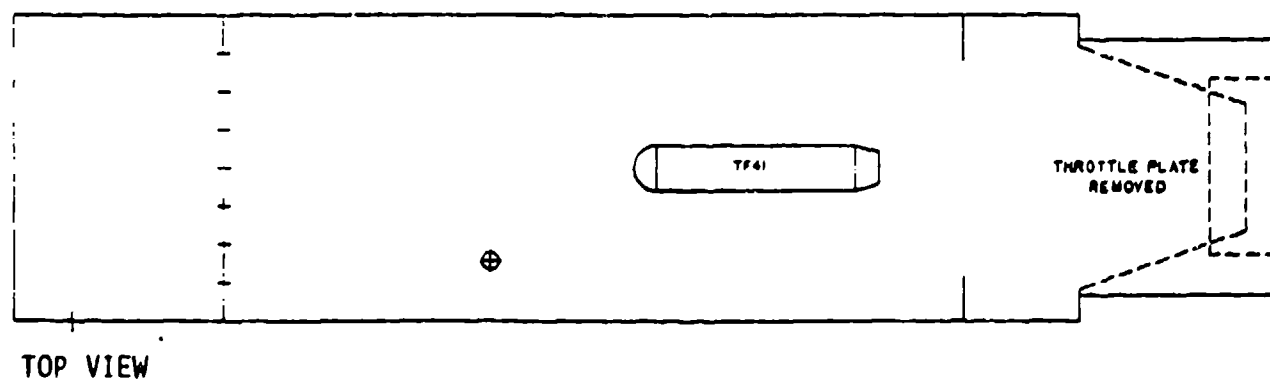
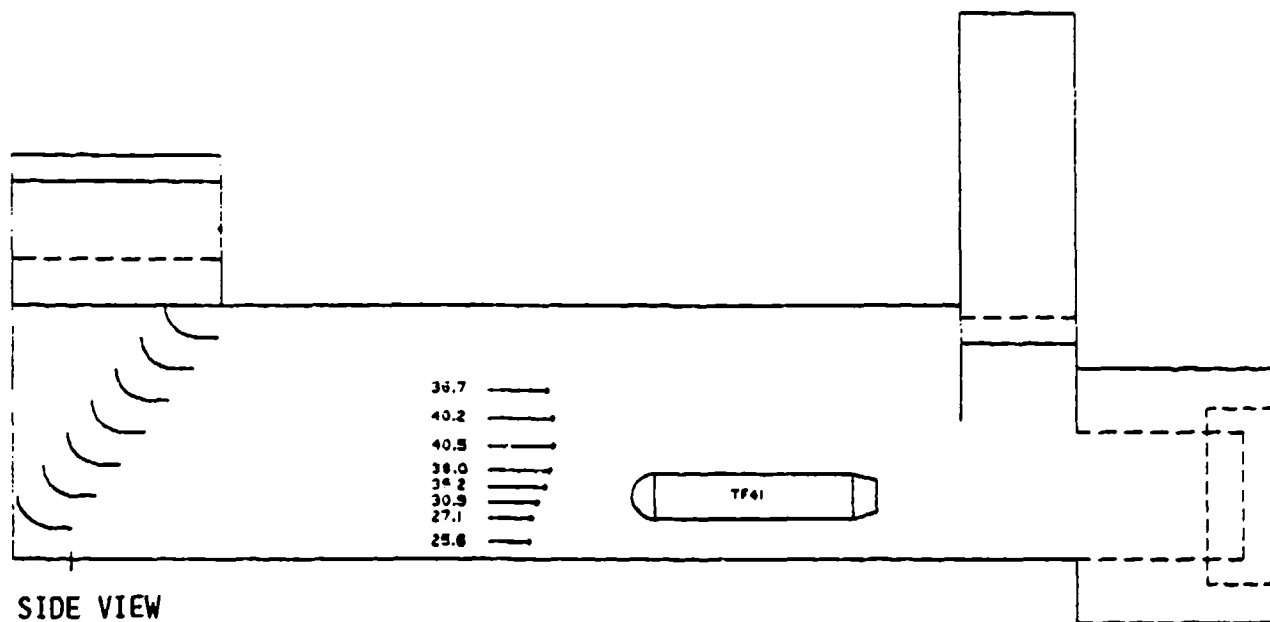


Figure 53. Airflows (ft/sec) inside test bay while testing TF41-A-2C at Mil.

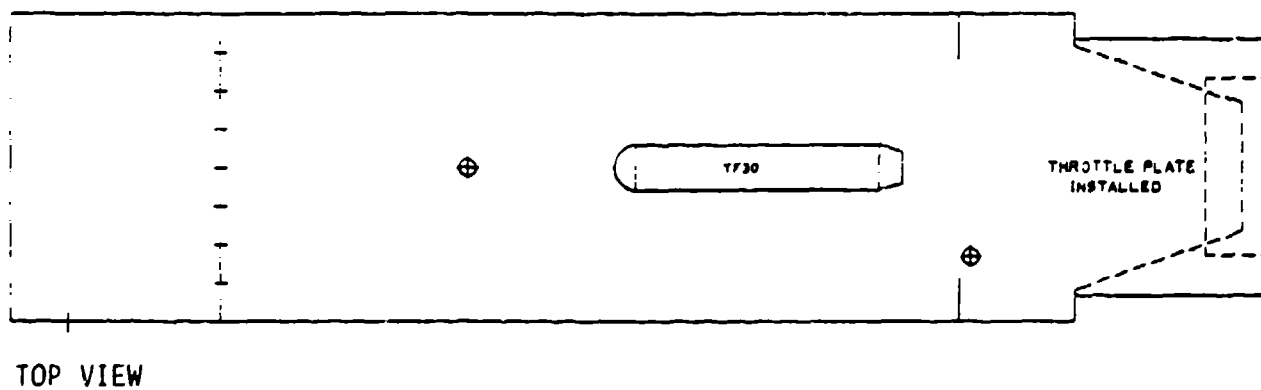
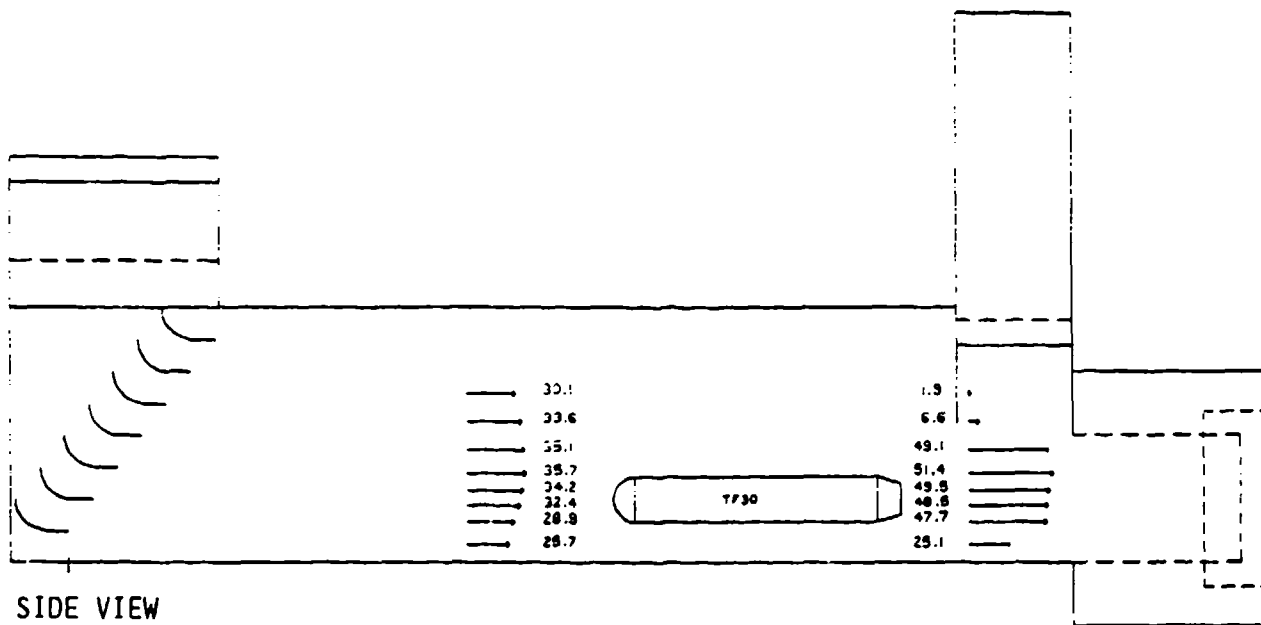


Figure 54. Airflows (ft/sec) inside test bay while testing TF30-P-414A at A/B.

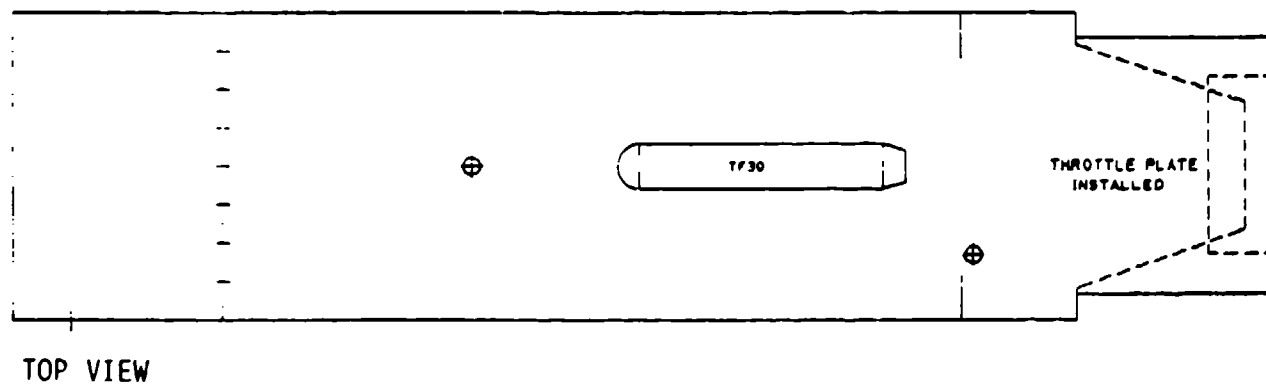
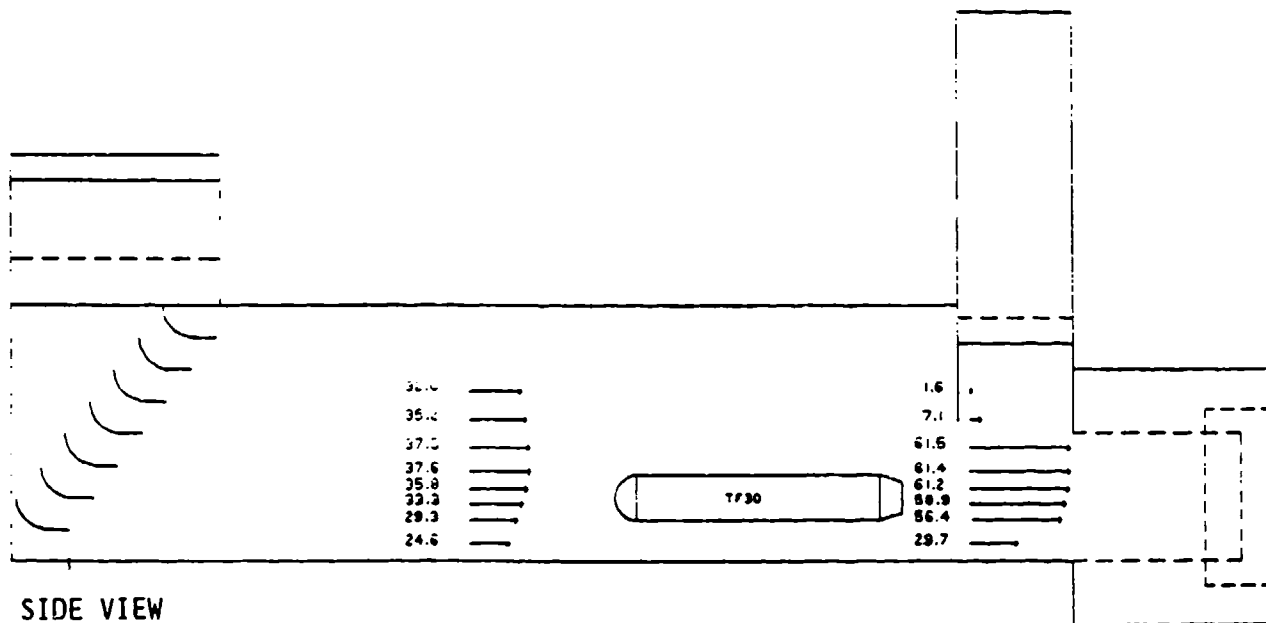


Figure 55. Airflows (ft/sec) inside test bay while testing TF30-P-414A at Mil.

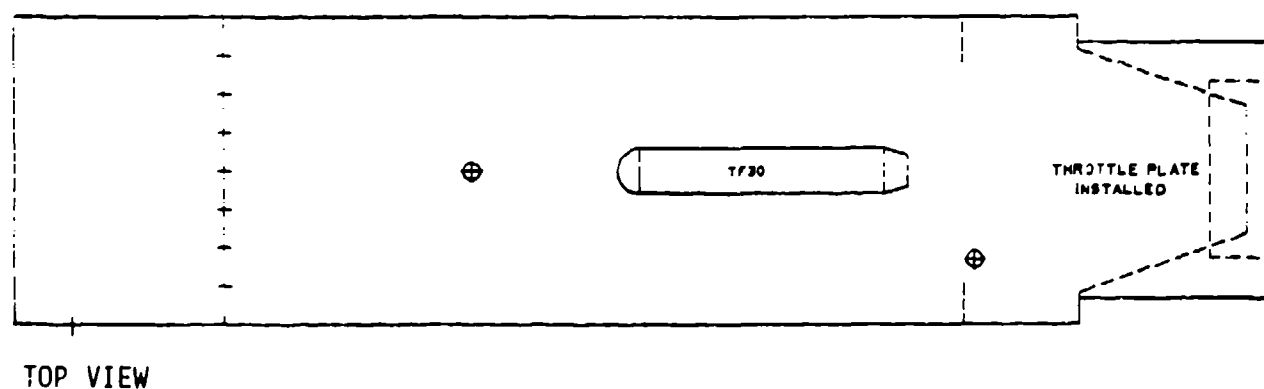
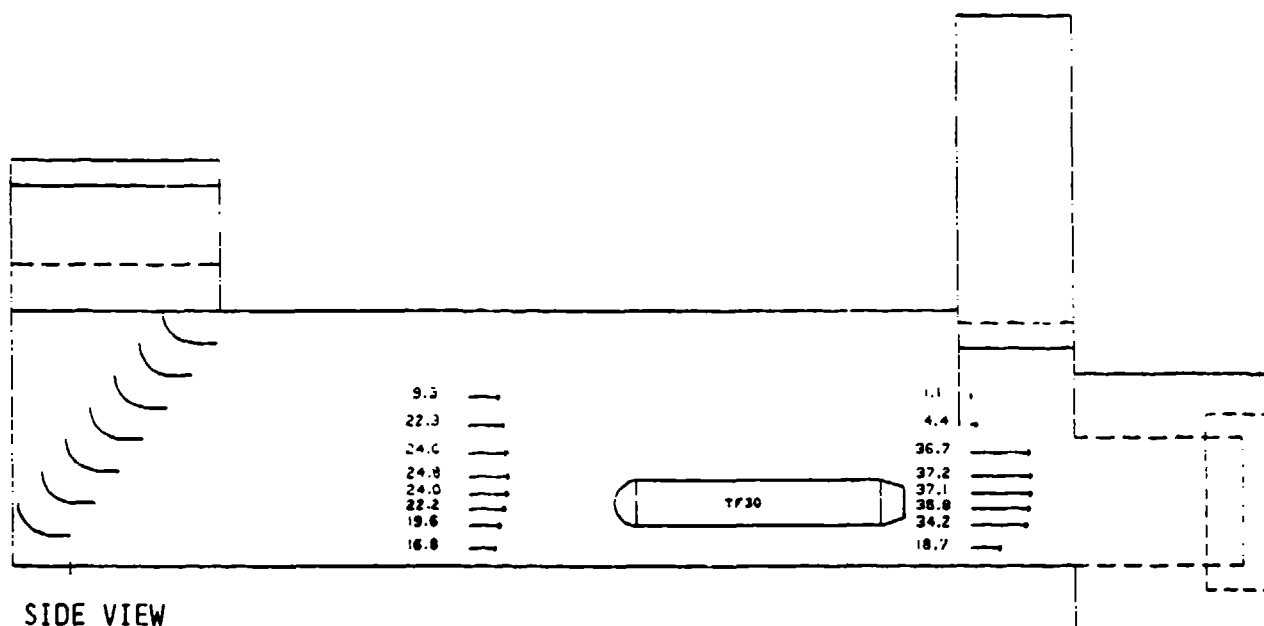


Figure 56. Airflows (ft/sec) inside test bay while testing TF30-P-414A at 85%.

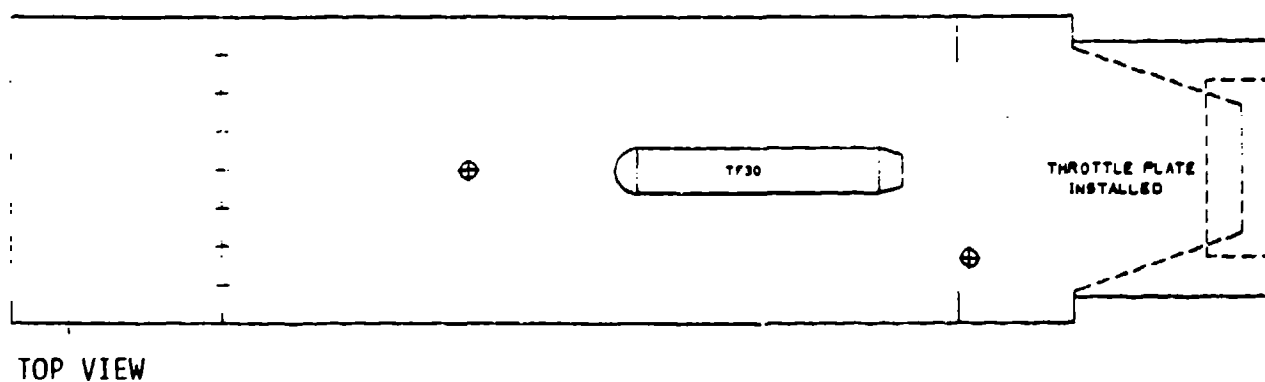
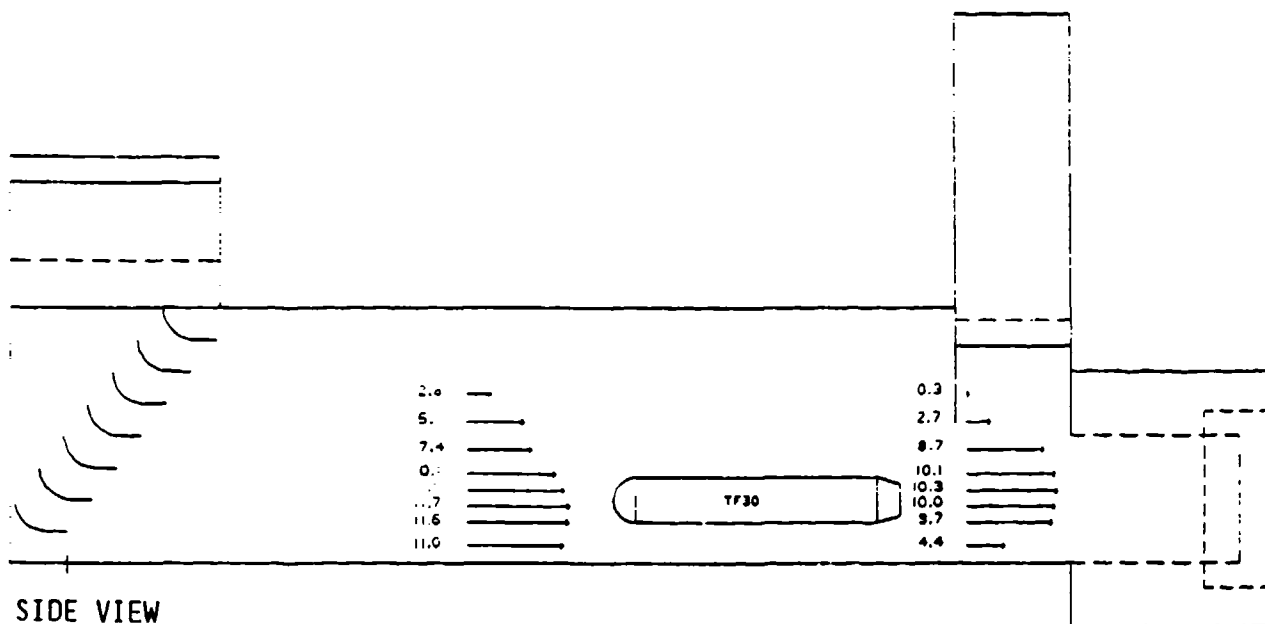


Figure 57. Airflows (ft/sec) inside test bay while testing TF30-P-414A at idle.

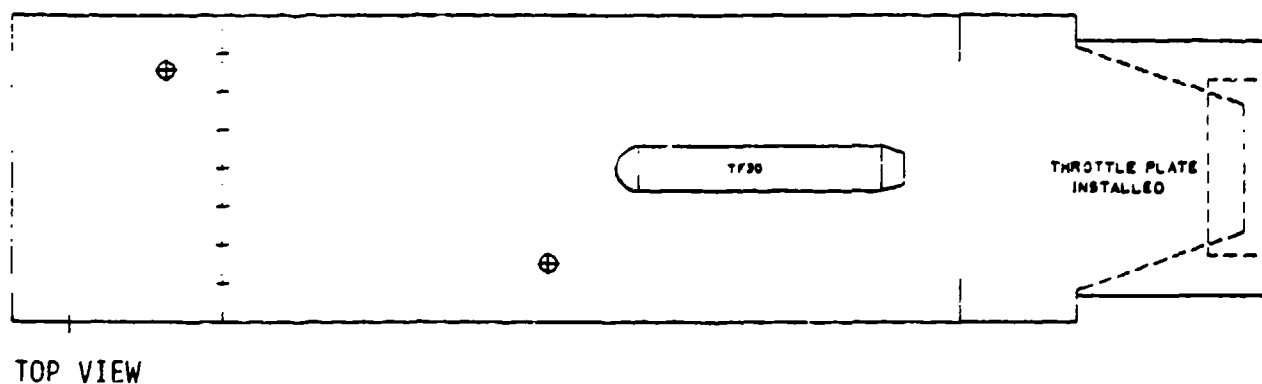
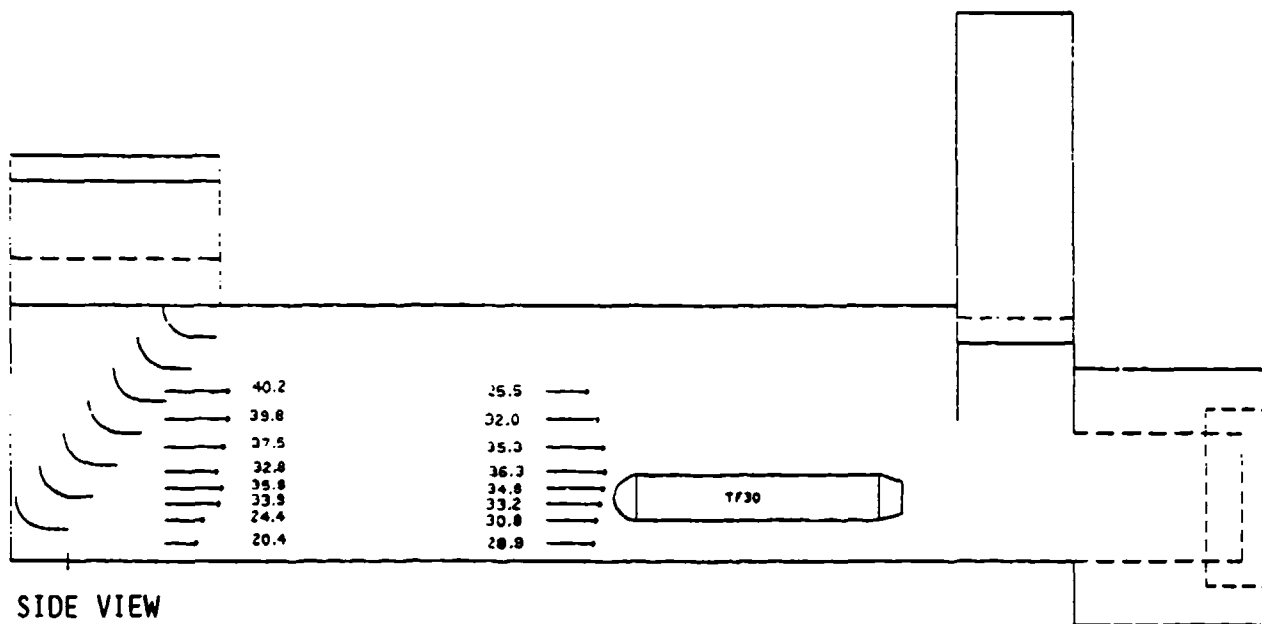


Figure 58. Airflows (ft/sec) inside test bay while testing TF30-P-414A at A/B with throttle plate.

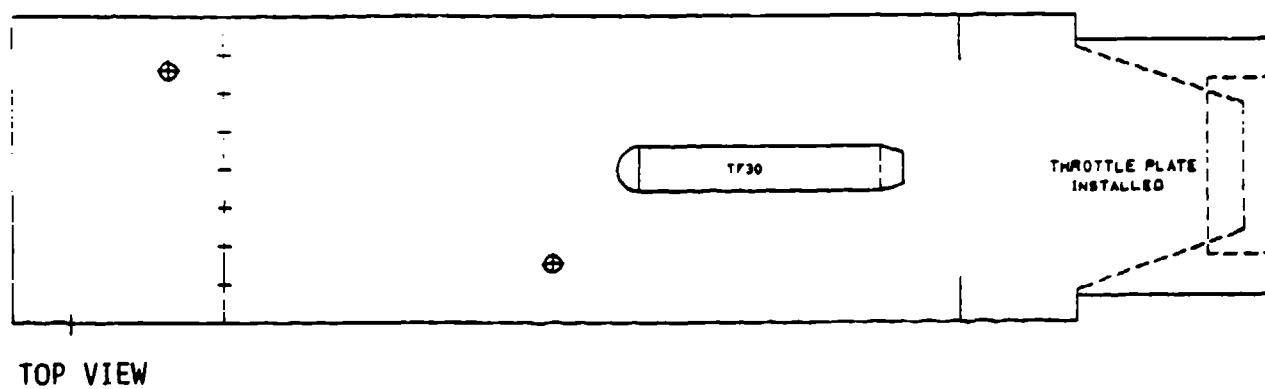
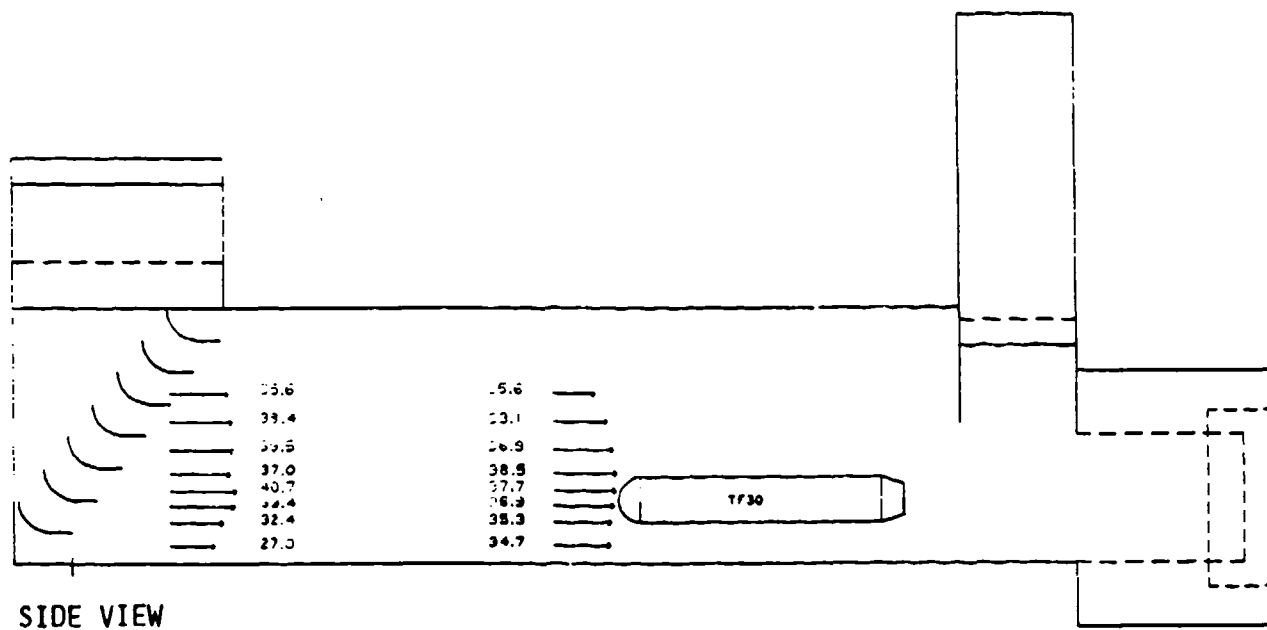


Figure 59. Airflows (ft/sec) inside test bay while testing TF30-P-414A at Mil.

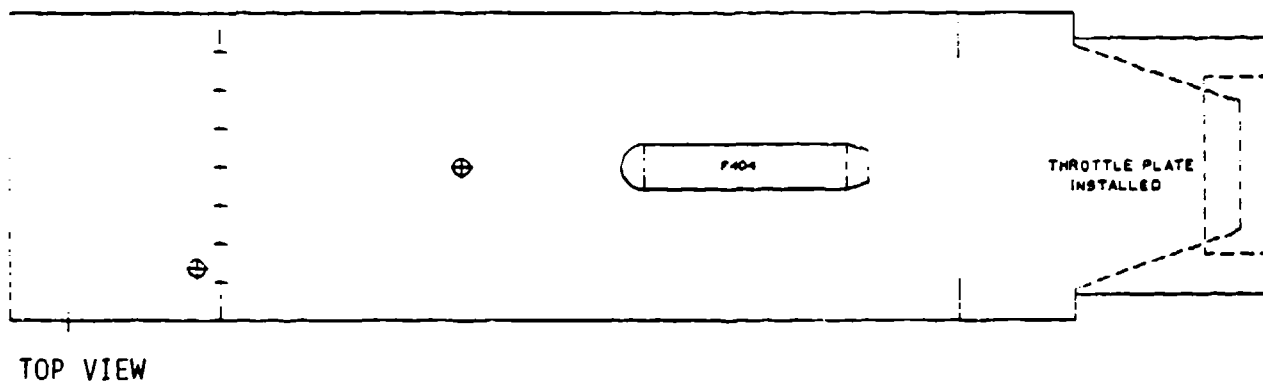
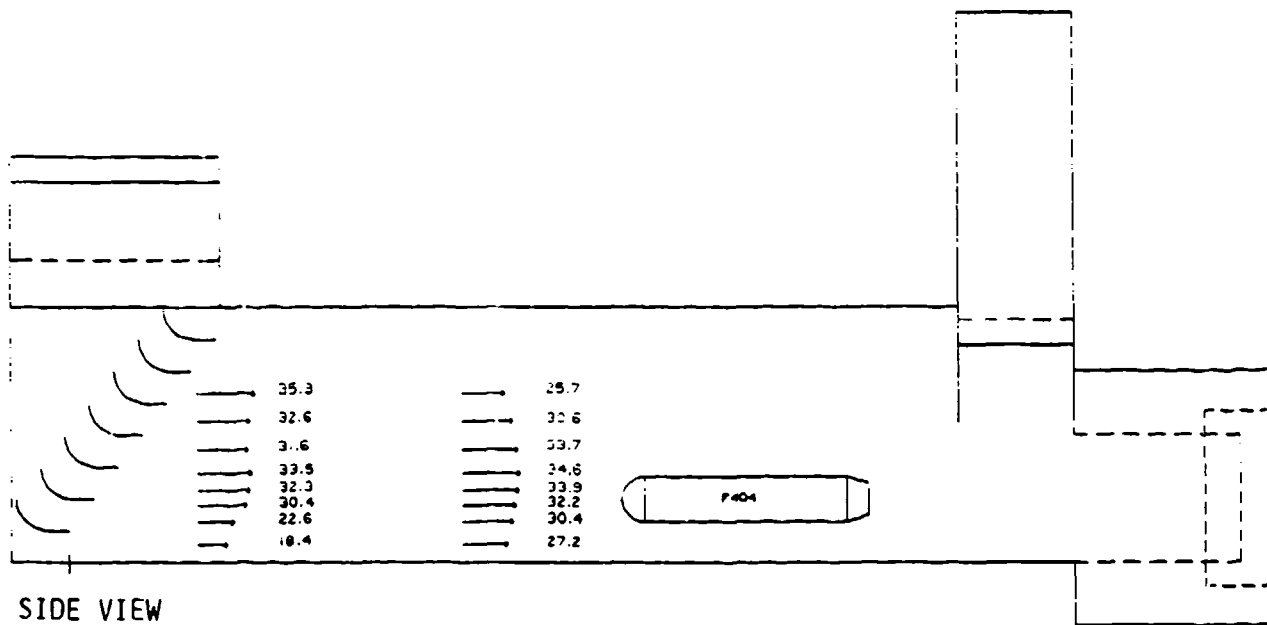


Figure 60. Airflows (ft/sec) inside test bay while testing F404-GE-400 at A/B.

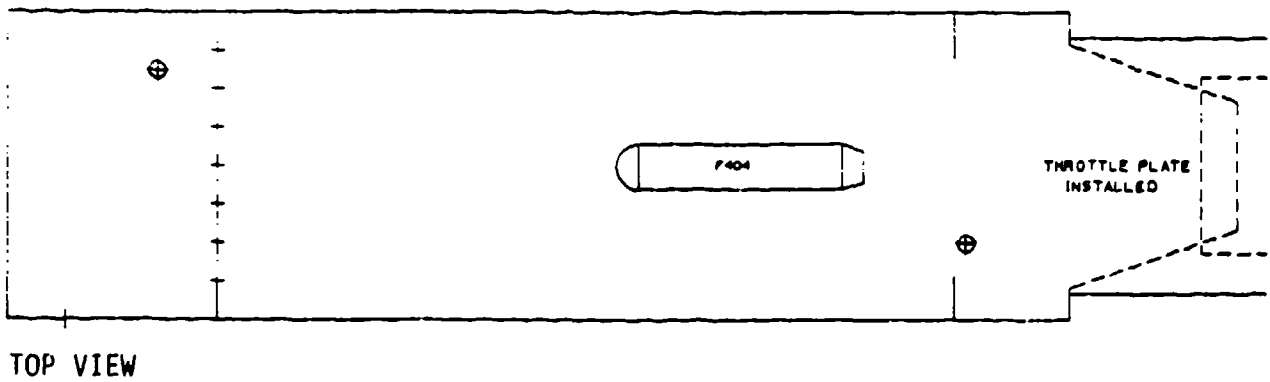
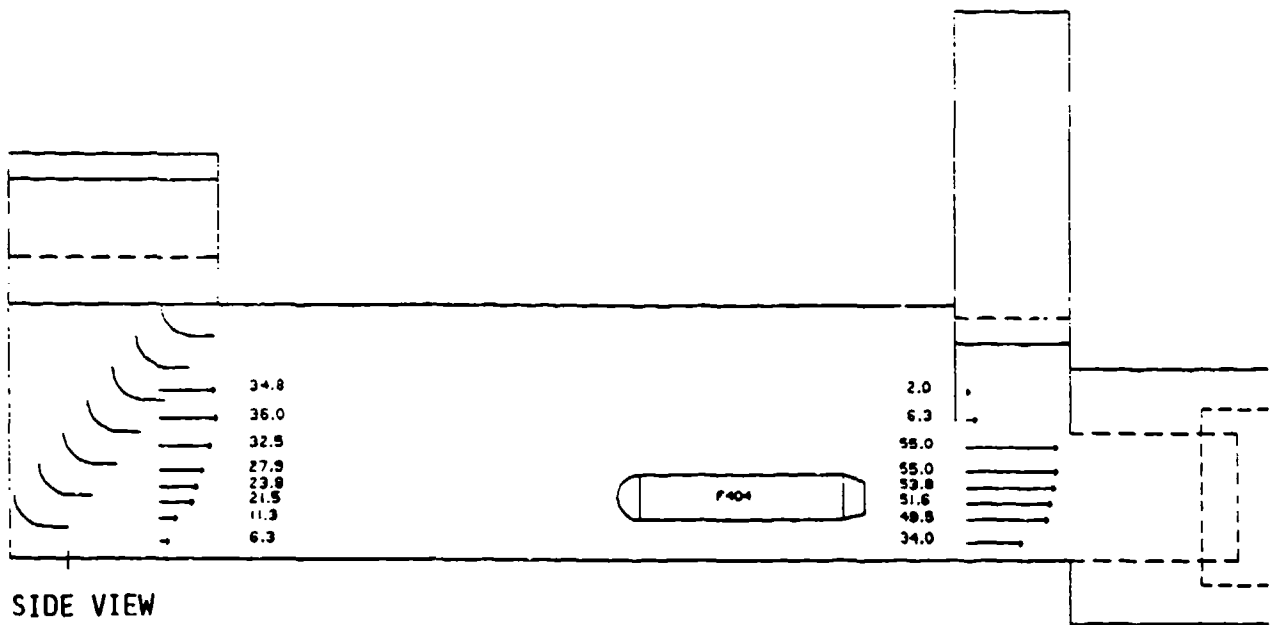


Figure 61. Airflows (ft/sec) inside test bay while testing F404-GE-400 at Mil with throttle plate.

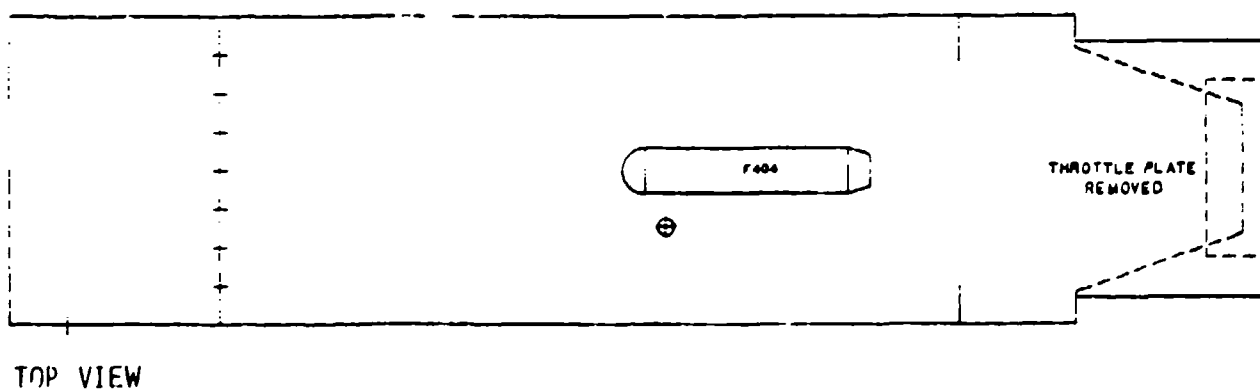
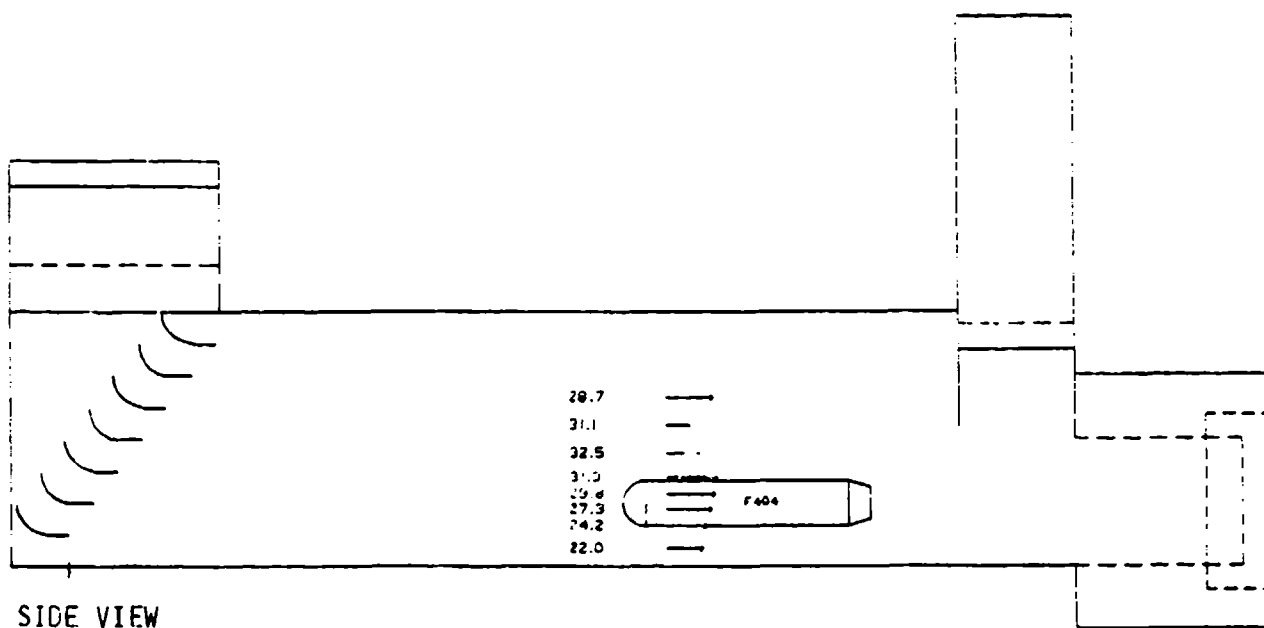


Figure 62. Airflows (ft/sec) inside test bay while testing F404-GE-400 at Mil without throttle plate.

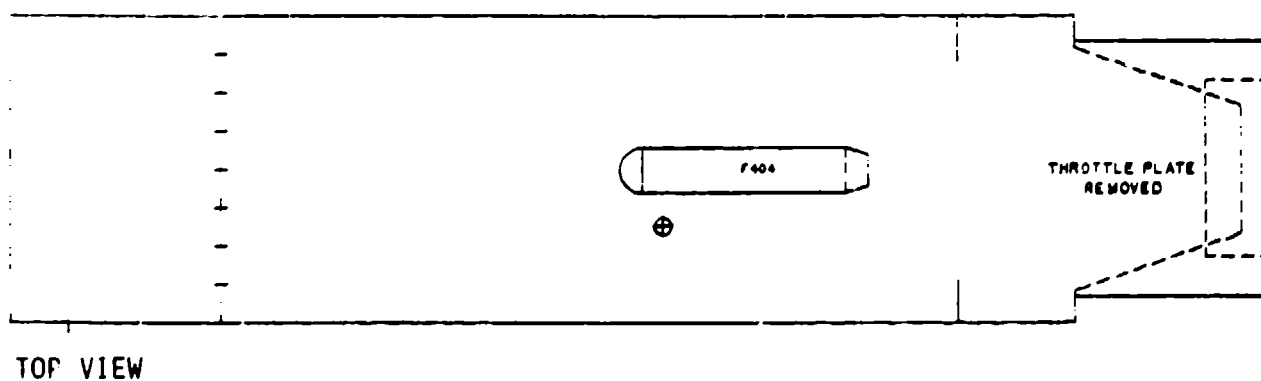
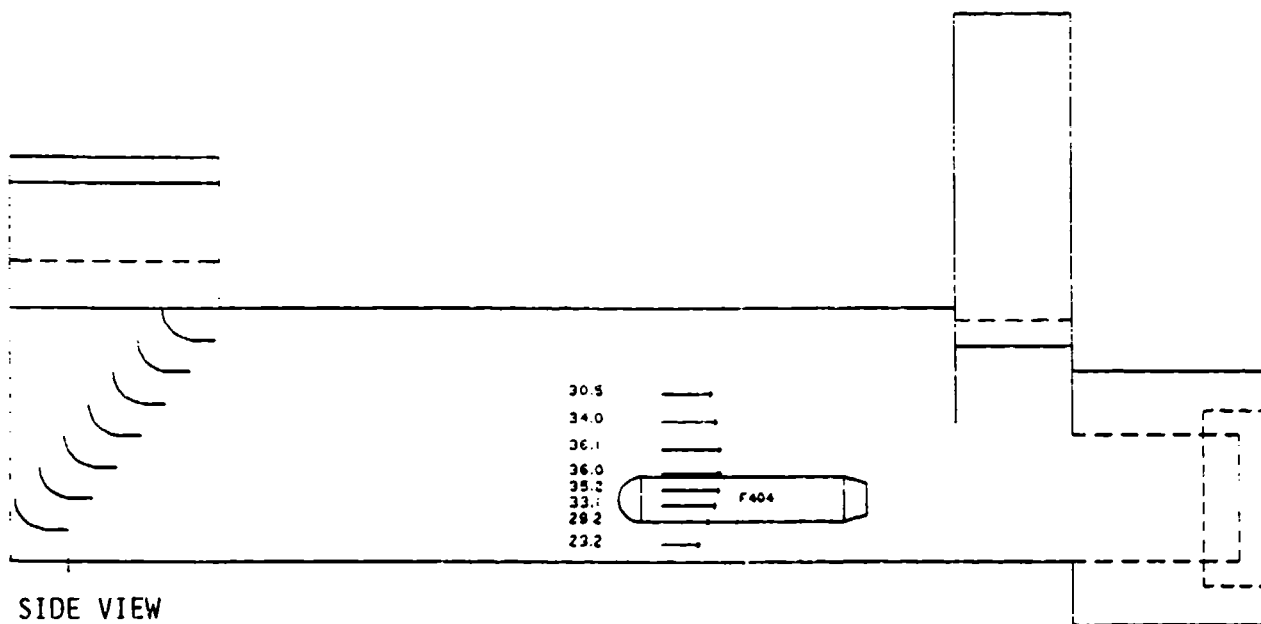


Figure 63. Airflows (ft/sec) inside test bay while testing F404-GE-400 at A/B.

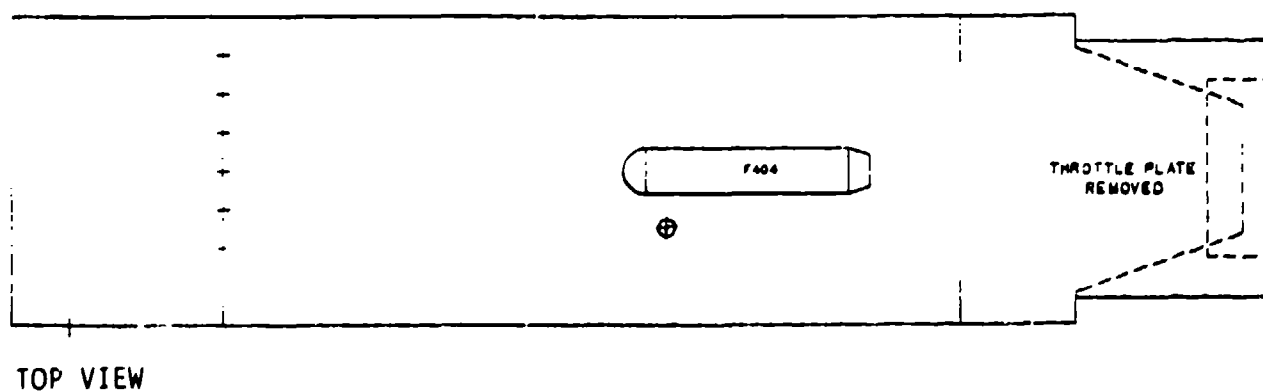
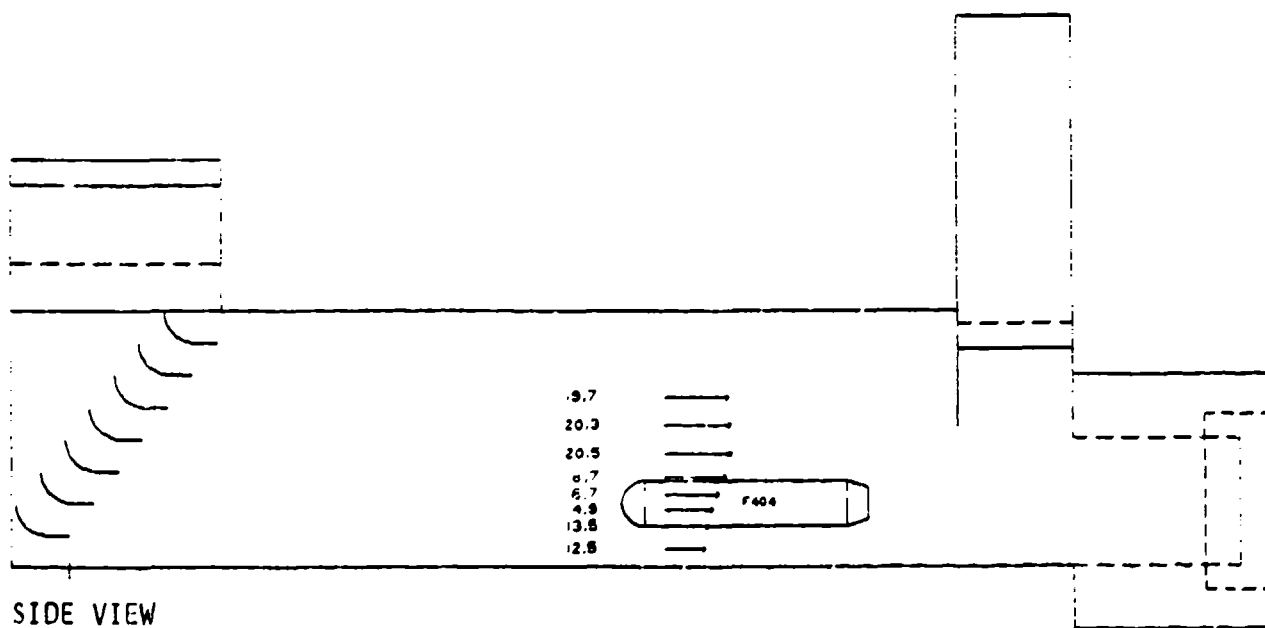


Figure 64. Airflows (ft/sec) inside test bay while testing F404-GE-400 at 85%.

Appendix A

DESCRIPTION OF THE STANDARD NAVY TEST CELL AT NAS CUBI POINT

Figure 3, duplicated here as Figure A-1, identifies the main components of the T-10 test cell at NAS Cubi Point, and indicates the paths of flow through the test cell.

The test cell is comprised of five sections: Primary intake, test bay, secondary intake, augmenter tube, and exhaust stack.

The T-10 test cell is a "dry augmenter" cell. This means that the cell is designed to draw in copious amounts of air through the primary and secondary intakes to mix with and cool the exhaust flow from the engine. Cooling the exhaust flow gases, particularly at the afterburner power setting, is needed for preventing damage to exhaust section components of the test cells. (Prior to acceptance of the T-10 design as the standard for Navy test cells, water was injected into the engine exhaust flows to cool the exhaust gases.)

The T-10 test cell acts as a large eductor. The momentum of the engine exhaust flow "pumps," or "drags," the copious amounts of air needed through the test cell. Exhaust flow leaves the engine as a high velocity, relatively small diameter, jet directed into the augmenter tube, and surrounded by ambient or slow speed air. A turbulent shear layer develops around the jet and pulls the ambient air along with the jet, i.e., the eductor effect. In pulling ambient air down the augmenter tube with the jet, a reduced pressure is created in the test bay. The difference between the test bay pressure and outside atmospheric pressure is the "cell depression." Cell depression causes air to be drawn in through the primary and secondary intakes to replace the air pulled down the augmenter tube.

Augmentation ratio is defined as follows:

$$\text{Augmentation ratio} = \left(\frac{(\text{inlet flow} - \text{engine flow})}{\text{engine flow}} \right)$$

In designing the test cell, the goal is to achieve a high enough augmentation ratio so that components of the augmenter tube and exhaust stack are not overheated, but keep a low enough augmentation ratio so that cell depression is minimal and flow condition approaching the engine approximate those of an open test stand. Augmentation ratio is a function of type of engine, engine power setting, and test cell geometry.

Specific test cell geometric features influencing augmentation ratio are augmenter tube size and intake area.

The function and essential features of each test cell section are explained below.

T-10 TEST CELL COMPONENTS

Primary Intake

The primary intake provides air for the engine during testing, plus some excess air that flows past the engine to mix with the exhaust flow and cool it down. Typically, about 60% of the air through the test cell comes through the primary intake. The primary intake has 12 vertical channels, 1.094 or 1.104 feet wide by 15.0 feet long by 9.08 feet deep, through which the air passes. The channels are separated by 11 baffles, 1.104 feet thick, constructed of sound absorbing materials. The interior walls of the intake stack are also lined with sound absorbing panels. The baffles and wall lining panels absorb engine noise tending to pass up the primary intake, thereby reducing noise on the outside of the test cell to acceptable levels.

Below the acoustic baffles are seven turning vanes, approximately 2.5 feet apart, which turn the vertical flow smoothly to the horizontal direction. The center section of the turning vanes can be lifted for installing or removing the engine through the front door. During tests, the vanes are lowered and the front door is closed and sealed.

Test Bay

The test bay is a large room, 56.0 feet long by 25.0 feet wide by 20.00 feet high, which encloses the engines during post-maintenance tests. The length and cross sectional area of the test bay allows the airflow leaving the turning vanes to "smooth out" and approach the engine with a fairly uniform profile, approximating conditions which would be encountered if the engine were being tested on an open test stand. Specifically, cell depression is monitored to ensure that it does not exceed 3.0 inches of H_2O (a limit dictated by structural design of the test bay walls rather than by engine performance), and airflow speed in the test bay is not to exceed 50 ft/sec.

During tests, the engines are rigidly clamped onto a thrust stand that is restrained by tie-downs in the thick concrete floor of the test bay. The engines are operated and monitored remotely from the control room, which is quiet due to acoustic isolation from the test bay. A window with layers of bulletproof glass allows the control room operator to view the engine in the test bay. The test bay is equipped with a water-deluge fire protection system. The walls and ceiling of the test bay are lined with panels of sound absorbing material to reduce transmission of engine noise to the outside.

Secondary Intake

The secondary intake provides air to mix with and cool the engine's exhaust flow, thereby reducing the temperatures in the exhaust section of the test cell. About 40% of the total air drawn into the test cell enters through the secondary intake. The secondary intake has nine vertical channels, 1.438 or 1.50 feet by 7.83 feet by 23.92 feet deep,

through which the air passes. The channels are separated by eight baffles, 1.50 feet thick, constructed of sound absorbing materials. Below the baffles, the secondary intake opens into a plenum where mixing between the jet exhaust flow and the augmentation air starts. The walls of the secondary intake, including the plenum and the stack, are lined with sound absorbing panels.

The secondary intake is taller than the primary intake because more noise attenuation is required of the secondary intake. The secondary intake stack is almost directly above the main sources of test cell noise, i.e., the jet engine and the jet exhaust.

Augmenter Tube

The functions of the augmenter tube are to: (1) Absorb and dissipate as much as possible the noise energy from the engine and exhaust flow, and (2) Mix the hot engine exhaust with the cool augmentation air. The augmenter tube may be thought of as a large cylindrical muffler, 80 feet long by 20 feet outside diameter.

The first 10 feet of the augmenter tube is a transition segment between the secondary intake and the 70-foot long main portion of the augmenter tube. The transition segment has sloping walls going from an obround opening 18.0 feet wide by 10.0 feet high to an obround opening 12.0 feet wide by 10.17 feet high. The walls of the transition segment are lined with high temperature acoustic panels.

The remaining 70 feet of the augmenter tube has a circular interior cross section, 13.67 feet in diameter. This portion of the augmenter tube is lined with corrugated, perforated stainless steel plate and high temperature acoustic pillows. The acoustic pillows do not extend to the outer structural shell of 20-foot diameter. There is a void between the outer structural shell and the acoustic pillows. Acoustic curtains are hung in this void to help with noise attenuation.

There is a discontinuity of cross sectional area at 10 feet down the augmenter tube, i.e., at the end of the transition segment. The cross sectional area goes from obround (12.0 feet by 10.17 feet) to circular (13.67 feet diameter). The smaller area in the transition segment was put in the design to restrict the spreading of the hot jet exhaust, and make impingement of the augmenter tube walls occur further downstream. The restrictive area also has the effect of reducing augmentation ratio slightly. In an attempt to move the impingement of exhaust gasses even further downstream, an extension (designated the "throttle plate") was added to the transition segment. The throttle plate is essentially a stainless steel conical frustum, extending 2.67 feet past the transition segment, and going from obround (12.0 feet by 10.17 feet) to circular (10.17 feet diameter).

Exhaust Stack

The function of the exhaust stack is to turn the exhaust flow and the noise in the vertical direction as they exit the test cell. The exhaust stack is 16.5 feet high by 28.3 feet long by 23.7 feet wide. It has a 45° ramp to divert the flow and noise vertically. The ramp and interior stack sidewalls are lined with sound absorbing panels. The three 16-inch-thick vertical walls of the stack are reinforced concrete.

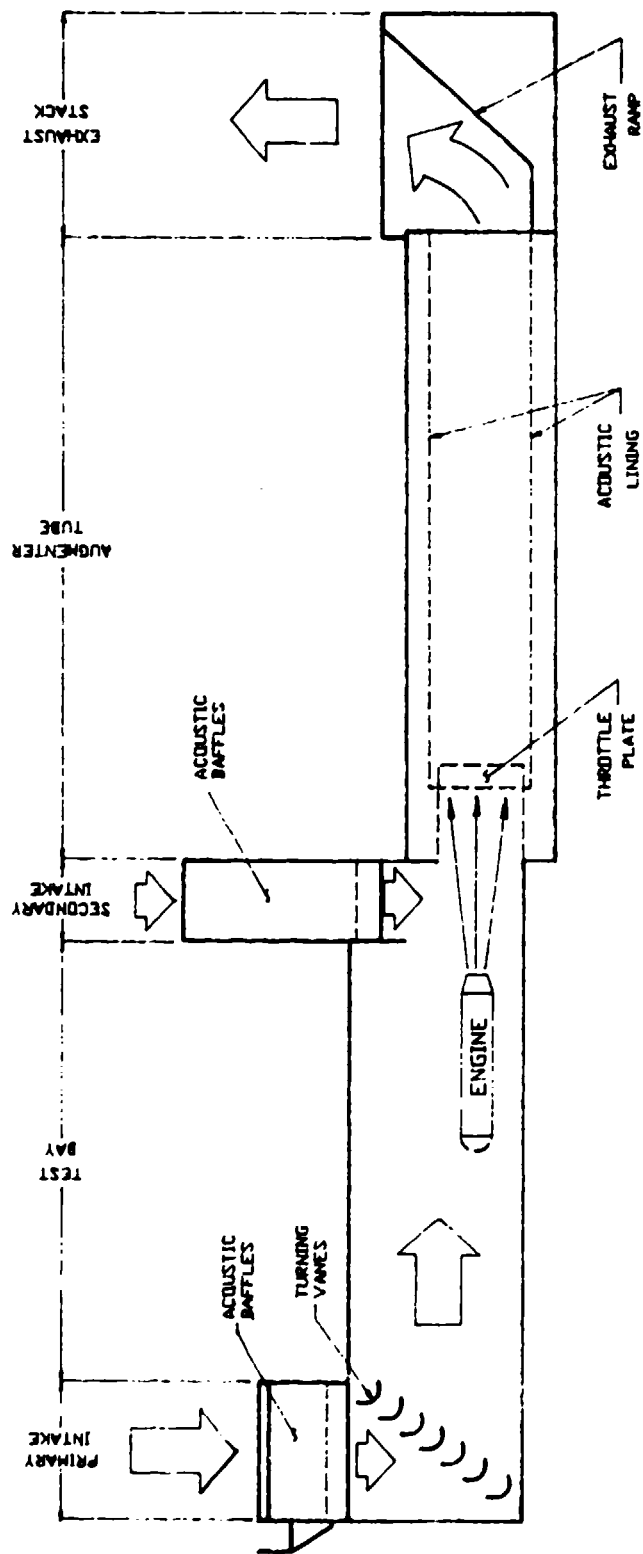


Figure A-1. Components of the standard Navy test cell, NAS Cubi Point.

Appendix B

INSTRUMENTATION

The tests included measuring and observing the flow parameters and temperatures throughout the test cell.

Intakes

- Primary Intake. Velocity and mass flow rate distribution at the top of the primary intake baffles.
- Secondary Intake. Velocity and mass flow rate distribution at the bottom of the secondary intake baffles.

Test Bay

- Velocity measurements up to 13 feet high at various positions in the test bay.
- Cell depression.
- Qualitative, overall flow patterns throughout the test bay.
- Air temperature.

Augmenter

- Velocity distribution and mass flow rate of the jet engine exhaust/augmentation air at 30 feet aft of the secondary intake.
- Velocity distribution and mass flow rate of the jet engine exhaust/augmentation air at 60 feet aft of the secondary intake.
- Temperature distribution of the jet engine exhaust/augmentation air at 30 feet and at 60 feet aft of the secondary intake.
- Temperature distribution of the perforated plate surfaces circumferentially and down the length of the augmentor tube.
- Static pressure distribution down the length of the augmentor tube.

Stack Ramp

- Temperature distribution on the stack ramp.

Figures B-1 and B-2 show locations of the instrumentation. Thermocouples TR1 and TW1 through TW12 were permanently installed during construction of the hush house. All other instrumentation was added for the tests, and was removed at the conclusion of the tests.

SCHEMATIC OF DATA ACQUISITION SYSTEM

A schematic of the data acquisition system is shown in Figure B-3. Instrumentation consisted of:

- 31 pitot-static tubes to measure airflow in the primary and secondary intakes: 12 in the primary intake, measuring flow in one quadrant and 19 in the secondary intake, measuring the flow across the entire secondary.
- 16 anemometers on two moveable stands, used to measure velocities in the test bay.
- 12 static pressure probes, all referenced to atmospheric pressure: 2 in the test bay to measure cell depression; 6 along the augments tube wall on the port side to measure static pressure distribution down the tube; and 4 (2 on each instrumentation rack in the augments tube) to measure static pressure in the vicinity of the rack total pressure measurements.
- 24 total pressure probes, all referenced to atmospheric pressure: 13 on the instrumentation rack in the augments tube located nearest the engine (30 feet downstream from the secondary intake) and 11 on the instrumentation rack in the augments tube located furthest from the engine (60 feet downstream from the secondary intake).
- 54 thermocouples: 13 permanently installed. One on the exhaust stack ramp, plus 12 on the augments tube walls, and 41 temporarily installed for these tests. Location of the 41 thermocouples were: 13 in the augments tube on the instrumentation rack located nearest the engine (30 feet downstream from the secondary intake); 11 in the augments tube on the instrumentation rack located furthest from the engine (60 feet downstream from the secondary intake); 9 on the exhaust stack ramp; 6 on the augments tube walls, 3 at each rack position; 1 on the test bay, starboard wall; and 1 in the secondary intake.

Except for the permanently installed thermocouples, all channels of instrumentation were connected to a MACSYM 250 digital datalogger manufactured by Analog Devices. The permanently installed thermocouples were connected to a Kaye Instrument Digistrip III programmable datalogger. All signals from the instrumentation were analog signals, i.e., voltage levels were proportional to the values of the variables being measured. The dataloggers, however, digitized the signals. For this

test series, the MACSYM 250 was programmed to digitize and sample the signals from the instruments, to record the data, to exercise subroutines to perform a time-average of several samples from an instrument, to convert from voltage to engineering units, then go to the next channel. The MACSYM 250 cycled through all channels approximately once per second. As the tests were in progress, current values of selected variables were displayed in engineering units on a CRT screen for quick-look "sanity" checks. Any of the variables could be displayed. The screen display was updated every 7 to 10 seconds. The Kayes Digistrip III data-logger was programmed to print time and current readings of all 13 permanently installed thermocouples at 10-second intervals.

Periodically the test sequence was interrupted to allow the MACSYM 250 to download and copy its data disk onto a COMPAQ PC data disk. This provided backup copies of the data. In addition, this procedure permitted preliminary analysis of results (computation of mass flow through the hush house and distribution of flow through the sections of the intake) at the site while testing continued. For compatibility with the MACSYM 250, the COMPAQ PC had dual disk drives, an Intel 8087 board, and an AD PCIO 1 communication card.

INTAKE PITOT-STATIC PRESSURE MEASUREMENTS

Pitot-static pressure probes were installed in both the primary and secondary intakes. Locations are shown in Figure B-1. There were 12 probes in the primary intake and 19 in the secondary intake.

The pitot and static ports of each pitot-static probe were connected by air-tight flexible plastic tubing to transducers. The transducers were manufactured by Omega Engineering, Inc. All transducers in the primary intake were Model PX163. The transducers in the secondary intake were a mixture of Model PX163 and Model PX162. Model PX163 is rated for 5-inch H_2O differential pressure between the pitot and static ports, while Model PX162 is rated for 27-inch H_2O differential pressure between the ports. The circuits of the piezoresistive element of each transducer were connected to an 8-volt DC power supply. Relevant characteristics of the transducer/pitot-static tube combinations are summarized below.

	PX163	PX162
Input voltage	8.0 volts	8.0 volts
Output voltage at 0 velocity (nominal)	3.5 volts	1.0 volts
Full-scale differential pressure rating	5-in. H_2O	27-in. H_2O
Output voltage at full scale differential pressure rating (nominal)	6.0 volts	6.0 volts
Velocity at full-scale differential pressure rating, ft/sec (temp = 85°F)	152	353

Specific curves of voltage versus differential pressure were obtained for each transducer, after installation, with the use of a Druck Digital Pressure Indicator Calibrator, Model DPI 600.

The relationship between transducer voltage and air velocity is obtained from the voltage-pressure calibrations and from the Bernoulli equation for incompressible flow:

$$PS_i = \left[PS_F \left(\frac{Volt - Volt(0)}{Volt(F) - Volt(0)} \right) \right]_i$$

$$Vel_i = \left[\frac{2g_c PS_i W}{\zeta_{ATM} \cdot 12} \right]^{1/2} = \left[\frac{2g_c R (T_{ATM} + 460) W PS_i}{144 \cdot P_{ATM} \cdot 12} \right]^{1/2}$$

The pitot-static probes in the primary intake were all mounted on one quadrant of the intake, the forward/starboard quadrant. The probes were placed midway between the noise suppression baffles, with the tips approximately 12 inches below the top of the baffles. Distance between the baffles is 1.104 feet (1.094 feet between outer baffles and sidewall acoustic panels). Six of the probes were 1.875 feet from the front wall of the intake, and six others were 5.625 feet from the front wall. These distances represent 12.5% and 37.5% of the 15-foot length of the baffles. Thus each probe was at the center of an area 3.75 feet by 1.104 feet = 4.14 square feet (4.103 square feet for the two probes located between the outer baffle and the sidewall acoustic panel). Assuming uniform flow in each of the 12 areas, and assuming symmetrical flow between quadrants, the mass flow rate in the primary intake is:

$$\dot{M}_{PRIM} = 4 \sum_{i=1}^{12} \dot{M}_i = 4 \sum_{i=1}^{12} \zeta_{ATM} A_i Vel_i$$

$$= \sum_{i=1}^{12} \left[\frac{144 \cdot P_{ATM}}{R (T_{ATM} + 460)} \right] A_i Vel_i$$

where: $A_1 = A_7 = 4.103 \text{ ft}^2$

$A_{2-6} = A_{8-12} = 4.14 \text{ ft}^2$

The pitot-static probes in the secondary intake were placed so that measurements were taken throughout the starboard half, while a sampling of measurements were taken on the port half to verify symmetry of the intake flow. The probes were positioned with the tips centered between baffles, approximately 16 inches above the transition from the vertical acoustically treated portion to the sheet-metal wedge at the bottom of the baffles. Distance between the baffles is 1.50 feet (1.438 feet between the outer baffles and the sidewall acoustic panels). The probes were located at distances of 1.306 feet, 3.917 feet, and 6.528 feet from the front surface of the secondary intake, which represent 16.7%, 50.0%, and 83.3% of the 7.833-foot length of the baffles. Thus each probe was centered in an area of 2.612 feet by 1.50 feet = 3.918 square feet (3.756 square feet for the probes between the outer baffles and the sidewall acoustic panels). Assuming uniform flow in each area, and assuming symmetry between the port and starboard sides, the mass flow rate in the secondary intake is:

$$\dot{M}_{SEC} = 2 \sum_{i=13}^{25} \dot{M}_i + \dot{M}_{26} = 2 \sum_{i=13}^{25} \zeta_{ATM} A_i Vel + \zeta_{ATM} A_{26} Vel_{26}$$

where: $A_{13-15} = 3.756 \text{ ft}^2$

$A_{16-25} = 3.918 \text{ ft}^2$

CELL DEPRESSION MEASUREMENTS

Static pressure relative to atmospheric pressure was monitored at two points in the test bay. Locations of the cell depression measurements are shown in Figure B-1. Cell depression was measured at each point by installing a section of 3/8-inch plastic tubing with one end open, mounted flush with the wall and pointing to the floor, and connecting the other end to one port of the Model PX163 transducer. Atmospheric pressure was sensed at the other port of the transducer by running plastic tubing from the transducer port out the secondary intake to an area undisturbed by engine operations.

The description of transducer circuitry and calibration techniques given in the discussion of Intake Pitot-Static Pressure Measurements applies to the Cell Depression Measurements as well.

FLOW VELOCITY MEASUREMENTS IN THE TEST BAY

Anemometers were used for quantitative measurements of flow velocity in the test bay. The anemometers were manufactured by R.M. Young Company, and are identified as Gill Type Anemometers (Cat No. 27103) with a 3-blade propeller, 20 cm diameter by 50 cm pitch (Cat No. 8253). The anemometers were mounted in two stands. Each stand had eight anemometers positioned at 15, 37.5, 52.5, 67.5, 82.5, 105, 132, and 157.5 inches above the floor. The anemometers on each stand were in the same vertical plane and faced the same direction. Figures B-4 and B-5 show

the stands. The stands could be moved to various positions in the test bay. Figure B-2 shows positions at which data were taken with the anemometers.

Rotational speed of the anemometer propellers is proportional to air speed. The propeller shaft turns a generator, with generator voltage proportional to air speed. Reversal of flow direction past an anemometer reverses the sign of the output voltage. Calibration of the rotational speed versus output voltage was accomplished with a reversible constant speed (1,800 rpm) motor, (Cat No. 27230) manufactured by R.M. Young Company, which would spin the anemometer at 1,800 rpm using a flexible coupling. A rotational speed of 1,800 rpm results in a nominal 0.5 volt output signal. To relate rpm to air speed, three of the anemometers available for the tests were sent to the manufacturer for calibration in their wind tunnel. The tunnel calibration confirmed company-supplied literature stating that 1,800 rpm corresponds to a wind velocity of 48.4 ft/sec (33 mi/hr). The nominal relationship between voltage and air velocity is:

$$Vel_j = 48.4 \left[\frac{\text{Volt}}{\text{Volt (1800)}} \right]_j = 48.4 \left[\frac{\text{Volt}}{0.5} \right]_j$$

Heights of the anemometers above the floor were chosen so that one was lower than the trailing edge height of the bottom turning vane, two were between the trailing edge heights of the bottom and second turning vanes, two were between the trailing edge heights of the second and third, one was between the third and fourth, one was between the fourth and fifth, and one was between the fifth and sixth. The highest anemometer was at just over 13 feet. The test bay ceiling was at 20 feet high, so no measurements were made in the top 6 feet 10 inches of the test bay.

FLOW VISUALIZATION

Two methods of flow visualization were planned for observing the overall flow patterns in the test bay: Streamers and smoke.

The intent was to videotape the streamers and the smoke patterns during engine runs, and study the videotapes for locations of dead spots, eddies, or recirculation flow. Early in the test program, however, it became evident that the flow patterns were very smooth. A videotape record was made only during the J52-P-88 engine runs. During all other engine runs, the streamers were watched simply to verify that flow in the test bay was smooth, but no permanent videotape records were made.

The one videotape record that was made was not clear. The video camera was hand-held. The cameraman was unable to prevent the camera from vibrating because of the noise in the test bay. Test cell operators say that the test bay noise in the test vibrations are higher during J52-P-88 engine runs than during runs with other engines, so

perhaps there would have been less difficulty in making clear pictures during runs with other engines. A decision was made not to video tape the remaining tests because of the poor quality of the first pictures, plus the smoothness of the flow.

Streamers were attached to the trailing edges of the primary intake turning vanes. Streamers were also attached to strings spanning the test bay in several locations, both forward and above the engines. Figures B-5 and B-6 show the streamers.

Smoke cannisters used to mark helicopter landing pads were obtained for flow visualization. The engine representative from General Electric stationed at the NAS Cubi Point jet maintenance shop was consulted about the effect of the smoke on the engines. The cannisters would be set off in the primary intake or in the test bay forward of the engine, and some of the smoke from them would be ingested through the engines. The chemical composition of the smoke had been provided with the cannisters. The General Electric representative recommended that the smoke not be used, since known corrosive agents were in the smoke. Correlation "gold plate" engines were being used in the test series, and since smooth flow patterns were being observed with the streamers, it was decided that the risk to the engines outweighed the use of the smoke and the small additional information that the smoke flow patterns would provide.

AUGMENTER TUBE STATIC PRESSURE MEASUREMENTS

Static pressure was measured at 10-foot intervals down the length of the augmentor tube. Figure B-1 shows that six of the static pressure measurements were taken along the port wall of the augmentor tube, and two static pressure measurements were taken on each of the racks erected in the augmentor tube at 30 and 60 feet aft of the secondary intake.

The static pressure probes along the port wall were fabricated by NCEL from sections of 1/4 inch stainless steel tubing. One end of each section of tubing was plugged with silver solder. Four inches back from the plugged end, four 1/16 inch diameter holes were drilled in the sides of the tubing. The tubing was mounted along the augmentor wall, parallel to the axis of the augmentor. The open end of each section of tubing was connected by a stainless steel airtight fitting to stainless steel tubing routed through the closest 1-inch pipe nipple built into the augmentor tube wall at 10-foot intervals. Outside the augmentor tube, i.e., outside the high temperature environment, clear tygon tubing was used to continue an airtight path between the stainless steel tubing and one port of the pressure transducer.

The static pressure measurements on the racks were taken with purchased pitot-static probes. The static pressure ports of the probes nearest the top and nearest the bottom of the vertical post of each rack were connected by stainless steel airtight fittings to stainless steel tubing routed via an adjacent 1-inch pipe nipple through the augmentor tube wall. Again, outside the augmentor, tygon tubing continued the path to the pressure transducer.

Transducers used to measure the augments tube static pressures were Model PX162. One port was connected to the tubing from the pressure probes, and the other port was left open to atmospheric pressure. The description of transducer circuitry and calibration techniques given in the Intake Pitot-Static Pressure Measurements section applies to the Augments Tube Static Pressure Measurements as well. The relationship between augments static pressure and measured voltage is:

$$S_n = \left[S_F \left(\frac{\text{Volt} - \text{Volt (0)}}{\text{Volt (F)} - \text{Volt (0)}} \right) \right]_n$$

AUGMENTS RACK TOTAL PRESSURE MEASUREMENTS

Two racks were erected in the augments tube for instrumentation to measure velocity and stagnation temperature of the flow in the core of the tube. Figure B-7 is a picture of the two racks with instrumentation installed. The racks were 30 and 60 feet aft of the secondary intake. The racks were made of 1-1/2- and 2-inch stainless steel tubing. Carbon steel gussets were welded to the tubing to make bolted joints, and carbon steel footings were welded on to allow the rack to be bolted to the augments tube wall at the top, bottom, and sides of the augments. Carbon steel supports were welded to the tubing at each location for a pressure probe or a thermocouple.

Figure B-1 shows the locations of pressure probes on the racks. The front rack had 13 probes, while the aft rack had 11. All the probes were purchased pitot-static tubes. Except for the top and bottom probes on each vertical post (see discussion of Augments Tube Static Pressure Measurements), however, only the total pressure ports of each probe were used. The pressure probes were clamped to the carbon steel supports and to the stainless steel tubing with hose clamps and aircraft stainless steel wire. Figure B-8 shows a typical installation. Airtight tube fittings connected the probes to 1/4-inch stainless steel tubing routed via one of the 1-inch pipe nipples through the augments tube wall. Outside the augments, clear tygon tubing completed the airtight path to the transducers.

Transducers Model LX1801DZ-1, for the rack total pressure measurements were manufactured by SenSym Corporation and were capable of measuring up to 5 psi differential pressure between ports. The leads from the pressure probes were connected to the high pressure port. The low pressure port was left open to atmospheric pressure. Nominal characteristics of the SenSym pressure transducers are presented:

Input voltage	20.0 volts
Output voltage at 0 velocity (nominal)	7.5 volts
Full-scale differential pressure rating	5 lbf/in. ²
Output voltage at full-scale differential pressure rating (nominal)	12.5 volts
Velocity at full-scale differential pressure rating, ft/sec (temp = 85°F)	725

Specific curves of voltage versus differential pressure were obtained for each transducer, after installation, with the use of the Druck Digital Pressure Indicator Calibrator, Model DPI 600. Leak checks were also performed with the calibrator on the installed probes/tubing/transducers. All transducers were leaking around the threads of the hose connector fittings. (RTV) Room Temperature Vulcanizing material sealed the leaks.

The relationship between transducer voltage and air velocity is obtained from the voltage-pressure calibration and from the pressure-velocity relationship for compressible, isentropic flow. The pressure-velocity relationship requires measurement of both total and static pressures. Static pressures were read on only two of the probes on each rack. The average of these two readings was used for static pressure at each probe.

$$S_{A \text{ AVG}} = \frac{S_3 + S_4}{2}$$

$$PA_k = \left[PA_F \left(\frac{\text{Volt} - \text{Volt}(0)}{\text{Volt}(F) - \text{Volt}(0)} \right) \right]_k$$

$$Vel_k = \left[1 - \frac{\frac{S_{A \text{ AVG}} \cdot W}{144 \cdot 12} + P_{ATM}}{PA_k + P_{ATM}} \frac{\gamma - 1}{\gamma} \frac{2 \gamma g_c R (TA_k + 460)}{\gamma - 1} \right]^{1/2}$$

The temperatures needed to evaluate the velocity were also measured on the racks. The measurement techniques are described in the section entitled Temperature Measurements. For each pressure measurement, there was a corresponding temperature measurement taken in the immediate proximity.

Mass flow rate in the augments tube can also be calculated from the measurements taken on the racks. For Rack A the method of computation is:

$$T_L = TA_k - \frac{\gamma - 1}{2 \gamma R g_c} (Vel_k)^2$$

$$\dot{M}_A = \sum_{k=1}^{13} \dot{M}_k = \sum_{k=1}^{13} \zeta_k A_k Vel_k$$

$$= \sum_{k=1}^{13} \frac{\frac{S_{A \text{ AVG}} \cdot W}{144 \cdot 12} + P_{ATM}}{R (T_k + 460)} \cdot 144 A_k Vel_k$$

$$\begin{aligned}
\text{where: } A_1 &= A_9 = 24.104 \text{ ft}^2 \\
A_2 &= A_8 = 7.658 \text{ ft}^2 \\
A_3 &= A_7 = 3.142 \text{ ft}^2 \\
A_4 &= A_6 = 1.571 \text{ ft}^2 \\
A_5 &= 0.785 \text{ ft}^2 \\
A_{10} &= A_{13} = 33.529 \text{ ft}^2 \\
A_{11} &= A_{12} = 2.945 \text{ ft}^2
\end{aligned}$$

For Rack B the method of computation is:

$$S_{B \text{ AVG}} = \frac{S_7 + S_8}{2}$$

$$PB_\ell = \left[PB_F \left(\frac{\text{Volt} - \text{Volt (0)}}{\text{Volt (F)} - \text{Volt (0)}} \right) \right]$$

$$Vel_1 = \left[1 - \frac{\frac{S_{B \text{ AVG}} \cdot W}{144 \cdot 12} + P_{ATM}}{PB_\ell + P_{ATM}} \frac{\gamma - 1}{\gamma} \right]^{1/2} \frac{2 \gamma g_c R (TB_\ell + 460)}{\gamma - 1}$$

$$T_\gamma = TB_\ell - \frac{\gamma - 1}{2 \gamma R g_c} (Vel_\ell)^2$$

$$\begin{aligned}
\dot{M}_B &= \sum_{\ell=1}^{11} \dot{M}_\ell = \sum_{\ell=1}^{11} \zeta_\ell A_\ell Vel_\ell \\
&= \sum_{\ell=1}^{11} \frac{\frac{S_{B \text{ AVG}} \cdot W}{144 \cdot 12} + P_{ATM}}{R (T_\ell + 460)} A_k Vel_\ell
\end{aligned}$$

$$\begin{aligned}
\text{where: } A_1 &= A_7 = 17.035 \text{ ft}^2 \\
A_2 &= A_6 = 12.566 \text{ ft}^2 \\
A_3 &= A_5 = A_9 = A_{10} = 6.283 \text{ ft}^2 \\
A_4 &= 3.142 \text{ ft}^2 \\
A_8 &= A_{11} = 29.602 \text{ ft}^2
\end{aligned}$$

Computation of the static temperatures T_1 and T_k from the measured stagnation temperatures and computed velocities^k is explained in the section entitled Temperature Measurements.

Accuracy of the mass flow rate computations, and more basically, of the measurements on the racks, can be evaluated by comparing the mass flow rates obtained at Rack A versus at Rack B versus the mass flow rates through the intakes. All should be equal (neglecting the small contribution of fuel flow to the engines). This is discussed further in Appendix C.

TEMPERATURE MEASUREMENTS

Temperatures were measured with thermocouples at 54 locations in the test cell. Figure B-2 shows the placement of thermocouples.

- 18 (12 permanent, 6 temporary) on the augmentor tube wall.
- 10 (1 permanent, 9 temporary) on the exhaust stack ramp.
- 13 (temporary) on Rack A, located 30 feet aft of the secondary intake.
- 11 (temporary) on Rack B, located 60 feet aft of the secondary intake.
- 1 (temporary) on the test bay wall.
- 1 (temporary) in the secondary intake.

The designation "permanent" means that the thermocouple was installed during construction and is wired into the control panel in the control room, allowing the operators to monitor wall temperatures in the augmentor/ramp sections of the test cell. Selected temperatures can be displayed. The control room panel sounds an alarm if wall temperature exceeds design limit.

The permanent thermocouples are all J-type junctions (iron-constantan).

The designation "temporary" means that the thermocouple was installed specifically for these tests, and was removed at the completion of the tests. The temporary thermocouples were K-type junctions (chromel-alumel).

The 17 temporary thermocouples installed on the augmentor tube wall, on the exhaust stack ramp, on the test bay wall, and in the secondary intake were purchased with the junctions already made and attached to flat washers 1/4-inch in diameter, which served as the sensing elements (NANMAC Corporation Washer Thermocouple A6-13K). Each washer and junction was held in contact with the metal surface by a screw threaded into the metal through the eye of the washer.

The 24 temporary thermocouples installed on Racks A and B in the augmentor tube were NANMAC Corporation Pencil Probe "Eroding" Thermocouples, Model E12-2K. Figure B-8 shows an installation of this type of thermocouple. This type of thermocouple was not good for this application. One problem was that the aft portion of the thermocouple was intended to be protected from the high temperatures and the large induced vibrations occurring at the racks. Some protection was provided by welding a stainless steel sleeve over the aft portion of the thermocouple

and by coating the base (at which point the connections were made between the thermocouple probe and the wires leading to the recording instruments) with high temperature RTV. Another problem was that the thermocouple junction was susceptible to degradation from impurities in the flow. During almost every test, some of the thermocouples would cease to read temperatures. The junctions could be renewed by filing or sanding the probe tips between runs.

During tests of the TF-30 engine, several of the pencil probe thermocouples in Rack A failed structurally and were blown out of the augments tube. These were replaced with field-made junctions, formed by soldering the wires leading to the recording instruments. The field-made junctions were held in position by passing the wires inside 1/4-inch stainless steel tubing clamped to the rack.

The thermocouples on Racks A and B measured stagnation temperatures, i.e., temperatures reflecting the random molecular motion (static temperatures) plus the ordered flow energy (kinetic energy). Static temperatures are calculated from the measured temperatures as shown.

$$T_{\text{STATIC}} = T_{\text{TOTAL}} - \frac{\gamma - 1}{2\gamma R_g} (\text{Vel})^2$$

The thermocouples on Racks A and B did not respond instantaneously to the flow. Several seconds were required for the thermocouples to reach a stable reading after an engine power setting was established. In most cases, stable thermocouple readings were taken about 60 seconds or more after an engine setting was established. At afterburner settings, however, stable thermocouple readings were sometimes not reached before the engine power had to be reduced. In these cases, estimates of the stable readings were made by extrapolating the temperature traces to asymptotic values or by referring to longer runs at afterburner power.

All temporary thermocouples were connected to a reference temperature junction (Kaye Instrument Uniform Temperature Reference). Omega Engineering, Inc.* explains how the reference temperature junction eliminates the need for calibrating individual thermocouples, and eliminates the need for ice bath reference junctions. Figure B-3 shows circuitry associated with the reference temperature junction. Confidence in the thermocouple temperature measurements using the reference temperature junction was established during tests at Marine Corps Air Station Cherry Point by comparison within 1°F with readings from a calibrated Fluke 8024A multimeter probe at ambient conditions.

The permanent thermocouple readings were printed by a Kayes Instrument Digistrip III datalogger. The Kayes datalogger was connected in parallel with the test cell control panel in the control room, allowing the permanent thermocouple readings to be displayed as usual and printed out at the same time. The Kayes datalogger was programmed to sample all permanent thermocouple values at 10-second intervals, and print them out in degrees Fahrenheit. The time and Julian date were also printed out with each sample. NCEL did not calibrate the permanent thermocouples.

*Omega Engineering, Inc. T6-T11: Complete temperature measurement handbook and encyclopedia, 1986.

LIST OF SYMBOLS

<u>Variables</u>	<u>Units</u>
A area	ft ²
C _p specific heat of air at constant pressure	0.24 BTU/lbm-°F
g gravitational acceleration	32.2 ft/sec ²
g _c gravitational conversion constant	32.2 ft-lbm/lbf-sec ²
H _v heating value of aircraft fuel	BTU/lbm
J Joule's constant	773 ft-lbf/BTU
m mass flow rate	lbm/sec
P pressure	lbf/in. ²
P _A pitot pressure on rack A	lbf/in. ² (gauge)
P _B pitot pressure on rack B	lbf/in. ² (gauge)
P _S difference between pitot and static pressures in intake	in. H ₂ O
R ideal gas constant for air	53.3 ft-lbf/lbm-°R
S static pressure in augmeter tube	in. H ₂ O (gauge)
T static temperature	°F
T _A stagnation temperature on rack A	°F
T _B stagnation temperature on rack B	°F
Vel speed of flow	ft/sec
Volt voltage	volts
w weight density of water	62.4 lbf/ft ³
Z height above augmeter tube centerline	ft
γ ratio of specific heats for air	1.4 (dimensionless)
ζ mass density	lbm/ft ³
144 conversion factor, ft ² to in. ²	144 in. ² /ft ²
12 conversion factor, ft to in.	12 in./ft
460 conversion factor, °F to °R	°R = °F + 460

Subscripts or Parenthesis

A denotes rack A

ATM denotes atmospheric conditions

AVE denotes average

B denotes rack B

f denotes aircraft fuel

F denotes value at maximum speed

i denotes inlet

j denotes anemometers

k denotes rack A

l denotes rack B

n denotes augmenter tube static pressure

O denotes value at zero speed

PRIM denotes primary intake

SEC denotes secondary intake

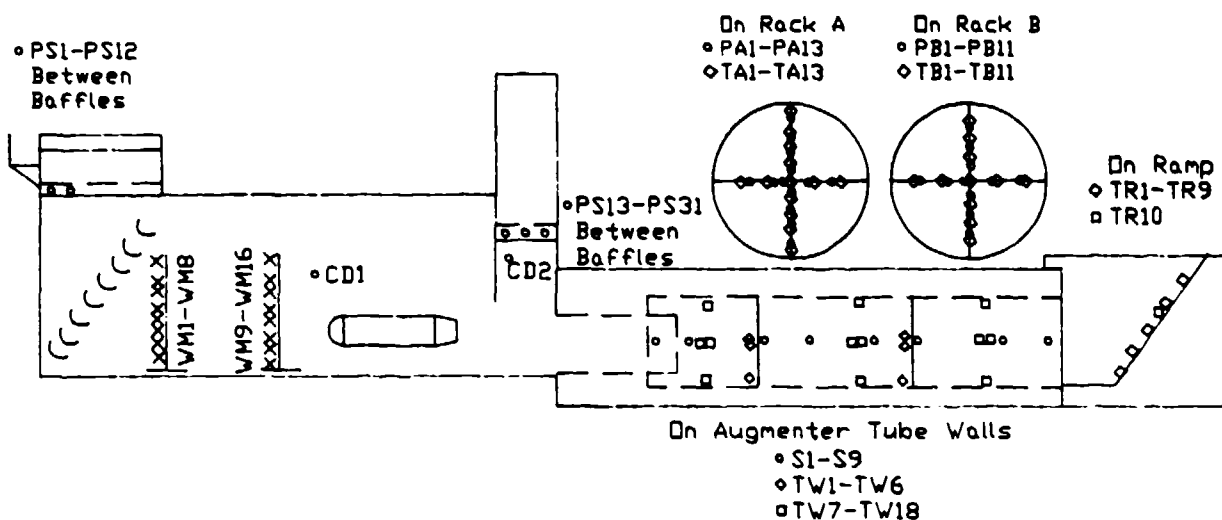


Figure B-1. Location of instrumentation for aerothermal tests at NAS Cubi Point T-10 test cell (side view).

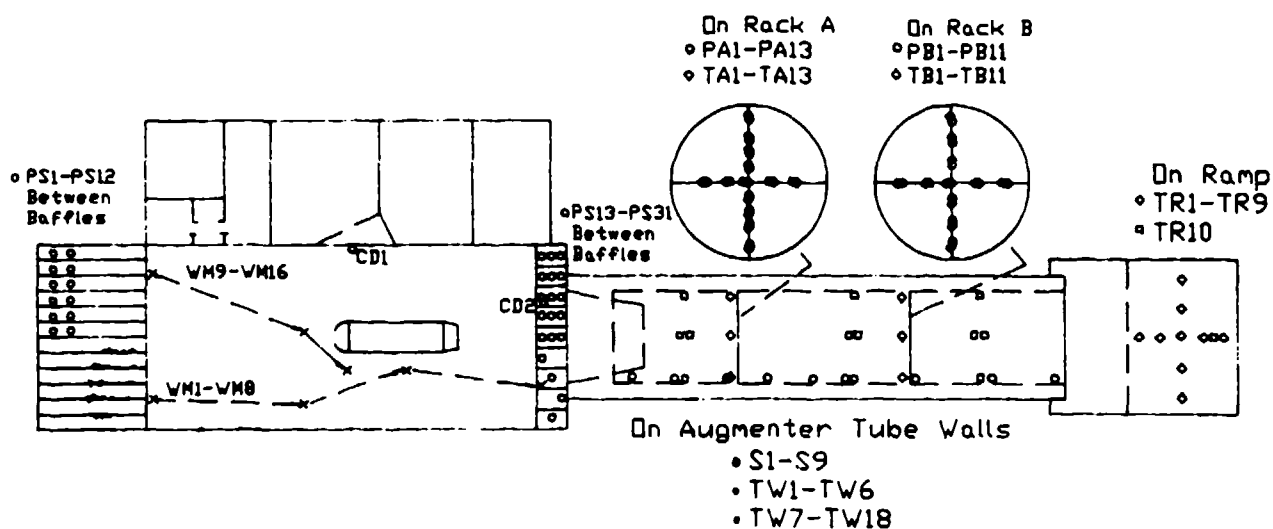


Figure B-2. Location of instrumentation for aerothermal tests at NAS Cubi Point T-10 test cell (top view).

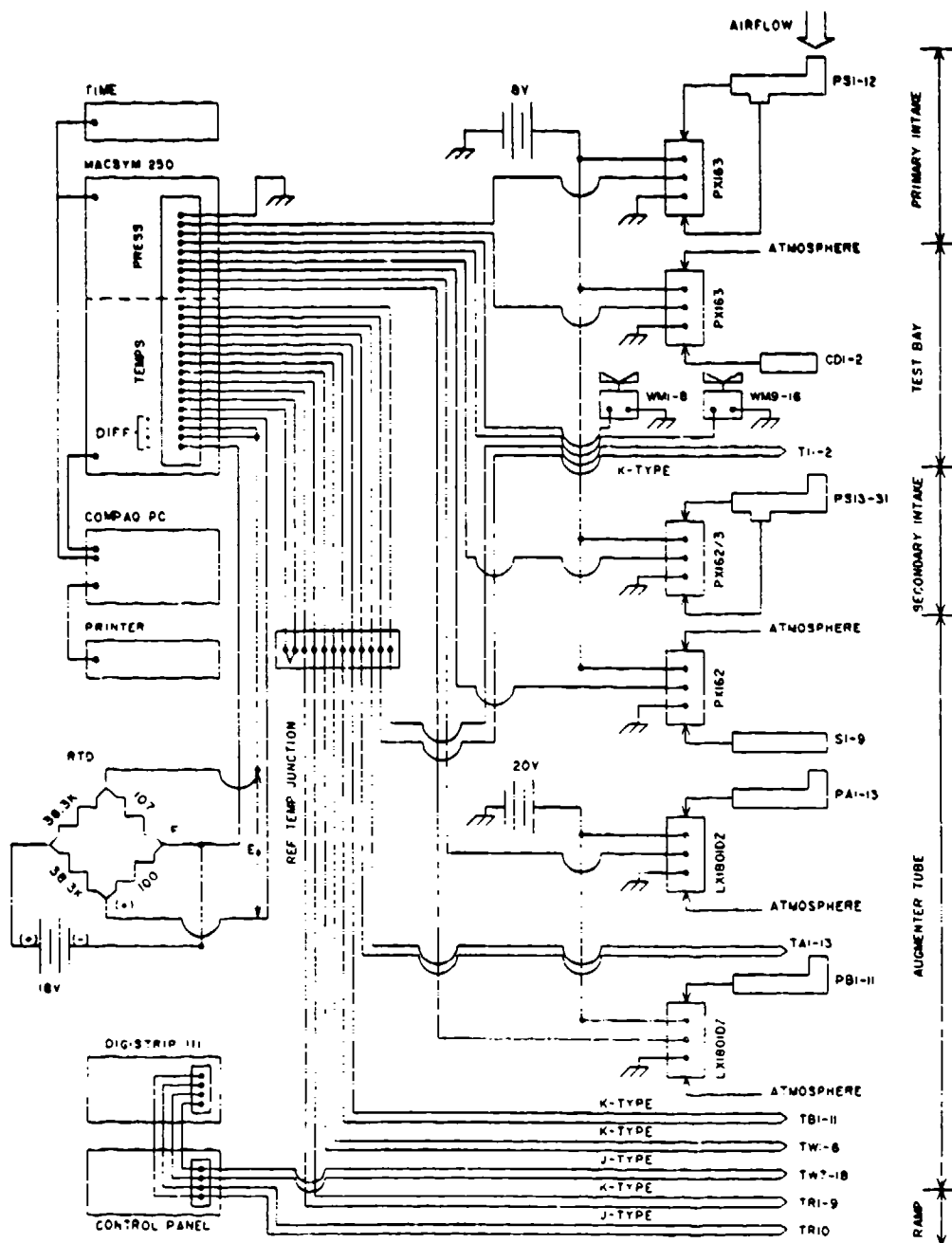


Figure B-3. Schematic of instrumentation for aerothermal tests at NAS Cubi Point.

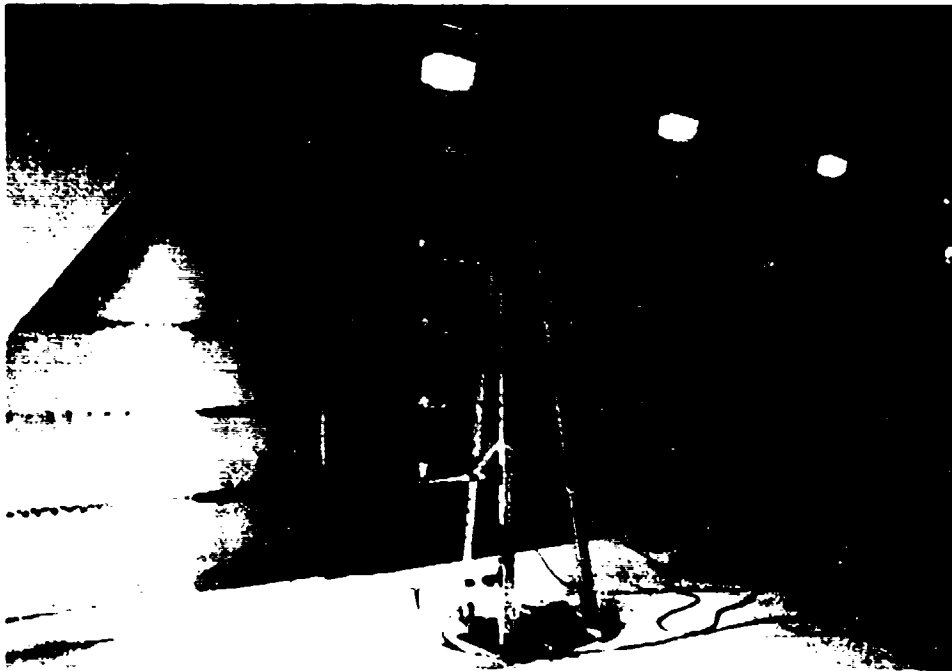


Figure B-4. Anemometer stand with seven anemometers, moveable within test bay.

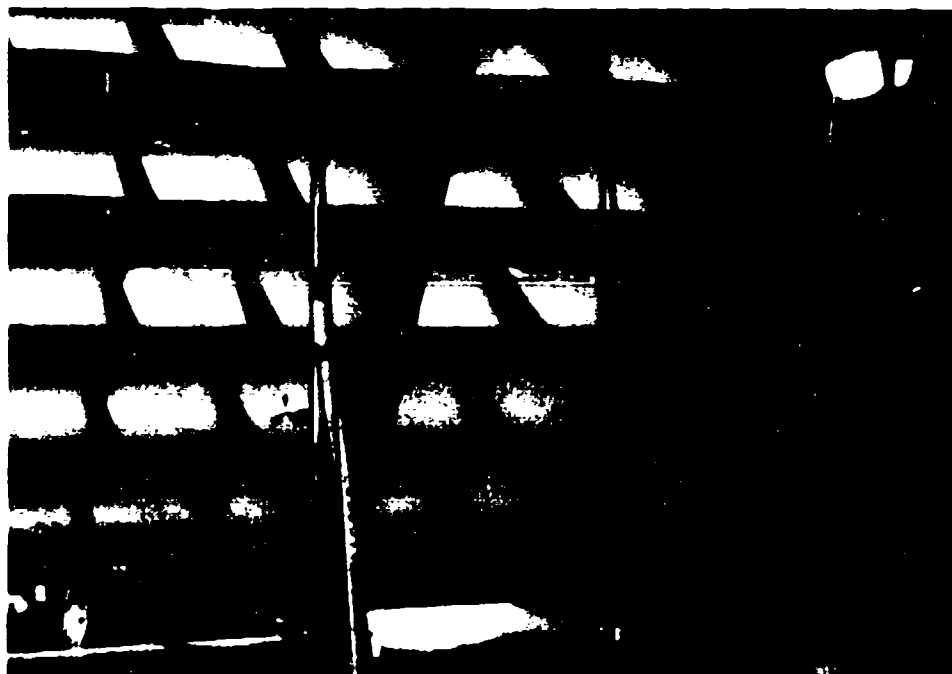


Figure B-5. Streamers attached to inlet turning vanes for flow visualization. Also both anemometers stands.

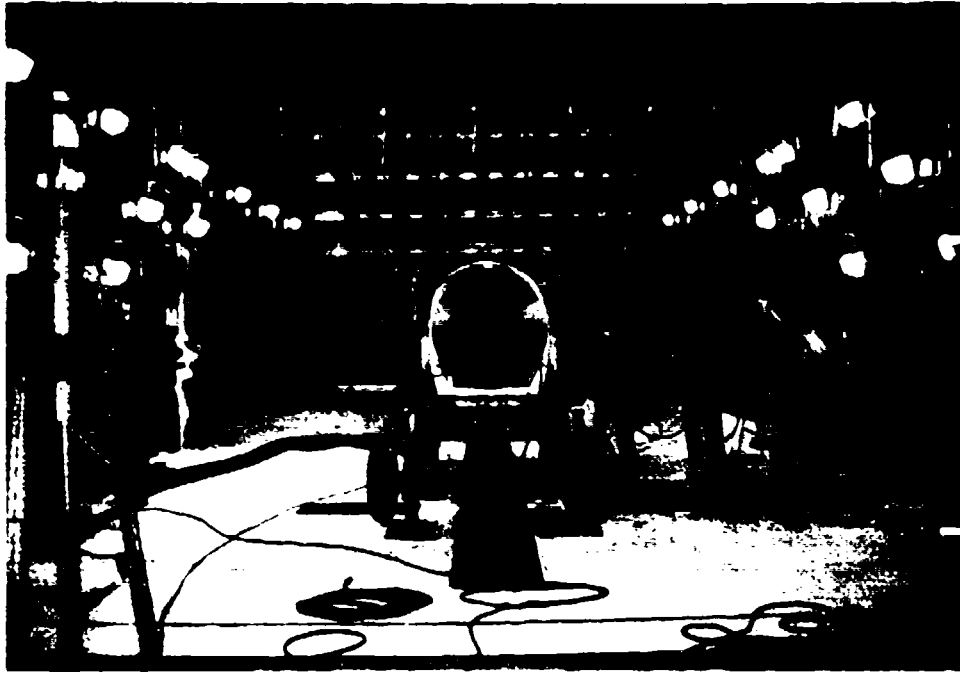


Figure B-6. Streamers across test bay for flow visualization.

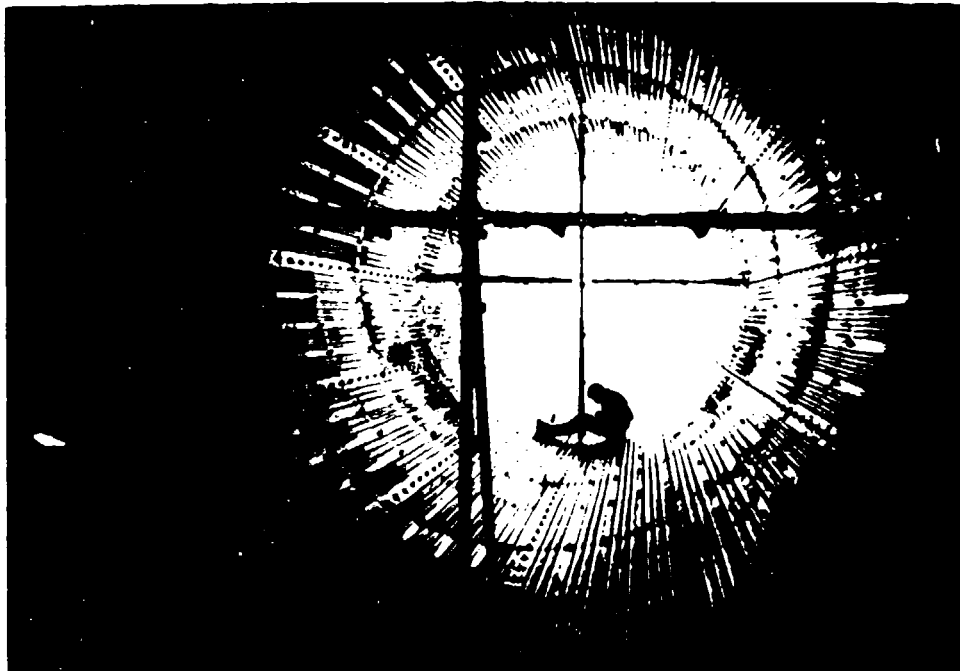


Figure B-7. Augmenter instrumentation racks A in foreground and B in background.

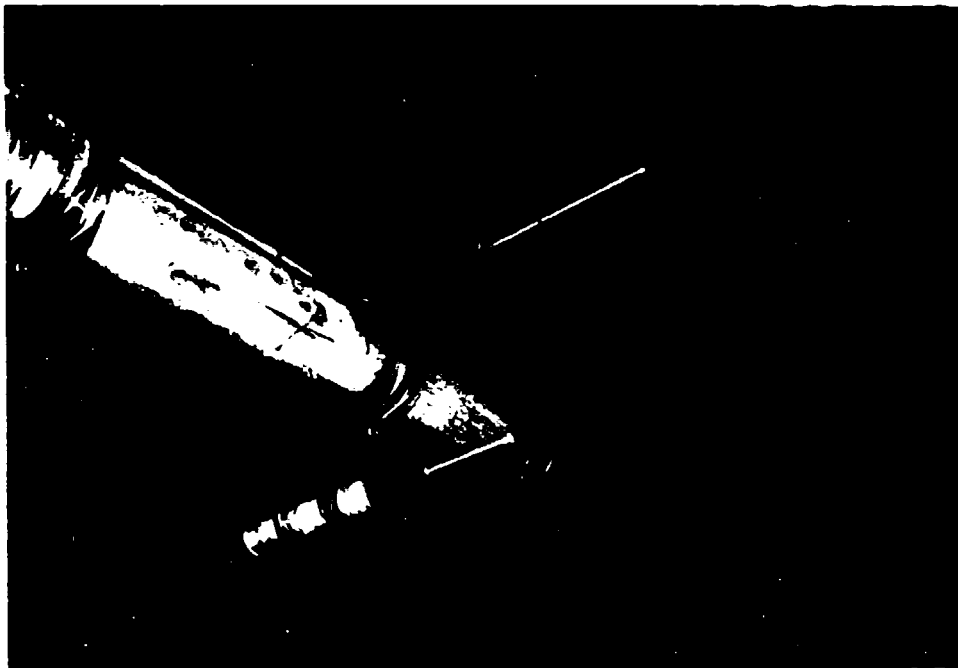


Figure B-8. Typical installation of pitot tube and pencil-probe "ending" thermocouple on augmeter instrumentation rack.

Appendix C

ACCURACY OF THE DATA

There are several methods of estimating the accuracy of the results of these tests: (1) the accuracy of both pressures and temperatures can be judged by examining how well mass and energy calculated from the data are conserved across the test cell, (2) the velocity of the air entering the primary inlet was measured by three independent techniques. From these velocities, mass flows can be calculated and compared, and (3) standard deviations of the data were calculated and, in part, provide another benchmark of the accuracy of the instrumentation.

CONSERVATION OF MASS

The mass entering the test cell, the primary plus secondary inlet air, must (neglecting the small contribution of the jet fuel) equal the total mass of the gases passing each of the instrumentation racks. Referring to Figure C-1.

$$M_{PA} + M_{SA} = M_A = M_B$$

As an illustration, consider the F404 being tested at A/B. The inlet flows are determined from pitot tubes mounted in each of inlets, assuming an incompressible symmetric flow as discussed previously. For example:

$$M_{PA} = 1005 \text{ lb/sec}, M_{SA} = 820 \text{ lb/sec}$$

or a total inlet flow of 1,825 pounds of air per second.

Gas flow through the augmentor tube was also determined from pitot tube pressure measurements; here the probes were attached to racks extending across the tube. The problem of calculating mass flow across these racks is difficult since both velocity and temperature vary greatly with radial location. It is best accomplished by calculating the mass flux at each probe, fitting a curve to the results, and integrating this curve over the entire cross section of the tube.

Continuing with the above example, the mass flux across rack "A" can be approximated with the relationship:

$$\dot{M}_A = 25.3 - 0.6r^2 \text{ lb/sec-ft}^2$$

This function and the mass fluxes calculated at each probe are shown together on Figure C-2 for comparison. Integrating over the cross sectional area of the augmentor tube:

$$\begin{aligned}
 \dot{M}_A &= \int_0^{6.9 \text{ ft}} 2\pi r \dot{M}_A \, dr \\
 &= 2\pi \int_0^{6.9} r (25.3 - 0.6 r^2) \, dr \\
 &= 1,650 \text{ lb/sec}
 \end{aligned}$$

The mass flow calculated in this manner is about 9% less than the mass measured at the two inlets.

Using an analogous procedure, the mass flow across rack "B" was 1,730 lb/sec, a value about 5% more than calculated at the first rack and approximately 5% less than the inlet flow.

Differences this small are certainly within the errors inherent in the methods used to calculate the mass flows. These mass flow comparisons and others are summarized as Table C-1.

CONSERVATION OF ENERGY

In the same manner, the energy entering the test cell, the thermal plus kinetic energy in the inlet air plus the chemical energy of the fuel, must equal the thermal plus kinetic energy passing each of the instrumentation racks. Referring to Figure C-3:

$$\begin{aligned}
 (\dot{M}_{PA} + \dot{M}_{SA}) (C_P T)_\infty + \dot{M}_f \text{HV}_f &= \dot{M}_A \left(C_P T + \frac{V^2}{2} \right)_A \\
 &= \dot{M}_B \left(C_P T + \frac{V^2}{2} \right)_B
 \end{aligned}$$

As with the mass balance, the energy flux is calculated from the rack data and a curve generated to fit these values. Another simple integration then yields the desired gas energies. For the validation of the F404 A/B run, the energy passing rack "A" was 0.30 MBtu/sec, passing rack "B" was 0.35 MBtu/sec, and the energy entering the test cell was 0.39 MBtu/sec. This energy balance is poorer than the mass balance but still close enough to give confidence to the data.

INDEPENDENT VELOCITY MEASUREMENTS

Mass flows through the primary inlet can also be determined from velocities measured with the anemometers. These velocities are discussed in Appendix B. Assuming incompressibility, a good assumption, a flat velocity profile between sets of vanes, perhaps a good assumption, and employing a computer model to extrapolate up beyond the highest anemometer (Ref C-1), the Bernoulli equation can be used to calculate a mass

flux. Some primary inlet airflows determined in this manner are also included on Table C-2 for direct comparison with airflows derived from the pitot tube pressures. Airflows measured with the anemometers were about 20% lower; than pitot tube measured airflows.

Using a hand-held anemometer, the correlation team also measured primary inlet airflows (Ref C-2). This is yet another comparison that can be used to evaluate the accuracy of the pitot tube velocity measurements. Table C-2 lists both sets of measurements. The airflow measured by the correlation team ranged from 0% up to 16% greater than the airflows measured using the pitot tubes.

STANDARD DEVIATION

The data used to generate the figures are average values, averages of readings taken every second for half a minute or more. This data varied greatly from reading to reading. Much of this variation is attributable to the actual physics of the problem, however; the variables are really fluctuating from second to second. Turbulence would account for much of this.

Therefore, the standard deviations of this data represent more than the errors in the system of data collection. With this reservation, Table C-3 is provided as another measure of the accuracy of the results. It includes standard deviations associated with the data collected during two runs that represent extremes encountered during the testing: the TF30 at A/B and then at idle. In terms of both absolute values and percentage of the arithmetic mean, fluctuations recorded during the A/B run are far more severe. This would tend to substantiate the expected contribution due to turbulence. Typically at A/B, standard deviations of the temperatures averaged around 10% of the average value. Standard deviations of pressures were 25% of the mean or higher. Standard deviations of the anemometers ranged from 5% to 10% of the mean velocity.

REFERENCES

C-1. Cham Ltd. Technical Report TR/100: Phoenix-beginners guide and user manual, by H.I. Rosten and D.B. Spalding, London. October 1986.

C-2. Naval Air Station, Cubi Point. NAPC-LR-87-8: Jet engine test cell correction, Republic of the Philippines, 31 March 1987.

Table C-1. Conservation of Mass and Energy Across
T-10 Test Cell at NAS Cubi Point

[All Runs With Throttle Plate Installed]											
Engine	TF30	TF30	F404	F404	F404	F404	TF41	TF41	J52- P48B	J52- 4P8B	J52- P408
Power	A/B	Mil	A/B	Mil	85%	Idle	Mil	85%	Mil	85%	85%
Inlet lb/sec	1844	1943	1825	1862	1140	368	1948	1254	1527	1167	1189
Rack "A" Mass	1853	1404	1650	1578	1317	305	1560	1554	1711	1343	1400
Rack "B" Mass	1945	1723	1730	1531	926	331	1833	1100	1445	1061	1067
Inlet MBtu/sec	0.50	0.29	0.39	0.28	0.16	0.05	0.30	0.19	0.24	0.17	0.18
Rack "A" Energy	0.43	0.20	0.30	0.24	0.19	0.04	0.23	0.22	0.25	0.19	0.19
Rack "B" Energy	0.48	0.27	0.35	0.24	0.13	0.05	0.29	0.16	0.22	0.15	0.15

Table C-2. Comparison of Independent Primary Inlet

[All Runs With Throttle Plate Installed]				
Engine	Power	Measured Primary Inlet Airflows (lb/sec)		
		Pitot Tubes	Anenometers	Correlation Team ^a
TF30	M11	1050	970 1075	
F404	A/B	1020	840	1021
		1005	820	
		1000	840	
	M11	990		
		1080		
		1000		
	85%	595	500	
		640		
	Idle	245	180	
J52-P-8B	M11	900	865	849
		840		
		910		
		920		
	85%	775	605	
		680		
	Idle	300	180	
		295		
TF41	M11	1170	880	1303
		1130	870	
		1140	930	
			930	

^aSee Reference C-2

TABLE C-3. TYPICAL STANDARD DEVIATIONS IN THE AEROTHERMAL DATA;
TESTING THE TF30 IN THE T-10 CELL AT HAS CUBI POINT

MEASUREMENT	A/B		MIL		85%		IDLE	
	AVERAGE OF 35 READINGS	STANDARD DEVIATION	AVERAGE OF 68 READINGS	STANDARD DEVIATION	AVERAGE OF 66 READINGS	STANDARD DEVIATION	AVERAGE OF 80 READINGS	STANDARD DEVIATION
CELL DEPRESSION, in. H_2O	-0.550	1.487	-0.695	0.412	-0.275	0.105	-0.055	0.032
PITOT-STATIC HEAD AT PRIMARY INLET, in. H_2O	1.005	0.284	1.139	0.099	0.411	0.114	0.085	0.018
PITOT-STATIC HEAD AT SECONDARY INLET, in. H_2O	4.226	4.360	2.366	0.628	1.000	0.161	0.129	0.037
AUGMENTER TUBE WALL STATIC PRESSURE, in. H_2O	-4.834	0.386	-4.901	0.013	-3.737	1.371	-0.386	0.137
TOTAL PRESSURE PROBE IN CENTER OF RACK "A", PSI	64.297	4.734	50.698	6.144	15.513	2.211	1.382	0.299
ANEMOMETER IN TEST BAY, FT/SEC	35.782	1.302	37.685	1.555	24.760	1.043	9.925	2.126
GAS TEMPERATURE AT CENTER OF RACK "A", °F	1034.712	143.759	270.160	78.110	167.034	27.865	142.326	0.818
AUGMENTER TUBE WALL TEMPERATURE NEAR RACK "B", °F	542.356	51.826	168.511	0.956	128.346	0.948	114.253	1.826
RAMP WALL TEMPERATURE, °F	468.084	61.737	176.543	0.990	126.176	1.185	104.380	1.704

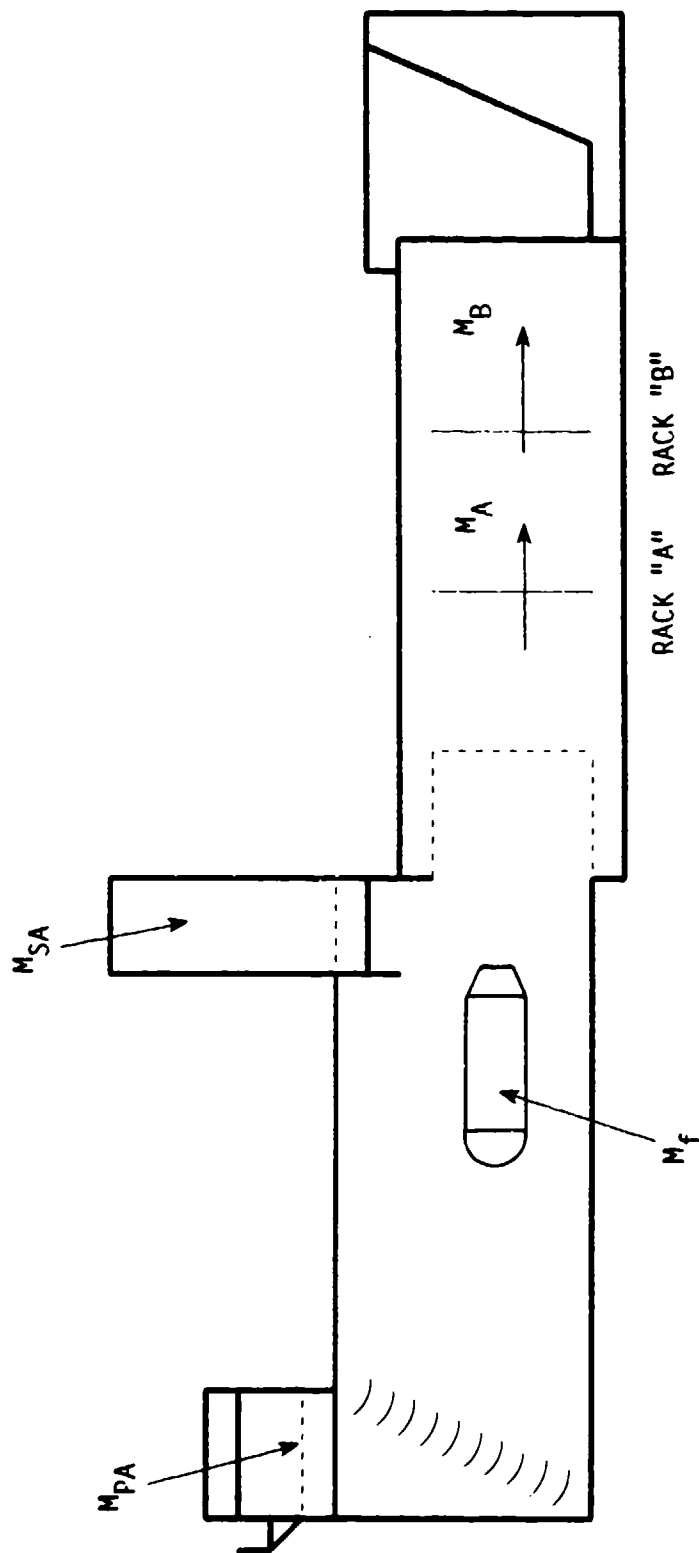


Figure C-1. Conservation of mass across T-10 test cell at NAS Cubi Point.

NOTES:

- (1) F404 AT A/B
- (2) RACK A IS 30 FT DOWN THE TUBE
- (3) r = DISTANCE FROM CENTER OF AUGMENTER TUBE

● CALCULATED FROM PRESSURES AND TEMPERATURES MEASURED 11/11/86

MASS FLUX = $25.3 - 0.6 r^2$

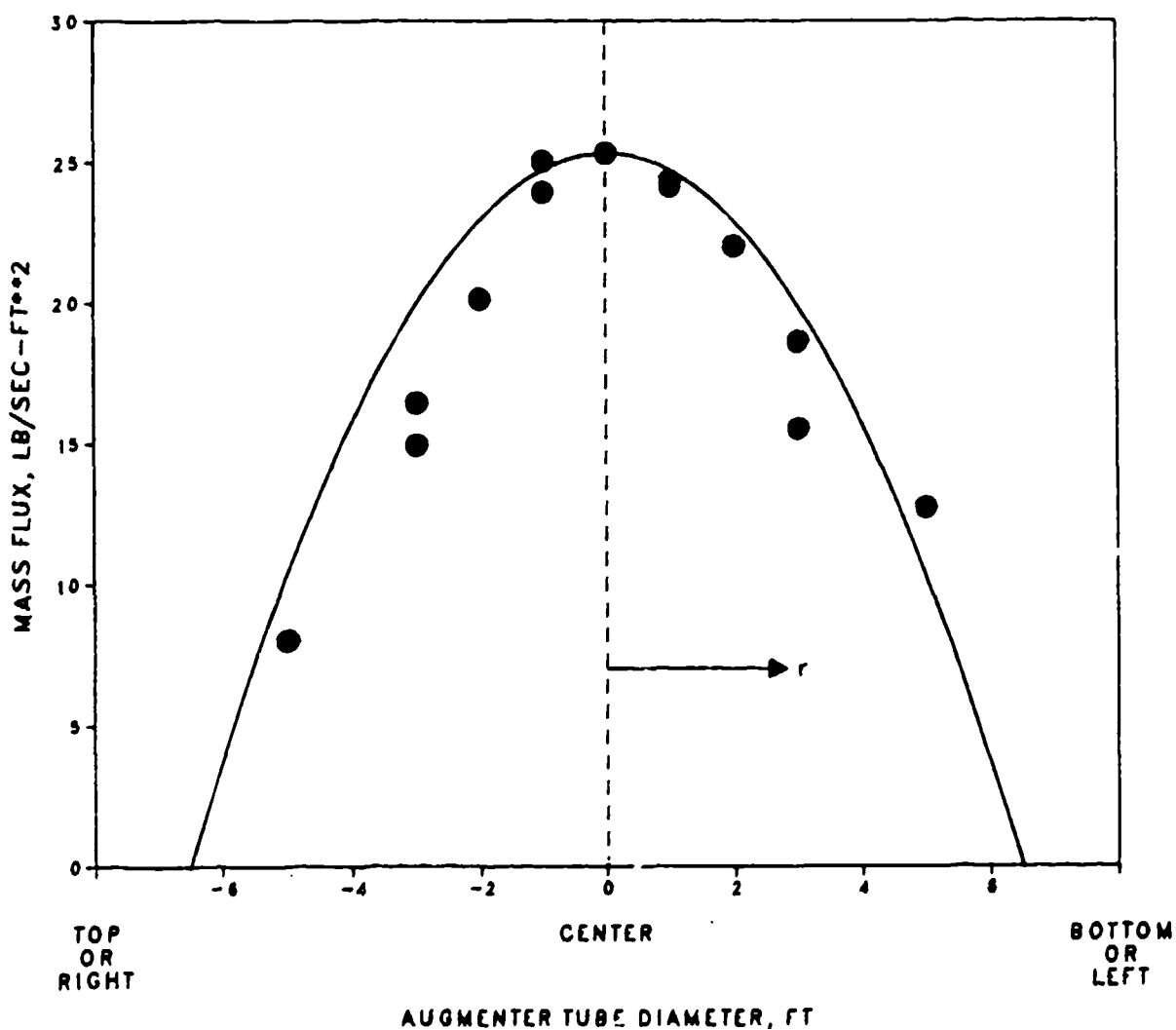


Figure C-2. Curve fitting to the mass flux of the gas flow at rack A.

M = mass flow
 C_p = specific heat
 T = temperature
 V = velocity
 HV = heating value

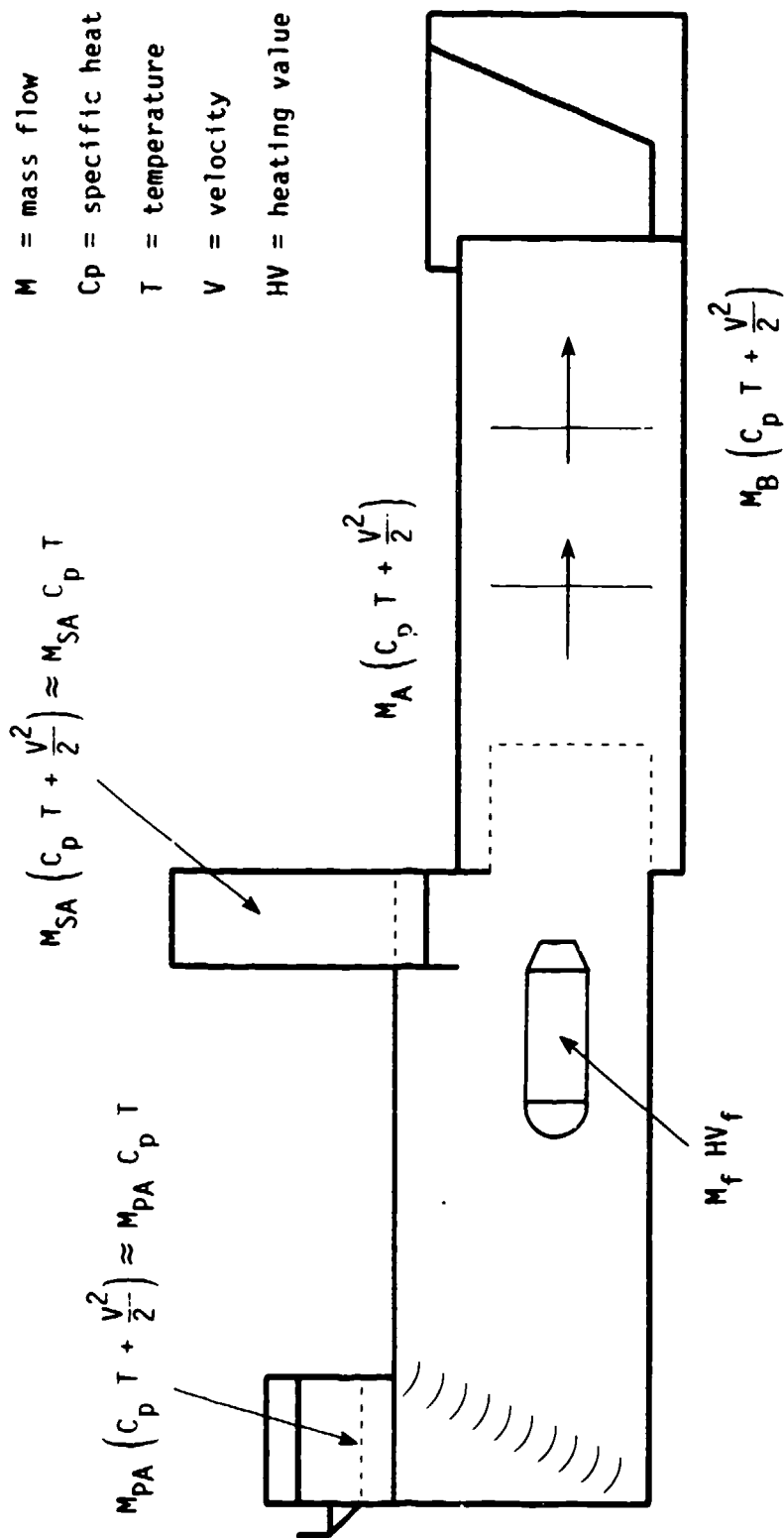


Figure C-3. Conservation of energy across T-10 test cell at NAS Cubi Point.

Appendix D

DATA REDUCTION TECHNIQUES

Periodically, the test sequence was interrupted to allow the MACSYM 250 to download and copy its data disk onto a COMPAQ PC data disk. This provided backup copies of the data. In addition, this procedure permitted preliminary analysis of results (computation of mass flow through the hush house and distribution of flow through sections of the intake) at the site while testing continued. For compatibility with the MACSYM 250, the COMPAQ PC had dual disk drives, an Intel 8087 board, and an AD PCID 1 communication card.

The calculations involved in the data reduction are described in Appendixes B and C. The BASIC program employed to make these calculations is provided here. Typical results are also included.

PROGRAM LISTING

```

10 REM    PROGRAM CMDT TO AVERAGE DATA AND CALCULATE VELOCITIES AND
20 REM    MASS FLOWS. SPECIFIC FOR NAS CUBI PT. TESTING 11/86.
30 REM    EDIT LINES 200-210 FOR WEATHER AND PRINT HEADING (ENG. ETC.)
40 REM    $USE 13.6 TO CONVERT INCHES OF MERCURY TO INCHES OF WATER.†
50 REM
60 CLS: CLEAR:  OPTION BASE 1
70 DIM DAT( 145), SUM( 145), C1( 145), AVE( 145), MMS( 145)
80 DIM O( 145), M(95), A(60), PR( 65), TR(75), V(77), RHO(40)
90 DIM PT(57), PS(57), VWM(18), WM(18), OS(13), DS(13), MS(13), EA(38)
100 REM
110 READ K1,K2,R,GC
120 DATA 1.41,1.39,53.36,32.174
130 FOR I=1 TO 20: READ A(I) : NEXT I
140 DATA 24.1,07.7,03.2,01.6,0.80,01.6,03.2,07.7,24.1,33.5,
      02.9,02.9,33.5,17.0,12.6,06.3,3.10,06.3,12.6,17.0
150 FOR I = 21 TO 40: READ A(I): NEXT I
160 DATA 29.6,06.3,06.3,29.6,04.6,04.4,04.4,04.4,04.4,04.4,
      04.6,04.4,04.4,04.4,04.4,04.4,4.42,4.42,4.42,4.42
170 FOR I = 41 TO 55: READ A(I): NEXT I
180 DATA 4.42,4.42,4.42,4.42,4.42,4.42,4.42,4.42,4.42,4.42,
      4.42,13.25,13.25,13.25,13.25
190 LPRINT
200 LPRINT "LOCATION: NAS CUBI POINT      ENGINE:          THROTTLE:
210 LPRINT "DATE: 11/  /86          BAROM. = 40 IN. H2O ;
      AMB. TEMP =  F. "      ; TR47 = 88 ; PR37 = 405
220 CN = 132: HRSLX= 1: TLIN=1: NLIN=11  '**** NUM CHANNELS,'HR' LOC ETC.
230 NCHAV = 129: EVSL = 4
240 OF$="OFFZCUPB"  ': LPRINT " CALIB OFFSET ZERO IS 'OFFZCUPB' PER L-240"
250 CONV$="CUPCONB"  ': LPRINT " CONVERTS/MULTIPLIER IS 'CUPCONB' PER L-250"
260 PRINT"    PROGRAM 'CMDT' TO AVERAGE DATA AND CALCULATE VELOCITIES AND"
270 PRINT"    MASS FLOWS. EDIT LINES 200 THRU 250 FOR HEADING, WEATHER, ETC."
280 PRINT"    "
290 PRINT:INPUT "ENTER THE DATA FILE TO BE ANALYZED  (ON DRIVE B:)";
      DA$:PRINT
300 NAM$ = "NOSAVE"
310 REM
320 OPEN "R",#1,"A:"+OF$+".DAT",40          'OFFSET FILE
330 FIELD #1, 4 AS OS(1), 4 AS OS(2), 4 AS OS(3), 4 AS OS(4), 4 AS OS(5),
      4 AS OS(6), 4 AS OS(7), 4 AS OS(8), 4 AS OS(9), 4 AS OS(10)
340 OPEN "R",#2,"B:"+DA$+".DAT",48          'DATA FILE
350 FIELD #2, 4 AS DS(1), 4 AS DS(2), 4 AS DS(3), 4 AS DS(4), 4 AS DS(5),
      4 AS DS(6), 4 AS DS(7), 4 AS DS(8), 4 AS DS(9), 4 AS DS(10),
      4 AS DS(11), 4 AS DS(12)
360 OPEN "R",#3,"A:"+CONV$+".DAT",40          'UNITS CONVERSION FILE
370 FIELD #3, 4 AS MS(1), 4 AS MS(2), 4 AS MS(3), 4 AS MS(4), 4 AS MS(5),
      4 AS MS(6), 4 AS MS(7), 4 AS MS(8), 4 AS MS(9), 4 AS MS(10)
380 OPEN "R",#4,"B:"+NAM$+".DAT",40          'STATISTICAL FILE
390 FIELD #4, 4 AS SS(1), 4 AS SS(2), 4 AS SS(3), 4 AS SS(4), 4 AS SS(5),
      4 AS SS(6), 4 AS SS(7), 4 AS SS(8), 4 AS SS(9), 4 AS SS(10)
400 REM

```

```

410 REM                                ***** LOAD IN CONV FILE
420 FOR J=1 TO 132 STEP 10
430 GET #3
440     FOR I= 1 TO 10
450         MMS(I+J-1)=CVS(M$(I))
460     NEXT I
470 NEXT J
480 REM                                *** LOAD IN OFFSET FILE
490 FOR J=1 TO 90 STEP 10
500 GET #1
510     FOR I= 1 TO 10
520         O(I+J-1)=CVS(O$(I))
530     NEXT I
540 NEXT J
550 CLOSE #1 :    CLOSE #3
560 REM
570 REM  A KEY TO SUCCESSFUL EXECUTION OF THE PROGRAM IS PROPER
580 REM  EVENT TIMES.  LOCAL REAL TIME WAS RECORDED IN DATA.
590 REM
600 PRINT:INPUT "ENTER START TIME          (HR, MIN, SEC)";H1,M1,S1
610 SEC1=3600*H1+60*M1+S1
620 PRINT:INPUT "ENTER FINAL TIME          (HR, MIN, SEC)";H2,M2,S2
630 SEC2=3600*H2+60*M2+S2
640 IF SEC2<SEC1 THEN PRINT:PRINT CHR$(7):PRINT "BAD ENTRY!":GOTO 600
650 INC=22
660 N=0
670 REC% = 0                                '*****START DATA GET LOOP AND
680 REC%=REC%+1                                'SEARCH FOR CORRECT TIME SPAN
690 GET #2,REC%
700 IF EOF(2) THEN GOTO 950
710 FOR I=1 TO 12: DAT(I)=CVS(D$( I)): NEXT I
720 PRINT DAT(HRSLX+TLIN-1);":":DAT(HRSLX+TLIN);":":DAT(HRSLX+TLIN+1)
730 SEC=DAT(HRSLX+TLIN-1)*3600+DAT(HRSLX+TLIN)*60+DAT(HRSLX+TLIN+1)
740 IF SEC<SEC1 THEN REC% = REC% + 10        'CHECK IF DATA IS WITHIN BOUNDS.
750 IF SEC<SEC1 THEN GOTO 680                ' THIS LINE ENDS THE TIME SEARCH LOOP
760 REM IF (N=0) AND (SEC>(SEC1+2*INC)) THEN GOTO 4600
770 N=N+1
780 REM
790 FOR J=13 TO 129 STEP 12                    '***** PULL IN DATA      **
800     REC%=REC%+1
810     GET #2,REC%
820     FOR I=1 TO 12: DAT(I+J-1)=CVS(D$(I)): NEXT I
830 NEXT J
840 IF N=1 THEN GOTO 920                        '****PRINT FOR 1st SECOND OF DATA
850 IF SEC>=(SEC2 + .6) THEN GOTO 940
860 REM                                FOR DATA STILL IN RAW VOLTAGE, DO
870 REM                                PRELIMINARY STATISTICAL ANALYSIS
880 FOR L=1 TO NCHAV
890     SUM(L)=SUM(L)+DAT(L): C1(L)=C1(L)+DAT(L)*DAT(L)
900 NEXT L
910 GOTO 680
920 LPRINT "FIRST TIME ARRAY IS AT:  ";DAT(1);":":DAT(2);":":DAT(3)
930 GOTO 680
940 N = N - 2
950 LPRINT "AVERAGED ";N+1;" READINGS THRU ";

```

```

960 LPRINT "TIME: ";DAT(TLIN+HRSLSX-1);";";DAT(TLIN+HRSLSX);";";
      DAT(TLIN+HRSLSX+1)
970 REM      *****CONVERT THE DAT() & SUM( ) FILES TO ENGINEERING UNITS
980 FOR K=1 TO NCHAV
990     DAT(K) = MMS(K)*(DAT(K)-O(K))
1000    SUM(K) = MMS(K)*(SUM(K)-N*O(K))
1010 NEXT K
1020 X=0
1030 FOR J=1 TO NCHAV STEP 10  'CLEAR 2 REM'S TO PRINT OUT AVERAGES **
1040     FOR K=1 TO 2:         ' REM LPRINT:LPRINT USING " ###. ";X+1;
1050         FOR I=1 TO 5: X=X+1
1060             AVE(X)=SUM(X)/N
1070 REM             LPRINT USING " ####.### ";AVE(X);
1080         NEXT I
1090     NEXT K
1100 NEXT J
1110 REM
1120 PR(37) = PR37             ' AMBIENT P; STILL IN IN. H2O,FM LINE 210
1130 TR(47) = TR47 + 459.7:   TR47 = TR47 + 459.7         ' DEG. RANKINE
1140 RHOIN = .03613*144*PR37/TR47/53.36
1150 MCELL(1) = 0: MSEC = 0
1160 REM     LOAD AVERAGED PRESSURE FILE FOR INLETS; CONV. TO PSF
1170 FOR J=1 TO 31
1180     PR( J ) = .03613*144*AVE( 40 + J )
1190 NEXT J
1200 REM CALCULATE PRIMARY INLET VELOCITIES AND MASS FLOWS
1210 FOR I = 1 TO 12
1220     V(I) = SQR(2*ABS(PR(I))*32.174/RHOIN)
1230         IF PR(I) < 0 THEN V(I) = 0
1240     M(I) = RHOIN*A(I + 24)*V(I)
1250     MCELL(1) = MCELL(1) + 4*M(I)
1260 NEXT I
1270 REM
1280 REM
1290 VFWMA = V(1): VFWMB = V(7)
1300 REM CALCULATE SECONDARY INLET VELOCITIES AND MASS FLOWS
1310 FOR I = 13 TO 31
1320     V(I) = SQR(2*ABS(PR(I))*32.174/RHOIN)
1330         IF PR(I) < 0 THEN V(I) = 0
1340     M(I) = RHOIN*A(I + 24)*V(I)          'A( ) FROM LINES ---
1350     MSEC = MSEC + M(I)
1360 NEXT I
1370 REM
1380 PRINT:PRINT " DO YOU WANT TO CALCULATE PRIMARY INLET AIRFLOWS "
1390 PRINT" USING WINDMILLS? ( 0 = YES, RACK 1; --- 1 = YES, RACK 2;
      --->2 = NO)"

1400 INPUT WMINANS
1410 IF WMINANS >1 GOTO 1540
1420 FOR I = 1 TO 8: VWM(I) = AVE (I+71+8*WMINANS): NEXT I
1430 REM     AVERAGE THE VELOCITY FOR 60 SQ.FT. SLOTS HAVING 2 WINDMILLS;
1440 REM     EXTRAPOLATE FOR SLOTS (9 & 10) WITHOUT WINDMILLS .
1450 VWM(2) = .5*(VWM(2)+VWM(3)): VWM(3)=0: VWM(4) = .5*(VWM(4)+VWM(5))
1460 VWM(5) = 0: VWM(9) = .5*VWM(4): VWM(10) = .28*VWM(4)

```

```

1470 FOR I = 1 TO 10
1480   MWM = MWM + 60*RHOIN*VWM(I)
1490 NEXT I
1500 LPRINT:LPRINT: LPRINT "INLET FLOW CHARACTERISTICS": LPRINT
1510 LPRINT "PRIMARY INLET"
1520 FOR I=1 TO 12: LPRINT USING " _V_ (##) = ###.## M(##) =
###.## PR(##) = ###.## ##.##;I,V(I);I;M(I);I;PR(I) _=
1530 NEXT I
1540 LPRINT:LPRINT USING "   PRIMARY INLET MASS FLOW = ###.## LB/SEC";
      MCELL(1)
1550 LPRINT:LPRINT USING "   PRIMARY INLET MASS FLOW MEASURED WITH
WINDMILLS = ###.## LB/SEC ";MWM
1560 LPRINT:LPRINT "SECONDARY INLET "
1570 FOR I=13 TO 31: LPRINT USING " _V_ (##) = ###.## M(##) =
###.## PR(##) = ###.## ##.##;I,V(I);I;M(I);I;PR(I) _=
1580 NEXT I
1590 LPRINT:LPRINT USING "   SECONDARY INLET MASS FLOW = ###.## LB/SEC ";
      MSEC
1600 LPRINT:LPRINT "SECONDARY INLET SYMMETRY CHECK "
1610 LPRINT USING " V(28) = ###.## CORRESPONDS TO V(22) = ###.##";
      V(28); V(22)
1620 LPRINT USING " V(29) = ###.## CORRESPONDS TO V(20) = ###.##";
      V(29);V(20)
1630 LPRINT USING " V(30) = ###.## CORRESPONDS TO V(18) = ###.##";
      V(30);V(18)
1640 LPRINT USING " V(31) = ###.## CORRESPONDS TO V(14) = ###.##";
      V(31);V(14)
1650 MCELL(1) = MCELL(1) + MSEC      ' TOTAL INLET AIRFLOW, PRI. + SEC.
1660 REM
1670 VMAX = V(1)
1680 FOR I=2 TO 31                      'LOCATE MAX TEST CELL INLET
1690   IF V(I) > VMAX, THEN VMAX = V(I)      'VELOCITY
1700 NEXT I
1710 REM AUGMENTATION AIRFLOW AND AUGMENTATION RATIO CALC VIA INLETS.
1720 PRINT: INPUT "ENTER ENGINE MASS FLOW IN LB/SEC, AND FUEL FLOW IN
      LB./HR." , MENG, FENG
1730 MSEC(1) = MCELL(1) - MENG
1740 AUGRAT(1) = MSEC(1)/MENG
1750 LPRINT
1760 LPRINT USING "TOTAL   INLET   AIRFLOW           = ###.## LB/SEC";MCELL(1)
1770 LPRINT USING "AUGMENTATION AIRFLOW OF INLETS = ###.## LB/SEC";MSEC(1)
1780 LPRINT USING "AUGMENTATION RATIO           =   ##.##"; AUGRAT(1)
1790 REM
1800 REM                      CALCULATE EXHAUST FLOWS
1810 KS1 = (K1 - 1)/K1
1820 KS2 = 2/(K1 - 1)
1830 REM   LOAD EXHAUST TEMPERATURES AND DP'S; CONVERT TO RANKINE & PSI
1840 PR37 = .03613*PR37
1850 FOR I = 1 TO 36
1860   TR(I) = 459.7 + AVE(I+ 95)
1870   PR(I) = .03613 * AVE(I+4)      ' PR(25) & PR(26) ARE CD'S
1880 NEXT I

```

```

1890 REM   CALCULATE EXHAUST FLOWS OF THE TWO EXHAUST RACKS
1900 FOR K = 1 TO 15 STEP 13
1910   FOR I = 1 TO 13
1920     PT(I) = PR(I + K -1) + PR37
1930     PS25 = PR(30 + INT(K/4) ) + PR37
1940     RHO(I) = 144*PS25/TR(I + K -1)/R
1950     MACH = SQR(KS2*ABS((PT(I)/PS25)*KS1 - 1))
1960     V(I + K -1) = MACH*(K1*GC*R*TR(I + K -1))*0.5
1970     IF ((PT(I)/PS25)*KS1-1) < 0 THEN V(I + K -1) = 0
1980     M(I + K -1) = RHO(I)*A(I + K -1 )*V(I + K -1)
1990   NEXT I
2000 NEXT K
2010 REM   ENERGY BALANCE CONSTANTS AND CALCULATIONS.
2020 HVF = 18069: CHEM = FENG*HVF/3600000000# ' FENG IN LB/HR
2030 EAIR = MCELL(1)*(.24*TR47 + .00002*V(30)*2)/1000000!
2040 EIN = CHEM + EAIR
2050 LPRINT:LPRINT USING "EAIR = ###.###, EFUEL = ###.###,
EIN = ###.### MBTU/SEC.";EAIR;CHEM;EIN
2060 LPRINT:LPRINT "EXHAUST RACK 'A' "
2070 FOR I=1 TO 13
2080   MCELL2A = MCELL2A + M(I)
2090   LPRINT USING "V(##) = ###.## FT/SEC";I,V(I);
2100   LPRINT USING " T(##) = ### DEG. F M(##) = ###.## LB/SEC";I;
TR(I)-459.7;I;M(I)
2110 NEXT I
2120 LPRINT:LPRINT USING "TOTAL AUGMENTATION TUBE AIRFLOW (BY SUM) =
###.## LB/SEC"; MCELL2A
2130 MCELL2A = 0 : ECELL2A = 0: M(1)=M(1)/A(1)
2140 FOR I = 5 TO 13: M(I) = M(I)/A(I): NEXT I
2150 A(1)=1:A(5)=1:A(9)=1
2160 EA(5) = M(5)*(.24*TR(5) + .00002*V(5)*2)
2170 EA(1) = M(1)*(.24*TR(1) + .00002*V(1)*2)
2180 EA(9) = M(9)*(.24*TR(9) + .00002*V(9)*2)
2190 EA(1) = .5*(EA(1) + EA(9)): C1 = (EA(1) - EA(5))/25: C2 = EA(5)
2200 LPRINT:LPRINT "EXHAUST RACK 'B'"
2210 FOR I = 14 TO 24
2220   MCELL2B = MCELL2B + M(I)
2230   LPRINT USING "V(##) = ###.## FT/SEC";I,V(I);
2240   LPRINT USING " T(##) = ### DEG. F M(##) = ###.## LB./SEC.";
I;TR(I)-459.7;I;M(I)
2250 NEXT I
2260 LPRINT:LPRINT USING "TOTAL AUGMENTATION TUBE AIRFLOW (BY SUM) =
###.## LB/SEC";MCELL2B
2270 M(1) = .5*(M(1)+M(9)): A(1)=(M(1)-M(5))/25
2280 A(2) = M(5)
2290 FOR I = 1 TO 7 : M(I+1) = A(1)*I*2 + A(2) :
M(I) = A(1)*(I-1)*2 + A(2)
2300   EA(I+1) = C1*I*2 + C2 : EA(I) = C1*(I-1)*2 + C2
2310   MCELL2A = MCELL2A + 3.14159*(M(I+1)+M(I))*(I*2-(I-1)*2)/2
2320   ECELL2A = ECELL2A + 3.14159*(EA(I+1)+EA(I))*(I*2-(I-1)*2)/2000000!
2330 NEXT I
2340 LPRINT:LPRINT USING "TOTAL AUGMENTATION TUBE AIRFLOW, RACK 'A'
(BY INTEGR.) = ###.## LB/SEC";MCELL2A
2350 MSEC2A = MCELL2A - MENG; AUGRAT2A = MSEC2A/MENG

```

```

2360 LPRINT USING "ENGINE GAS FLOW" = ###. LB/SEC"; MENG
2370 LPRINT USING "AUGMENTATION (SECONDARY) AIRFLOW = ###. LB/SEC"; MSEC2A
2380 LPRINT USING "AUGMENTATION RATIO" = ###. "; AUGRAT2A
2390 LPRINT USING " E - RACK 'A' = ###. MBTU/SEC."; ECELL2A
2400 MCELL2B = 0; ECELL2B = 0
2410 FOR I = 1 TO 24: M(I) = M(I)/A(I): A(I) = 1: NEXT I
2420 EA(17) = M(17)*(.24*TR(17) + .00002*V(17)^2)
2430 EA(14) = M(14)*(.24*TR(14) + .00002*V(14)^2)
2440 EA(20) = M(20)*(.24*TR(20) + .00002*V(20)^2)
2450 EA(14) = .5*(EA(14) + EA(20)): C3 = (EA(14) - EA(17))/36: C4 = EA(17)
2460 M(14) = .5*(M(14)+M(20)): A(14)=(M(14)-M(17))/36
2470 A(2) = M(17)
2480 FOR I = 1 TO 7: M(I+1) = A(14)*I^2 + A(2): M(I) = A(14)*(I-1)^2 + A(2)
2490 EA(I+1) = C3*I^2 + C4: EA(I) = C3*(I-1)^2 + C4
2500 MCELL2B = MCELL2B + 3.14159*(M(I+1)+M(I))*(I^2-(I-1)^2)/2
2510 ECELL2B = ECELL2B + 3.14159*(EA(I+1)+EA(I))*(I^2-(I-1)^2)/2000000!
2520 NEXT I
2530 MSEC2B = MCELL2B - MENG: AUGRAT2B = MSEC2B/MENG
2540 LPRINT: LPRINT USING "TOTAL AUGMENTATION TUBE AIRFLOW, RACK B
(BY INTEGR.) = ###. LB/SEC" ; MCELL2B
2550 LPRINT USING "ENGINE GAS FLOW" = ###. LB/SEC"; MENG
2560 LPRINT USING "AUGMENTATION (SECONDARY) AIRFLOW = ###. LB/SEC";
MSEC2B
2570 LPRINT USING "AUGMENTATION RATIO" = ###. "; AUGRAT2B
2580 LPRINT USING "E - RACK 'B' = ###. MBTU/SEC. "; ECELL2B
2590 PMIN = AVE(29): IF AVE(30)<AVE(29) THEN PMIN = AVE(30)
2600 LPRINT: LPRINT "STATICS IN AUGMENTER TUBE -- IN. H2O"
2610 LPRINT USING " S( 1 -- 5 ) ###. ###. ###. ###. ";
AVE(31); AVE(32); AVE(33); AVE(34); AVE(35)
2620 LPRINT USING " S( 6 -- 10 ) ###. ###. ###. ###. ";
AVE(36); AVE(37); AVE(38); AVE(39); AVE(40)
2630 TMAX1 = 25 'TMAX1 IS FOR AUG. TUBE WALL TEMP.
2640 FOR I=1 TO 6
2650 IF DAT(I+89) > TMAX1, THEN TMAX1 = DAT(I+89)
2660 IF DAT(I+89) = TMAX1 THEN IMAX = I
2670 NEXT I 'TEMP
2680 REM CONVERT BACK TO DEGR F IS NOT NEEDED;
2690 TMAX2 = 25
2700 FOR I=1 TO 9
2710 IF DAT(I+119) > TMAX2, THEN TMAX2 = DAT(I+119)
'LOCATE MAX RAMP TEMP.
2720 NEXT I
2730 FOR I = 1 TO 16
2740 WM(I) = AVE(I + 71)
2750 NEXT I
2760 LPRINT: LPRINT "WINDMILL VELOCITIES ---- FT./SEC,";
2770 FOR J = 1 TO 8
2780 LPRINT USING " VWM(##) = ###.
VWM(##) = ###. "; J; WM(J); J+8; WM(J+8)
2790 NEXT J
2800 REM
2810 LPRINT
2820 LPRINT
2830 LPRINT USING "CELL DEPRESSION = ###. INCHES WATER"; PMIN
2840 LPRINT USING "MAX TEST CELL INLET VELOCITY = ###. FT/SEC"; VMAX

```

```

2850 LPRINT USING "MAX AUGMENTOR TUBE WALL TEMP. = ###.## DEG.F
AT STA. ## ";TMAX1;IMAX
2860 LPRINT USING "MAX EXHAUST RAMP TEMPERATURE = ###.## DEG.F "; TMAX2
2870 LPRINT USING "INLET TOTAL AUGMENTATION RATIO = ##.## "; AUGRAT(1)
2880 LPRINT USING "EXHAUST AUGMENTATION RATIO, RACK 'A' = ##.## ";AUGRAT2A
2890 LPRINT USING "EXHAUST AUGMENTATION RATIO, RACK 'B' = ##.## ";AUGRAT2B
2900 REM
2910 REM LPRINT FLAGS ALERTING TO POTENTIAL TEST CELL PROBLEM AREAS
2920 IF PMIN < -1.5, THEN LPRINT "** CELL DEPRESSION > 1.5 INCHES H2O **"
2930 PRINT "DONE" : LPRINT "END OF SUMMARY"
2940 GOTO 2980
2950 REM
2960 PRINT CHR$(7):PRINT "TIME ";H1;": ";M1;": ";S1;" DOES NOT OCCUR!":
GOTO 2980
2970 PRINT CHR$(7):PRINT "TIME ";H2;": ";M2;": ";S2;" DOES NOT OCCUR!
CHECK DATA FILE NAME"
2980 PRINT "DONE"
2990 PRINT;PRINT:PRINT:INPUT "PRESS RETURN TO RETURN TO MAIN MENU",A$
3000 REM LOAD "MENU",R
3010 END

```

TYPICAL RESULTS

LOCATION: NAS CUBI POINT ENGINE: F404-GE-400 THROTTLE: A/BURN.
 DATE: 11/11/86 BAROM. = 405 IN. H2O ; AMB. TEMP = 88 F.
 FIRST TIME ARRAY IS AT: 17 : 43 : 55.03333
 AVERAGED 26 READINGS THRU TIME: 17 : 44 : 25.03333

INLET FLOW CHARACTERISTICS

PRIMARY INLET

V(1) =	65.2	M(1) =	21.6	PR(1) =	4.8
V(2) =	68.9	M(2) =	21.8	PR(2) =	5.3
V(3) =	67.4	M(3) =	21.4	PR(3) =	5.1
V(4) =	62.7	M(4) =	19.9	PR(4) =	4.4
V(5) =	62.7	M(5) =	19.9	PR(5) =	4.4
V(6) =	62.9	M(6) =	20.0	PR(6) =	4.4
V(7) =	66.0	M(7) =	21.9	PR(7) =	4.9
V(8) =	68.1	M(8) =	21.6	PR(8) =	5.2
V(9) =	64.2	M(9) =	20.4	PR(9) =	4.6
V(10) =	64.4	M(10) =	20.4	PR(10) =	4.6
V(11) =	64.3	M(11) =	20.4	PR(11) =	4.6
V(12) =	65.0	M(12) =	20.6	PR(12) =	4.7

PRIMARY INLET MASS FLOW = 999.4 LB/SEC

PRIMARY INLET MASS FLOW MEASURED WITH WINDMILLS = 849.5 LB/SEC

SECONDARY INLET

V(13) =	81.5	M(13) =	26.0	PR(13) =	7.4
V(14) =	89.5	M(14) =	28.5	PR(14) =	9.0
V(15) =	90.7	M(15) =	28.9	PR(15) =	9.2
V(16) =	85.5	M(16) =	27.3	PR(16) =	8.2
V(17) =	117.4	M(17) =	37.4	PR(17) =	15.4
V(18) =	114.5	M(18) =	36.5	PR(18) =	14.7
V(19) =	94.9	M(19) =	30.2	PR(19) =	10.1
V(20) =	136.7	M(20) =	43.6	PR(20) =	20.9
V(21) =	94.5	M(21) =	30.1	PR(21) =	10.0
V(22) =	102.6	M(22) =	32.7	PR(22) =	11.8
V(23) =	104.6	M(23) =	33.3	PR(23) =	12.3
V(24) =	116.6	M(24) =	37.2	PR(24) =	15.2
V(25) =	101.9	M(25) =	32.5	PR(25) =	11.6
V(26) =	82.5	M(26) =	26.3	PR(26) =	7.6
V(27) =	100.7	M(27) =	32.1	PR(27) =	11.4
V(28) =	102.8	M(28) =	98.2	PR(28) =	11.8
V(29) =	96.1	M(29) =	91.8	PR(29) =	10.4
V(30) =	109.7	M(30) =	104.8	PR(30) =	13.5
V(31) =	96.4	M(31) =	92.1	PR(31) =	10.4

SECONDARY INLET MASS FLOW = 869.3 LB/SEC

SECONDARY INLET SYMMETRY CHECK

V(28) = 102.8	CORRESPONDS TO	V(22) = 102.6
V(29) = 96.1	CORRESPONDS TO	V(20) = 136.7
V(30) = 109.7	CORRESPONDS TO	V(18) = 114.5
V(31) = 96.4	CORRESPONDS TO	V(14) = 89.5

TOTAL INLET AIRFLOW = 1868.7 LB/SEC
 AUGMENTATION AIRFLOW OF INLETS = 1728.7 LB/SEC
 AUGMENTATION RATIO = 12.35

EAIR = 0.246, EFUEL = 0.155, EIN = 0.401 MBTU/SEC.

EXHAUST RACK 'A'

V(1) = 158.8 FT/SEC	T(1) = 264 DEG. F	M(1) = 206.4 LB/SEC
V(2) = 352.5 FT/SEC	T(2) = 380 DEG. F	M(2) = 126.2 LB/SEC
V(3) = 472.4 FT/SEC	T(3) = 454 DEG. F	M(3) = 64.6 LB/SEC
V(4) = 588.5 FT/SEC	T(4) = 530 DEG. F	M(4) = 37.1 LB/SEC
V(5) = 674.3 FT/SEC	T(5) = 580 DEG. F	M(5) = 20.2 LB/SEC
V(6) = 671.2 FT/SEC	T(6) = 586 DEG. F	M(6) = 40.1 LB/SEC
V(7) = 561.7 FT/SEC	T(7) = 518 DEG. F	M(7) = 71.7 LB/SEC
V(8) = 441.2 FT/SEC	T(8) = 429 DEG. F	M(8) = 149.3 LB/SEC
V(9) = 259.4 FT/SEC	T(9) = 299 DEG. F	M(9) = 321.7 LB/SEC
V(10) = 425.5 FT/SEC	T(10) = 753 DEG. F	M(10) = 458.9 LB/SEC
V(11) = 646.4 FT/SEC	T(11) = 565 DEG. F	M(11) = 71.4 LB/SEC
V(12) = 594.0 FT/SEC	T(12) = 529 DEG. F	M(12) = 68.0 LB/SEC
V(13) = 274.9 FT/SEC	T(13) = 384 DEG. F	M(13) = 426.2 LB/SEC

TOTAL AUGMENTATION TUBE AIRFLOW (BY SUM) = 2061.7 LB/SEC

EXHAUST RACK 'B'

V(14) = 171.4 FT/SEC	T(14) = 266 DEG. F	M(14) = 158.7 LB./SEC.
V(15) = 228.9 FT/SEC	T(15) = 355 DEG. F	M(15) = 139.8 LB./SEC.
V(16) = 274.7 FT/SEC	T(16) = 377 DEG. F	M(16) = 81.7 LB./SEC.
V(17) = 298.8 FT/SEC	T(17) = 396 DEG. F	M(17) = 42.8 LB./SEC.
V(18) = 306.2 FT/SEC	T(18) = 400 DEG. F	M(18) = 88.6 LB./SEC.
V(19) = 276.8 FT/SEC	T(19) = 382 DEG. F	M(19) = 163.6 LB./SEC.
V(20) = 232.1 FT/SEC	T(20) = 344 DEG. F	M(20) = 193.9 LB./SEC.
V(21) = 251.0 FT/SEC	T(21) = 372 DEG. F	M(21) = 352.7 LB./SEC.
V(22) = 283.6 FT/SEC	T(22) = 388 DEG. F	M(22) = 83.3 LB./SEC.
V(23) = 265.3 FT/SEC	T(23) = 376 DEG. F	M(23) = 79.0 LB./SEC.
V(24) = 218.6 FT/SEC	T(24) = 354 DEG. F	M(24) = 313.9 LB./SEC.

TOTAL AUGMENTATION TUBE AIRFLOW (BY SUM) = 1697.9 LB/SEC

TOTAL AUGMENTATION TUBE AIRFLOW, RACK 'A' (BY INTEGR.) = 1730.6 LB/SEC

ENGINE GAS FLOW = 140. LB/SEC

AUGMENTATION (SECONDARY) AIRFLOW = 1590.6 LB/SEC

AUGMENTATION RATIO = 11.36

E - RACK 'A' = 0.317 MBTU/SEC.

TOTAL AUGMENTATION TUBE AIRFLOW, RACK B (BY INTEGR.) = 1764.5 LB/SEC

ENGINE GAS FLOW = 140.0 LB/SEC

AUGMENTATION (SECONDARY) AIRFLOW = 1624.5 LB/SEC

AUGMENTATION RATIO = 11.60

E - RACK 'B' = 0.342 MBTU/SEC.

STATICS IN AUGMENTER TUBE -- IN. H2O

S(1 -- 5)	-5.00	-4.85	-4.76	-4.72	-1.60
S(6 - 10)	-0.05	0.06	0.89	0.73	1.62

WINDMILL VELOCITIES ---- FT./SEC.

VWM(1) = 26.2	VWM(9) = 35.4
VWM(2) = 30.5	VWM(10) = 32.5
VWM(3) = 33.5	VWM(11) = 31.2
VWM(4) = 34.3	VWM(12) = 33.6
VWM(5) = 33.6	VWM(13) = 32.1
VWM(6) = 31.8	VWM(14) = 30.2
VWM(7) = 29.7	VWM(15) = 22.3
VWM(8) = 26.3	VWM(16) = 18.1

CELL DEPRESSION = -0.641 INCHES WATER

MAX TEST CELL INLET VELOCITY = 136.7 FT/SEC

MAX AUGMENTOR TUBE WALL TEMP. = 416.7 DEG.F AT STA. 6

MAX EXHAUST RAMP TEMPERATURE = 353.3 DEG.F

INLET TOTAL AUGMENTATION RATIO = 12.35

EXHAUST AUGMENTATION RATIO, RACK 'A' = 11.36

EXHAUST AUGMENTATION RATIO, RACK 'B' = 11.60

END OF SUMMARY

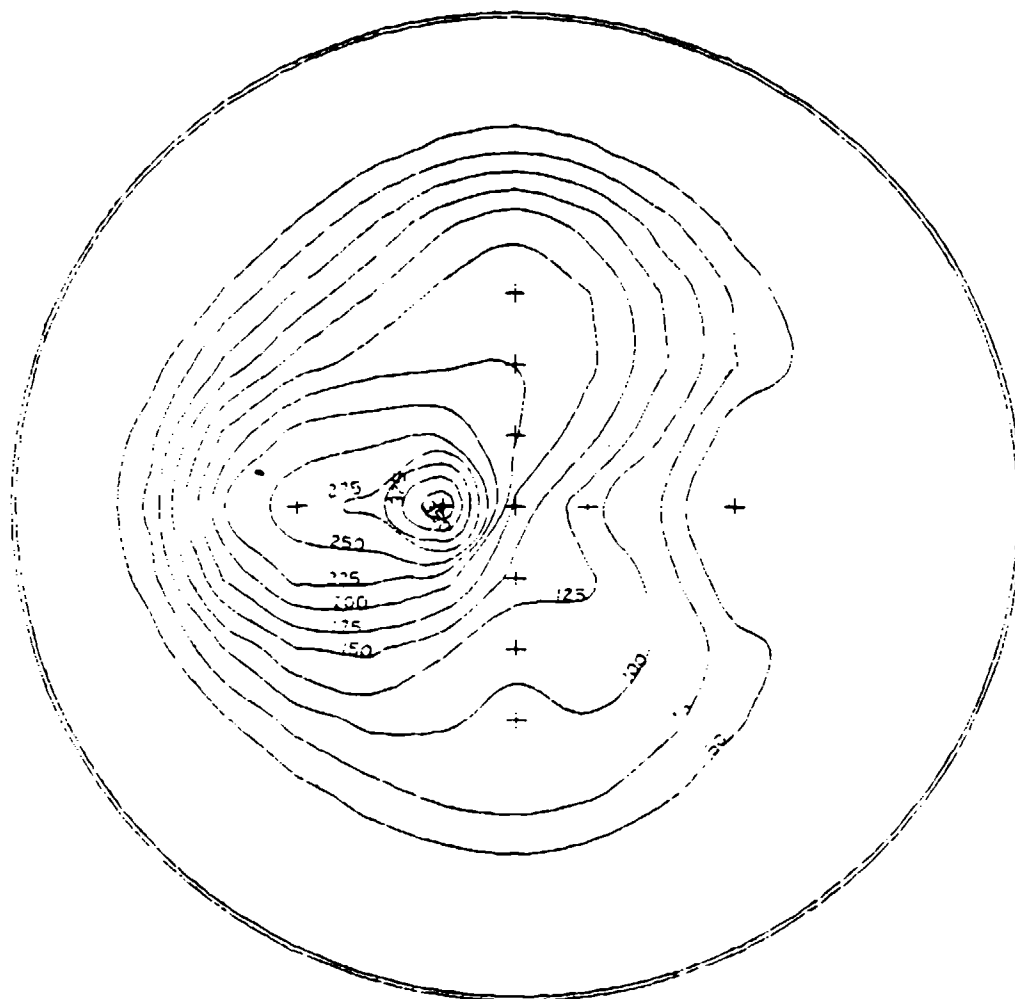
Appendix E

VELOCITY CONTOUR PLOTS

Figures E-1 through E-6 are contour plots of the augmentor tube velocities calculated from pressures measured at the forward instrumentation rack. The contours were generated using Computervision Corporation's CADD5 4X Site Engineering Package.* Interpolation was employed, requiring assumptions to be made concerning the weighting of the different velocities. These contours, therefore, are not "data." They are offered as a less accurate but perhaps more enlightening method of presenting the results. In particular, the effects of engine misalignment are clearly illustrated.

*Computervision Corporation. User's Manual: CADD5 4X site engineering reference. Boston, MA. May 1984.

J52 MISALIGNED BY 2.3 DEGREES



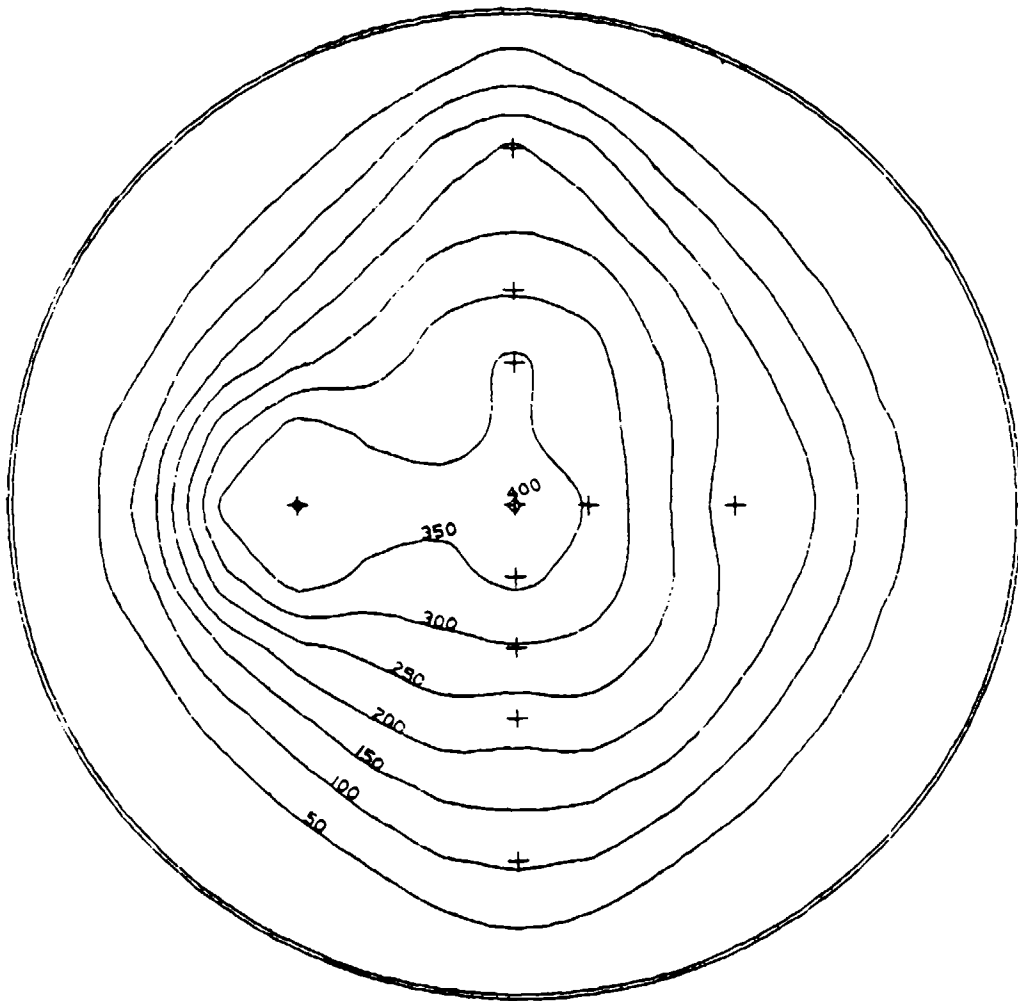
NOTES:

- (1) VELOCITY CONTOURS IN A PLANE CUTTING AUGMENTER TUBE 30 FT FROM TUBE INLET
- (2) VELOCITIES IN FT/SEC
- (3) MISALIGNMENT TO THE LEFT WHEN FACING ENGINE
- (4) J52-P-39 AT MIL

(a) J52 misaligned by 2.3 degrees.

Figure E-1. Effect of horizontal misalignment on the aerothermal performance of T-10 test cell at the NAS Cubi Point.

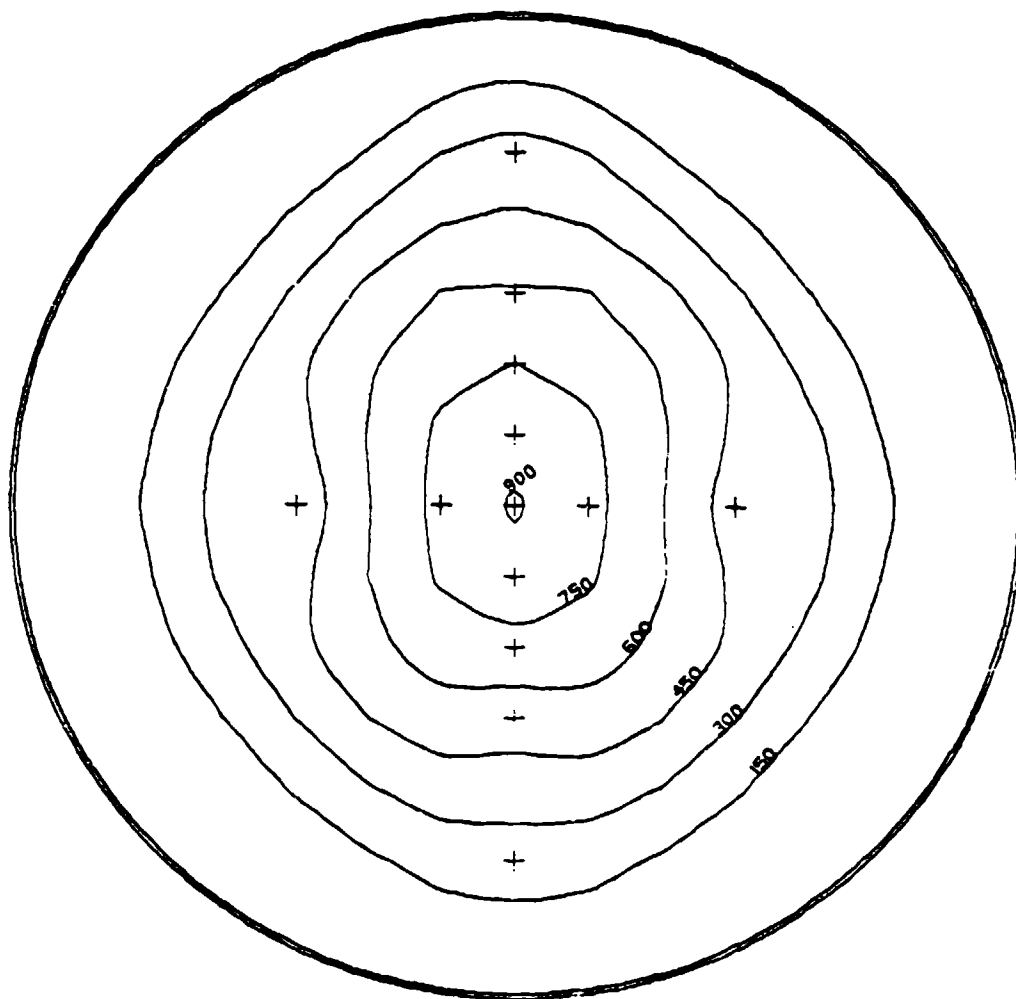
J52 MISALIGNED BY 1.0 DEGREES



NOTES:

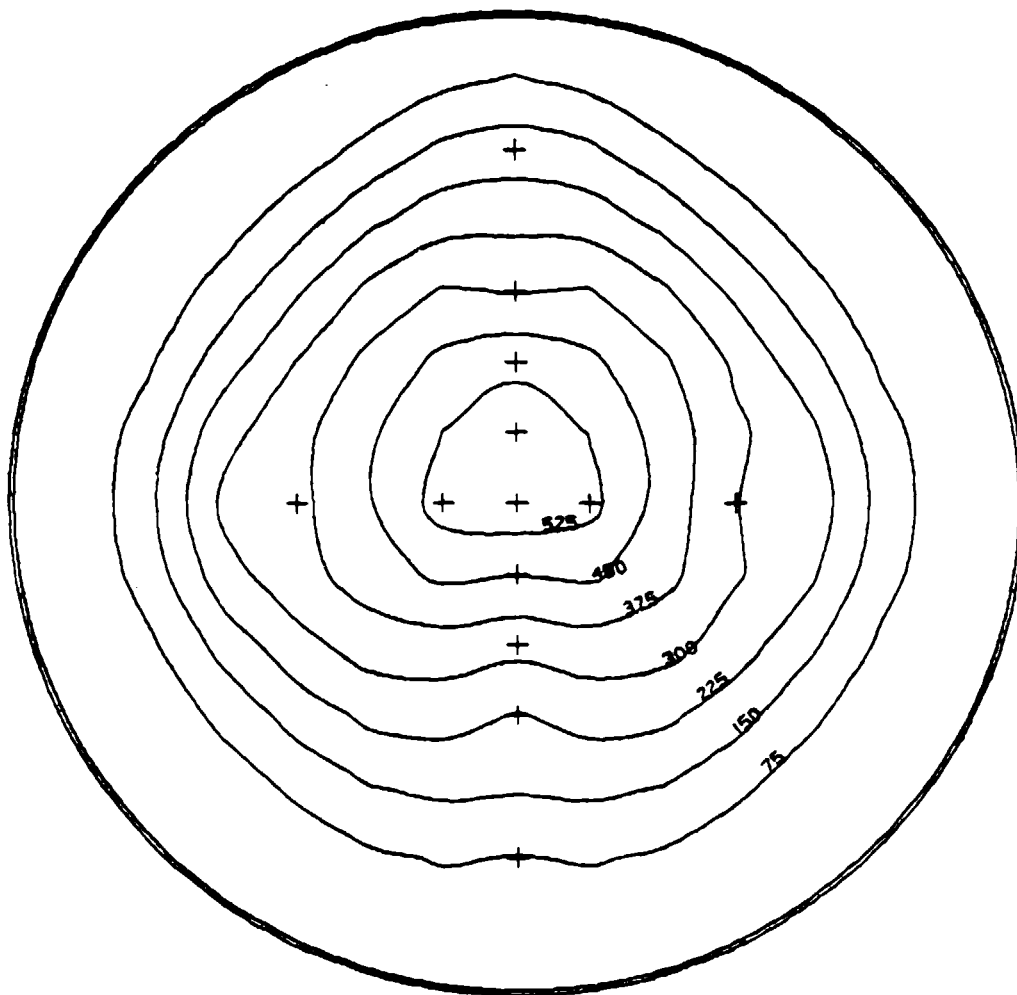
- (1) VELOCITY CONTOURS IN A PLANE CUTTING AUGMENTER TUBE 30 FT FROM TUBE INLET
- (2) VELOCITIES IN FT/SEC
- (3) MISALIGNMENT TO THE LEFT WHEN FACING ENGINE
- (4) J52-P-8B AT MIL

(b) J52 misaligned by 1.0 degree.



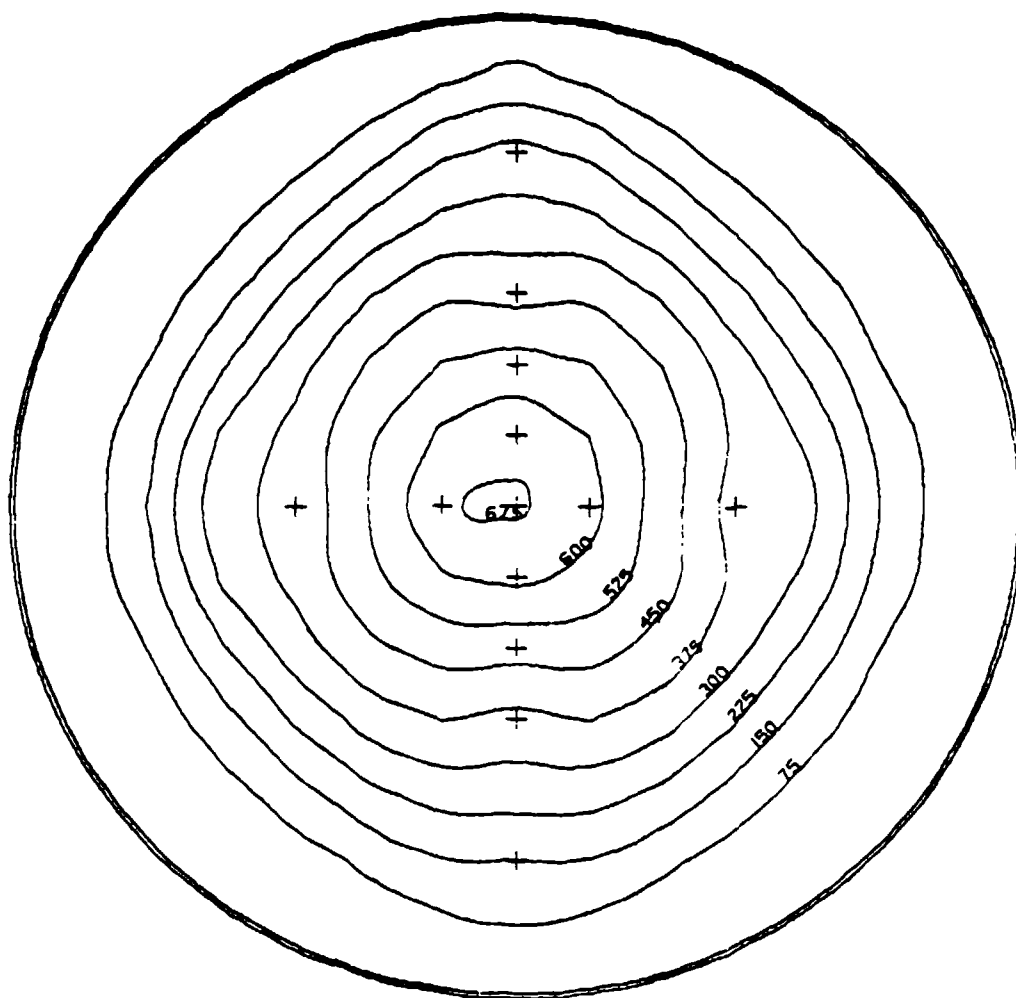
- NOTES: (1) VELOCITIES IN FT/SEC
(2) LOOKING BACK TOWARD ENGINE
(3) 30 FT DOWN THE TUBE: 73.1 FT FROM ENGINE NOZZLE
(4) AVERAGED OVER A 37 SECONDS RUN

Figure E-2. Velocity contours across augmentor tube while testing TF30-P-414A at A/B with throttle plate.



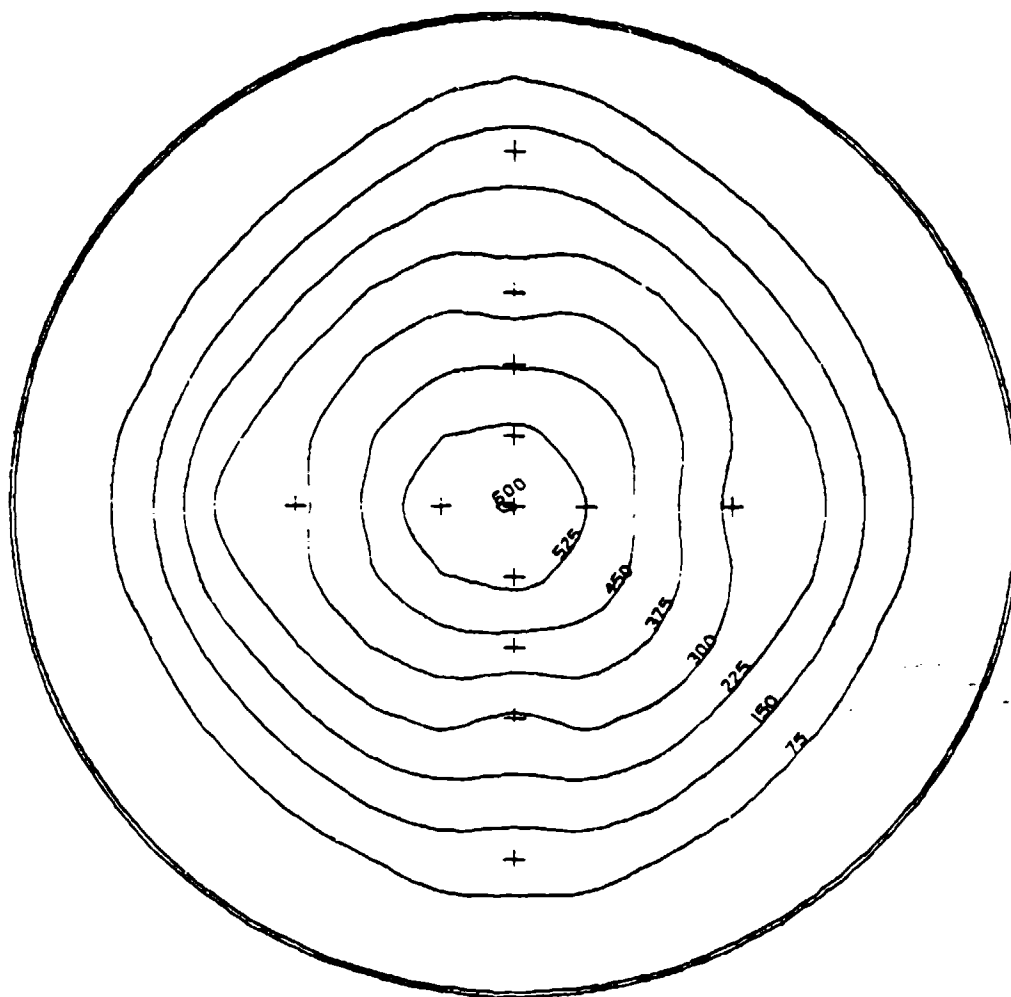
NOTES: (1) VELOCITIES (PRESSURES) AVERAGED OVER A 60 SECONDS RUN
(2) VELOCITIES IN FT/SEC
(3) 30 FT DOWN THE TUBE: 43.1 FT FROM ENGINE NOZZLE

Figure E-3. Velocity contours across augmeter tube while testing TF30-P-414A at Mil with throttle plate.



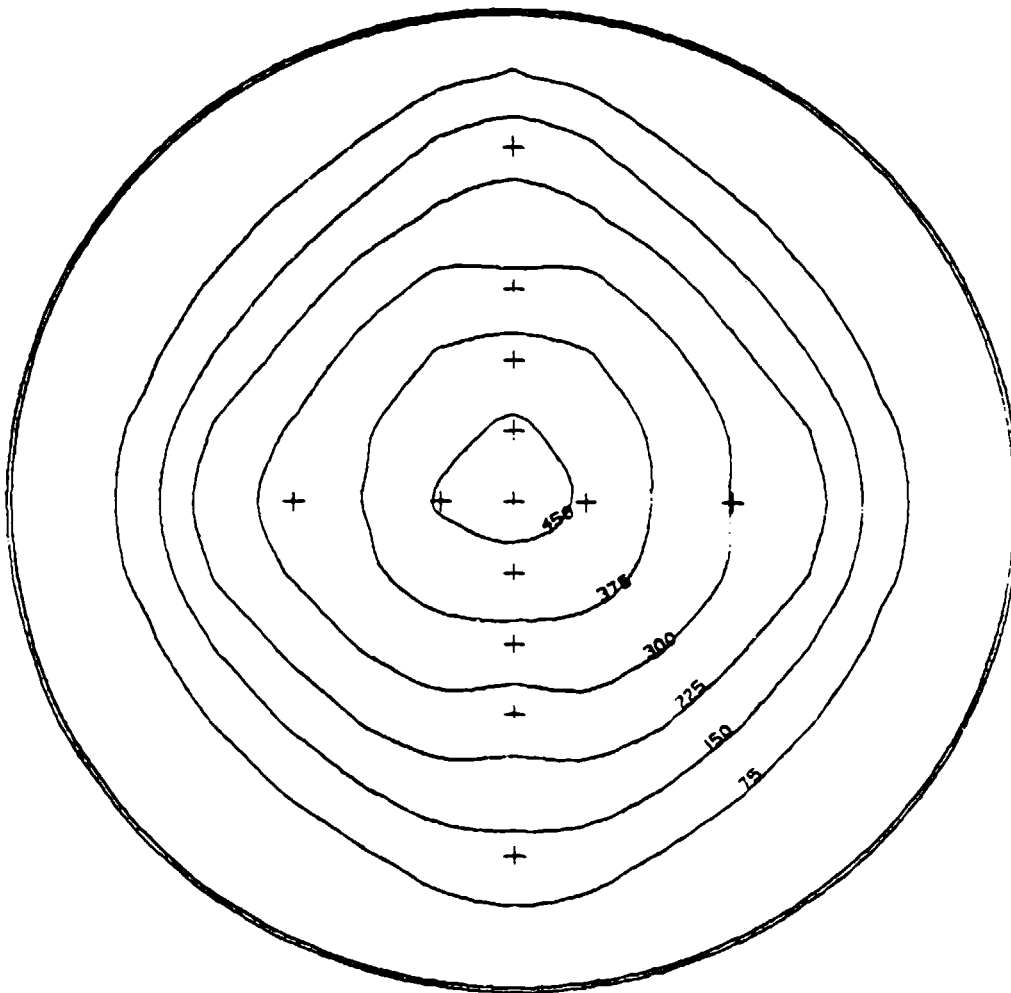
NOTES: (1) VELOCITIES (PRESSURES) AVERAGED OVER A 26 SECONDS RUN
(2) VELOCITIES IN FT/SEC
(3) 30 FT DOWN THE TUBE: 45.7 FT FROM ENGINE NOZZLE

Figure E-4. Velocity contours across augmenter tube while testing F404-GE-400 at A/B with throttle plate.



NOTES: (1) VELOCITIES (PRESSURES) AVERAGED OVER A 78 SECONDS RUN
(2) VELOCITIES IN FT/SEC
(3) 30 FT DOWN THE TUBE: 45.3 FT FROM ENGINE NOZZLE

Figure E-5. Velocity contours across augmentor tube while testing TF41-A-2C at Mil with throttle plate.



NOTES: (1) VELOCITIES (PRESSURES) AVERAGED OVER A 91 SECONDS RUN
(2) VELOCITIES IN FT/SEC
(3) 30 FT DOWN THE TUBE: 48.0 FT FROM ENGINE NOZZLE

Figure E-6. Velocity contours across augmeter tube while testing J52-P-408 at M11 with throttle plate.

Appendix F

CUBI POINT WEATHER SUMMARIES

The weather was never a factor influencing the tests. It rained several nights and during the afternoon on the 13th and 14th of November, but tests were not conducted during any period of heavy precipitation. Winds were always light, rarely exceeding ten knots.

Table F-1 summarizes weather conditions encountered during the period of the tests.

Table F-1. Weather Summaries For Cubi Point During 9-19 November 1986

Condition	Dates and Times						
	9 Nov 1053	11 Nov 0900	11 Nov 1630	12 Nov 2000	13 Nov 1445	19 Nov 1100	19 Nov 1820
Dry Bulb, °F	87	88	89	83	77	92	85
Wet Bulb, °F	79	79	76	74	74	79	76
Humidity, %	75	66	62	76	90	56	72
Barometer, in./Hg	29.77	29.85	29.76	29.80	29.70	29.75	29.71
Wind Velocity, Kn	5	6 - 12	6	3	9	3	4
Wind Direction	090	060	050	120	350	Var- able	315

DISTRIBUTION LIST

AF 6550 ABG/DER, Patrick AFB, FL; AFIT/DET (Hudson), Wright-Patterson AFB, OH; AFIT/DET, Wright-Patterson AFB, OH
 AF HQ ESD/DEE, Hanscom AFB, MA
 AFB AUL/LSE 63-465, Maxwell AFB, AL
 ARMY ERADCOM Tech Supp Dir (DELS-D), Ft Monmouth, NJ
 ARMY BELVOIR R&D CEN STRBE-BLORE, Ft Belvoir, VA
 ARMY CERL CERL-ZN, Champaign, IL; Library, Champaign, IL. **CECER-EM (Hayes), Champaign, IL**
 ARMY EHA Bio-Aco Div, Aberdeen Proving Grnd, MD; HSHB-EW, Aberdeen Proving Grnd, MD
 ARMY EWES WESGP-E, Vicksburg, MS
 CBC Code 10, Davisville, RI; Code 15, Port Hueneme, CA; Code 430, Gulfport, MS; Library, Davisville, RI;
 PWO (Code 400), Gulfport, MS; PWO (Code 80), Port Hueneme, CA; Tech Library, Gulfport, MS
 CBU 401, OIC, Great Lakes, IL; 405, OIC, San Diego, CA; 411, OIC, Norfolk, VA; 417, OIC, Oak Harbor, WA
 COMDT COGARD Library, Washington, DC
 COMFAIR SEC, Naples, Italy; WESTPAC DET, OIC, Cubi Point, RP
 COMNAVAIRSYSCOM Code 4223F, Washington, DC
 COMNAVRESFOR Code 823, New Orleans, LA
 DOE Wind/Ocean Tech Div, Tobacco, MD
 DTIC Alexandria, VA
 EPA Air Prgm Off, Ann Arbor, MI
 FAA Code APM-740 (Tomita), Washington, DC
 FCTC LANT, PWO, Virginia Bch, VA
 FMFLANT CEC Offr, Norfolk, VA
 LIBRARY OF CONGRESS Sci & Tech Div, Washington, DC
 MARCORBASE PWO, Camp Pendleton, CA
 MCAF Code C144, Quantico, VA
 MCAS PWO, Yuma, AZ
 MCRD PWO, San Diego, CA
 MCRDAC M & L Div Quantico, VA
 NAF AROICC, Midway Island; Dir, Engrg Div, PWD, Atsugi, Japan; PWO, Atsugi, Japan
 NAS AIMD Pwrplnts (Chambers), Cubi Point, RP; Chase Fld, Code 18300, Beeville, TX; Chase Fld, PWO, Beeville, TX; Code 072E, Willow Grove, PA; Code 110, Adak, AK; Code 15, Alameda, CA; Code 70, South Weymouth, MA; Code 8, Patuxent River, MD; Miramar, PWO, San Diego, CA; PW Engrg (Branson), Patuxent River, MD; PWD Maint Div, New Orleans, LA; PWO (Code 182) Bermuda; PWO, Dallas, TX; PWO, Glenview, IL; PWO, Kellavik, Iceland; PWO, Kingsville TX; PWO, New Orleans, LA; PWO, Sigonella, Italy; PWO, South Weymouth, MA; SCE, Cubi Point, RP; SCE, Norfolk, VA; Whiting Fld, PWO, Milton, FL
 NAVAIRDEVCCEN Code 832, Warminster, PA
 NAVAIRENGCEN Code 182, Lakehurst, NJ; Code 52611 (Croce), Lakehurst, NJ; PWO, Lakehurst, NJ
 NAVAIRPROPCEN Code PE21 (Zimmerman), Trenton, NJ; Code PE31 (Klarman), Trenton, NJ
 NAVAIRTESTCEN Code SY53 (Lynch), Patuxent River, MD; PWO, Patuxent River, MD
 NAVAVIONICEN Code D/701, Indianapolis, IN; PWO, Indianapolis, IN
 NAVAVNDEPOT Code 643.7 (Douglas), San Diego, CA
 NAVCAMS PWO (Code W-60), Wahiawa, HI; SCE, Guam, Mariana Islands
 NAVCOASTSYSCEN Tech Library, Panama City, FL
 NAVCONSTRACEN Code B-1, Port Hueneme, CA
 NAVFACENGCOM Code 00, Alexandria, VA; Code 03, Alexandria, VA; Code 03R (Bersson), Alexandria, VA; Code 03T (Essoglou), Alexandria, VA; Code 04A, Alexandria, VA; Code 04A1, Alexandria, VA; Code 04A5 (E. Ference), Alexandria, VA; Code 0631, Alexandria, VA; Code 083, Alexandria, VA; Code 09M124 (Lib), Alexandria, VA
 NAVFACENGCOM - CHES DIV, FPO-IPL, Washington, DC
 NAVFACENGCOM - LANT DIV, Br Ofc, Dir, Naples, Italy; Code 1112, Norfolk, VA; Library, Norfolk, VA
 NAVFACENGCOM - NORTH DIV, Code 04, Philadelphia, PA; Code 04A1, Philadelphia, PA; Code 202.2, Philadelphia, PA
 NAVFACENGCOM - PAC DIV, Code 09P, Pearl Harbor, HI; Code 101 (Kyi), Pearl Harbor, HI; Library, Pearl Harbor, HI
 NAVFACENGCOM - SOUTH DIV, Code 1112, Charleston, SC; Code 403 (Foster), Charleston, SC; Code 406, Charleston, SC; Library, Charleston, SC
 NAVFACENGCOM - WEST DIV, Code 04A2.2 (Lib), San Bruno, CA; Code 04B, San Bruno, CA; Pac NW Br Ofc, Code C/50, Silverdale, WA
 NAVFACENGCOM CONTRACTS Code 460, Portsmouth, VA; DROICC, Lemoore, CA; OICC, Guam; OICC/ROICC, Norfolk, VA; ROICC, Corpus Christi, TX; ROICC, Point Mugu, CA; OICC/ROICC, Virginia Beach, VA; SW Pac, OICC, Manila, RP

NAVHOSP Hd. Fac Mgmt. Camp Pendleton, CA
NAVMARCORESCEN LTJG Davis, Raleigh, NC
NAVOCEANSYSCEN Code 524 (Lepor), San Diego, CA
NAVPGSCOL Code 61WL (O. Wilson), Monterey, CA; Code 69ZC (Salinas), Monterey, CA
NAVSTA Dir, Engr Div, PWD, Guantanamo Bay, Cuba; Util Engrg Offr, Rota, Spain
NAVSWC Code H31 (Gibbs), Dahlgren, VA
NAVWARCOL Code 24, Newport, RI
NAVWPNCEN AROICC, China Lake, CA; PWO (Code 266), China Lake, CA
NETC Code 42, Newport, RI; PWO, Newport, RI
NMCB 3, Ops Offr: 40, CO: 5, Ops Dept
PACMISRANFAC III Area, PWO, Kekaha, HI
PWC Code 10, Oakland, CA; Code 101 (Library), Oakland, CA; Code 1013, Oakland, CA; Code 123-C, San Diego, CA; Code 400, Great Lakes, IL; Code 400, Pearl Harbor, HI; Code 400, San Diego, CA; Code 421 (Kaya), Pearl Harbor, HI; Code 420, Great Lakes, IL; Code 420B (Waid), Subic Bay, RP; Code 500, Great Lakes, IL; Code 500, Norfolk, VA; Code 500, Oakland, CA; Library (Code 134), Pearl Harbor, HI; Library, Guam, Mariana Islands; Library, Norfolk, VA; Library, Pensacola, FL; Library, Yokosuka, Japan; Tech Library, Subic Bay, RP
USCINCPAC Code J44, Camp HM Smith, HI

INSTRUCTIONS

The Naval Civil Engineering Laboratory has revised its primary distribution lists. The bottom of the label on the reverse side has several numbers listed. These numbers correspond to numbers assigned to the list of Subject Categories. Numbers on the label corresponding to those on the list indicate the subject category and type of documents you are presently receiving. If you are satisfied, throw this card away (or file it for later reference).

If you want to change what you are presently receiving:

- Delete – mark off number on bottom of label.
- Add – circle number on list.
- Remove my name from all your lists – check box on list.
- Change my address – line out incorrect line and write in correction (PLEASE ATTACH LABEL).
- Number of copies should be entered after the title of the subject categories you select.

Fold on line below and drop in the mail.

Note: Numbers on label but not listed on questionnaire are for NCEL use only, please ignore them.

Fold on line and staple.

DEPARTMENT OF THE NAVY

NAVAL CIVIL ENGINEERING LABORATORY
PORT HUENEME, CALIFORNIA 93043-5003

OFFICIAL BUSINESS
PENALTY FOR PRIVATE USE, \$300
NCEL-2700/4 (REV. 10-87)
0030-LL-L70-0044



BUSINESS REPLY CARD

FIRST CLASS PERMIT NO. 69

POSTAGE WILL BE PAID BY ADDRESSEE

Commanding Officer
Code L08B
Naval Civil Engineering Laboratory
Port Hueneme, California 93043-5003

NO POSTAGE
NECESSARY
IF MAILED
IN THE
UNITED STATES



DISTRIBUTION QUESTIONNAIRE

The Naval Civil Engineering Laboratory is revising its primary distribution lists.

SUBJECT CATEGORIES

1 SHORE FACILITIES

- 2 Construction methods and materials (including corrosion control, coatings)
- 3 Waterfront structures (maintenance/deterioration control)
- 4 Utilities (including power conditioning)
- 5 Explosives safety
- 6 Aviation Engineering Test Facilities
- 7 Fire prevention and control
- 8 Antenna technology
- 9 Structural analysis and design (including numerical and computer techniques)
- 10 Protective construction (including hardened shelters, shock and vibration studies)
- 11 Soil/rock mechanics
- 14 Airfields and pavements

15 ADVANCED BASE AND AMPHIBIOUS FACILITIES

- 16 Base facilities (including shelters, power generation, water supplies)
- 17 Expedient roads/airfields/bridges
- 18 Amphibious operations (including breakwaters, wave forces)
- 19 Over-the-Beach operations (including containerization, materiel transfer, lighterage and cranes)
- 20 POL storage, transfer and distribution

28 ENERGY/POWER GENERATION

- 29 Thermal conservation (thermal engineering of buildings, HVAC systems, energy loss measurement, power generation)
- 30 Controls and electrical conservation (electrical systems, energy monitoring and control systems)
- 31 Fuel flexibility (liquid fuels, coal utilization, energy from solid waste)
- 32 Alternate energy source (geothermal power, photovoltaic power systems, solar systems, wind systems, energy storage systems)
- 33 Site data and systems integration (energy resource data, energy consumption data, integrating energy systems)

34 ENVIRONMENTAL PROTECTION

- 35 Solid waste management
- 36 Hazardous/toxic materials management
- 37 Wastewater management and sanitary engineering
- 38 Oil pollution removal and recovery
- 39 Air pollution

44 OCEAN ENGINEERING

- 45 Seafloor soils and foundations
- 46 Seafloor construction systems and operations (including diver and manipulator tools)
- 47 Undersea structures and materials
- 48 Anchors and moorings
- 49 Undersea power systems, electromechanical cables, and connectors
- 50 Pressure vessel facilities
- 51 Physical environment (including site surveying)
- 52 Ocean-based concrete structures
- 54 Undersea cable dynamics

TYPES OF DOCUMENTS

- 85 Techdata Sheets
- 86 Technical Reports and Technical Notes
- 83 Table of Contents & Index to TDS

82 NCEL Guides & Abstracts

91 Physical Security

92 None—
remove my name